Synaptic mechanisms in experience-dependent processes responsible for the development of central neural maps of visual space.

A thesis submitted for the degree of
Doctor of Philosophy in the University of London

by

Stephen G Brickley

Division of Neurophysiology and Neuropharmacology
National Institute for Medical Research
Mill Hill, London NW7 1AA

ProQuest Number: 10106700

ProQuest 10106700

Abstract

Experience-dependent synaptic plasticity has been demonstrated in the binocular visual system of the aquatic frog *Xenopus laevis*. This thesis offers further support for the role of correlated patterns of neural activity in this synaptic plasticity and demonstrates, for the first time, that *N*-methyl-D-aspartate (NMDA)-type glutamate receptors contribute to synaptic transmission in the optic tectum of *Xenopus*.

Electrophysiological mapping techniques assessed the capacity for synaptic reorganisations to occur in the binocular visual system of *Xenopus*. The intertectal system, a series of connections that mediates binocular vision in lower vertebrates, reorganised its pattern of synaptic connections in response to large changes in the orientation of both eyes.

Stroboscopic illumination was shown to interfere with correlated patterns of neural activity in the tectum, but the development of the retinotectal projection was not affected by this procedure. However, the intertectal systems capacity to modify its pattern of synaptic connections, in response to changes in eye position, was disturbed by this visual environment.

Next, *in vivo* and *in vitro* preparations of the optic tectum were developed to monitor pre and postsynaptic activity in the visual system of *Xenopus*. It was established that mono-synaptic transmission between retinal fibres and tectal neurons was mediated by non-NMDA type glutamate receptors. However, when the optic tract of the adult animal was electrically stimulated the late poly-synaptic (U2) component of the evoked response was reduced by $\sim 30\%$ in the presence of $50 \mu M$ AP5. This NMDA mediated component of the late U2 response was at its most significant 1 month after metamorphosis, was regulated by visual experience, and was not present in another species of frog, *Rana pipiens*.

Finally, a thin slice preparation of the optic tectum was developed which enabled tight-seal whole cell recordings to be made from identified tectal neurons.

List of Contents

Chapter 1
Introduction

Chapter 2
Materials and Methods

Chapter 3
Intertectal plasticity:
limitations and morphological correlates

Chapter 4
Intertectal plasticity:
correlated firing patterns in the tectum

Chapter 5
Synaptic transmission *in vivo*

Chapter 6
Synaptic transmission *in vitro*

Chapter 7
Intertectal plasticity:
AP5 sensitivity of the long latency U2 response

Chapter 8
Slice preparation of the optic tectum

Chapter 9
General Discussion

Appendix

List of Figures

List of Tables

Abbreviations

AMPA	α-amino-3-hydroxy-4-isoxazole propionic acid
ANOVA	analysis of variance
AP5	2-amino-5-phosphonovaleric acid
CC	cross correlation
CNQX	6-cyano-7-nitroquinoxaline-2,3-dione
CNS	central nervous system
CPP	3-(($\pm$)-2-carboxypiperazin-4-yl)propyl-1-phosphonic acid
D-TC	D-tubocurarine
EB	ethidium bromide
FDA	fluorosceine diacetate
GABA	γ-Aminobutyric acid
HRP	horse radish peroxidase
LED	light emitting diode
LY	lucifer yellow
MS222	Tricaine-methanesulphonate
MURF	multi-unit receptive field
NI	nucleus isthmi
NMDA	N-methyl-D-aspartate
PSTH	post-stimulus time histogram
RGC	retinal ganglion cell
SC	superior colliculus
TTX	tetrodotoxin

Chapter 1
Introduction

1.1. Overview

The elaboration and maintenance of topographic representations of sensory space offer a compelling insight into the processes governing neural development. These maps can be demonstrated with electrophysiological and anatomical techniques. One electrophysiological approach is to record neural activity at systematically varied positions in the central nervous system (CNS) in response to stimuli at defined locations in the external world or on the body surface. This approach demonstrates that topographic maps precisely convey the spatial information of a given sensory modality within the neural array and that these arrays are joined by orderly patterns of nerve connections. However, the processes governing the development of order within these nerve connections are poorly understood. The initial elaboration of maps is thought to be governed by intrinsic genetically determined factors, such as cell surface markers, which guide the early afferent inputs to their appropriate locations in the CNS array to establish the initial order of the projection. However, it is evident that in some developing neural systems disturbance in the normal pattern of neural activity, during critical developmental periods, results in long-term changes in the order of connections. It is hypothesised that activity-dependent processes are involved in the final generation of topographic order within the CNS subsequent to the successful completion of genetically determined events.

Neural activity in the brain can be generated by two different sources: either intrinsically, by the spontaneous firing of CNS neurons themselves, or extrinsically as a result of stimuli in the environment. A role for both spontaneous and evoked neural activity in the changes which occur within the synaptic circuitry of the CNS has been demonstrated in several disparate neuronal systems. Early experience seems to exert a particularly powerful influence on the elaboration and maintenance of those synaptic connections which are concerned with integrating information from two receptor surfaces, such as the two eyes. This thesis describes experiments concerned with the development of binocular visual connections in the main visual centre, the mid-brain optic tectum, of the frog, *Xenopus laevis* (figure 1.1). Experiments were designed to investigate the experience-dependent synaptic changes that occur in this binocular visual system and to examine possible synaptic mechanisms which underlie

them. Before describing these experiments I will discuss work describing synaptic plasticity in the optic tectum and has suggested a role for spontaneous and visually evoked activity in these changes.

1.2. Visual maps in the optic tectum

The optic tectum, a bi-lobed nucleus situated in the mid-brain, is the primary visual centre in anuran amphibia and mediates prey catching and behaviour (Ewert, 1976). In the aquatic frog *Xenopus laevis* each tectal lobe receives a topographically organized representation of visual space originating from the contralateral and ipsilateral eye (Gaze, 1958b). This is not true for all lower vertebrates, for example there is no ipsilateral input to the tectal lobe in the goldfish, *carassius auratus*. In these visuotectal topographic representations information from the nasal portion of the visual field projects through both eyes to the rostral aspect of each tectal lobe, the temporal visual field projects to caudal tectum, the superior visual field projects to medial tectum and the inferior visual field projects to lateral tectum (see figure 1.2). Input from the contralateral eye is direct and mediated by the completely crossed retinotectal projection (Gaze, 1958a). Input from the ipsilateral eye arrives via a commissural (intertectal) projection involving a relay at the nucleus isthmi (NI), another bilateral nucleus situated caudal to the tectum (Gruberg and Udin, 1978). The intertectal relay between the tectal lobes involves a projection between the tectal lobe and the ipsilateral NI (the uncrossed tecto-isthmic projection) followed by a crossed projection from that ipsilateral NI to the opposite tectal lobe (the crossed isthmo-tectal projection). The projection between each tectal lobe and its ipsilateral NI is a reciprocal one (the uncrossed isthmo-tectal projection). In adult frogs the presence of this intertectal relay is organised such that one point in the binocular visual field projects through both eyes to a common point on each lobe of the nucleus (see figure 1.1). This intertectal system of connections may provide the stereoscopic cues necessary for the computation of visual depth during prey-catching in anuran amphibians (Collett, 1977).
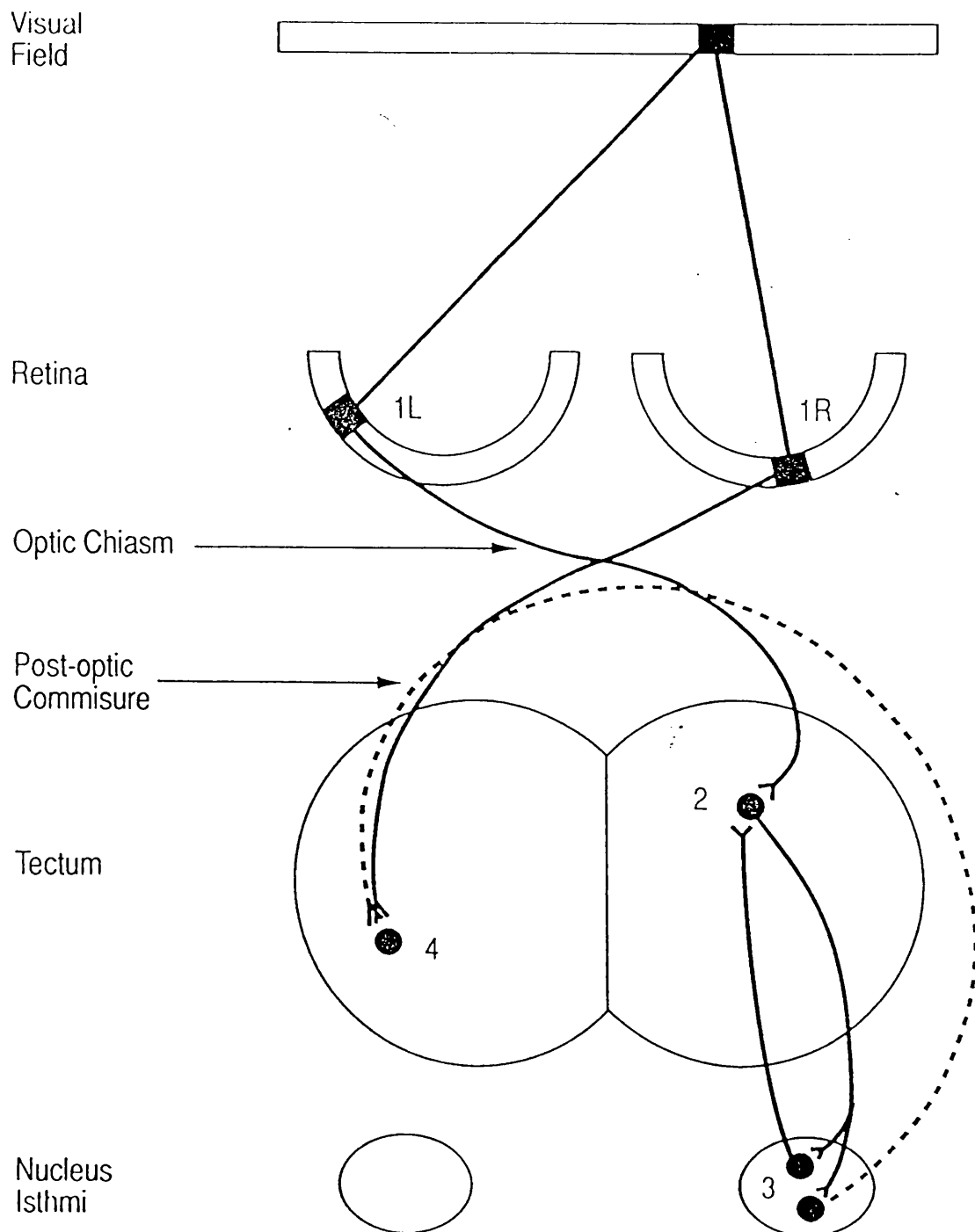
Figure 1.1. The pathways responsible for the dual topographic projections of the binocular visual field present on each tectal lobe in adult frogs.

If we consider a point in the binocular visual field it projects to one point on each retina (1R and 1L). The point on the left retina (1L) projects directly to point 2 on the right tectal lobe via the crossed retinotectal pathway and the corresponding point on the right retina (1R), which receives matched binocular input, projects to point 4 on the left tectum via its crossed pathway. Point 2, on the right tectum, is reciprocally linked to point 3 in another topographically organized mid-brain structure; the nucleus isthmi. The crossed isthmotectal projection (dotted line), conveys information about point 2, back across the mid-line through the post-optic commissure to its binocularly matched input, point 4, on the opposite tectal lobe. Point 4 on the left tectal lobe also projects to a point on its ipsilateral nucleus isthmi, which sends a projection, in turn, to point 2 on the right tectal lobe (Not shown). This means that a point in the binocular visual field can be mapped at one position on each tectal lobe through both eyes. In adult frogs, the "intertectal" system links all paired tectal locations receiving matched visual input from the binocular portion of visual space. Because the pathway from an eye to its ipsilateral tectum is polysynaptic, visual information usually arrives through this pathway some 10-30msec after its arrival through the direct retinal pathway from the contralateral eye.

Note: in the depiction of the crossed and uncrossed isthmotectal pathways, the projections are shown as arising from different populations of isthmic neurons. This arrangement has been described in *Rana pipiens* (Grobstein and Comer, 1983), but whether this arrangement also exists in *Xenopus* is unknown.

1.3. The retinotectal projection

1.3.1. The chemoaffinity hypothesis.

The notion of specific chemoaffinity markers establishing order within the developing CNS achieved prominence following experiments Roger Sperry performed on the entirely crossed retinotectal projection (reviewed by Sperry, 1963). After regeneration of the optic nerve, in newts and anura which had one eye rotated by 180°, Sperry showed that the animals oriented incorrectly to visual stimuli (Sperry, 1943). Sperry interpreted the results of these behavioural experiments as indicating that the optic nerve fibres had regenerated to their specified target sites in the tectum. He concluded that ordered synaptic connections are the product of neuronal specificity. The chemoaffinity hypothesis states that specific markers exist on pre- and postsynaptic elements such that synaptic connections are only established between those neurons bearing the appropriate labels. Indeed, the polarity of the retinotectal projection is specified very early in larval development. Gaze and colleagues (1979b) have demonstrated that 180° rotation of the eye primordium in *Xenopus* between stages 21-30, before retinal ganglion cell (RGC) axons have arrived in the tectum, results in the establishment of an inverted map, implying that the mapping polarity is specified before this stage of development. We now know that optic fibres arrive in the tectal neuropil at very early stages of development before any postsynaptic targets have matured (Gaze and Grant, 1992a). Older fibres lie deep within the optic tract displaced medially toward the midline of the brain and newly arriving fibres are positioned superficially in the lateral edge of the tract. The order of these fibres within the optic tract establishes much of the early topography within the tectum. However, it is still supposed that labels on presynaptic fibres and postsynaptic cells play a key role in organizing the polarity of the early projection and in establishing its initial topographic order across the tectum. More recent work (Bonh**ö**ffer and Gierer, 1984) has attempted to identify growth factors on the rostro-caudal and medio-lateral axis of the retina and the tectum which could specify this polarity.

1.3.2. Early experiments challenging the chemoaffinity hypothesis.

The view that connections between RGC axon terminals and tectal neurons are solely determined by intransigent sets of markers was first challenged by the outcome of so called "size-disparity" experiments. The first of these (Attardi and Sperry, 1963) supported the chemoaffinity hypothesis by showing that a half retina, when regenerating into a whole tectum, initially re-establishes connections with the appropriate half of the nucleus. Jacobson and Gaze (1965) then showed, in the converse experiment, that a full retina will not compress its regenerated projection onto half a tectum. These seemingly unequivocal demonstrations that RGCs respect tectal boundaries based upon their matching positional specificities did not withstand further experimentation. In 1970 Gaze contradicted his previous findings by describing the compression of an intact retina onto a half tectal lobe (Gaze and Sharma, 1970). This was followed by a series of papers demonstrating that a half retina will also expand onto a whole tectum (Horder, 1971; Yoon, 1972a&b; Schmidt et al., 1974 & 1977). The only change in the experimental procedure was time. The earlier experiments examined the initial regenerated retinotectal projection up to 3 weeks after the manipulation whereas the later studies examined the status of the projection after at least 1½ months. This result does not support the idea that chemospecific markers restrict absolutely the termination of retinal fibres to pre-defined areas of the tectum.

1.3.3. Shifting synaptic connections in the developing retinotectal projection.

It is now apparent that, in addition to the synaptic plasticity exhibited by the retinotectal projection during certain conditions of regeneration, the maturation of the retinotectal projection also proceeds in a manner inconsistent with immutable markers. In *Xenopus,* the retina grows by addition of new neurons to the ciliary margin throughout larval life and this continues into adulthood, while neurons are added to the tectum only at its caudal margin during larval life after which tectal histogenesis appears to cease (Straznicky and Gaze, 1971; 1972; Grant and Keating, 1986). The observation that a topographically organized retinotectal projection is demonstrable from very early larval stages (Gaze et al., 1974) led to the suggestion that a progressive shift of retinotectal synapses occurs throughout development. Initially new temporal RGC axons invade the rostral tectum causing a progressive shift of retinal fibres into caudal tectum as the developing retinotectal projection expands across the growing tectum (Gaze et al., 1979a). Later in development the number of

RGCs projecting to the tectum still increases but with no corresponding increase in the tectal cell number. It has been suggested that newly arriving retinal ganglion cell axons may compete for target space and/or trophic molecules derived from the optic tectum. This process should lead to the stabilization of connections formed by competing cells and to the death and elimination of cells that fail to compete successfully. Therefore, development of the retinotectal projection should be accompanied by cell death in the retina. Neuronal cell death is emerging as a fundamental feature of nervous system development in vertebrates. Indeed, in the cat 80% of RGCs are eliminated at birth (Williams *et al.*, 1986). It has recently been shown in *Xenopus* that cell death begins at the onset of metamorphosis, at about stage 57, and is completed by the end of metamorphosis. However, only 10% of the total RGC population is lost during this time (Gaze and Grant, 1992b) and so it is uncertain to what degree this phenomenon contributes to the developing retinotectal projection. Therefore, it has been suggested that, in *Xenopus*, changes are made in the pattern of synaptic connections formed between retinal fibres and tectal cells from at least stage 45 of larval life until adulthood (Gaze *et al.*, 1979a). Evidence for shifting synaptic connections between optic axons and tectal dendrites also exists in the developing retinotectal projection of another frog, *Rana pipiens,* (Reh and Constantine-Paton, 1984) and the goldfish, *carassius auratus* (Easter and Stuermer, 1984).

1.3.4. The possible role of neural activity in the developing retinotectal projection.

What cues could orchestrate these orderly shifts in synaptic connectivity? One possibility is that these synaptic changes are activity-dependent. It is known that spontaneous firing patterns between neighbouring RGCs exhibit much greater temporal correlation than do the firing patterns of separated ganglion cells (Arnett, 1978). It has been proposed that spontaneous correlated firing patterns stabilize synaptic connections in the retinotectal projection due to the ability of the tectal neurons to respond to the coincident neural activity of neighbouring RGCs. Neighbouring RGCs would selectively make synaptic connections on the dendrites of common tectal neurons due to the coincident neural activity they exhibit. Spontaneous firing patterns are not removed by visual deprivation so dark-rearing should not alter the plasticity demonstrated in the retinotectal projection. In support of this, investigations into the normal developmental changes in this pathway in *Xenopus* have shown that the precision of the retinotectal projection does not depend upon visual experience (Dawes

18

et al., 1984; Keating *et al.*, 1986). Animals reared in total darkness from stage 35/36, prior to the onset of visually driven electrical activity in the retina (Witkovsky *et al.*, 1976), showed no change in the topographic order, receptive field size and the distribution of retinotectal unit types within the superficial layers of the tectal lobe.

So what evidence is there to implicate the spontaneous neural activity of RGCs in the normal development of the retinotectal projection. Harris (1980 & 1984) directly investigated the role of neural activity in the developing retinotectal projection of the newt. The embryonic eye cup from *Ambystoma trigrinum* was transplanted into an embryonic newt of the species *Taricha toross*. This latter species manufactures Tetrodotoxin (TTX), a Na$^+$ channel blocker, in sufficient quantities to suppress action potentials in a TTX-sensitive species such as *Ambystoma*. The transplanted eye from *Ambystoma* grew in an environment in which it was incapable of generating action potentials. Anatomical assessment established that the retinotectal projection was topographically organized. Recently, Stuermer *et al.* (1990) reported that in embryonic zebra fish intraocular injection of TTX had no effect on the normal development of the retinotectal map. These data casts some doubt on the role of spontaneous neural activity in the generation of the precise pattern of connections which distinguishes the mature retinotectal projection. However, electrophysiological mapping of the retinotectal projection was not possible in the presence of TTX and the anatomical tracing techniques may not reveal small differences in the precision of the topographic projection.

In the "three eyed frog" preparation, a third eye primordium is implanted into an embryo so that two retinae innervate one tectal lobe. In this artificial situation the axon terminals of two retinotectal projections segregate into a pattern of eye-specific stripes in the doubly-innervated tectal lobe (Constantine-Paton and Law, 1978). Repeated intra-ocular injections of TTX, to block neural activity, prevents the eye specific segregation of afferent terminals (Boss and Schmidt, 1982; Meyer, 1982; Reh and Constantine-Paton, 1985). In other experiments the exceptional capacity of the optic nerve to regenerate into the optic tectum has been used to investigate activity-dependent synaptic plasticity in the retinotectal system. It has been shown that intraocular injection of TTX disrupts the topographic order of the regenerated retinotectal projection (Meyer, 1983; Schmidt and Edwards, 1983; Olson and Meyer, 1991). Finally, it has been shown that exposing animals to stroboscopic illumination, a procedure which is postulated to interfere with the correlated patterns of spontaneous retinal activity, disrupts the topographic order of the regenerated retinotectal

projection (Schmidt and Eisele, 1985; Cook and Rankin, 1986; Cook, 1987 & 1988). Dark-rearing is also reported to have no effect on the topographic order of the regenerated retinotectal projection (Cook and Becker, 1990; Olson and Meyer, 1991) indicating that the important information is carried by the spontaneous neural activity of RGCs rather than by visually-evoked activity. The only reported exception to this is a study by Schmidt and Eisele (1985) which showed an enlargement of receptive fields in the regenerated projection of visually deprived animals.

In light of the evidence supporting a role for spontaneous neural activity in the experimentally induced reorganisation of this projection it has been postulated that a postsynaptic mechanism exists in the tectum to detect correlated patterns of neural activity in neighbouring retinal fibres. Stabilization of convergent synaptic inputs onto common tectal cells could occur through a postsynaptic mechanism ensuring topographic order in the developing retinotectal projection. However, in *Xenopus*, there is no evidence to suggest that patterned neural activity plays any role in the normal development of the retinotectal projection. Therefore, the effect of chronic exposure to stroboscopic illumination on the development of the retinotectal projection in *Xenopus* was examined in Chapter 4. As part of this study the acute effects of stroboscopic illumination on correlated firing patterns recorded through the retinotectal projection was examined to assess whether this pattern of stimulation did disturb the spontaneous firing patterns of RGCs.
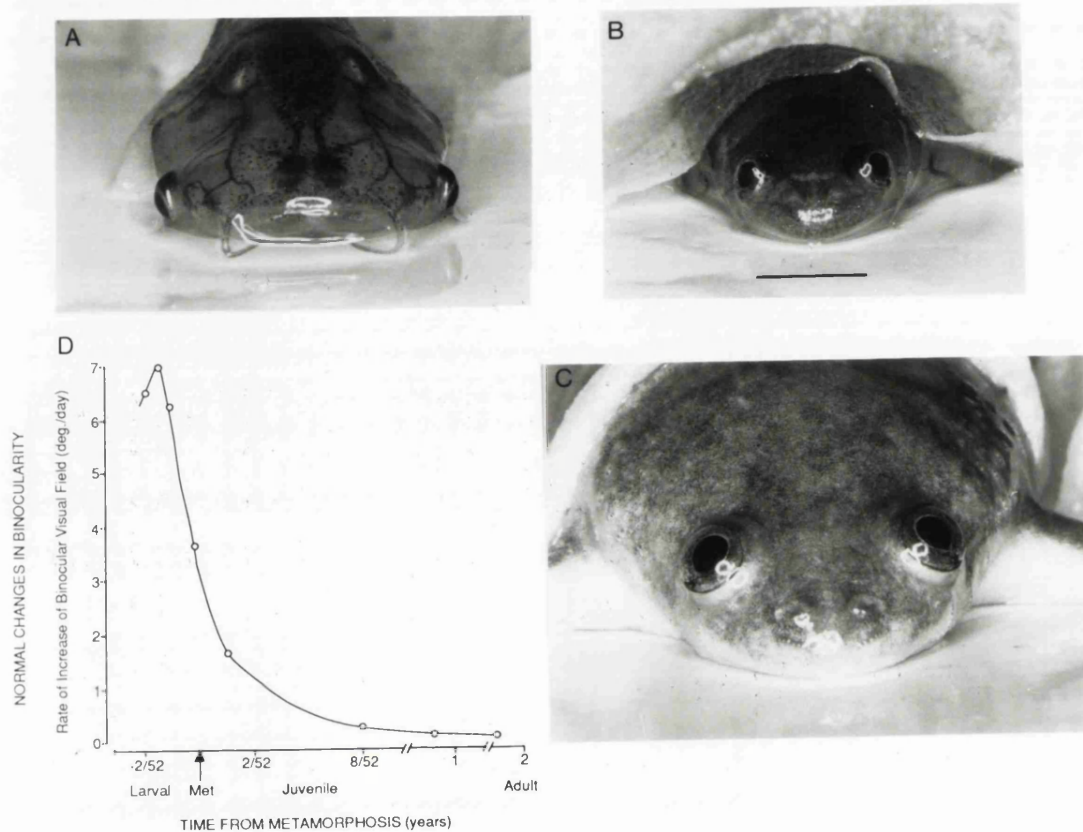
Figure 1.2. Growth-related changes in eye position in developing *Xenopus laevis*.

The photographs show frontal views of the head, illustrating the changing position of the two eyes, in animals at three developmental stages: (A) stage 58 of larval life; (B) ~2 weeks later, at metamorphic climax (Stage 66); (C) 1 year after metamorphic climax. Scale bar in B = 5mm and applies to all photographs. During this developmental period, the eyes migrate from lateral to frontodorsal positions in the head. As a result, the binocular visual field enlarges. (D) Shows the rate of this enlargement, expressed in degrees/day and plotted as a function of age. The data used to construct this function were derived from quantitative ophthalmoscopic studies of eye migration in *Xenopus*. These have shown that at the following developmental stages the average horizontal extent of the binocular field of view, as measured in the plane containing the two optic axes are: stage 58 = 20°; stage 60 = 33°; stage 62 = 55°; stage 64 = 82°; stage 66 = 100°; 2 weeks postmetamorphosis (PM) = 122°; 13 weeks PM = 138°; 1 year PM = 148°; adult (>2years PM) = 160°. The average time that elapses between these various developmental stages are: stages 58-60, 2 days; stages 60-62, 3 days; stages 62-64, 4 days; stages 64-66, 5 days.

(Taken from: M.J.Keating and S.Grant, "The critical period for experience-dependent plasticity in a system of binocular visual connections in *Xenopus laevis*: its temporal profile and relation to normal developmental requirements". European Journal of Neuroscience, (1992), Vol 4, pp 27-36.)

21

1.4. The intertectal system

1.4.1. Intertectal plasticity during development.

In *Xenopus*, the commissural system of connections described in section 1.2 is confronted with a difficult developmental problem which is also related to growth changes in the periphery (figure 1.2). Maturational changes in skull shape and size continuously alter the geometrical relationship between the two eyes. In larval life the two eyes are situated on the side of the head and so face laterally with little binocular overlap present between the two eyes. During metamorphosis the two eyes move in a nasal and dorsal direction as the skull changes shape and so the degree of binocular overlap increases. These movements continue until adulthood when the two eyes reach their final position on the top of the head (Grobstein and Comer, 1977; Grant and Keating, 1986). Consequently, the nasotemporal extent of the binocular visual field, assayed using optical techniques, increases from 30° to 162° between the onset of metamorphic climax at stage 60 and adulthood, some years after metamorphosis (Grant and Keating, 1989a).

Electrophysiological mapping experiments also demonstrate that the portion of the optic tectum which receives binocular visual input increases as the degree of binocular overlap gets larger. It has been shown that the proportion of each tectal lobe devoted to the representation of the binocular visual field increases from 11% at stage 60 to 77% in the adult (Grant and Keating, 1989a). In addition, changes in ocular geometry affect the points on each retina which are receiving matched binocular visual input. The intertectal series of connections has to accommodate for this expansion and link those changing points on each tectal lobe which receive matched binocular visual input. Electrophysiological mapping experiments have demonstrated that, between stage 60 and adulthood the ipsilateral visuotectal projection, which is a product of the intertectal system, increases in size as the binocular visual field and its tectal representation enlarges. Moreover, throughout this period, the ipsilateral visuotectal projection maintains its spatial registration with the contralateral visuotectal projection from the other eye. These data suggest that during the course of normal maturation the intertectal system undergoes a process of expansion and ordered remodelling of its synaptic connections.

The normal maturation of the intertectal system in *Xenopus* has been shown by electrophysiological mapping experiments to rely upon visual experience (Keating, 1974; Feldman, 1975; Keating and Feldman, 1975; Keating, 1981). Animals were

placed into total darkness before the onset of visual function in the intertectal pathway until terminal electrophysiological experiments were performed. It was shown that visual deprivation did not affect the developmental ocular migration that normally occurs in *Xenopus* (Grant and Keating, 1989b), nor did it affect the normal maturation of the contralateral visuotectal projection (Grant *et al.*, 1986; Keating *et al.*, 1986). However, abnormalities were observed in the ipsilateral visuotectal projection. Following short periods of dark-rearing the spatial registration of the binocular visual inputs was fairly precise, even though there were no visual cues available during the initial construction of the projection (Grant and Keating, 1989b). But later in development, following longer periods of visual deprivation, the order in this projection and its registration with the contralateral visuotectal projection deteriorated. Quantitative analysis of the degree of spatial registration of the ipsilateral visuotectal projection revealed that it was considerably poorer and was systematically shifted, compared to the pattern of connections observed in normal controls (Grant and Keating, 1989b). Also, ipsilateral multi-unit receptive fields in dark-reared animals were considerably larger than in normal animals (Keating and Kennard, 1987). This evidence suggests that, in *Xenopus*, the initial elaboration of the intertectal series of connections is intrinsically derived but later modifications, in response to changing eye positions, require visual experience.
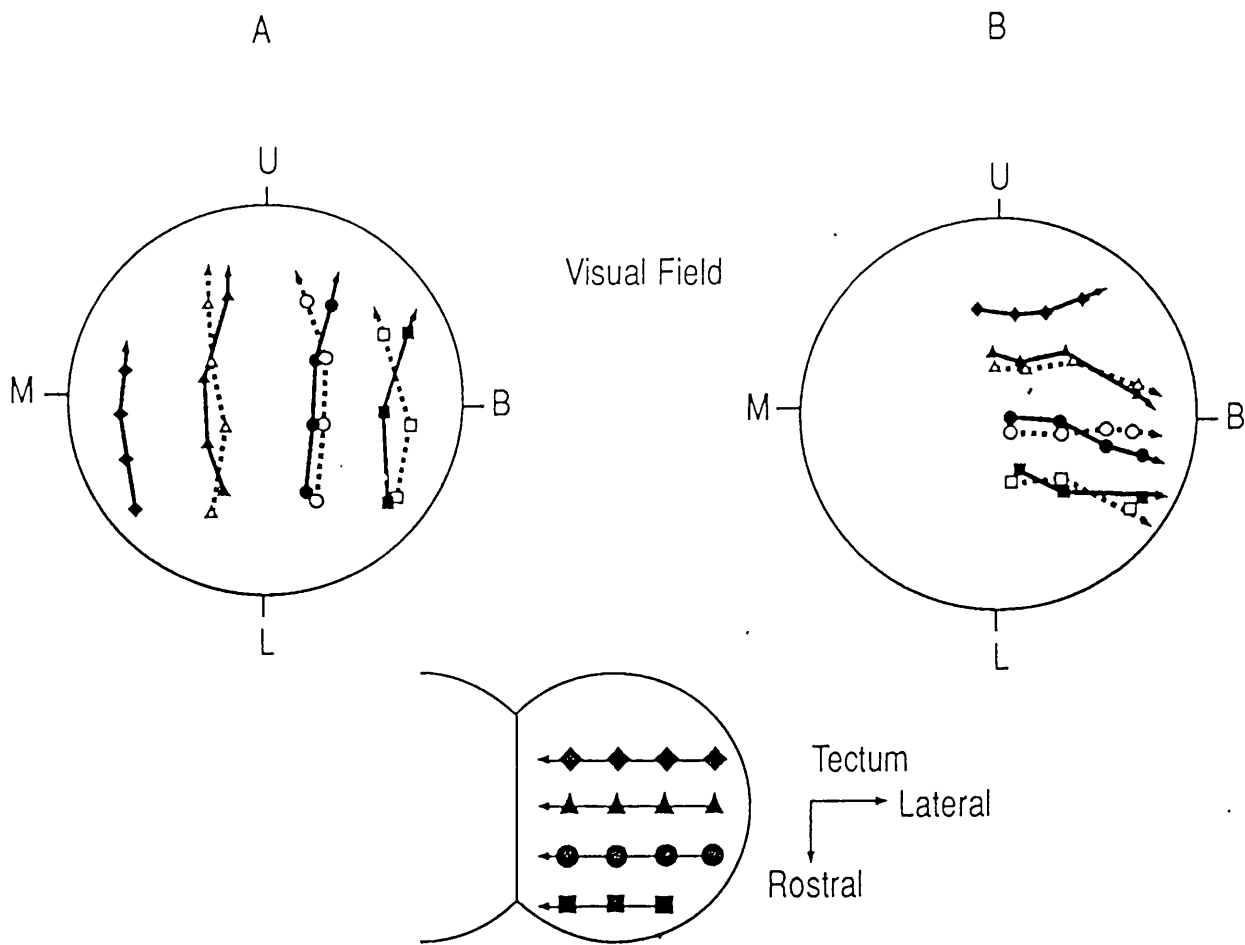
Figure 1.3. The effect of a single eye rotation on the electrophysiologically derived contralateral and ipsilateral tectal maps of visual space after 1 year of visual experience.

The diagram of the optic tecta shows the outlines, transposed from a photograph of the dorsal surface, upon which a 100μm grid was superimposed. Rostral and lateral directions are indicated by the label. The symbols on the tectal diagram represent the sites of vertical microelectrode penetrations. The two large circles (A & B) denote perimetric chart representations of the visual field, with the optic axis of the right eye centred on the fixation point of the perimeter. In A the maps from the contralateral (solid lines) and ipsilateral (dotted lines) eyes are shown from a normal animal 1 year postmetamorphosis. In B the contralateral and ipsilateral maps are depicted from a 1 year postmetamorphic animal at the same age which had received a 90° rotation of its (left) eye in larval life. The indirect nature of the ipsilateral visuotectal pathway is indicated by the dotted lines and open symbols within the visual field representations. For each microelectrode penetration the centre of the region of visual space, stimulation of which produced unitary potentials at that electrode site, when viewed by either the contralateral (solid symbols) or ipsilateral (open symbols) eye, is indicated by the corresponding symbol on the chart representation. M, B, U and L are the monocular, binocular, upper and lower aspects of the visual field of the tested eye. Note that the two visual projections to each tectum are in full spatial register in both the normal (A) and the eye rotated animal (B).

24

1.4.2. Experimental assay for intertectal plasticity.

Further evidence that experience-dependent mechanisms contribute to the alterations which take place in the developing intertectal pathway was derived from observing the effects of experimental perturbations on this pathway. Larval animals were given a single eye rotation to rotate the visual input that is relayed directly to the opposite tectal lobe (figure 1.3). So, following a 180° eye rotation the nasal portion of the visual field no longer projects to the rostral aspect of the opposite tectal lobe but now projects to caudal tectum: similarly, the superior visual field no longer projects to the medial aspect of the opposite tectal lobe but now projects to lateral tectum. Electrophysiological mapping of binocular visual inputs one year after a single eye rotation demonstrated that the ipsilateral map of binocular visual space, mediated by the intertectal pathway, alters the pattern of its connections so that it acquires alignment with the rotated contralateral map (Gaze *et al.*, 1970) but that this synaptic plasticity fails to occur if the animals are dark-reared after the operation (Keating and Feldman, 1975). However, the experience-dependent synaptic modifications which take place in the intertectal pathway do not occur immediately. In accordance with earlier conclusions, about the importance of intrinsic mechanisms in the initial elaboration of this pathway, the orientation of the earliest ipsilateral visuotectal projections were found to be normal. The visual input from the ipsilateral eye is initially out of register with that recorded through the rotated, contralateral eye. Modifications in the intertectal system were not seen until several weeks after metamorphosis (Grant and Keating, 1992). Electrophysiological mapping experiments described in Chapter 3 investigated whether intertectal plasticity could also take place following a double eye rotation in larval life.

The capacity of the intertectal system to adapt to a single eye rotation reduces with age. In the extensive study of Keating and Grant (1992) one eye was rotated to different degrees (from 20° to 180°) in 238 animals of various developmental stages (from mid-larval to adult life) and the intertectal pattern of connections was electrophysiologically mapped 1-2 years post-operatively. It was found that in animals which received a single eye rotation up to 2 weeks before metamorphosis the intertectal system completely modified its pattern of connections in response to any size of eye rotation. However, no animal exhibited this intertectal plasticity in response to even the smallest eye rotation if the operation was performed at 3 months postmetamorphosis or older. At intervening ages, altered intertectal connections were found only in response to progressively smaller eye rotations (figure 1.4). Therefore,

a "critical period" was defined around the time of metamorphosis at which intertectal plasticity would occur. Moreover, the temporal profile of this critical period was shown to correlate with the changes in eye position which normally occur in *Xenopus* as a consequence of growth. So, the capacity for intertectal plasticity is greatest at that stage in development when growth related changes in eye position are at their most drastic (figure 1.2).
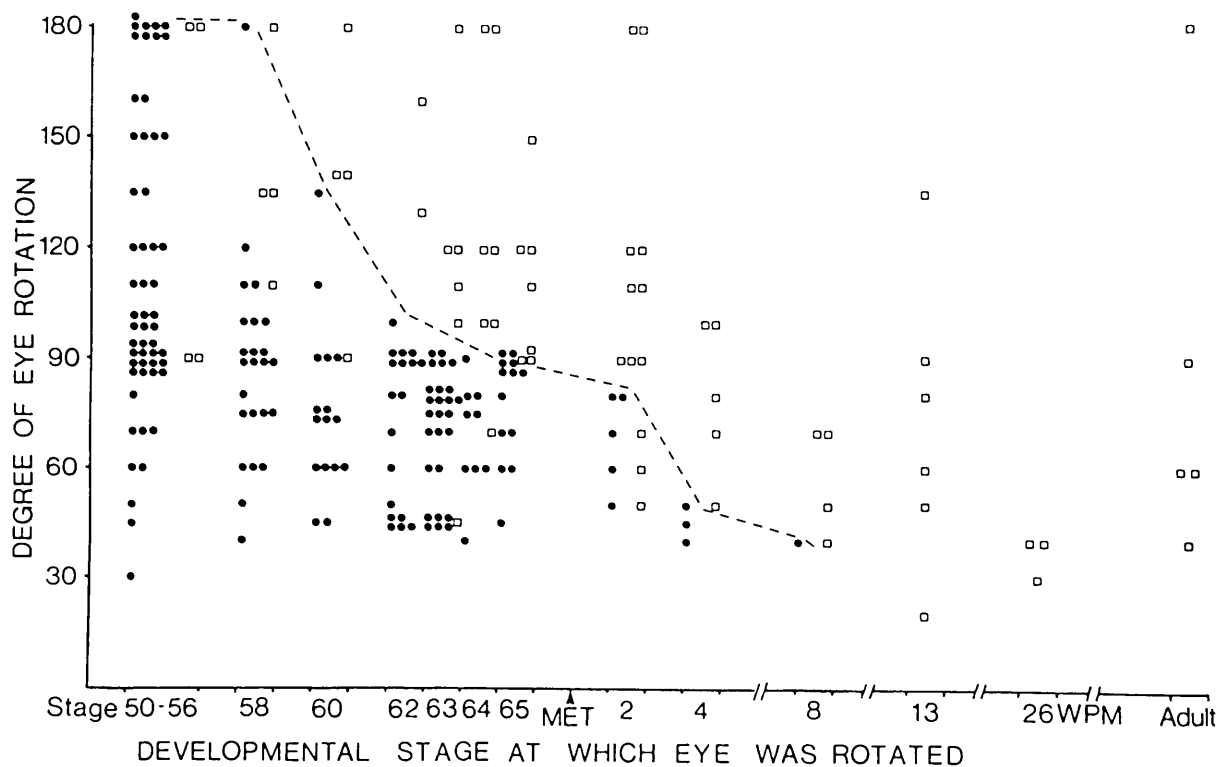
Figure 1.4. The age-dependent response of the intertectal system to eye rotations of different sizes.

The abscissa shows the age at which the eye rotation was given. The ordinate shows the size of the eye rotation present at terminal mapping. Each symbol depicts the result obtained from one animal; filled circles, animal showing "binocular interaction", indicative of a reorganized intertectal system; open squares, animals showing "non-interaction", indicating no change in the intertectal system. The dotted line shows the transition point between the two results obtained from groups of animals at the same age. (Taken from: M.J.Keating and S.Grant, "The critical period for experience-dependent plasticity in a system of binocular visual connections in *Xenopus laevis*: its temporal profile and relation to normal developmental requirements." European Journal of Neuroscience, (1992), Vol 4, pp 27-36.

1.4.3. Morphological correlates of intertectal plasticity.

Horseradish peroxidase (HRP) labelling studies have shown that the alterations demonstrated electrophysiologically in the intertectal series of connections take place in the crossed projection from the NI to the tectal lobe (Udin and Keating, 1981; Udin, 1983). This crossed isthmotectal projection is the final part of the relay which is responsible for the dual representation of binocular visual space on each tectal lobe (see figure 1.1). Following HRP injection into the NI it was shown that HRP labelled crossed isthmotectal fibres follow abnormal trajectories in eye rotated animals (Udin, 1983). Tracing of individual axons in flat-mounted, unsectioned tecta (Udin and Keating, 1981) demonstrated that crossed isthmotectal axons in normal *Xenopus* follow a route which is approximately rostrocaudal, with neighbouring axons exhibiting a tendency to run parallel with one another. Analysis of crossed isthmotectal axon trajectories in eye rotated *Xenopus* suggest that these axons reach their new locations after passing through their normal locations. The axons now cross one another and run in medial and lateral directions as well as the normal rostrocaudal polarity. It has been postulated that terminal arbors travel first to normal unrotated locations and then follow a circuitous route to the newly appropriate tectal location. Data in Chapter 3 demonstrates that, under certain conditions, these earlier termination sites can also be identified electrophysiologically.

It is more difficult to demonstrate anatomically that ordered shifts in the crossed isthmotectal projection occur during normal development. However, Udin and Fisher (1985) demonstrated that at stage 60, when binocular overlap is limited to 11% of the tectal neuropil, dense terminal arbors of crossed isthmotectal fibres were only present in the rostral portion of the tectum where this limited binocular overlap is represented. Such dense terminal arbors were found at progressively more caudal tectal locations as the tectal area responsible for the representation of the binocular visual field increased (Udin, 1989). However, many of the axons have branches growing away from the main arbor into monocular tectal areas, while others branch extensively over the tectum and have no obvious dense terminal arbor. Udin *et al.* (1992) demonstrated, following analysis of HRP impregnation at the electron microscope level, that crossed isthmotectal axons do make synapses in monocular tectal regions. Extending earlier work by Udin, Fisher and Norden (1990) in adult Xenopus, they also demonstrated that the vast majority of crossed isthmotectal synapses in young animals, including those located ectopically in caudal tectum were located on the dendrites of tectal neurons rather than a pre-synaptic profile. ?

Therefore, it appears that the majority of crossed isthmotectal synaptic connections are made with the dendrites of tectal neurons, but the distribution of these connections changes with development.

1.4.4. The lack of intertectal plasticity in other anuran amphibia.

Not all anurans are capable of the synaptic plasticity which has been described in the binocular visual system of *Xenopus laevis*. Dark-rearing did not affect the normal degree of spatial alignment between the two visual projections to the tectum in the frog *Rana pipiens* although multi-unit receptive fields (MURFs) recorded through the ipsilateral eye were enlarged (Jacobson, 1971). This suggests, the frog *Rana pipiens* is also not able to adapt its series of intertectal connections to a monocular eye rotation apportioned in early larval life even, after over 200 days of normal visual experience. (Jacobson and Hirsch, 1973). However, it is now known that *Rana* does not face the same developmental obstacles that *Xenopus* is confronted with. Throughout its pre- and postmetamorphic development the changing ocular geometry experienced by *Xenopus* necessitates systematic alterations in the alignment of its binocular tectal maps. In *Rana*, these changes in relative eye positions are much smaller (Grobstein and Comer, 1977) and, hence, the requirement for intertectal plasticity is considerably reduced. Kennard and Keating (1985) demonstrated that a genuine species difference did exist between *Xenopus* and *Rana*, in the capacity of this system to respond to early eye rotation and postulated that the manifestation of intertectal plasticity in *Xenopus* was related to the larger changes in eye position which occur during development. In another species of anuran, the Australian green and golden tree frog (*Hyla moorei*), the eyes also maintain their relative positions from metamorphic climax onwards. *Hyla* also resembles *Rana* in not adjusting its intertectal connections in response to early eye rotation (Beazley, 1979).

1.5. "Hebb" synapses and synaptic plasticity.

In 1949, D.O. Hebb proposed a specific mechanism for producing functional change at developing synapses suggesting that:

"When an axon of cell A is near enough to excite a cell B and repeatedly or persistently takes part in firing it, some growth process or metabolic change takes place in one or both cells such that A's efficiency, as one of the cells firing B, is increased."

(Hebb, D.O., 1949)

The Hebbian synapse rule postulates, with little experimental evidence to support it, that synaptic stability improves when there is temporal correlation of firing between pre- and postsynaptic elements. This rule, in its elementary form, does not explain many forms of activity-dependent synaptic plasticity in the CNS. For example, Carew *et al.* (1984) have demonstrated that firing of the postsynaptic neuron is not required in the synaptic plasticity which underlies conditioning in *Aplysia*. This form of activity-dependent synaptic plasticity only requires that the neural activity in the presynaptic cell be paired with a facilitatory input. Similar modification of the Hebbian synapse rule may make it applicable to the consolidation of appropriate retinotectal and isthmotectal inputs onto common tectal dendrites. The activity-dependent synaptic plasticity which is exhibited in the experimentally manipulated retinotectal projection may only require that the spontaneous neural activity of neighbouring RGCs be sufficiently correlated for synaptic stabilisation to occur. In the intertectal system it would require that the presynaptic neural activity arriving through the retinotectal and crossed isthmotectal projections be sufficiently correlated before synaptic stabilization would occur.

1.6. The coicidence detection hypothesis and intertectal plasticity

We know that intertectal synaptic plasticity accommodates the binocular visual system of *Xenopus laevis* to drastic changes in eye position. The plasticity is orchestrated by visual experience and is restricted to a critical period of development when eye positional changes are occurring. Moreover, the phenomenon has been demonstrated to involve actual anatomical shifts in the spatial location of crossed isthmotectal terminal arbors. The coincidence detection hypothesis, as suggested by Keating (1968), could explain the modifications which take place in the intertectal system following normal changes in eye position and following experimentally induced alterations in ocular geometry.

The hypothesis states:

"..connections are formed, not by the action of the innate mechanism of neuronal specificity but by a functional interaction between the two eyes. Those positions on the two tecta that are simultaneously receiving a similar spatiotemporal pattern of impulses through the two eyes from a stimulus at one position in the binocular visual field, become neuronally linked together."

(Gaze, Keating, Székely and Beazley, 1970).

Or, in brief this adaptation of the Hebbian rule states that **connections that fire together, wire together.** It is currently supposed that those positions on each tectal lobe which receive their direct contralateral input from positions of retinal correspondence will exhibit correlated firing patterns (see Chapter 4 for a demonstration of this phenomenon). The ability to recognise this coincident neural activity is thought to enable systematic changes in the anatomy of this system to occur. As the eyes change position so those neural elements which receive matched binocular visual input and, therefore exhibit correlated firing, would alter. The capacity to link changing positions on each tectal lobe which exhibit coincident neural activity would enable intertectal plasticity to occur. This hypothesis is supported by dark-rearing, a procedure which completely removes correlated firing between matched binocular inputs. In the absence of all visual cues intertectal synaptic plasticity does not take place. Experiments were undertaken to further test the validity of the coincidence detection hypothesis (Chapter 4) with relation to intertectal plasticity. Stroboscopic illumination was used to subvert the correlated patterns of neural activity which occur during binocular visual stimulation. Following each strobe flash all points in the visual field and, therefore, all points across the retina should be simultaneously activated. If this is the case, then strobe-rearing should make the process of coincidence detection impossible for the binocular visual system and obstruct intertectal plasticity. However, this procedure could also interfere with activity-dependent synaptic plasticity in the developing retinotectal projection and so the order of this pathway was also monitored following strobe-rearing.

NMDA receptor
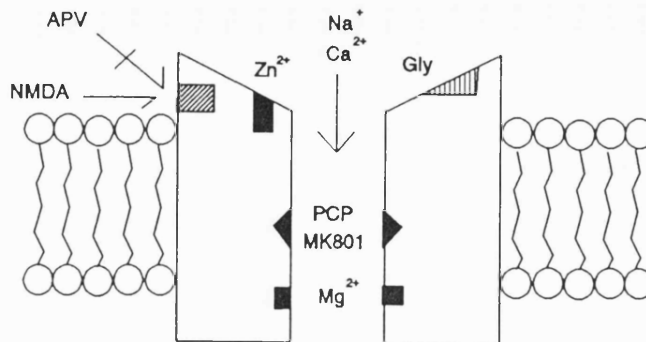
AMPA receptor
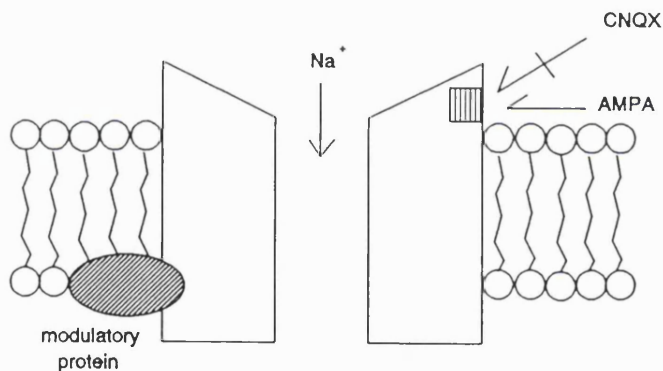
Figure 1.5. The NMDA and non-NMDA type glutamate receptor complexes.

Diagrammatic representations of the NMDA and AMPA (or non-NMDA)-type glutamate postsynaptic receptors. Both types are ligand gated ion channels whose endogenous agonist is L-glutamate; the major excitatory neurotransmitter in the vertebrate CNS. The NMDA receptor comprises an agonist binding site which is blocked by specific antagonists (eg. AP5 & CPP), modulatory sites for glycine and zinc, and an ion channel permeable to Na^+ and Ca^{2+} which is blocked by Mg^{2+} and specific antagonists (eg. PCP & MK801). However, the binding of the agonist to the receptor binding site at normal resting membrane potential will not result in an agonist induced opening of the associated ion channel. Only when the membrane is sufficiently depolarised, resulting in Mg^{2+} block removal, will agonist binding induce ion channel opening. The non-NMDA receptor consiste of an agonist binding site (AMPA) which is blocked by specific antagonists (eg. CNQX & DNQX). At normal resting membrane potentials agonist induced opening of the ion channel will occur allowing Na^+ to depolarise the cell.

32

1.7. The NMDA receptor: a molecular coincidence detector?

What is now needed to complete a mechanistic description of changes in synaptic connectivity is a molecular coincidence detector which is able to respond, given adequate depolarization at the target dendrites, to the degree of temporal correlation exhibited in the neural activity of convergent afferent inputs. There are theoretical reasons for believing that the N-methyl-D-aspartate (NMDA)-type glutamate receptor fulfils these requirements (figure 1.5). The ion channel associated with the NMDA receptor is blocked by magnesium ions when the local membrane is at resting potential, but when excitatory input is sufficient, the resulting depolarisation expels the magnesium ion block and permits the opening of the ion channel (Mayer *et al.*, 1984; Nowak *et al.*, 1984). The NMDA receptor channel has slow kinetics (Stern *et al.*, 1992; Lester *et al.*, 1990) and high Ca^{2+} permeability (Ascher and Nowak, 1988). Therefore, opening of the NMDA receptors ion channel allows Ca^{2+} to flow into the postsynaptic cell, and it is this chemical signal which is proposed to trigger a variety of biochemical cascades which stabilize connections between pre- and postsynaptic elements. In contrast, the non-NMDA-type glutamate receptor channel can be opened at resting membrane potentials and has fast kinetics (Trussel and Fischbach, 1989; Jonas and Sakmann, 1992; Colquhoun *et al.*, 1992) and low Ca^{2+} permeability (Iino *et al.*, 1990).

These theoretical considerations have led to the suggestion that the NMDA receptor could mediate both retinotectal and intertectal synaptic plasticity. In the case of the retinotectal projection, sufficient excitatory input to activate the NMDA receptor would only be achieved once the spontaneous firing patterns of RGCs was sufficiently correlated. Thus, neighbouring RGCs which exhibit correlated spontaneous firing would be selectively stabilized onto common tectal neurons. In the case of intertectal plasticity, it may be that sufficient excitatory input to activate the NMDA receptor is only achieved once the neural activity derived from binocularly convergent inputs is correlated. This situation would only occur when the information arriving through the retinotectal and crossed isthmotectal inputs onto common tectal dendrites was temporally coincident. Thus, in intertectal synaptic plasticity only binocularly convergent retinotectal and isthmotectal inputs onto common tectal neurons would be stabilized due to their correlated patterns of evoked neural activity, whereas other isthmotectal inputs would be de-stabilized. However, in *Xenopus* arrival of visual information from the ipsilateral eye is delayed by ~20msec relative to the arrival of information from the direct retinotectal projection, this delay being

due to the polysynaptic nature of the intertectal relay. Consequently, the postsynaptic mechanism responsible for intertectal plasticity should be responsive to this delay.

What empirical reasons are there for implicating the NMDA receptor in retinotectal and intertectal synaptic plasticity? When the optic tectum of a three-eyed *Rana pipiens* was continuously perfused with the NMDA receptor antagonist D,L-2-amino-5-phosphonovaleric acid (AP5), which was slowly released from a polymer implant (Elvax), eye specific stripes were actively desegregated (Cline *et al.*, 1987). This procedure also disrupted the normal development of the retinotectal projection (Cline and Constantine-Paton, 1989). The terminal arbors of HRP impregnated RGCs were significantly larger following chronic AP5 treatment than those normally encountered in the retinotectal projection. However, similar results have been obtained when all neural activity was removed from the system by intraocular administration of TTX (Boss and Schmidt, 1982; Meyer, 1982; Reh and Constantine-Paton, 1985). The NMDA receptor has also been implicated in the synaptic modifications described in the binocular visual system of *Xenopus*. In these experiments the optic tectum of *Xenopus* was constantly perfused with AP5 from the slow releasing polymer implant and the intertectal systems ability to adapt to a single eye rotation, given at larval stage 58, was monitored (Scherer and Udin, 1989). The animals were reared, before and after the eye rotation, in a normal visual environment and electrophysiologically mapped at 3 months post metamorphosis. The binocular maps obtained from these animals showed considerable disturbance, in a manner analogous to dark-rearing, and were out of register with the retinotectal projection through the rotated eye. Therefore, activation of NMDA receptors appears to be necessary for both activity-dependent synaptic plasticity in the retinotectal projection and experience-dependent synaptic plasticity in the intertectal projection.

It is not certain whether these types of phenomenon represent interference with a specific postsynaptic mechanism concerned with synaptic stabilization or merely reflect interference with normal levels of neural activity. Although these chronic experiments implicate postsynaptic glutamate receptors in synaptic plasticity in the frog tectum there has been no direct demonstration that the receptors actually mediate any aspect of synaptic transmission in this nucleus. Indeed, it was previously believed that retinotectal synaptic transmission were mediated by the cholinergic system (Freeman *et al.*, 1980). Therefore, *in vivo* and *in vitro* preparations of the optic tectum were developed (Chapter 5 & 6) to examine the effects of postsynaptic glutamate receptor blockers on visually evoked and electrically stimulated responses in

the visual system of *Xenopus*. The major aim was to determine whether glutamate receptors mediate retinotectal synaptic transmission in *Xenopus* and whether NMDA receptors are activated by this input. The role of cholinergic and of GABA receptors in synaptic transmission within the tectum was also evaluated. A late polysynaptic component of the response evoked by electrical stimulation of the retinal inputs *in vitro* was shown to be depressed by AP5. This observation formed the basis of further experiments designed to investigate whether this NMDA receptor mediated component of tectal synaptic transmission is regulated by age, visual experience or by species, in accordance with the requirements for the mechanism underlying intertectal plasticity in *Xenopus* (Chapter 7). Finally a slice preparation of the *Xenopus* optic tectum was developed from which tight-seal whole cell current and voltage clamped recordings could be made, using a similar methodology to that of Edwards *et al.*, (1989). The purpose of these experiments was to gain insight into the classes of tectal neuron that possess NMDA and non-NMDA receptors, by combining intracellular dye-injection and intracellular recording (Chapter 8).

Chapter 2

Materials and methods

2.1. Animals and rearing conditions

2.1.1. Normal animals.

Two species of frog were used in this study. Most of the experiments involved
Xenopus laevis, the aquatic South African clawed toed frog, which were bred from
stocks maintained at the National Institute for Medical Research. Amplexus was
induced by injecting female *Xenopus* with 400 *i.u.* of human chorionic gonadotrophin
into the dorsal lymph sac, and males similarly with 200 *i.u.*. Embryos and larval
animals were placed in batches of 10-15, in large tanks containing 5-7 litres of aerated
tap water supplemented with iodine, maintained at 24°C. This solution was changed
every 10 days. Larval animals were fed 3 times weekly on a Complan diet. Once
regression of the tail had begun animals were transferred in groups of 2-5 into perspex
boxes (22.5 x 12.0 x 7.5cm), containing tap water which was changed every week.
Normal animals were reared in diurnal light/dark conditions and fed twice a day on
tubifex worms. The other frog was *Rana pipiens*, which were supplied from an
outside breeding colony (Blades Biological) when aged approximately one year post-
metamorphosis.

2.1.2. Developmental staging.

Larval and metamorphic *Xenopus* were staged according to standard criteria of
external morphology (Nieuwkoop and Faber, 1967). In *Xenopus*, metamorphosis
begins at stage 49 and is complete by stage 66 but significant changes in skull shape,
heralding the transition from tadpole to frog, do not occur until stage 60. In this
study the term "late larval" has been used to denote stages 55 to 59, "metamorphic
climax" to cover stages 60-66, "early juvenile" to describe animals aged 1-13 weeks
post-metamorphosis and "late juvenile" for those aged 6-12 months post-
metamorphosis. The term "adult" was only applied to sexually mature animals aged 2
or more years post-metamorphosis. The estimation of age for *Rana pipiens* was
purely based upon body size, because exact birth-dates and time of metamorphosis
were not available from the supplier.

2.1.3. Dark-reared animals.

A number of larvae were transferred at stage 57-58 of development, before functional binocular connections are established (Beazley et al., 1972), into light-tight cupboards and reared in total darkness until the terminal recording experiment. Groups of 2-5 animals were placed in separate perspex containers (22.5 x 12.0 x 7cm) whose sides were covered with black opaque plastic. The feeding and water changing regime was identical to the visually experienced animals. The feeding and water changing period did result in exposure to a 1 minute period of very dim red safe light (Patersons). Animals were anaesthetized with i.p. injections of 12-15mg of Tricaine-methanesulphonate (MS222) before transfer to the laboratory in a light-tight box.

2.1.4. Strobe-reared animals.

Late larval animals were reared for one year in constant stroboscopic illumination until they were electrophysiologically mapped. Throughout this period the strobe flash duration was maintained at 10μsec, with a constant frequency of either 1Hz or 0.2Hz. The strobe rearing conditions were optimised so that the minimum of contrast information was presented to the animal during each strobe flash. Individual animals were placed in separate perspex containers (22.5cm x 11.5cm x 7cm) whose sides were covered with black opaque plastic so that the strobe flash could only enter the box from above. The boxes were placed inside a light-proofed cupboard which housed the strobe unit (Dawe Instruments Limited). The inside walls of the cupboard were also blacked out so that a minimum of contrast information was produced during each strobe flash. The animals were fed and their water replaced twice a week. This procedure was performed in a dark room under minimal lighting. This feeding and cleaning regime meant that each animal was removed from stroboscopic illumination for an average of ~5 minutes per week but during this period a very dim red safe light was used. Before electrophysiological mapping the animals were anaesthetized and transferred in a light proof box to the laboratory.

2.1.5. Eye-rotated animals.

Eye rotations were administered between stages 55 and 58 of larval development (Nieuwkoop and Faber, 1967). Animals were anaesthetized in an aqueous solution (1:12000) of MS222. Dissecting needles and watchmakers forceps were used to separate the periocular tissue from its investment of the globe. The eye was rotated about its optic axis and held in its new position for a few minutes whilst

the periocular tissue adhered to it. The animals were permitted to recover and survive for at least one year post-metamorphosis. In most cases the eye had de-rotated after the operation so that the final rotation was less than the original 90° or 180°. The final degree of the eye rotation was calculated from two parameters; the position of the iridial notch and the orientation of the electrophysiologically derived contralateral visuotectal projection.
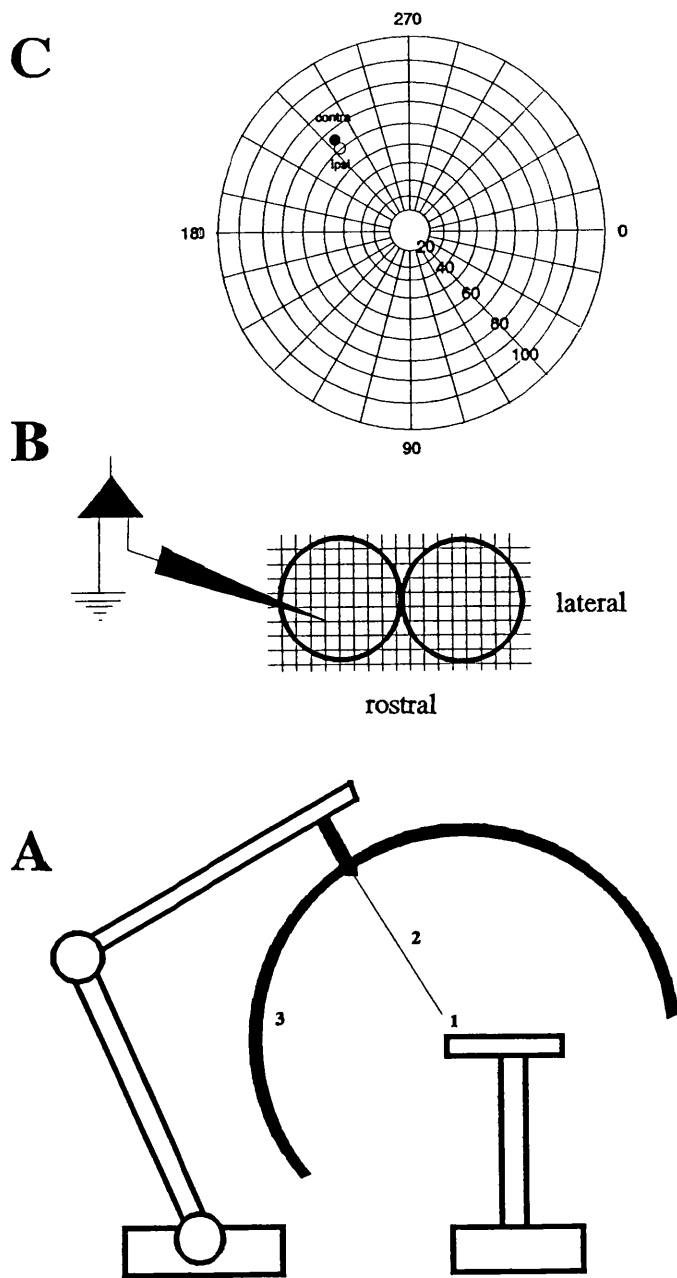
Figure 2.1 A,B & C. Electrophysiological mapping of topographic representations of visual space in the frog optic tectum.

A, the animal is placed at the centre of an Air-mark perimeter (1). The optic axis of one eye is aligned with the centre of the arc (2). Visual stimuli can be presented on the perimeter arc (3) at any position in the animals visual field.

B, The optic tectum is exposed and photographed (x50). A 1cm grid is superimposed onto the photograph so that accurate placement of the electrode at specified tectal locations can be achieved.

C, The position in visual space at which neural activity is elicited at a specified tectal location through the eye contralateral (filled circle) or ipsilateral (open circle) is marked on a perimeter card. A polar co-ordinate system is used to record the radial and circumferential position of the receptive field centres with respect to the origin of the perimeter and the optic axis of the aligned eye.

2.2. Electrophysiological mapping of binocular visual space.

2.2.1. Preparation of animals.

These experiments were performed on *Xenopus*, aged between 1 and 3 years post-metamorphosis. The animal was anaesthetized with i.p. injections of 12-15mg MS222 and the skull opened with a dental drill. The meninges covering the surface of the tectal lobes were removed and the tecta covered with mineral oil to prevent dryness. The tecta were photographed at a magnification of x50 and a 1cm rectangular grid superimposed on the photograph (figure 2.1). The intricate melanophore pattern present on each tectal lobe facilitated the placement of recording electrodes at specified surface locations and the re-establishment of those positions later in an experiment.

2.2.2. Recording methods.

The animal was placed in the centre of an Aimark projection perimeter (Mark IV, U.K. Optical Bausch & Lomb Ltd.) of radius 33cm, with one eye centred on the fixation point of the perimeter arc. The perimeter could be tilted to accommodate for the optic axis of *Xenopus* which looks upwards and outwards. The recording microelectrodes were tungsten-in-glass tipped with platinum with a tip diameter of 2-5μm and an impedence of 0.5-2MΩ. The tip of the microelectrode was placed on positions corresponding to the intersections of the grid on the tectal photograph. Visually elicited signals were A.C. coupled and amplified by X1000 (Neurolog A.C. Preamp NL103, A.C. Amp NL105) before being monitored both on an oscilloscope and through an audio amp. Window discriminators (Digitimer D130) were used to time the arrival of individual action potentials at the tectal recording locations.

2.2.3. Mapping procedure.

The topographic organization of contralateral and ipsilateral visuotectal projections was assessed electrophysiologically. Visual stimuli were black discs subtending 5° of visual angle presented against a uniform background, the mean luminance of which varied between 0.5 and 4.5 x 10^3 candela/m^2. For each tectal recording position the optimal position within the visual field was determined at which a stimulus elicited robust unitary activity at the microelectrode. The position in space of each receptive field was recorded on a polar co-ordinate card for future analysis. When the visual field through one eye was being mapped, the other eye was covered

with an opaque shield. In most animals a total of four visuotectal projections were mapped (see figure 3.1) corresponding to the two separate projections of visual space present on each tectal lobe. First, the ipsilateral eye was covered and the position of visual receptive fields were recorded at specified tectal locations through the direct retinotectal projection. Then, the position of visual receptive fields resulting from the ipsilateral visuotectal projection was mapped with the contralateral eye covered. So, two visuotectal projections were mapped onto each tectal lobe, with accurate re-establishment of recording position effected if required, using the photograph of the optic tectum.

2.2.4. Analysis of topographic order in the visuotectal maps.

Each visuotectal projection from a given eye consists of a collection of receptive field centres determined by the above method. The topographic order of the projection was assessed by analyzing whether each visual field position within the projection was appropriately located with respect to its neighbours recorded from the adjacent tectal location. Therefore, the order of the projection in experimental animals was compared to that expected from normal animals.

2.2.5. Analysis of spatial registration between binocular inputs.

The degree of spatial registration between binocular maps, recorded from normal, eye rotated and strobe-reared animals, was analyzed by calculating the absolute disparity between the receptive field centres of the responses recorded through the contralateral and ipsilateral eyes. The location of each receptive field centre is recorded on a perimeter card in terms of radial (R) and circumferential (C) positions in visual space. The absolute disparity value for the binocular inputs was then calculated by a two stage process:

1. The polar plot co-ordinates (R and C) recorded on the perimeter card are converted into Cartesian co-ordinates (x and y), where;

$$x = R(\cos C)$$
$$y = R(\sin C)$$

2. The absolute disparity (D) was then calculated between these two points, where;

$$D = SQRT\ [(x_1-x_2)^2+(y_1-y_2)^2]$$

According to this method, if the two receptive field centres occupied exactly the same position in visual space their absolute disparity would be zero degrees. The larger the absolute disparity between the position of these receptive field centres the greater the mis-alignment between the two binocular inputs to each tectal p[osition. For example, if the receptive field centres of two inputs are such that; for position 1, R = 75° & C = 230°; and, for position 2, R = 70° & C = 230°. The absolute disparity values is 5.1°.

Mann-Whitney non-parametric un-paired statistics were employed to establish levels of significance between the average absolute disparity values obtained from normal and experimental animals.

2.3. Effects of stroboscopic illumination.

2.3.1. Monitoring the acute effects of stroboscopic illumination on correlated firing patterns in the tectum.

To examine the effects of exposure to stroboscopic illumination, two tungsten-in-glass recording electrodes were used to simultaneously monitor the multi-unit neuronal activity evoked at two disparate tectal locations during stimulation with the strobe flash. First, multi-unit receptive fields (MURFs) of the contralateral eye were identified for each of the tectal recording positions, on the same or opposite tectal lobes. For a recording to be characterized as a multi-unit we required that it be constituted of at least three different spikes as revealed by difference in spike height and shape. The full extent of each MURF was marked on the perimeter card so that the area of visual space in which a robust unitary response was elicited in the tectal neuropil was established. A 5° black disk moving across the perimeter arc was used to elicit this activity. The perimeter arc was the only source of illumination, maximum 4.5×10^3 cdm^{-2}, and so the opaque disc had a degree of contrast with the perimeter. The MURFs were classified according to their response properties to moving black stimuli, to spots of light and to changes in background illumination (Maturana *et al.*, 1960). "Sustained" units respond with a prolonged burst of activity when an object is moving into their receptive field and held stationary there. "Event" units respond to both the ON and OFF of background illumination and to moving stimuli. "Dimmer" units respond with discreet bursts of activity to each decrement in background illumination, the response becoming more vigorous when darkness is approached. These units form a laminar distribution in the superficial neuropil (layers 8 and 9) of the tectum with sustained units at the surface and

dimmer units deepest in the tectum (Keating *et al.*, 1986).

The tectal recording positions were adjusted so that the two MURFs were either partially overlapping or completely non-overlapping in visual space. Once the MURFs had been fully classified in terms of size, unit-type and position in visual space 30 minutes of spontaneous activity was recorded from them in the dark. The response of the two MURFs to constant stroboscopic illumination was then recorded for a two hour period. The strobe flash unit (Strobotorch, Type 1222A, Dawe Instruments) was placed 30cm from the animal either in line with both overlapping receptive fields or approximately equidistant between the two non-overlapping receptive fields. The strobe flash duration (10μsec) and rate (either 0.2Hz or 1Hz) were set to that of the stroboscopic rearing conditions. At intervals during the experiment the response of the two MURFs, to the black disk moving through the receptive field during stroboscopic illumination, was evaluated. The electrical signals were conventionally amplified, and the spikes processed through separate channels adjusted to discriminate signals 100% above the noise-level. The time of this spike activity in relation to the strobe flash was recorded using a CED 1401 laboratory interface on which on-line analysis could be carried out.

2.3.2. Analysis of acute strobe data.

Event data was recorded at two tectal locations during the entire course of the experiment. The raw timing data was depicted as "raster" plots in which the time of each individual event was recorded for the entire experiment. When a strobe frequency of 1Hz was being examined the experimental data was divided into 1 second epochs. At a strobe frequency of 0.2Hz the data was divided into 5 second epochs. The "raster" was examined to evaluate any change in the response of a MURF to constant stroboscopic illumination. This analysis would reveal whether the MURFs response to the strobe flash always occurs at the same latency poststimulus. The number of events which occur following each strobe flash were also calculated to assess changes in the firing rate during an experiment.

Cross correlations (CCs) were constructed between the event data recorded at both tectal locations. One event channel was considered to be the "stimulus" and the other event channel the "response". For each event in the stimulus channel the times at which events occurred in the response channel, during the 1 second before and after it, were calculated with the response data seperated into 10msec bins. An average CC was computed from all events which occurred during a 20 second period, at 15 minute intervals during the entire experiment. Those events which are coincident (*ie* occur at

0 seconds) in the CC were used to estimate the degree of correlation. Any increase in this value, during stroboscopic illumination, would indicate an improvement in the degree of correlation between the firing patterns recorded at the two tectal sites.

2.3.3. Analysing the effects of strobe-rearing on the development of the retinotectal projection.

Three aspects of the topographic rpecision were were assessed electrophysiologically in the retinotectal proejction of strobe-reared animals:

(i)   The overall topographic order of the projection. This was assayed by mapping the contralateral visuotectal projection with standard electrophysiological techniques (Section 2.2.3) and establishing whether the receptive field centres recorded at neighbouring tectal locations were correct or incorrect (section 2.2.4).

(ii)   The depth distribution of terminals from different classes of RGCs. MURFs recorded at different depths in the superficial tectal neuropil were classified as either sustained, event or dimmer type-units (see section 2.3.1). The distribution of these different unit-types within the tectal neuropil of strobe-reared animals was compared to that previously observed in normal animals.

(iii)   MURF size. The size of "event" MURFs were plotted quantitatively using computer control of the visual stimulus and analysis of the acquired spike data. Visual stimuli consisted of square dark stimuli moved systematically, under computer control, across a large television screen. The screen was situated 38cm from the animal's eye so that the effective stimulus area of the screen was 64.5° in the naso-temporal and 34.5° in the superior-inferior axis of the field. The stimulus routinely used was a dark square of side 6° moved at a velocity of $44°s^{-1}$. The background luminance of the screen was $170cdm^{-2}$ and the contrast between the visual stimulus and the background was 0.98.

The screen was traversed systematically by the visual stimulus. Starting at one corner, the stimulus moved across the screen either vertically or horizontally in 1.5° steps. Spikes occurring during the traverse were recorded and stored on computer (CED 502 & PDP11). The computer produced a two-dimensional matrix representation of the screen, in which thein each bin field was divided into 1.5°x1.5° bins and the number of events was represented as an element in the matrix. The measurement of a MURF size involved the pooling of matrices from several traverses, involving stimulus movement in either the horizontal or vertical direction: the horizontal diameter was measured from responses to vertical stimulus directions, and the vertical diameter from responses to horizontal movements. To eliminate spurious readings due to occasional spontaneous or

artefactual spikes, the MURF size was considered to be that in which individual matrix elements were 10% or more of the maximum element size. Pseudo-three-dimensional plots of this information were generated, in which the x axis represented the nosotemporal dimension of the field, the y axis the superoinferior dimension of the field and the z axis the number of spikes evoked in response to stimulation of the corresponding 1.5°x1.5° of the visual field.

The signifance of any differences in MURF size between normal and experimental groups was estimated using Mann-Whitney non-parametric un-paired statistics.

2.3.4. Analysing the chronic effects of stroboscopic illumination on the intertectal projection.

Procedures were identical to those described in sections 2.2.4 and 2.2.5 of this chapter. The topographic order of the visuotectal projections and the degree of spatial alignment between binocular inputs were assessed in normal and strobe-reared animals.

2.4. Examining synaptic transmission in the optic tectum *in vivo*, using physiological stimuli.

2.4.1. Recording pre- and postsynaptic visually elicited activity from the optic tectum *in vivo*.

In this preparation, visually-evoked activity was recorded in both tectal lobes through the remaining eye of monocularly enucleated frogs. In each experiment, a tungsten-in-glass microelectrode was inserted at a point of approximate visual correspondence in each tectal lobe and to a depth of 100-150μm below their surface, as these locations favoured optimal responses. Recordings were always made from regions of the tectum that would normally be binocularly driven, although the exact topographic positions at which the two recordings were made varied between experiments. It is believed that activity, recorded in the tectum contralateral to the eye, emanates directly from the terminal arbors of its topographically distributed retinal axons (see chapter 3). However, visually-evoked activity recorded in the tectum ipsilateral to the eye originates from the topographically distributed terminal arbors of crossed isthmotectal axons (Udin and Keating, 1981). This activity is itself contingent upon direct retinotectal transmission through the stimulated eye, and reflects postsynaptic output from the opposite tectum (see Figure 1.1). This *in vivo* preparation exploits the postsynaptic nature of the crossed isthmotectal pathway.

2.4.2. Examining the effect of specific postsynaptic blockers on synaptic transmission.

The tectum forms the roof of the midbrain and so removal of the overlying cranium creates a natural well into which drugs can be infused and gain access to the tectal surface. To facilitate this process, the tectum of each animal was continuously superfused during the experiment with an aspirated (95% O_2/5% CO_2) physiological medium of normal frog Ringer that could be administered from one of two available reservoirs. These consisted of graduated 50ml syringes, each fitted with a stop-valve, and with a common outlet tube leading into the tectal well which was driven by a perfusion pump, set to a flow-rate of 0.2ml/min. After an initial period of control observations, drugs were added to the passive reservoir and applied to the tectum, by switching between the available solutions. Wash-out was later attempted by switching back to drug-free bathing medium.

Visually evoked responses were recorded simultaneously from the tectal lobes contralateral and ipsilateral to the one remaining eye, before, during, and after drug application. Controlled visual stimuli were delivered by a high intensity light-emitting diode (LED), that could be mounted at any position in the visual field of the remaining eye. Each stimulus was of 1 second duration and was presented every 30 seconds. Accurate timing of the onset and cessation of the stimulus was achieved by the generation of a step function from a digital to analogue converter (1401 laboratory interface) using an IBM PS/2 computer. The simultaneous recordings were conventionally amplified, and the spikes processed through separate channels adjusted to discriminate signals 50% above the noise-level. The spike activity detected by the system was recorded using a CED 1401 laboratory interface on which on-line analysis could be carried out. Post-stimulus time histograms (PSTHs) were constructed fropm this event data by counting the number of spikes occurring in each 5msec bin for a period of 1 second after stimulus onset (the ON response) and for the same period after its offset (the OFF response). The responses obtained from 20 consecutive stimulations were summed to produce the a single PSTH. The first visually evoked response was considered to be elicited when 5 or more spikes occurred in an individual time bin. This parameter was used to calculate the latency for the ON and OFF responses.

2.4.3. Analysing the effect of postsynaptic receptor antagonists *in vivo*.

Visually-evoked activity was confirmed as relatively stable at both recording sites for a minimum of 20 minutes, before any pharmacological agents were applied to the

46

tectum. The effects of these agents were then typically monitored for a similar period, before attempting to wash the drug from the tissue. The experiment was then terminated. The tectum of each animal was exposed to only one drug at one concentration. Drug effects were assessed in each experiment by comparing the PSTHs obtained before, during and after application of the antagonist. For a given perturbation the percentage change in the ON and OFF response at the contralateral and ipsilateral tectum could then be calculated. Also, the level of spontaneous activity could also be calculated by coumting the number of events which occur during a 25 second period between each visual stimuli. Any drug related change in the level of spontaneous activity could then be calculated.

A paired non-parametric two-tailed t-test was used to confirm any statistical significance in the change in the average firing rate following a given manipulation. One-way analysis of variance (ANOVA) was used to determine any statistical difference in the average firing rates between groups.
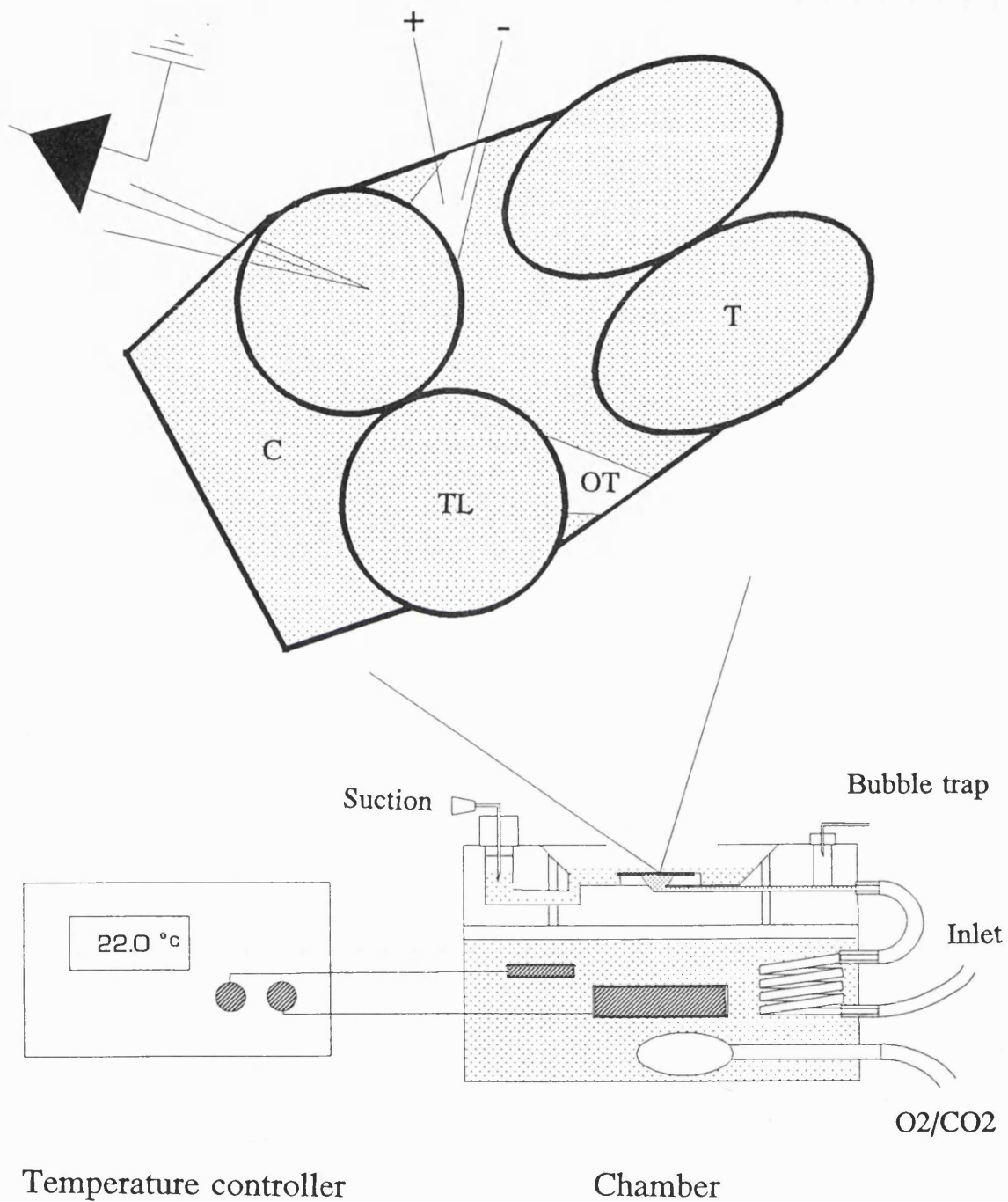
Figure 2.2. The whole mid-brain *in vitro* preparation.

The top schematic illustrates a dorsal representation of the whole brain preparation with the apparatus used to study the effect of pharmacological antagonists *in vitro*. A large portion of the frog brain (including the telencephalon **T**, the optic tract **OT**, the two tectal lobes **TL** and the cerebellum **C**) was quickly dissected out at ~1°C. This whole brain preparation was continuously perfused with oxygenated frog ringer in a perspex chamber which was maintained at 22°C. The optic tract was stimulated with a concentric stimulating electrode and an extracellular microelectrode was placed in the superficial layers of the tectal lobe.

48

2.5. Recording extracellular responses from the whole mid-brain *in vitro*.

2.5.1. Tissue preparation. ,

Animals were anaesthetized by immersion in an oxygenated solution (1:1500) of MS222. The midbrain (including the optic tecta, chiasma and caudal portion of the optic nerve) was rapidly dissected out intact into normal frog Ringer (composition in mM; NaCl 111; KCl 2.5; $CaCl_2$ 2.5; $NaHCO_3$ 17; $NaH_2PO_4.2H_2O$ 0.1; glucose 4; $MgSO_4$ 1.5; pH 7.4, 198 mosmols/mg) at approximately 1°C (see figure 2.2). The Ringer was constantly aspirated with 95% O_2/ 5% CO_2.

2.5.2. Recording methods.

The whole mid-brain preparation was transferred to the supporting nylon mesh of a perspex chamber (Scientific Systems Design) where it was maintained at 22°C. The tissue was left to equilibrate for at least one hour before any recordings were made. The total volume in the submersion chamber and the supplementing reservoir was approximately 40ml with a flow rate of 2ml/minute. The preparation was continuously superfused with an aspirated (95% O_2/5% CO_2) physiological medium of normal frog Ringer that could be administered from one of two available reservoirs. These consisted of graduated 50ml syringes, each fitted with a stop-valve, and with a common outlet tube leading into the perspex recording chamber which was driven by a perfusion pump. Drugs were bath-applied through individual superfusion lines with a common entry into the bath.

Throughout the experiment the midbrain preparation was viewed at x40 magnification with a binocular dissection microscope (Weiss). The optic tract was clearly visible due to the myelination of the RGCs which lie within it. A concentric bi-polar electrode (Clark Electromedical Instruments) was used for stimulation of the optic tract. A maximum current of 100mA was passed in the form of a rectangular pulse of 20-50μsec duration. The recording microelectrodes were made from glass pipettes filled with 2% Pontamine Sky Blue in 0.5M sodium acetate. The resistance of these electrodes, with tip diameters between 1.5 and 2μm, ranged from 1-8 MΩ. The recording electrode was placed, under visual control, in the superficial layers of the tectal neuropil. Estimation of the recording depth was made from the micromanipulator (Narishige). Conventional recordings of extracellular field potentials from the tectal neuropil were made through either a d.c. or a.c. pre-amplifier with wideband filtering between 0.1Hz and 10kHz. The signals were digitised at a sampling rate of

400μsec/sample and stored on a PC, via an analogue to digital converter (CED 1401).

2.5.3. Physiological assessment of whole midbrain viability.

The midbrain preparation was constantly viewed at x40 magnification to evaluate the degree of oedema and physical change in the gross topographic anatomy of the brain. Little change was observed in the size or physical appearance of the preparation over long periods of time (typically 4-8 hours, but in one case 24 hours). In order to assess this *in vitro* preparations physiological viability we repeated the experiments described in a previous *in vivo* study (Chung *et al.*, 1974a). Specifically, the characteristics of the waveforms were recorded at different depths below the pial surface (between 0-150μm) and we examined the effects of increased stimulus strength and paired pulse stimulation. Extracellular recordings were routinely made from this *in vitro* preparation for several hours (in one case 24 hours) with no change in the various physiological properties tested. Moreover, the extracellulr field potentials recorded from this *in vitro* were very similar to those previously reported *in vivo* (Chung *et al.*, 1974a). In all subsequent experiments we concentrated on the two most pronounced and superficial components of the evoked response which were previously classified by Chung *et al.* (1974a), as the U1 and U2 response.

2.5.4. Calculating the U1 and U2 peak amplitude and latency to peak amplitude.

All experiments involving drug application and other manipulations were carried out at a constant 150μm depth and the optic tract was stimulated 1/50 seconds. The duration of the current pulse was maintained at 20-50μsec and the current applied was varied between 0 and 100mA until the threshold for the extracellular response was determined. All subsequent recordings were made at 2x this threshold stimulus intensity. The peak amplitude of this response was calculated from the digitised traces using a computer program written specifically for the purpose (Appendix 1). Two cursers were positioned at the beginning and the end of each response and the maximum and minimum amplitudes were computed. The difference between these two values was defined as the peak amplitude of the response. The time at which the maximum negative deflection occurred between these two cursor positions was defined as the latency to peak amplitude for this response. The two cursers were also placed between a portion of the trace in which no response was present, usually during the 10 msec preceding each stimulus, to calculate the noise level in each recording.

50

2.5.5. Analysing the effect of experimental perturbations on the peak amplitude of the U1 and U2 responses.

To asses the effects of experimental perturbations a stable control response was recorded for at least 30 minutes. 10 consecutive responses obtained within the last 10 minutes of this control period were used to calculate the average peak amplitude and the average latency to peak amplitude for U1 and U2 responses. These parameters were then compared to those obtained from 10 consecutive responses, once the effect of a given perturbation had stabilised. The effect of each perturbation, including, anoxia, ion substitution, tetanic stimulation of the optic tract, and the application of specific pharmacological antagonists at known concentrations, were each assessed on a naive preparation.

Ten peak amplitudes were averaged before the manipulation and another ten once the response to the manoeuvre had stabilized. From these calculated values, and the calculated noise level of the trace, the change in the peak amplitude was derived for a given perturbation.1 The signifance of any change was then calculated using a paired non-parametric two-tailed t-test.
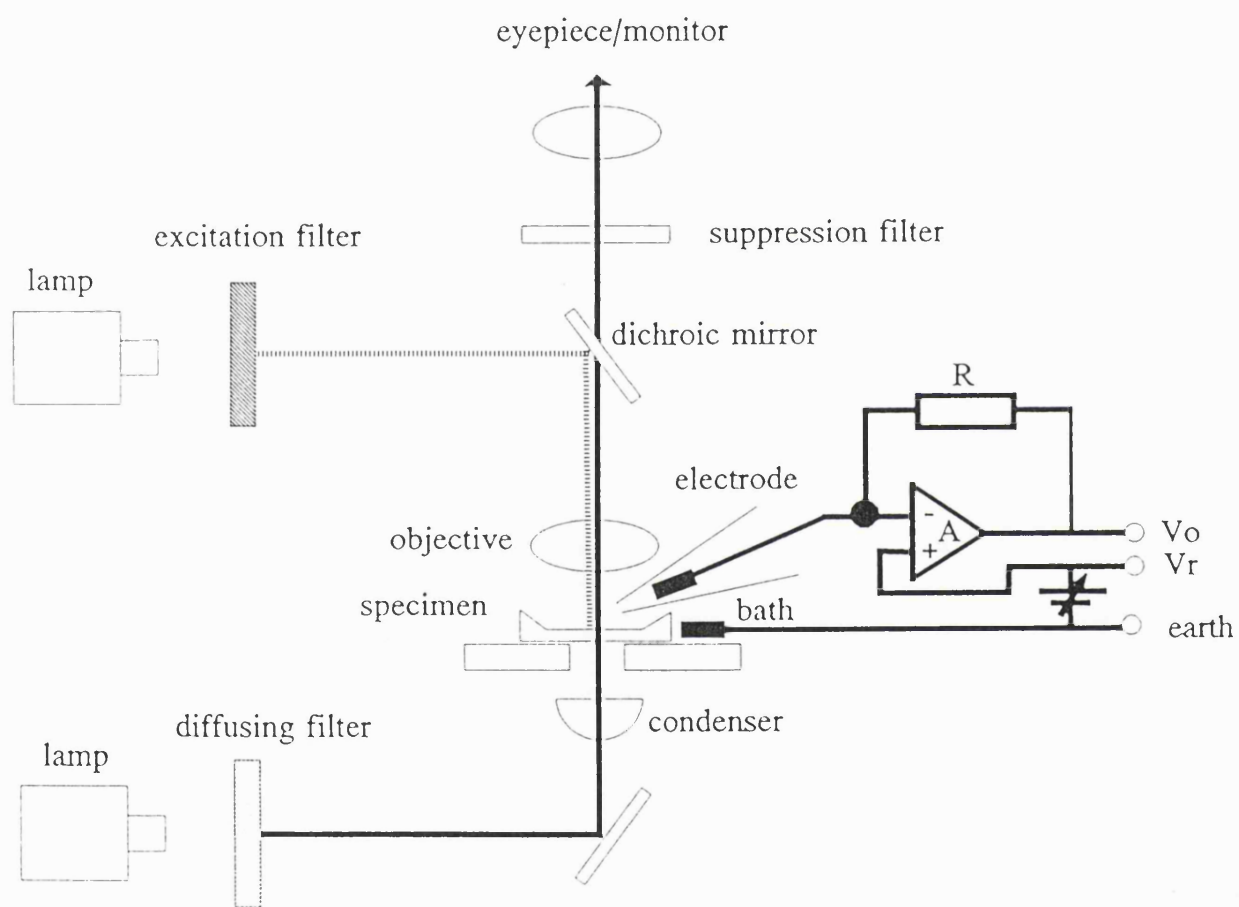
Figure 2.3. Visualisation and recording from thin slices of the optic tectum.

A schematic representation of the equipment used to visualise and make electrophysiological recordings from tectal neurones in thin slices. The specimen is maintained in a perspex holder mounted on a fixed stage microscope (Zeiss, Axioscop), Köhler illuminated and viewed with a x40 water immersion objective with Normaski optics. Cell attached and whole cell recordings were made from identified tectal neurons.

2.6. Intracellular recording from tectal slices.

2.6.1. Slicing the optic tectum.

Animals were anaesthetized by immersion in an oxygenated solution of MS222 (1:1500). The midbrain (including the optic tecta, chiasma and caudal portion of the optic nerve) was rapidly removed from the cranium in oxygenated frog ringer (composition in mM: NaCl 111; KCl 2.5; $CaCl_2$ 2.5; $NaHCO_3$ 17; $NaH_2PO_4.2H_2O$ 0.1; glucose 4; $MgSO_4$ 1.5; pH 7.4; 198 mosmols/mg) at $\sim 1°C$. Next, the brain was secured with fine insect pins and cut along the mid-line with a scalpel blade. The two bilaterally symmetrical halves were both used in the subsequent manufacture of slices. These were firmly attached onto the surface of a metal block by application of a thin layer of cyanoacrylate glue. Each half was attached to the block by its cut surface to ensure rigid support for this small piece of tissue. The block and specimen were then fully submerged in low Ca^{2+} oxygenated frog ringer (Composition in mM: NaCl 111; KCl 2.5; $CaCl_2$ 1; $NaHCO_3$ 17; $NaH_2PO_4.2H_2O$ 0.1; glucose 4; $MgSO_4$ 1.5; pH 7.4; 198 mosmols/mg) maintained at $\sim 1°C$.

Serial sagittal sections, 200μm thick, were prepared with the blade (Camden Instruments) approaching the specimen from the dorsal side. It is important that the tissue does not move as the blade cuts and that vibration, due to the oscillation of the blade, is minimised. Selection of an appropriate forward blade speed and a suitable amplitude of blade oscillation minimised this problem. An Oxford Vibratome was found to be a good sectioning instrument for this procedure. This instrument has a fixed frequency of blade oscillation ($\sim 25Hz$) with variable speed of forward blade movement and variable amplitude of vibration. The specimen was viewed under a magnifying glass throughout the slicing procedure and the speed and amplitude of the blade adjusted to ensure that the brain was not distorted during the passage of the blade.

Due to the relatively small size of the frog brain it was not possible to produce more than 6 slices from one animal. The slices were transported, in a fire polished pasteur pipette, to an incubation chamber. They were maintained at room temperature, for at least 1 hour, in normal oxygenated frog ringer (2.5mM Ca^{2+}). This whole procedure, from the induction of adequate anaesthesia to incubation of the slices, takes no longer than 30 minutes. Quick dissection of the brain into cold oxygenated physiological saline, optimally in less than 30 seconds, was found to be a critical step in the production of viable slices.

2.6.2. Optical assessment of slice viability.

The slice was positioned in the perspex recording chamber and held in place with a grid of parallel nylon threads attached to a flattened platinum U-shaped frame. The slice was constantly perfused with aspirated frog ringer at a flow rate of ~ 2ml/min. The normal frog ringer was not thermo-regulated and so the temperature of the slice was dependent on the ambient conditions of the room ($\sim 22°$C). The recording chamber was mounted on a fixed stage microscope (Zeiss, Axioskop) which was equipped with a bright field 100W tungsten-halogen lamp and an epifluorescence unit (fluorescence incident light excitation). The slice was viewed with a x40 water immersion objective (1.5mm working distance, 0.75 Numerical aperture) through x16 eye pieces (see figure 2.3). A TV camera was also mounted on the microscope (Avcam, 405) and the image was displayed on a video monitor (Hitachi, VM 129E/K). The cell bodies of tectal neurons could clearly be seen with Normaski differential interface contrast optics present in the microscope. The video camera afforded enhanced contrast information which greatly improved the quality of the image.

The visual characteristics of healthy neurons in thin slices prepared from the spinal cord, hippocampus, cerebellum and visual cortex of mammals has been described previously. Therefore, viable slices could, in theory, be identified purely on their appearance in this optical system. However, the good condition of this slice preparation was also assessed using fluorescent dyes to stain for living and dead cells. The slices were incubated for 1 minute in 10μg/ml Fluorescein diacetate (FDA) or 0.2mg/ml ethidium bromide (EB). FDA is not inherently capable of fluorescence but when it crosses the membrane of a healthy cell it is enzymically broken down and fluoresceine is released. This fluorochrome is retained by the cell and when excited with blue light (excitation wavelength ~ 490nm) fluorescence occurs (fluorescence emission wavelength ~ 525nm). EB is a fluorochrome which intercalates with double stranded DNA. If the membrane of a cell is damaged this fluorochrome will accumulate in the nucleus of the cell. Therefore, dead or damaged cells will accumulate EB and when they are excited with green light (excitation wavelength ~ 570nm) will exhibit strong fluorescence (fluorescence emission wavelength ~ 625nm). This labelling of healthy and damaged cells with specific fluorochromes was utilised, in conjunction with bright field microscopy and DIC optics, to establish the viability of slices.

2.6.3. Cell-attached and tight-seal whole-cell recording from tectal neurons.

In order to form a high resistance (GΩ) seal an unimpeded access to the cell

membrane is needed. Cells located in the upper surface of the slice were sufficiently exposed to allow this. However, cells located deeper in the slice were covered with tissue and cell debris which could be removed by "cleaning". A "cleaning" pipette (a patch pipette pulled with a large tip diameter of $\sim 20\mu$m) was filled with frog ringer and positioned above the neuron to be exposed. The unwanted tissue above the cell body was removed by applying gentle positive and negative pressure to the pipette. The removal of tissue covering the neuron was continuously monitored by focusing up and down the slice.

Patch clamp recordings were made from clean cell bodies situated in specific layers of the tectum. Patch pipettes were prepared using a two stage pulling procedure (David Kopf Instruments, Model 700C) from borosilicate glass of 1.5 mm outer diameter and 1.17 mm inner diameter. The pipette, $\sim 1\mu$m tip diameter, was filled (composition in mM: K-Gluconate 100: K.HEPES 5; NaATP 2; $MgSO_4$ 2; KCl 20; pH 7.4; 198 mosmols/mg) and the shank was coated with sylgard to minimise the capacitance which results from deep immersion of the pipette in the bath. The current, at the electrode tip, was set to zero and the pipette resistance monitored in response to a 5mV step-change in $V_{command}$. To form a high resistance seal between the pipette and the cell membrane the tip of the electrode was pressed against the cell body and gentle suction applied. Cell-attached recording of current elicited by voltage-dependent ion channels situated in the isolated patch of membrane were made once a giga-ohm seal was achieved.

The membrane patch could be broken by a short pulse of suction following the formation of a giga-seal establishing a conductive pathway between the pipette and the cell interior. The capacitive current elicited in cell attached mode by the 5mV step-change were compensated with the "fast" capacitance compensation of the patch clamp amplifier. The potential in the pipette ($V_{command}$) was adjusted to a level similar to the anticipated resting membrane potential of the cell (typically -70mV). Strong suction was applied to the pipette and large capacity transients appeared when the membrane was ruptured. This current, associated with charging the cell capacitance, were compensated with the "slow" capacitance compensation of the patch clamp amplifier.

The current record (I_o, mV/pA), the holding potential (V_{pip}, mV) and spoken information, were stored on separate channels of a tape recorder (Racal, 4 store) at a tape speed of 3.75 inch/s. In several experiments the raw data was saved onto video via a pulse code modulator (Ferguson Videostar & Sony PCM-701). Data was subsequently digitised (CED, 1401) at a sampling rate of 10KHz.

2.6.4. Dye-injection experiments.

Lucifer yellow (LY) was included in the patch pipette at a final concentration of $10\mu g/ml$. In whole cell configuration the dye passively diffused into the neuron but, in some cases current was injected into the cell to improve this process. When cells containing this fluorochrome are excited with blue light (mean excitation wavelength $\sim 440nm$) fluorescence occurs (fluorescence emission wavelength $> 470nm$). The filled cells were viewed under incident light fluorescence after 15 minutes of whole cell recording. The preparation was photographed under bright field and fluorescence illumination using 400ASA colour film (AGFA) at varying exposure settings ranging from 10 to 120sec. It proved difficult to remove the pipette without damaging the cell so we could not histologically process filled cells.

2.6.5. Recording spontaneous and evoked responses from tectal slices.

Tight-seal whole cell recordings were made from small tectal cell bodies ($\sim 10\mu m$ diameter) in layer 6, 8 & 9 and from larger ($\sim 30\mu m$ diameter) cell bodies in the deeper layers of the tectal slice. A concentric bi-polar electrode was used for stimulation (Clark Electromedical Instruments) of the optic tract, immediately before it enters the tectal neuropil, and the superficial layers of the tectum. In some experiments the efferent fibres running through layer 7 of the tectal neuropil were also stimulated. A current of 100mA was passed in the form of a rectangular pulse of 20-50μsec duration. The holding potential ($V_{command}$) could be varied between resting membrane potential (typically, -70mV) and +30mV to assess the I-V relationship of any spontaneous or evoked events.

2.6.6. Analysis of cell attached and whole cell recordings.

The seal resistance was calculated in cell-attached configuration before the resting membrane potential, cell capacitance and series resistance was calculated in whole cell mode. Before contact between the pipette tip and the identified tectal neuron was made the impedance of the patch pipette was calculated and the holding potential ($V_{command}$) of the pipette adjusted to zero. In cell attached configuration the resistance of the seal was calculate from the current passed at the pipette tip (I_p) during a given voltage step ($V_{command}$).

$$R_{seal} = V_{command} / I_p$$

In whole cell configuration the resting membrane potential of the neuron was calculated from the holding potential ($V_{command}$) at which no current (I_p) was being passed. The cells capacitance (C) was estimated from the change in charge (ΔQ) observed during

a given voltage step (ΔV) prior to capacitance compensation.

$$C = \Delta Q / \Delta V$$

The series resistance (R_s) between the pipette and the cell was then calculated from this measure of cell capacitance and the time constant (τ) for the decay in the capacitive current.

$$R_s = \tau / C$$

Single exponential equations were fitted to the decay of the capacitive transient to calculate τ. The quality of voltage clamp can be ascertained from how well the decay of the capacitive transient is explained by a single exponential fit. If this decay is best explained by a double exponential then this implies that adequate voltage clamp of the entire membrane is not possible.

The rise time, peak amplitude and decay time of spontaneously occurring events were calculated from the digitised records. Averaging of these spontaneous current was possible with the use of a window discriminator (Digitimer, D130) to identify the start of each event and trigger the sampling of the transient signal.

2.7. Pharmacological agents.

Atropine sulphate (AS), Evans.

Bicucculin, Sigma.

3-(($\pm$)-2-carboxypiperazin-4-yl)propyl-1-phosphonic acid (CPP), 6-cyano-7-nitroquinoxaline-2,3-dione (CNQX), D,L-2-amino-5-phosphonovaleric acid (AP5), Tocris Neuroamine.

D-Tubocurarine (D-TC), Wellcome.

Ethidium Bromide (EB), Sigma.

Fluorosceine diacetate (FDA), Sigma.

Lucifer Yellow (LY), Sigma.

Picrotoxin, Sigma.

All pharmacological antagonists (excepting AS & D-TC which were supplied in solution at 600mg/ml and 15mg/1.5ml respectively), were dissolved in external normal frog ringer to the required concentration before dilution to the final concentration in the external bathing medium.

Chapter 3

Intertectal plasticity:

limitations and morphological correlates

3.1. Introduction

Binocular vision in frogs is afforded by the presence of a dual visuotectal projection to the optic tectum (Gaze, 1958). The neural activity recorded from the superficial layers of the tectum in response to visual stimuli is believed to emanate from the terminal arbors of either the direct retinotectal or crossed isthmotectal fibres. The assumption as to the origin of the electrical transients recorded from the superficial layers of the tectal neuropil is based upon several observations which were first described by Maturana *et al.* (1960).

(1)   A microelectrode on the surface of the optic tectum records activity from a localized region of the visual field. Movement of the electrode tip, even by just 100μm, results in a shift in the effective region of visual space. No such orderly shift in the receptive field position would occur if the electrode were recording from fibres of passage. However, this observation does not rule out the possibility that the transients represent postsynaptic activation of tectal neurons.

(2)   The receptive field properties of single units recorded from the superficial tectum are the same as those recordable from the optic nerve.

(3)   The receptive field properties of units recorded from deeper tectal locations are very different from those recorded in the superficial tectum. These deeper tectal units presumably do reflect the postsynaptic activation of tectal neurons as no visual afferents terminate in these layers.

(4)   The electrical characteristics of the superficial units are similar to those of optic axons but those of the deeper units are not.

For these reasons it seems likely that the recordings made from the superficial tectal regions represent the distribution of the incoming afferent fibres. The entirely crossed nature of the retinotectal projection means that when the ipsilateral eye is covered only activity via this direct retinotectal projection will be recorded at the contralateral tectal lobe. When the contralateral eye is covered activity via the indirect intertectal projection will be recorded at the ipsilateral tectal lobe (see figure 1.1). The probable site of origin of the signal would be the terminal arborization of the retinotectal and isthmotectal fibres as the terminal branching patterns could be

expected to increase the signal to noise ratio specifically at these tectal locations. We also assume that synaptic connections are formed between the terminal arbor and the tectal dendrites and so this mapping procedure also reveals the sites of synaptic connections formed by the retinotectal and isthmotectal projection. The spatial location of this neural activity can be compared to determine whether the synaptic connections formed by the dual projections are in or out of register. If the activity, elicited by stimulation of the same portion of visual space, is detectable at the same spatial location in the tectal neuropil then the two inputs can be considered in register. If neural activity at a tectal location is elicited following stimulation of disparate portions of visual space then the two inputs are considered out of register.

Surgical rotation of one eye about its optic axis by 180° results in inversion of both the nasotemporal and dorsoventral axes of the retina. Therefore, the retinotectal projections representation of the visual field on the tectal lobe is rotated by 180°. However, the isthmotectal projection, to that tectal lobe receiving the rotated retinotectal projection, will not have been rotated. This will initially result in a mis-alignment of the crossed isthmotectal projection by 180°. It has been demonstrated that, following a single eye rotation, appropriate synaptic modifications take place in the crossed isthmotectal projection which realigns the isthmotectal projection with the rotated retinotectal projection. We currently only know of 3 limiting factors to this remarkable form of synaptic plasticity. This plasticity is only normally present up to 3 months after metamorphosis. After this critical period of development the intertectal system is not capable of adapting its pattern of synaptic connections to a single eye rotation. Also, the response of the intertectal system to a single eye rotation, surgically apportioned at an early period of development, can be blocked by either visually depriving the animal (Keating and Feldman, 1975) or by the application of the NMDA receptor antagonist AP5 to the tectum (Scherer and Udin, 1989). Therefore, the experience-dependent synaptic plasticity of the frog binocular system is contingent upon visual experience and correct NMDA-receptor function during a critical period of development.

Are there any other limitations to this experience-dependent plasticity? The response of the intertectal system to a double eye rotation has not yet been established. In a single eye rotation experiment only one of the contralateral visuotectal projections is in an abnormal orientation. It could be that following a single eye rotation some information is imparted to the system by the normally oriented retinotectal projection. A double eye rotation removes all intrinsic positional

cues which could be derived from the correct orientation of one direct retinotectal projection. If this information is important then the intertectal system should not be able to realign the binocular maps of visual space on each tectal lobe following a double eye rotation. Therefore, both eyes were rotated at late larval stages 55-58 and the response of the intertectal system was assayed electrophysiologically one year postmetamorphosis.

The second part of this study investigates what influence an intact retinotectal projection has on the electrophysiologically derived spatial location of crossed isthmotectal terminal arbors. The location of isthmotectal inputs to a tectal lobe was examined before and after the removal of the eye responsible for the retinotectal projection to that tectal lobe. These experiments were carried out on animals which had received double eye rotations in late larval life. After one year of normal visual experience the direct retinotectal projection and the crossed isthmotectal projection was electrophysiologically mapped to both tectal lobes. As far as possible the animal was not moved from its position in the coordinate frame during enucleation. During surgical anaesthesia the periocular tissue was cut with dissecting needles and watchmakers forceps. The ocular muscles and optic nerve were also cut and the eye removed from the socket. The crossed isthmotectal input to the right tectal lobe was then mapped again to see if the influence of the retinotectal projection altered the spatial location of the electrophysiologically derived crossed isthmotectal input to that tectal lobe which is no longer receiving direct retinal input.

3.2. Results

3.2.1. Double eye rotation experiments.

A total of 24 animals were given double eye rotations and the spatial location of binocular inputs were mapped at 277 tectal locations. All binocular inputs encountered arose from corresponding points in the visual field; indicating that extensive modifications in the crossed isthmotectal projection had occurred following double eye rotation. However, only 15 animals had retained double eye rotations, of 45° or more for each eye. The derotation of an eye is common in this preparation and so the degree of eye rotation performed is calculated at the final stage of mapping. In 10 of these animals, sufficient electrophysiological data was available to define the degree of eye rotation still present in both eyes and to evaluate the spatial registration between the binocular inputs to both tectal lobes (see table 3.1). A

representative example is shown in figure 3.1. It can be seen that full registration has been achieved between the dual binocular projections to each tectal lobe (the visuotectal projection in **A** is in register with **B**, and **C** is in register with **D**). The direct retinotectal projection which has been mapped through the right eye (**A**) shows a progression through space which indicates that the right eye has been rotated clockwise by 90°. The visuotectal progression displayed by the direct retinotectal projection mapped through the left eye (**D**) indicates that the left eye has been rotated anti-clockwise by 200°. Both crossed isthmotectal projections (**B** & **C**) have rearranged their pattern of synaptic connections to achieve alignment with the two rotated retinotectal projections (**A** & **D**). This pattern of aligned retinotectal and isthmotectal inputs was observed in all 10 animals following double eye rotation indicating full adaptation of the binocular visual system to these drastic changes in eye orientation.

Two criteria were used to satisfy the inclusion of mapping data in the final quantitative analysis of the absolute disparity in binocular alignment. The first was that the double eye rotation was of significant size; 45° or more for each eye. The degree of an eye rotation can easily be calculated from the electrophysiologically derived visual space map of the contralateral projection. The correct nasotemporal and dorsoventral progression through space of rostrocaudal and mediolateral penetrations across each tectal lobe has been well characterised. Therefore, the rotation was calculated in experimental animals by comparing the visual space map orientation with that obtained from normal animals. The average rotation in the final group was 82° clockwise for the right eye and 128.5° anti-clockwise for the left eye (see table 3.1). The second criteria was that the receptive field locations had been mapped for both the retinotectal and crossed isthmotectal inputs to the tectum so that the absolute disparity could be calculated. This left a total of 165 pairs to be included in the final quantitative analysis. In all 10 animals the 165 paired points appeared to arise from the same location in the visual field indicating that the intertectal system was able to rearrange its connections in response to a double eye rotation. The quantitative analysis confirms this. For the ten animals used in this study the mean absolute disparity was 8.01 ± 2.28 (std). In a previous study the absolute disparity for 191 paired points gathered from 7 normal animals of comparable ages was 9.6 ± 5.6 (Grant and Keating 1989a). The difference between these values was not significant (Mann-Whitney unpaired non-parametric two-tailed U-test).
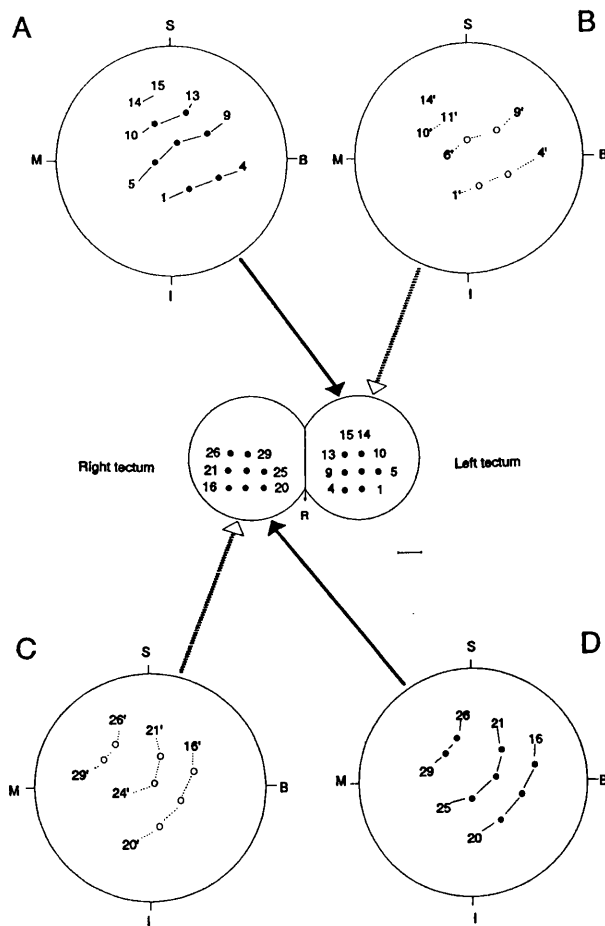
Figure 3.1. The effect of binocular eye rotation on the electrophysiologically derived contralateral and ipsilateral tectal maps of visual space after 1 year of visual experience.

The diagrams of the optic tecta show their outlines, transposed from a photograph of the dorsal surface, upon which a 100μm grid was superimposed. Rostral is indicated by the direction of the mid-line arrow labelled R. Numbers and intermediate dots on the tectal diagram represent the sites of vertical microelectrode penetrations. Large circles denote perimetric chart representations of the visual field, with the optic axis of the right eye centred on the fixation point of the perimeter. The animal was not moved within the coordinate frame during the recording session, thus the four chart representations plot identical areas of visual space. For each microelectrode penetration the centre of the region of visual space, stimulation of which produced evoked unitary potentials at that electrode site, when viewed by either the right or left eye, is indicated by the corresponding number of intermediate dots on the relevant chart representation. A, the contralateral visuotectal projection onto the left tectal lobe through the right eye. B, the ipsilateral visuotectal projection onto the left tectal lobe through the left eye. C, the ipsilateral visuotectal projection onto the right tectal lobe through the right eye. D, the contralateral visuotectal projection onto the right tectal lobe through the left eye. The indirect nature of the ipsilateral visuotectal pathway is indicated by the discontinuous lines within and from the visual field representations. B, M, S and I are the binocular, monocular, superior and inferior aspects of the visual field of the tested eye. Note that the two visual projections to each tectum are in full spatial register even though both contralateral projections have been rotated by $\sim 180°$.

62

3.2.2. Eye removal experiments.

In a total of 8 animals the crossed isthmotectal projection to a tectal lobe was mapped with the direct retinotectal projection intact. In all 8 animals the binocular input was mapped to the right tectal lobe such that a total of 97 isthmotectal receptive fields were identified (see table 3.1). Before eye removal all 97 isthmotectal receptive fields mapped were in full spatial register with the rotated retinotectal projection indicating that full modification of the intertectal system had occurred (figure 3.2). In 2 of these animals (LBR22 & LBR24) eye removal did not affect the location of the crossed isthmotectal inputs. In these 2 animals the 26 isthmotectal receptive fields mapped following eye removal occupied positions in visual space which would have been congruent with the retinotectal projection. However, the removal of the retinotectal input in 6 out of the 8 animals revealed that, for a total of 36 isthmotectal receptive fields, 23 isthmotectal inputs now occupied totally inappropriate positions in visual space. Figure 3.2 illustrates the results from one animal LBR13. **A** shows the mapping data obtained before the eye was removed. 16 retinotectal and 16 isthmotectal receptiver fields have been mapped to the left tectal lobe through the right (filled circles) and left (open circles) eye. All these binocular inputs occupied corresponding locations in visual space. Following removal of the right eye the ipsilateral inputs from the remaining left eye to the left tectal lobe was mapped again and the data is shown in **B**. 12 receptive fields remain unchanged but 11 others have appeared at previously unidentified locations. Therefore, a total of 23 isthmotectal receptive fields can now be identified at only 12 tectal locations. For example, at the tectal recording location **7** an isthmotectal receptive field is now located at **7'** and **7''** in the visual field whereas before eye removal an isthmotectal receptive field was only detected at location **7'** which was aligned with the retinotectal receptive field **7**.

The location of these previously unidentified ipsilateral receptive fields corresponded to positions in visual space appropriate to an unrotated retinotectal projection. In the 5 animals in which this effect was observed, 21 inappropriate isthmotectal receptive fields could be recorded simultaneously with the original receptive field positions which had been identified before the eye removal (dual points in table 3.1). So, for a single recording location on the tectum we could elicit a response through the isthmotectal projection at two disparate positions in visual space; one in register with the now removed rotated retinotectal projection and the other in a totally unmodified position out of register with the rotated retinotectal projection. After eye removal 2 isthmotectal receptive fields were detected only at the newly

inappropriate positions and the receptive fields which were recorded before eye removal were no longer present. Therefore, after monocular enucleation in 5 animals, 83 crossed isthmotectal receptive fields could be recorded from only 36 tectal locations and 23 of these receptive fields were in totally inappropriate locations in visual space. However, , in 2 animals this effect was not observed, and 26 isthmotectal receptive fields were still recorded from 26 tectal locations and these receptive fields occupied identical positions in visual space before and after monocular enucleation.
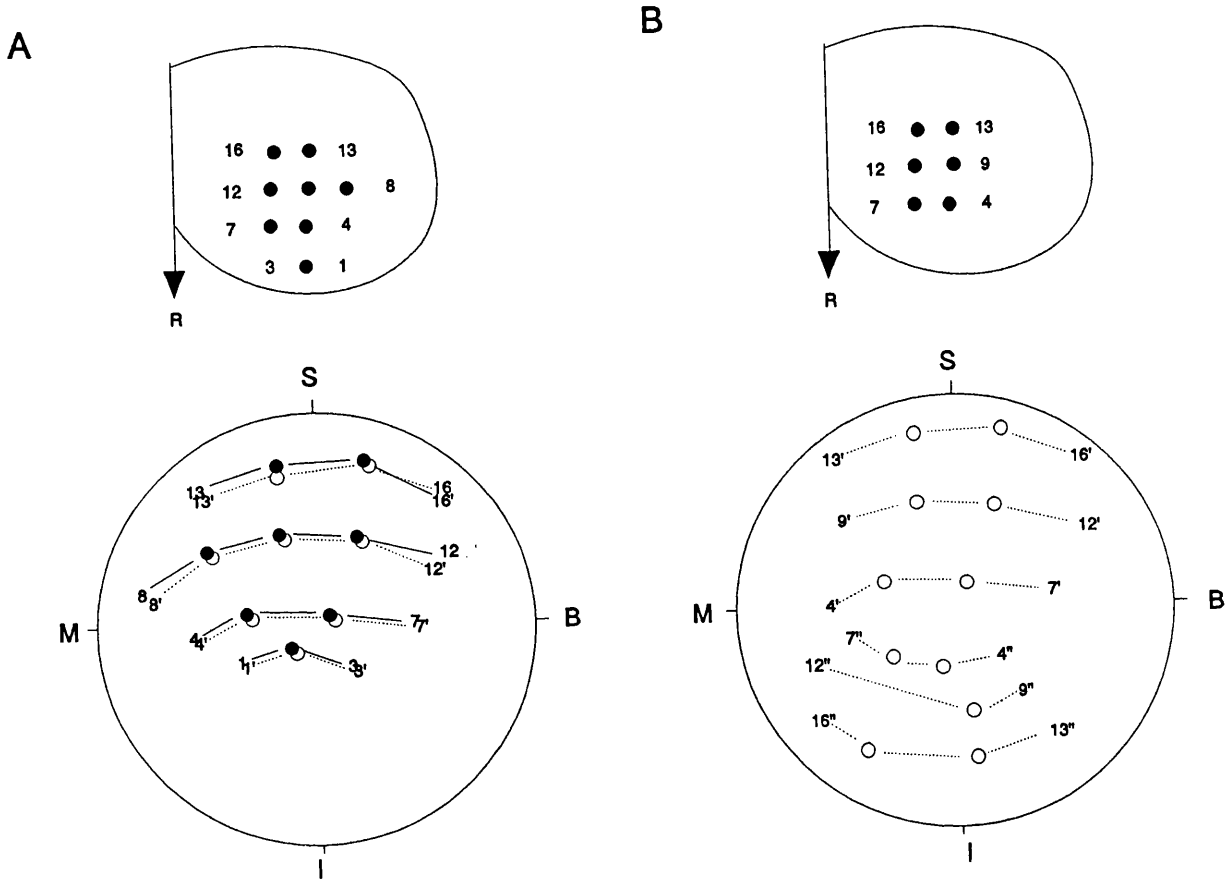
Figure 3.2. The effect of removing the direct retinotectal input on the correct binocular alignment of the isthmotectal projection.

The two diagrams of the optic tecta show their outlines, transposed from a photograph of the dorsal surface, upon which a 100μm grid was superimposed. Rostral is indicated by the direction of the mid-line arrow labelled R. Numbers and intermediate dots on the tectal diagram represent the sites of vertical microelectrode penetrations. Large circles denote perimetric chart representations of the visual field, with the optic axis of the right eye centred on the fixation point of the perimeter. B, M, S and I are the binocular, monocular, superior and inferior aspects of the visual field of the tested eye. For each microelectrode penetration the centre of the region of visual space, stimulation of which produced evoked unitary potentials at that electrode site, when viewed by the ipsilateral eye, is indicated by the corresponding number of intermediate dots on the relevant chart representation.

A depicts the visuo-tectal progression through space of crossed-isthmotectal connections before the removal of the direct retinotectal input to this tectal lobe. All the isthmotectal receptive fields recorded (open circles) in this animal were in spatial register with the rotated retinotectal input.

In B the retinotectal input has been removed. The animal was not moved within the coordinate frame during the recording session. The majority of isthmotectal connections previously recorded in A are still present arising from the same location in visual space (open circles 4'-16'). However, previously undetected receptive fields are now recorded at totally inappropriate locations in visual space (open circles 4''-16'').

3.3. Discussion

The present study demonstrates that experience-dependent plasticity will occur in the connections of the intertectal system following the surgical rotation of both eyes by ~180° in late larval life. The severity of the change to one or both eyes does not limit the manifestation of experience-dependent intertectal plasticity in the binocular visual system of *Xenopus laevis*. Moreover, adaptations in the binocular visual system will occur, even though the frog would exhibit mal-adaptive behaviour; *ie*, frogs orient incorrectly to a visual stimuli placed in the visual field of the rotated eye (Sperry, 1943). Following a double eye rotation both visual fields have been rotated so mal-adaptive behaviour will be exhibited following stimulation of either visuotectal projection. However, even in these circumstances, drastic alterations in the series of intertectal connections do take place.

In the mammal a gating mechanism is believed to exist which constrains the synaptic plasticity of the binocular visual system on the basis of behavioral relevance (Singer *et al*, 1982). Monocular deprivation in the cat during a critical period of development leads to alterations in the percentage of cells receiving binocularly driven input. Eye rotation coupled with monocular deprivation does not produce this characteristic loss in the percentage of cells driven from the deprived eye. Therefore, central gating of this developmental plasticity in the kitten visual cortex has been postulated. When there is no behavioral advantage in adapting the circuitry underlying binocular vision in the cat visual cortex functional adaptations do not occur. It is also believed that neuro-modulators, such as the cetacholaminergic system, are involved in this mechanism. Indeed, catecholamine depletion interferes with the construction of ocular dominance columns following monocular visual deprivation in the cat visual cortex (Bear and Singer, 1986; Daw *et al*, 1983). However, in *Xenopus*, catecholamine depletion does not affect the experience-dependent plasticity of the binocular visual system (Udin *et al.*, 1985). It seems to be the case that there are no identified gating mechanisms operating in the binocular visual system of *Xenopus*.

The unmasking of previously unidentified isthmotectal connections by the removal of the retinotectal projection to a tectal lobe has interesting implications. In the eye removal experiments the previously unidentified isthmotectal connections occupied positions on the tectum roughly corresponding to those positions the isthmotecial projection would have adopted if no rotation had been present. The connections that were presumably formed earlier in development, at inappropriate

tectal locations, were not electrophysiologically detectable later in development when the isthmotectal projection was mapped. Only positions related to a modified isthmotectal projection were now detectable. It was only after the rotated retinotectal projection had been removed that inappropriate, non-adapted, connections were observed. Therefore, eye removal seems to unmask previously unidentified isthmotectal connections which occupy binocularly inappropriate tectal locations. These masked inputs may represent the initial, intrinsically generated, location of the crossed isthmotectal projection.

Intertectal plasticity is thought to be characterised by an ordered movement of crossed isthmotectal terminal arbors from one location in the tectal neuropil to another newly appropriate situation. This conclusion is almost exclusively based upon electrophysiological mapping studies which are believed to monitor the neural activity recorded from the terminal arbors of the crossed isthmotectal projection. However, anatomical changes in the isthmotectal projection following larval eye rotation have been shown by analysing the distribution of HRP labelled cells in the nucleus isthmi and optic tectum (Udin and Keating, 1981; Udin, 1983). Analysis of crossed isthmotectal axon trajectories in eye rotated *Xenopus* suggest that these axons reach their new locations after passing through their normal locations. It is supposed that the terminal arbors travel first to normal unrotated locations and then follow a circuitous route to the newly appropriate tectal location. We also know, from electron microscopy, that during normal development crossed isthmotectal arbors make ectopic synaptic connections in monocular regions of the tectum (Udin *et al.*, 1992). The current eye removal data supports the anatomical data, demonstrating that under certain conditions the original binocularly inappropriate termination sites can be electrophysiologically detected.

67

Double eye rotation experiments

Experiment	Right Tectum (points in map)		Left Tectum (points in map)		Rotation (degrees)		Absolute
(LBR)	Retinotectal	Isthmotectal	Retinotectal	Isthmotectal	Right	Left	Disparity
9	17	9	20	10	90	120.0	9.18
11	16	9	23	6	60	135.0	9.51
13	19	8	17	2	30	120.0	13.42
16	18	7	3	7	110	130.0	6.08
17	19	7	21	14	75	115.0	7.03
18	13	5	4	3	180	90.0	9.24
19	17	9	5	7	60	180.0	6.56
21	15	13	15	10	90	200.0	5.13
22	16	12	15	14	80	90.0	6.67
24	14	12	15	11	45	105.0	7.26
Total	164	91	138	84			
			Average		82	128.5	
					Average		8.01
					Std		2.28

Acute enucleation experiments

Before eye removal

Experiment	Isthmotectal	Incongruent	Congruent	Dual
(LBR)	points	positions	positions	points
13	17	0	17	0
14	10	0	10	0
17	14	0	14	0
18	11	0	11	0
19	10	0	10	0
21	10	0	10	0
22	14	0	14	0
24	11	0	11	0
Total	97	0	97	0

After eye removal

Experiment	Isthmotectal	Incongruent	Congruent	Dual
(LBR)	points	positions	positions	points
13	13	12	1	11
14	8	4	4	4
17	2	0	2	0
18	3	2	1	1
19	6	3	3	3
21	4	2	2	2
22	13	0	13	0
24	13	0	13	0
Total	62	23	39	21

Table 3.1. Results from double eye rotation and eye removal experiments.

Chapter 4

Intertectal plasticity:

correlated firing patterns in the tectum

4.1. Introduction

It has been hypothesized that local coincident firing patterns, resulting from binocular visual stimulation, are utilized during intertectal plasticity (Grant and Keating, 1989a, 1989b, 1992). This coincidence detection hypothesis is supported by dark-rearing experiments (Keating and Feldman, 1975) a situation in which intertectal plasticity will not take place. If this hypothesis is to be believed, then procedures, other than visual deprivation, that interfere with the cues necessary for coincidence detection should similarly prevent the occurrence of intertectal plasticity. One such procedure could involve rearing animals in a visual environment consisting entirely of stroboscopic illumination. In this environment all points in the visual field and therefore all points across the tectum should be simultaneously activated (figure 4.1). Local coincident firing patterns, resulting from binocular visual experience, should not occur in a strobe environment. If no contrast information is supplied with the strobe flash then local coincidence detection will not be possible. Therefore, if stroboscopic illlumination does interfere with correlated patterns of neural activity and the coincidence detection hypothesis is correct then strobe-rearing should block intertectal plasticity in an analogous manner to dark-rearing.

4.1.1. Acute effects of stroboscopic illumination.

Experiments were designed to determine whether stroboscopic illumination interfered with firing patterns recorded in the superficial tectal neuropil. The anaesthetized animal was placed in an environment consisting entirely of stroboscopic illumination and multi-unit activity was recorded from the tectum. The time at which individual events occurred was extracted from the extracellular responses using a window discriminator so that changes in the firing patterns of MURFs could be established. First we examined the acute effect of constant stroboscopic illumination, at 0.2Hz and 1Hz, on the firing patterns of the three types of visual units which are present in the optic tectum. What was the optimal strobe frequency in terms of entraining evoked and spontaneous neural activity in the tectum?

Next, we examined the effect of normal visual stimulation on the firing

patterns recorded from two tectal locations (figure 4.4). Simultaneous recordings were made from overlapping and non-overlapping receptive fields and cross-correlations performed on the firing patterns recorded during normal visual stimulation. Does visual stimulation cause correlated patterns of neural activity between tectal locations receiving matched binocular input? Do disparate tectal locations which are receiving information from different parts of the visual field also exhibit correlated firing? Finally, we investigated how stroboscopic illumination altered the firing patterns recorded simultaneously from these separate tectal locations. Does the degree of correlation exhibited by the dual firing patterns change during exposure to stroboscopic illumination? If stroboscopic illumination does interfere with correlated patterns of activity then this environment could represent an appropriate method of testing the validity of the coincidence detection hypothesis.
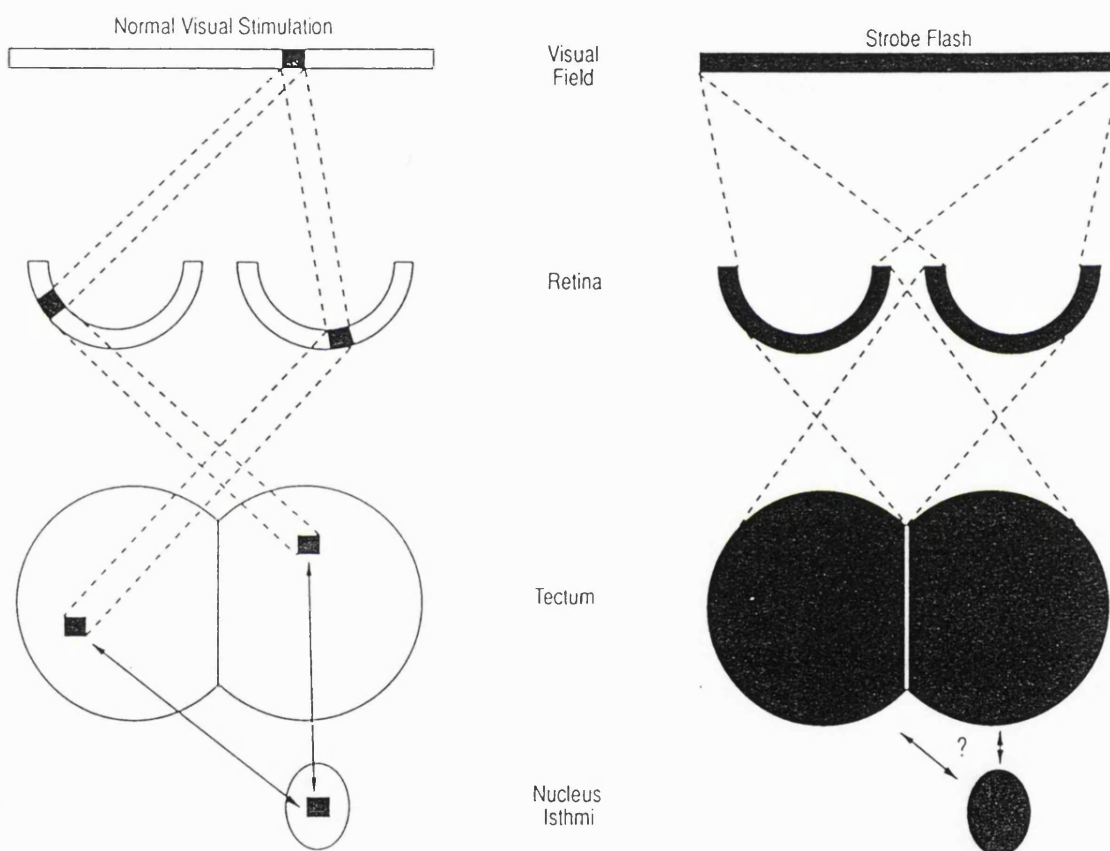
Figure 4.1. A schematic diagram illustrating how stroboscopic illumination disrupts the intertectal systems ability to detect correlated neural activity

Normal binocular vision results in discreet neural activity on each tectal lobe. The intertectal system is believed to detect the correlated neural activity which is produced at these tectal locations. The intertectal system proceeds to link points on the tectum receiving matched binocular input. It is believed that the intertecal system uses the correlated neural activity to keep the dual topographic representations of binocular space in register during normal development and to rearrange intertectal connections in response to a surgically induced eye rotation.

A strobe flash stimulates all of the visual field in synchrony. The discreet patterns of neural activity deriving from binocular vision is lost and the intertectal system is unable to detect areas of correlated neural activity. If the coincidence detection hypothesis is true then in constant stroboscopic illumination no modifications should occur in the intertectal system following a single eye rotation.

4.1.2. Chronic effects of stroboscopic illumination.

The detection of correlated firing patterns has also been implicated in the development of synaptic connections in the developing retinotectal projection (see Introduction). The detection of correlated patterns of neural activity between the spontaneous firing patterns of neighbouring retinal ganglion cells (RGCs) is thought to mediate the activity-dependent refinement of the retinotectal projection (Schmidt and Edwards, 1983). It could be that prolonged exposure to stroboscopic illumination disrupts the normal topographic precision of this pathway and that any disruption we observe in the isthmotectal projection is merely a reflection of the retinotectal projections disorder. Therefore, we assessed the topographic precision of the retinotectal projection following chronic exposure to stroboscopic illumination. Animals were placed into continuous stroboscopic illumination from stage 35-36 of larval development which is before the onset of visually driven electrical activity in the retina (Witkovsky et al., 1976). Animals were reared in constant stroboscopic illumination until a terminal experiment in which the retinotectal projection was mapped electrophysiologically. Three aspects of the retinotectal projections precision were assessed: **(1)** the topographic order of the projection; **(2)** the the MURF size; **(3)** the differential depth distribution of terminals from different classes of RGCs.

Finally, experiments were undertaken to determine what effect prolonged exposure to stroboscopic illumination would have on the experience-dependent plasticity of the binocular visual system in *Xenopus*. The plasticity of this series of connections was assayed by standard electrophysiological mapping techniques. We began by monitoring the ability of the intertectal system to adapt its pattern of connections in response to the normal changes in eye position which occur during development. The intertectal system of animals reared in normal diurnal lighting will maintain the dual projections of binocular visual space in spatial register throughout these developmental changes in eye position. However, if animals are reared in total darkness for a period of 12 months then the isthmotectal projection becomes out of register with the retinotectal projection appearing compressed on the tectal neuropil. To test whether stobe-rearing has similar effects to dark-rearing *Xenopus*, staged between 55-58 of late larval development, were reared in constant stroboscopic illumination until they were electrophysiologically mapped one year postmetamorphosis. We also know, from previous experiments, that given normal visual experience the binocular visual system of *Xenopus* is capable of adapting its pattern of intertectal connections to a single eye rotation. However, following

prolonged dark-rearing the isthmotectal projection remains out of alignment with the rotated retinotectal projection. If stroboscopic illumination does disrupt the cues necessary for intertectal plasticity in an analogous manner to dark-rearing then this environment should also affect the response of the intertectal system to a single eye rotation. So, before being placed into stroboscopic illumination another group of animals were given a 180° eye rotation at stage 55-58 of late larval life. These animals were mapped electrophysiologically one year postmetamorphosis to appraise the degree of registration between the rotated retinotectal projection and the unrotated isthmotectal projection.

4.2. Results

4.2.1. The acute effects of 1Hz and 0.2Hz stroboscopic illumination on the firing patterns of sustained, event and dimmer units.

A total of 32 classified MURFs (see Chapter 2 for definition of different types) were examined. 12 sustained type units; 7 at 1Hz and 5 at 0.2Hz. 18 event type units were also examined; 12 at 1Hz and 6 at 0.2Hz. Only 2 dimmer type units were recorded in this study; 1 at 1Hz and 1 at 0.2Hz. In total 20 MURFs were exposed to 1Hz stroboscopic illumination for ~ 1 hour and 12 were exposed to 0.2Hz stroboscopic illumination for ~ 1 hour. In all 32 receptive fields the firing patterns changed during exposure to stroboscopic illumination. The raster displays illustrate this stroboscopic entrainment effect very well (figure 4.2; A, B, & C). After a 30 minute period of quiescence stroboscopic illumination began. The initial response to the strobe was an amorphous response in terms of the latency profile to individual strobe flashes. The entire period 1 second post-stimulus was filled with visually elicited responses. This initial homogeneous burst of activity exhibited a high rate of firing which habituated quite strongly within 20 seconds of continued stroboscopic illumination. A distinct banding then occurred in the latency profile with early, middle and late responses periodically firing after the strobe flash in a highly synchronous manner. The periodic firing of these bands of activity sharpened, in terms of latency, with prolonged exposure to the strobe. Occasionally, a band at a particular latency would disappear from the response but on other occasions a new band of activity, at a new latency to strobe flash, would be detected.

Once this "entrainment effect" had occurred each response to strobe flash lasted up to 2 seconds post-stimulus and so at a strobe flash frequency of 0.2Hz

spontaneous activity was present during the remaining 3 seconds (figure 4.3). At a frequency of 1Hz the evoked response to each strobe flash was interrupted so spontaneous activity was not present. No other difference was noted in the response of MURFs to 1Hz or 0.2Hz stroboscopic illumination in terms of this entrainment effect. All three MURF types exhibited the stroboscopic entrainment effect. The distribution of early, middle and late responses to each strobe flash were not noticeably different in each group. A marked laminar distribution of latencies to strobe flash was seen in each case at both strobe frequencies. The initial response to strobe occupied the first 200msec post-stimulus. The middle latency band occurred between 300 and 500msec post-stimulus and the final response occurred in the final 600 to 1000msec period. However, it is evident from this study that 1Hz stroboscopic illumination provides a more efficient means of controlling the levels of correlated firing observed in the tectum as no spontaneous activity will be present at this frequency. For this reason in future acute and chronic experiments we only examined the effects of 1Hz stroboscopic illumination.

Figure 4.2. The acute effects of 1Hz stroboscopic illumination on the firing patterns recorded from sustained, event and dimmer type MURFs.

The times at which action potentials (events) were recorded in the superficial layers of the optic tectum are illustrated using raster plots. The ordinate describes the time in seconds during a recording session. During each 1 second period the time of each event is recorded along the abscissa. During the first 300 seconds of each recording session the animal is in darkness so any events recorded during the 1 second intervals are spontaneously occurring. Constant 1Hz stroboscopic illumination begins ~300 seconds into the recording session. The MURFs response to each strobe flash is then shown for a continuous 1 hour period. Initial exposure to stroboscopic illumination elicits a burst of events for the entire 1 second period following the strobe flash. This initial response profile changes during the stroboscopic entrainment effect. Events occupy early intermediate and late bursts of activity. This complicated phasic bursting pattern was apparent in sustained (see page 76), event (see page 77) and dimmer (see page 78) type MURFs.

A continuous display of the firing rate (events/second along the abscissa) has also been calculated for the duration of the recording session (seconds along the ordinate). The spontaneous rate is low during the first 300s of recording when the animal is in darkness (~ 1.5 events/second). Constant stroboscopic illumination increases this firing rate to over 150 events/second but this initially very high rate habituates rapidly. Following continued exposure to stroboscopic illumination the firing rate gradually increases. In the case of the sustained unit the firing rate increases from 20 events/second to 45 events/second over a 40 minute period.

SUSTAINED

76
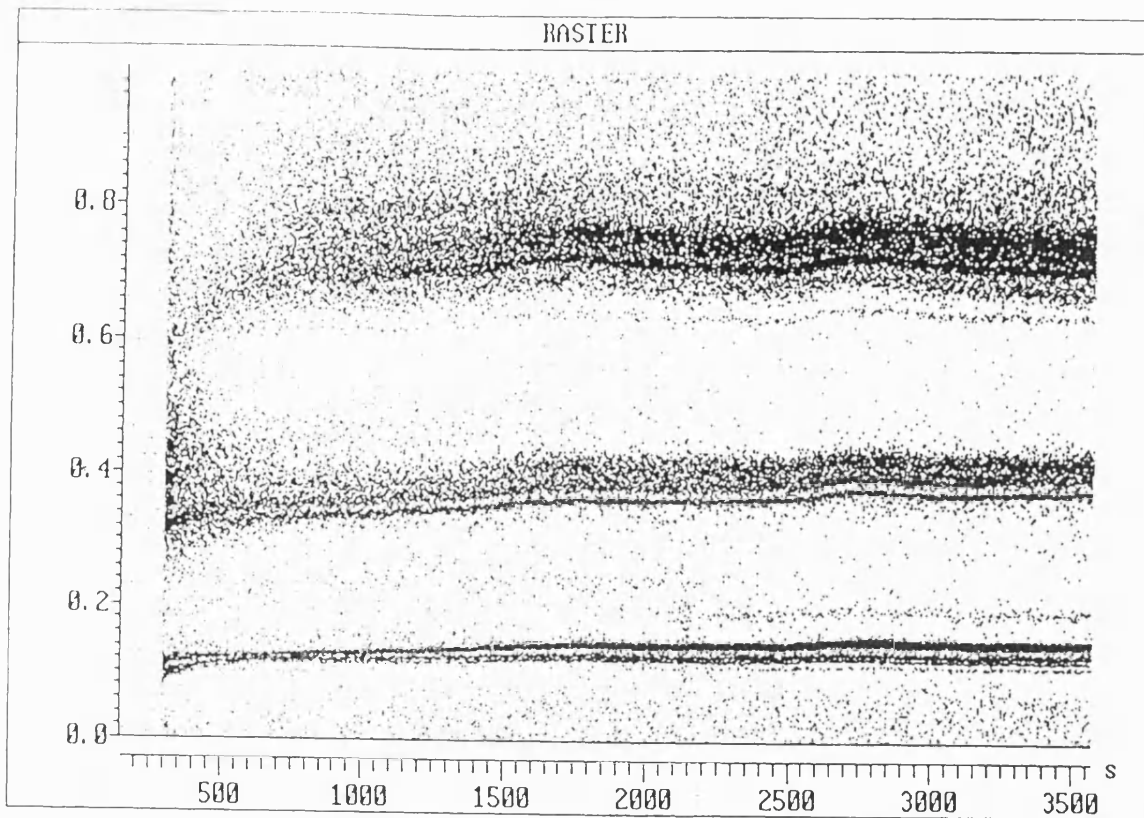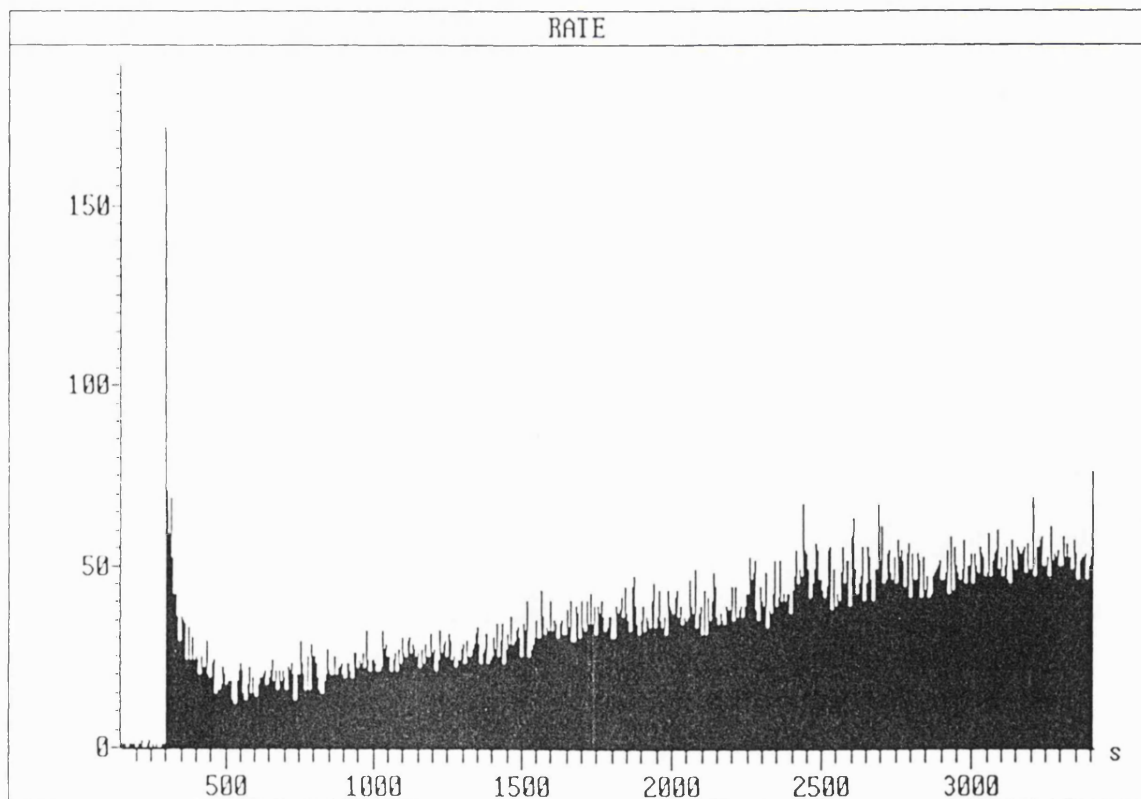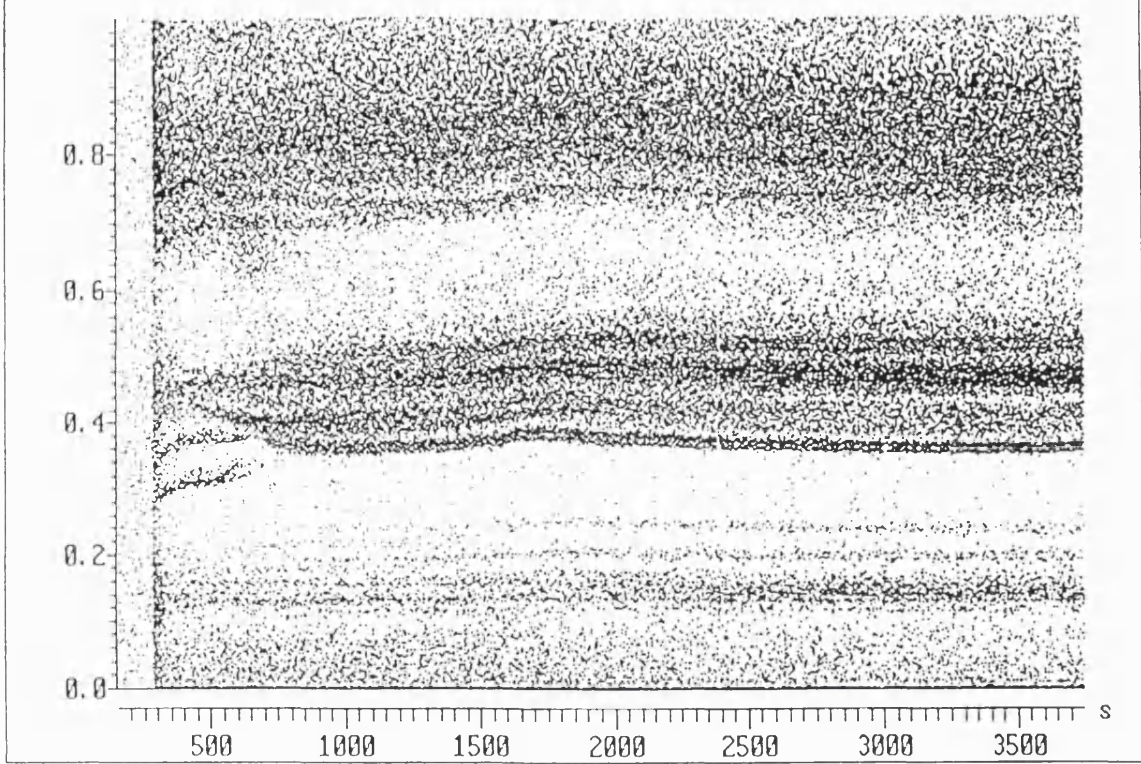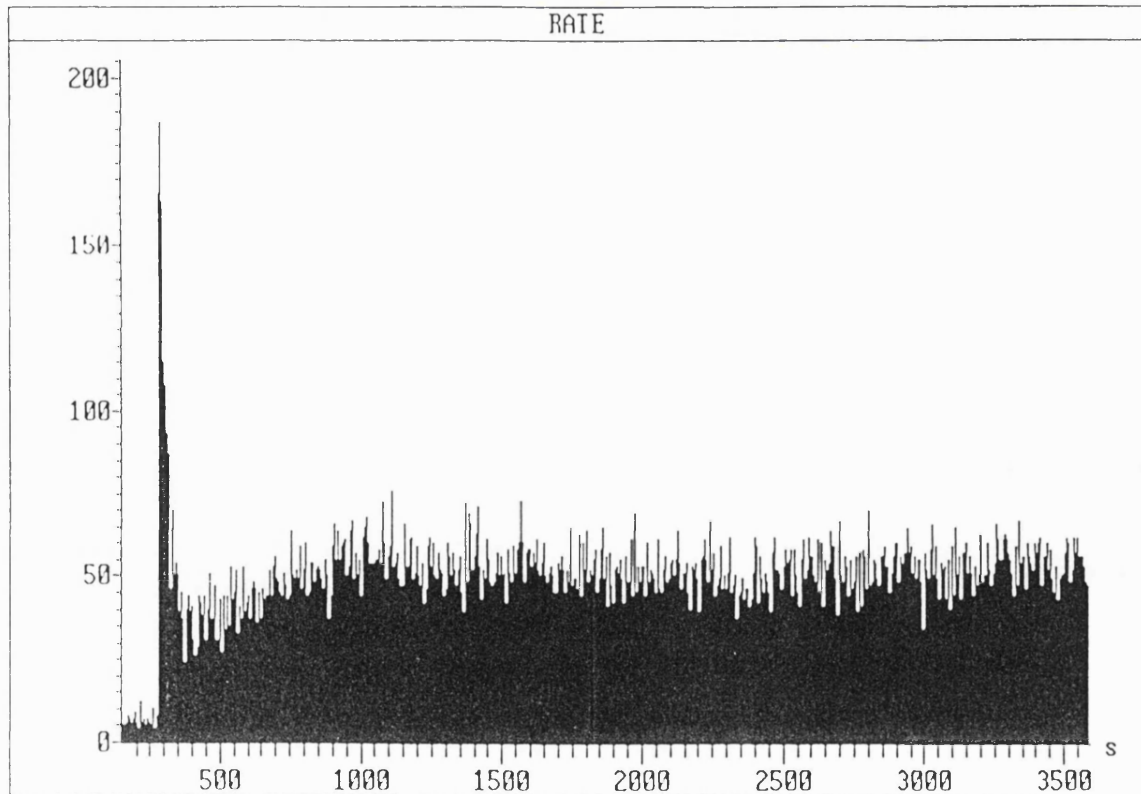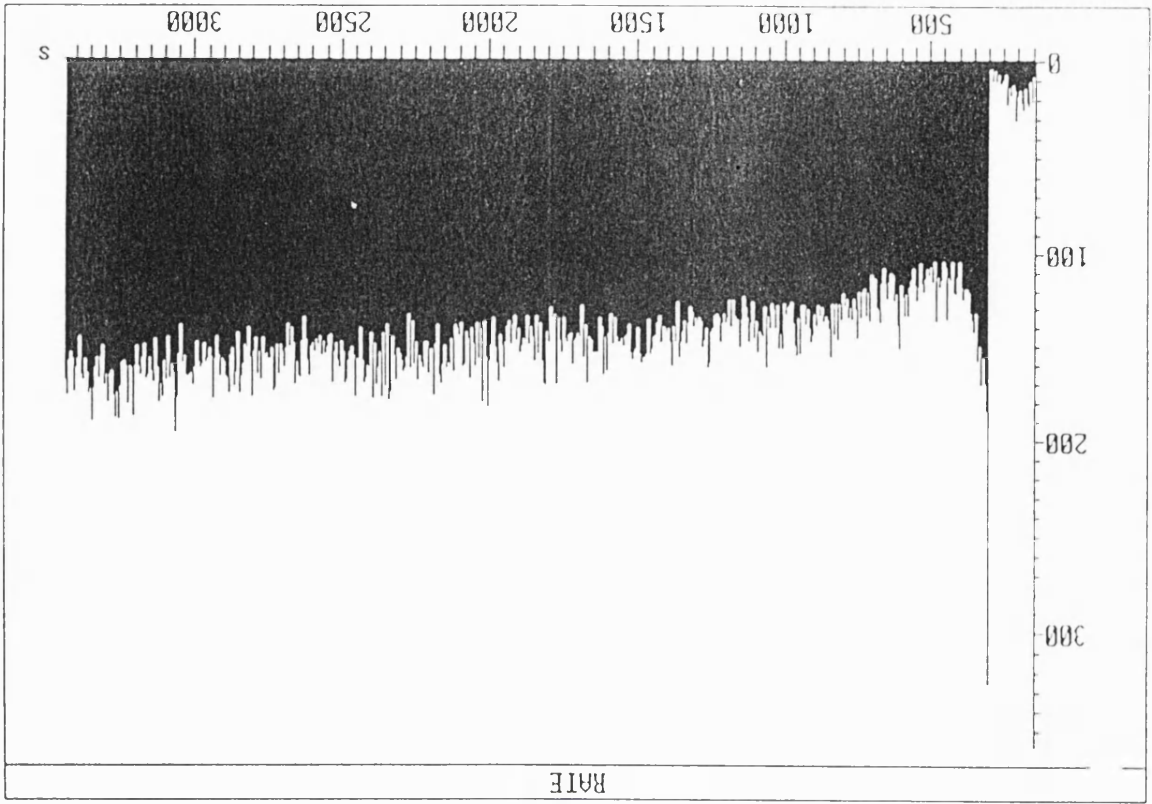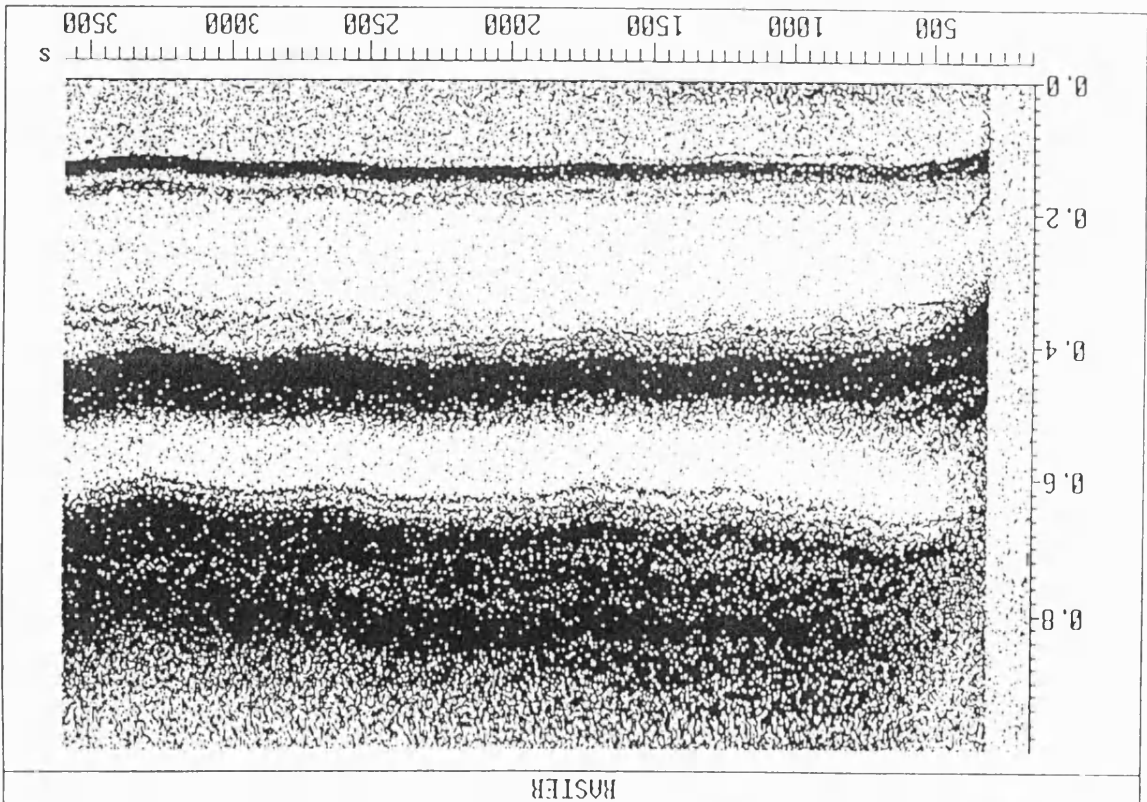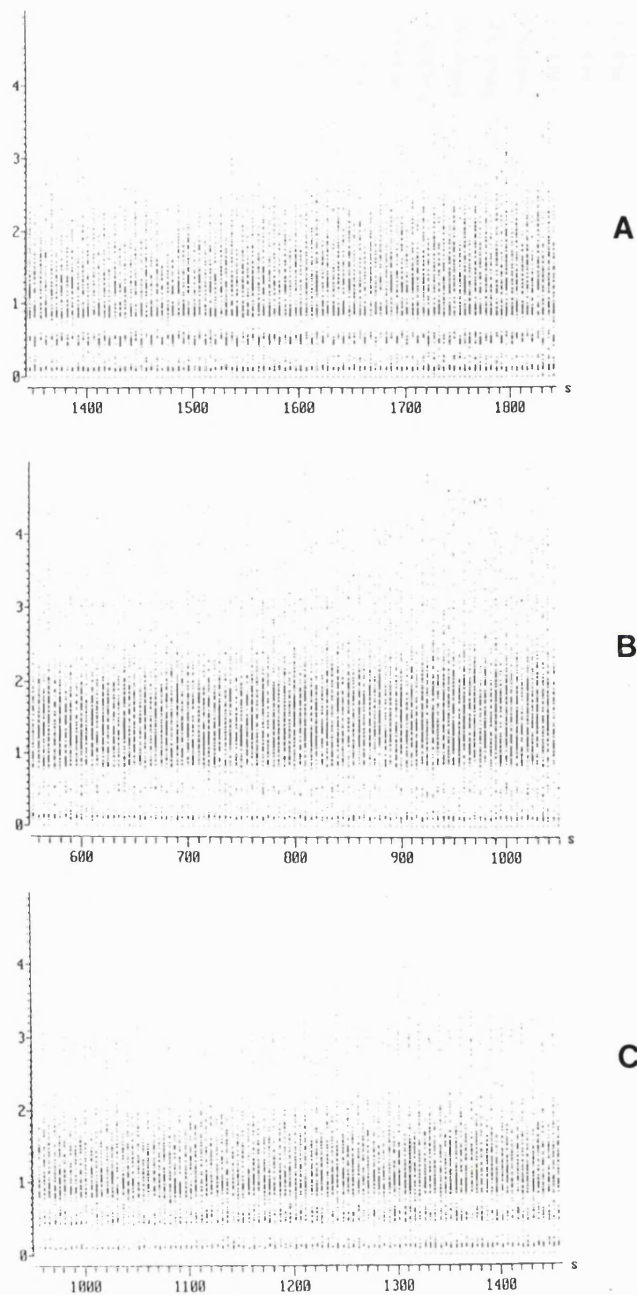
EVENT

Figure 4.3. The acute effects of 0.2Hz stroboscopic illumination on the firing patterns recorded from sustained, event and dimmer type MURFs.

Raster plots showing the response to 0.2Hz stroboscopic illumination recorded from a sustained (A), event (B) and dimmer (C) MURF. Conventions are similar to the raster plots in figure 4.2 but the duration of each response as plotted on the abscissa is now 5 seconds. The phasic bursting phenomenon is still apparent with the late burst occurring upto 2 seconds after the strobe flash but in the last 2 seconds of the response spontaneous events are occurring. Only ~500seconds of the recording session are illustrated following exposure to constant stroboscopic illumination at 0.2Hz.

79

4.2.2. Correlated patterns of neural activity in the tectum and normal visual experience.

Simultaneous recording from two tectal locations was achieved in 5 animals with a total of 24 MURFs. This included 6 pairs from overlapping receptive fields and 6 pairs from non-overlapping receptive fields (figure 4.4). In each of these groups 2 of the pairs were recorded from opposite tectal lobes and the other 4 were recorded from the same tectal lobe. Before the correlated firing patterns of the MURFs were examined the receptive fields were marked out on a perimeter card using a 3cm diameter black disc to identify the receptive field size of the MURFs (26.6° ± 9.0°sem, n=19) and their position in visual space. The result of visual stimulation with a black disc during normal light conditions is shown for a pair of overlapping and non-overlapping receptive fields recorded from two tectal locations in shown in figure 4.4. No qualitative difference was observed between those pairs recorded from opposite or the same tectal lobes. It should be noted that there is no cross-talk between the two recording sites and the signal to noise ratio is sufficient in both cases to identify the time of individual action potentials present in the MURFs. Cross-correlations (CCs) calculated from the firing patterns of overlapping receptive field responses to visual stimuli reveals a broad peak at $t = 0$ seconds (figure 4.5) irrespective of whether they were recorded from the same or opposite tectal lobes. CCs from non-overlapping receptive fields were flat with no cental peak indicating, not surprisingly, no correlation between the two firing patterns.
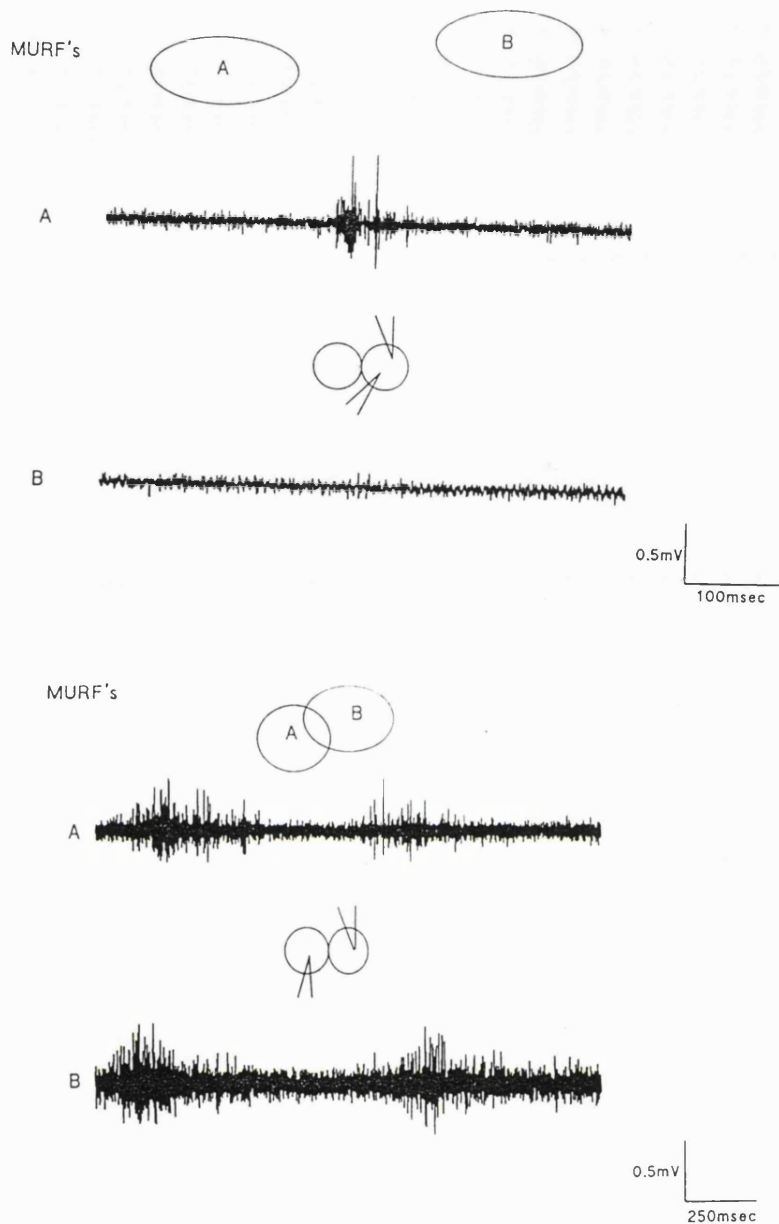
Figure 4.4. Examples of simultaneous extracellular recordings made from the same and opposite tectal lobes during stimulation of non-overlapping and overlapping visual receptive fields.

The top two traces are simultaneously recorded from two separate locations on the same tectal lobe (as depicted diagramatically by the inset). Stimulation of receptive field **A**, with a black disk, results in action potentials of varying amplitudes in trace **A** with no response recorded in **B**. The opposite effect was observed when receptive field **B** was stimulated (not shown). The receptive fields of these multi-units were plotted on perimetric mapping co-ordinates (see chapter 3) to determine their size and location in visual space. Note that no artifactual cross-talk is apparent when the recording locations are in the same tectal lobe.

The bottom two traces were recorded simultaneously from opposite tectal lobes during stimulation of overlapping receptive fields with a black disk. In this case neuronal activity is recorded at both tectal locations in response to visual stimulation of the overlapping visual fields. The time base is longer (250msec) to allow the documentation of two consecutive visual stimulations. As the recordings are made from opposite tectal locations the pathways giving rise to these events are entirely separate. However, the time at which the activity occurs at both tectal locations seems to be correlated.

81

Non-overlapping fields
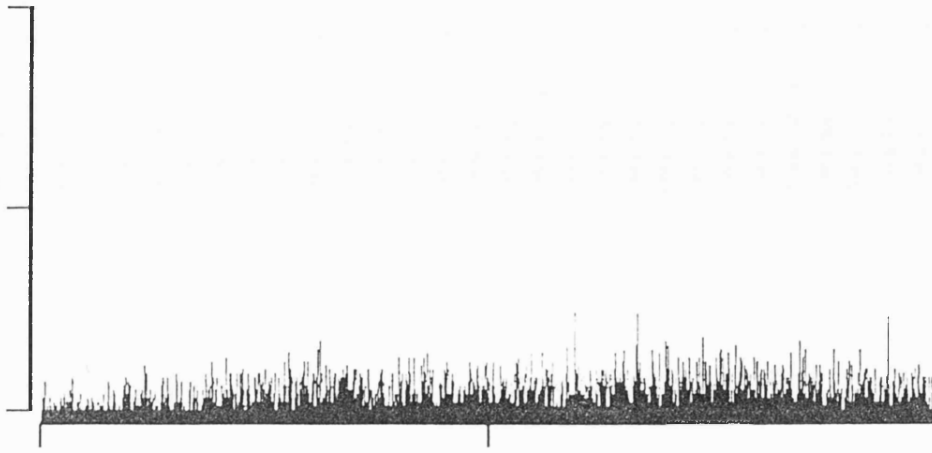
Overlapping fields
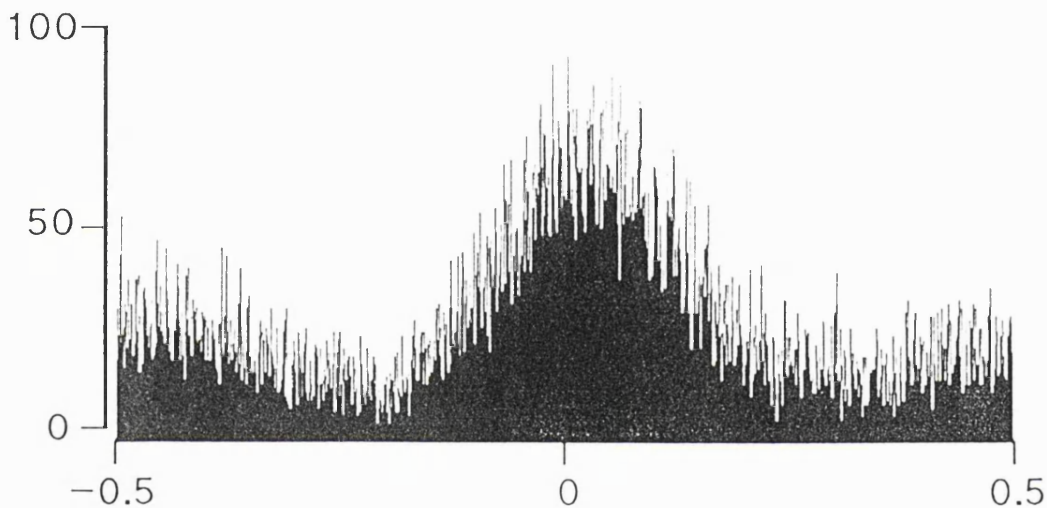
Figure 4.5. Cross-correlations calculated from non-overlapping and overlapping receptive fields during visual stimulation.

Event data was recorded simultaneously at two tectal locations (channel A & B) in response to a black disk moving through the receptive field. This timing data was used to construct a cross-correlation between the two separate sets of events. The algorithm adopted to construct the cross-correlation can be summarised; for each event in A calculate the time (over a period of ±0.5 seconds) at which events occur in B. This was calculated for all events in A which occurred over a 20 second period dividing the data into 500μsecond time bins. The cross-correlations describe the temporal relationship between events in A relative to those events in B.

For each plot the abscissa shows the time in seconds (±0.5sec) at which events were recorded. The number of events recorded in each of these 500μsecond time bins is shown on the ordinate scale. When the two MURFs are non-overlapping in visual space stimulation of one receptive field causes no activity at the other tectal location. The cross-correlation is flat with no central peak suggesting that neuronal activity at the two tectal locations is not correlated. When the two MURFs are overlapping activity at the two tectal locations is correlated. Stimulation of the overlapping portion of visual space causes activity at both tectal locations. Therefore, a central peak is produced in the cross-correlation around 0 seconds.

4.2.3. The acute effects of 1Hz stroboscopic illumination on correlated firing patterns in the tectum.

Simultaneous recording in response to constant 1Hz stroboscopic illumination from two tectal locations for a period of up to 2 hours was achieved in 12 animals. In 6 of the animals the two receptive fields were non-overlapping in visual space and in the other 6 they were overlapping (Table 4.1). In all overlapping receptive fields the cross-correlations, at the beginning of stroboscopic illumination, revealed a large central peak indicating synchronised firing behaviour. After prolonged exposure to stroboscopic illumination the number of events which occurred coincidently (*ie* at t = 0 seconds) increased indicating an improvement in the degree of correlation between the firing patterns recorded from these overlapping receptive fields (figure 4.6). Non-overlapping receptive fields revealed a different behaviour pattern to prolonged stroboscopic illumination. The CC at the start of stroboscopic entrainment was, in all cases, flat with no central peak but after longer periods of strobing a central peak at 0 seconds would appear (figure 4.7).
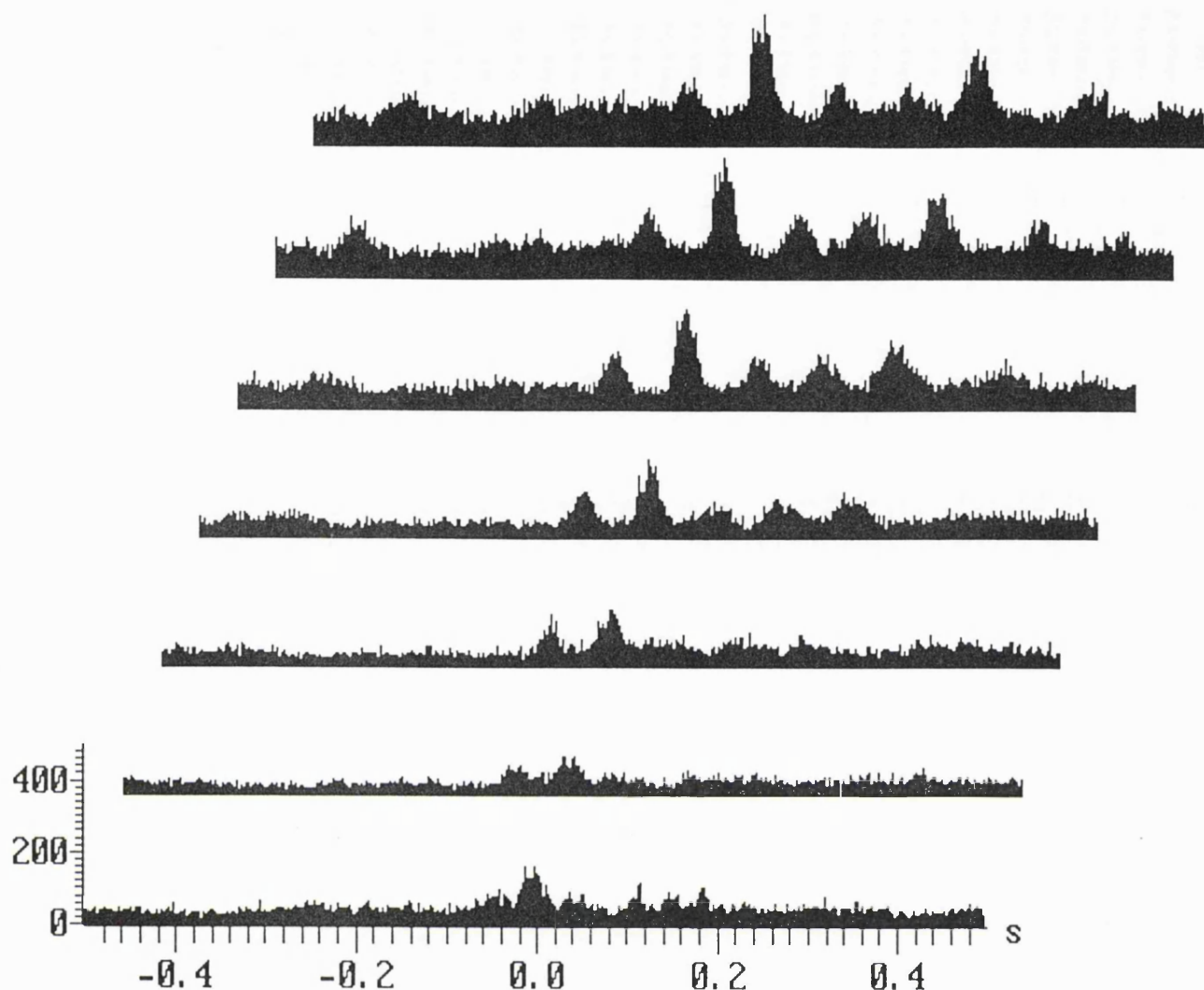
Figure 4.6. Cross-correlations calculated from overlapping receptive fields during 1Hz stroboscopic illumination.

Event data was simultaneously recorded from overlapping receptive fields. Cross-correlations were calculated at 15 minute intervals (consecutive correlelograms from bottom to top) during constant exposure to 1Hz stroboscopic illumination. The first graph was obtained during a 20 second period immediately following the initial exposure to stroboscopic illumination. The number of events occurring at a given time is depicted on the ordinate and the time at which these events occur is on the abscissa. A central peak is present in the first graph indicating correlation of firing patterns immediately on exposure to the strobe. This peak gets larger with continued exposure to stroboscopic illumination as do other peaks either side of the central peak at 0 seconds. For example a peak at +0.2 seconds is clearly visible after 1 hour of constant stroboscopic illumination. This implies that an event appears in one MURF which is consistently 200msec out of phase with the events in the second MURF. This stroboscopic entrainment effect was documented in the raster displays in figure 4.2. It is also apparent from this series of cross-correlation plots that the level of background gets greater during exposure to constant 1Hz stroboscopic illumination. This is consistent with the gradual increase in firing rate shown in the rate plots in figure 4.2 which were calculated from individual sustained, event and dimmer type MURFs during 1Hz stroboscopic illumination.
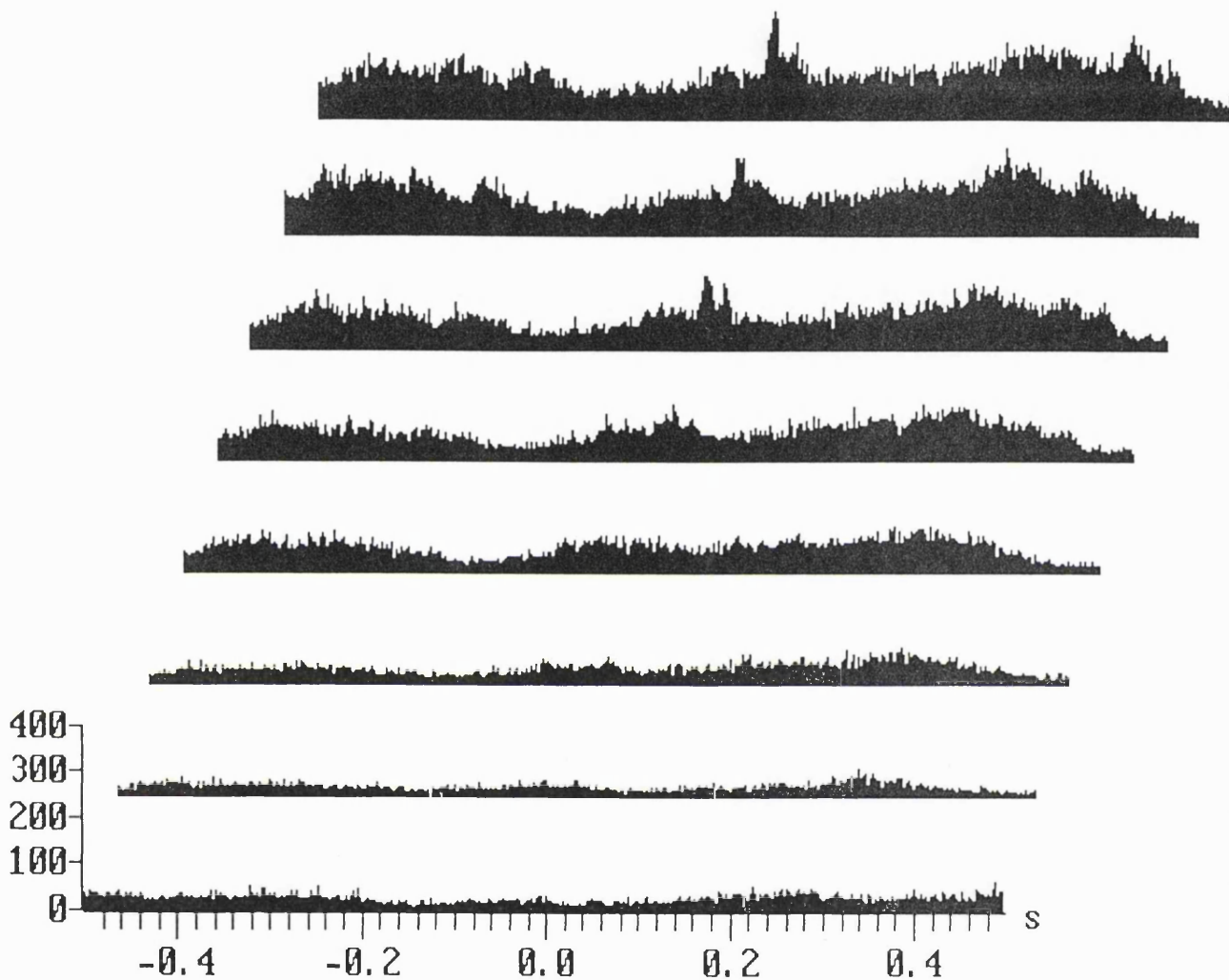
Figure 4.7. Cross-correlations calculated from non-overlapping receptive fields during 1Hz stroboscopic illumination.

In this experiment event data was simultaneously recorded from non-overlapping receptive fields. Cross-correlations were calculated at 15 minute intervals (consecutive correlelograms from bottom to top) during constant exposure to 1Hz stroboscopic illumination. The first graph was obtained during a 20 second period immediately following the initial exposure to stroboscopic illumination. Conventions are the same as figure 4.6. However, no central peak is present in the first cross-correlation which was calculated from the initial response to stroboscopic illumination. After 1 hour of constant stroboscopic illumination a central peak was observed in the correlelogram symptomatic of correlated neuronal activity.

4.2.4. The chronic effects of stroboscopic illumination on the developing retinotectal projection.

The retinotectal projection of animals reared in constant 1Hz stroboscopic illumination from stage 35-36 of larval life was assessed in a total of 16 animals aged at least 12 months post-metamorphosis. Control data was obtained from 14 animals reared in normal diurnal lighting to the same stage of development. A total of 370 receptive field positions, resulting from the direct retinotectal projection to each tectal lobe, were mapped in the strobe-reared animals. The topographic order in these maps was indistinguishable from those obtained from animals reared in normal diurnal lighting. The superior-inferior and nasal-temporal progression through visual space of receptive fields recorded from different tectal locations were no different from normal. Serial penetrations from rostral to caudal tectum still resulted in receptive field positions moving from temporal to nasal portions of the visual world whereas medial to lateral penetrations resulted in a progression from superior to inferior visual space. This visuotectal progression is a consequence of the retinotopic organisation of the direct retinotectal projection and was not affected by strobe-rearing.

The size of the MURFs which constitute the retinotectal projection were quantitatively measured. The size of event MURFs were recorded at one tectal location using computer control of the visual stimulus and analysis of the acquired spike data. Visual stimuli were moved systematically across a large television screen and the computer produced a two-dimensional matrix representation of the MURFs response to the stimulus. Pseudo-three-dimensional plots of this information are shown in figure 4.8. The x axis represents the nasotemporal dimension of the field, $\times$ the y axis the superoinferior dimension and the z axis the number of spikes evoked in response to stimulation of the corresponding $1.5° \times 1.5°$ of the visual field. The excitatory receptive field size of the MURF was considered to be that in which individual matrix elements were 10% or more of the maximum element size. The horizontal MURF diameter was measured from responses to vertical stimulus directions and the vertical MURF diameter from responses to horizontal movements. In a control group the average dimensions of MURFs were $28.4° \pm 6.3°$ in the vertical dimension and $23.9° \pm 4.4°$ (std, n=40) in the horizontal. When the MURF sizes of strobe-reared animals were calculated using this system the dimensions were $31.1° \pm 7.2°$ in the vertical and $24.3° \pm 3.3°$ (std, n=36) in the horizontal dimension. These values were not statistically significant (un-paired non parametric two tailed Mann-Whitney U-test) and so no quantitative difference between the MURF

size of control and strobe-reared animals could be found. It should also be noted that when MURF size was examined by marking the receptive fields out on a perimeter card using a 3cm diameter black disc to identify the extent of the receptive field an average MURF diameter of 26.6° ± 39.0° (std, n=19) was obtained in normal animals.

We also examined the relative distribution of sustained, event and dimmer type MURFs within the tectal neuropil in normal and strobe-reared animals. We found no difference in the relative distribution of these unit types within these two groups. In the control group a total of 64 radial penetrations of the tectum were made in 16 animals. 32 penetrations resulted in a sustained/event/dimmer combination of responses. So, a sustained type response was encountered first in the most superficial tectum and then an event followed by a dimmer type unit were recorded at progressively deeper tectal locations. In 21 penetrations a sustained unit was encountered first and then an event unit deeper in the tectum but no dimmer was found. In 10 penetrations an event unit was the first to be recorded followed by a dimmer unit and in 1 penetration a sustained unit was followed by a dimmer type response. The same distribution pattern was found in the 66 penetrations recorded from 31 strobe-reared animals. A sustained/event/dimmer combination was observed in 38 penetrations; a sustained/event combination in 15; an event/dimmer combination in 8 and a sustained/dimmer combination in 5 penetrations.
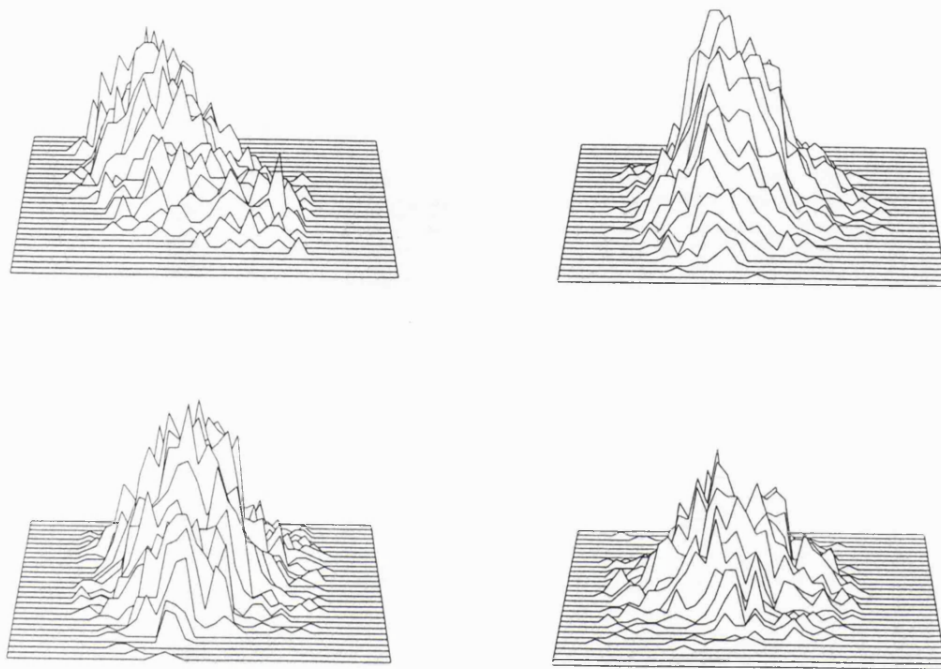
Figure 4.8. The effect of 1Hz stroboscopic illumination on MURFs recorded through the retinotectal projection.

Pseudo-three-dimensional plots of event MURFs. The top two plots were obtained from normal one year post-metamorphic animals. The bottom two plots were from animals reared in constant 1Hz stroboscopic illumination until on year post-metamorphosis from stage 35/36. The horizontal axis represents 64.5° of the nasotemporal field axis and the vertical axis represents 34.5° of the superoinferior field axis. The z ax records the number of events recorded in each 1.5° x 1.5° matrix element.

4.2.5. The chronic effects of stroboscopic illumination on the developing binocular visual system.

20 animals were reared in constant stroboscopic illumination from stages 55-58 of larval life until ~1 year after metamorphosis. In 12 of these animals sufficient data was available from the electrophysiological mapping experiments to compare the degree of registration exhibited in the binocular visuotectal projections (Table 4.2). The retinotectal and isthmotectal projections were mapped to both tectal lobes with at least 10 binocular inputs recorded at one tectal lobe. From a qualitative assessment of the alignment apparent between the retinotectal and isthmotectal projections 7 animals were totally normal (LNS4, LNS14, XSC21, XSC23, XSC24, XSC25, LRS8); 2 (LNS8, LRS18) showed indications of poor registration but were generally in good order; and 3 animals (LNS9, LRS6, LRS17) showed marked compression of the isthmotectal projection and poor registration with the retinotectal projection. Figure 4.9 shows the results from one of the 3 animals (LRS6) in which the isthmotectal projection was compressed in terms of the receptive fields location in binocular visual space. A depicts the retinotectal and isthmotectal projections to the right tectal lobe. The dorsal representation of the tectal lobe shows the position of the electrode penetrations from which the visual responses were recorded. The visual chart representations account the location of the retinotectal receptive fields (filled symbols) and the isthmotectal receptive fields (open circles) recorded at each tectal location. The progression through visual space is the same for the retinotectal and isthmotectal projections but the extent of the isthmoctectal projection is relatively restricted in space. This compression of the visuotectal projection, as conveyed by the isthmotectal pathway, is also observed in the binocular projection to the left tectal lobe in **B**.

The absolute disparity for binocular visual inputs recorded from a total of 15 strobe-reared animals was 13.7° ± 6.0° (std). In the 7 strobe-reared animals which appeared normal the absolute disparity was 9.0° ± 3.7°. In the remaining 8 animals the absolute disparity was 17.8° ± 4.3°. In the 16 control
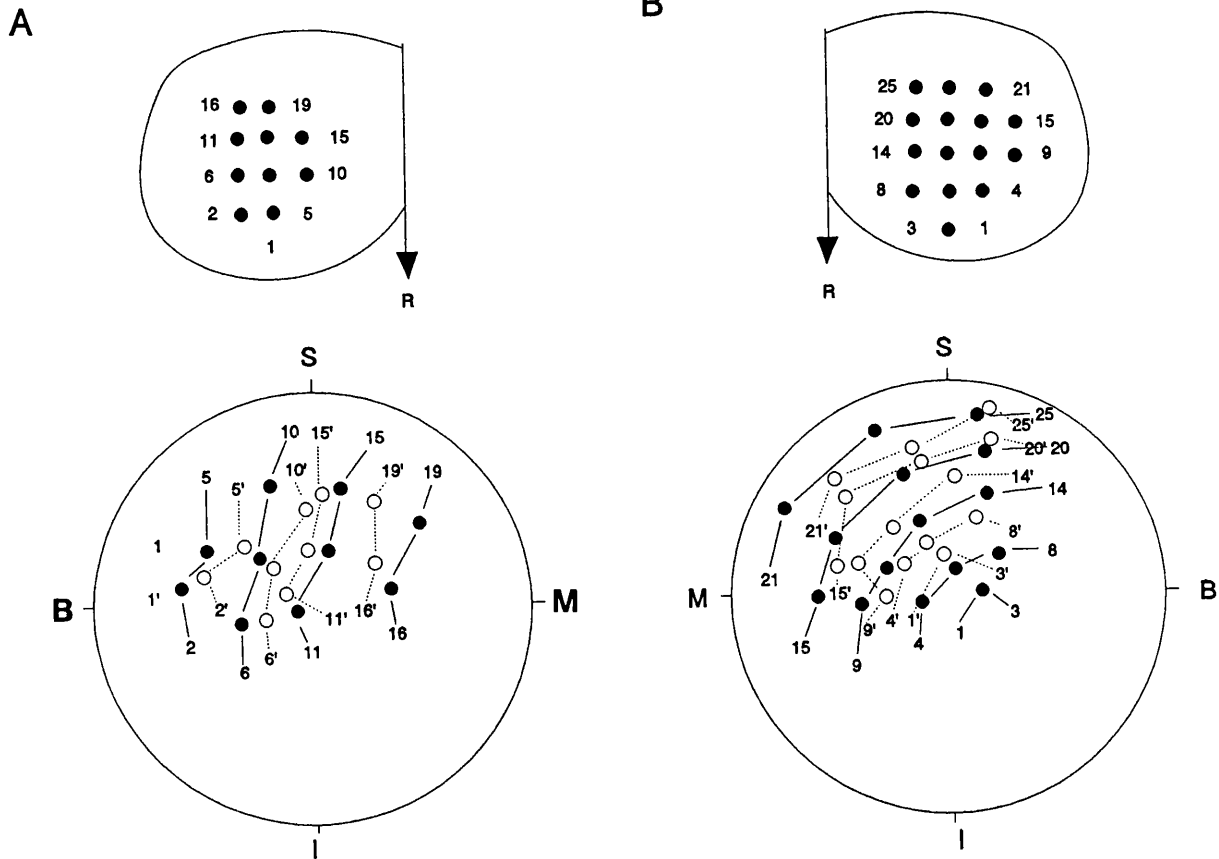
Figure 4.9. The results of mapping experiments illustrating how constant stroboscopic illumination can disrupt the ability of the intertectal system to adapt to normal changes in eye position.

Contralateral and ipsilateral visuotectal projections to the right (A) and left (B) tectal lobes of a strobe-reared animal. A dorsal representation of the tectal lobe shows the recording positions for this electrophysiological mapping experiment. The large circle denotes the perimeter card representation of the visual field. S,I,M & B are superior, inferior, monocular and binocular aspects of the visual field. During this experiment the optic axis of the left eye is aligned with the centre of the perimeter arc. The animal may be imagined positioned behind the chart representation with the optic axis of the left eye centred on the origin of the chart, looking out at the reader. The disc is the outline of a standard perimetric chart representing the visual field extending out for 100° of visual angle in all directions from the centre. The numbers in the visual field indicate the localized visual field position stimulation of which evoked activity at the corresponding tectal location. In the visual field representations filled symbols linked by solid lines represent the position of receptive field centres recorded via the retinotectal projection and open circles linked by dashed lines represent the position of receptive field centres recorded via the crossed isthmotectal projection.

animals, which were reared in normal diurnal lighting, the absolute disparity was 9.6° ± 2.5°. In contrast, the average absolute disparity obtained from 10 animals which had been reared in total darkness for a similar period was 26.6° ± 6.6°. The absolute disparity values from all 15 strobe-reared animals were compared with the values from the 15 control animals using a Mann-Whitney unpaired non-parametric test. A significant two-tailed p value of 0.042 was obtained. However, when the stobe-reared values were compared with those obtained following dark-rearing the two-tailed p value was extremely significant (p=0.0005) as was the p value obtained when comparing normal and dark-reared values (p<0.0001).

4.2.6. The chronic effects of stroboscopic illumination on intertectal plasticity following single eye rotation.

Of the 22 animals which received a single eye rotation at stage 55-58 of late larval life only 5 retained a rotation of 90° or more at the time of mapping (Table 4.2). In every animal there was a lack of registration between the dual binocular maps but there were cases in which the intertectal system did show signs of modification. Figure 4.10 illustrates the results of electrophysiological mapping experiments from one animals in which both projections to the left and right tectal lobe were mis-aligned by the degree of eye rotation apportioned. **A** shows the result of electrophysiological mapping of the right tectal lobe revealing that the left eye was rotated by approximately 180° (see the orientation of the retinotectal projection in figure 4.9 **A** for comparison). Constant stroboscopic illumination has totally disrupted the ability of the intertectal system to alter its synaptic connections to this degree of eye rotation. The approximate positions on the tectum at which neural activity was recorded is represented on a schematic of the tectal lobe. In the visual field chart the positions, at specified tectal locations, eliciting a response from the intertectal system are represented by the appropriate open symbols. Those eliciting a response from the retinotectal system, at corresponding tectal locations, are represented by filled symbols. **B** shows the retinotectal and isthmotectal input to the left tectal lobe. The retinotectal input to this lobe was not rotated (see the orientation of the retinotectal projection in figure 4.9 **B** for comparison) but because the isthmotectal input is relayed via the rotated left eye it is also 180° out of registration.

In the 5 animals a total of 163 isthmotectal inputs were electrophysiologically mapped of which 134 were in totally inappropriate positions in visual space indicating that, in the majority of cases, the intertectal system had not modified its synaptic

connections to accommodate for the rotation present in the retinotectal projection. However, it should be noted that in 2 of the 15 remaining animals the retinotectal projection from the left eye was found to be rotated by 75° or less indicating that only partial de-rotation had occurred in this eye. In these animals only 3 out of 72 isthmotectal inputs were out of alignment with the rotated retinotectal projection. The rotated eye in the remaining 13 animals had completely de-rotated so these animals were excluded from this study.
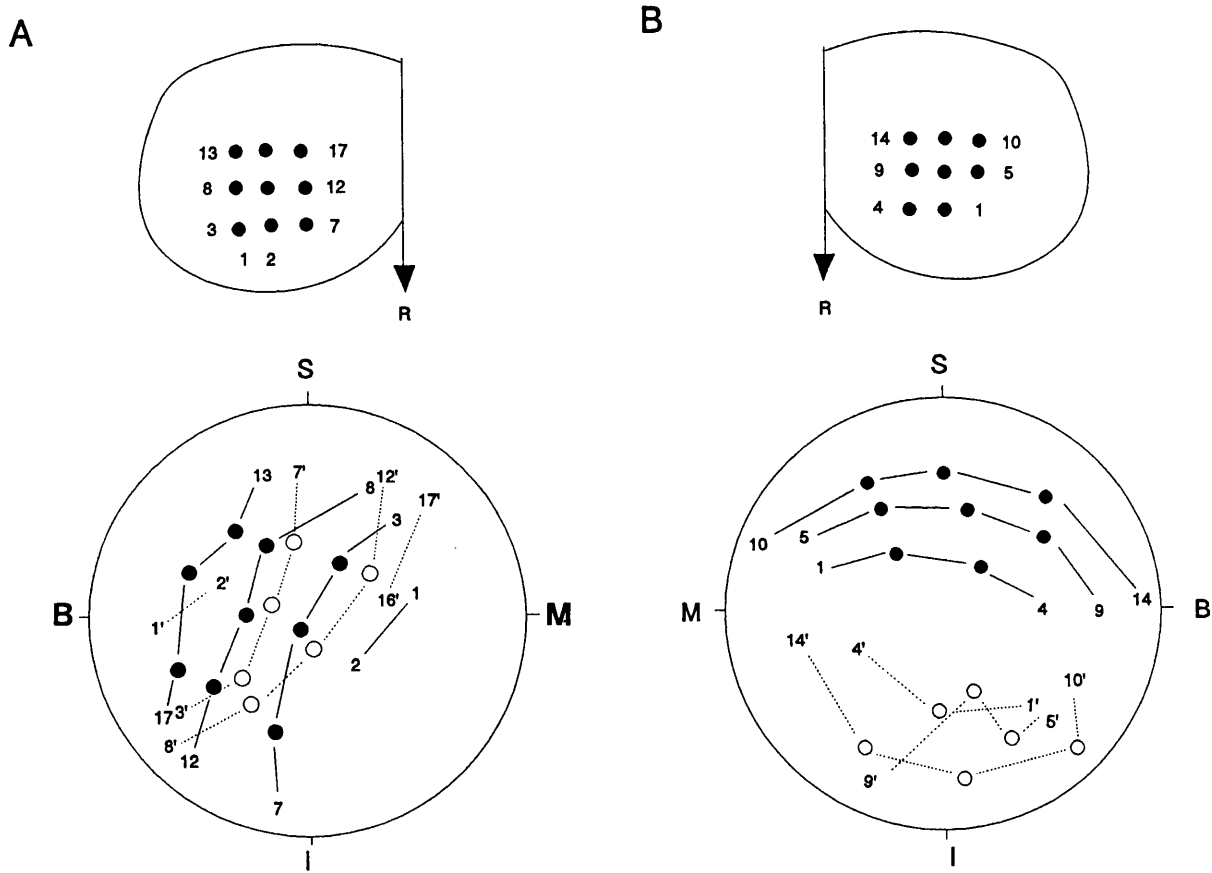
Figure 4.10. The results of mapping experiments illustrating how constant stroboscopic illumination can disrupt the ability of the intertectal system to adapt to a single eye rotation.

Contralateral and ipsilateral visuotectal projections to the right (A) and left (B) tectal lobes of a strobe-reared animal following a single eye rotation at stage 55/58 of development. Conventions are the same as figure 4.9.

4.3. Discussion

Prolonged exposure to stroboscopic illumination was shown to alter the firing patterns recorded in the tectum. This was true for sustained, event and dimmer type units (Hodos *et al*, 1982), which occupy different laminar distributions in the tectal neuropil, and was observed at strobe frequencies of 0.2Hz and 1Hz. However, at a strobe frequency of 0.2Hz spontaneous neuronal activity was not removed from these firing patterns. The detection of spontaneous neural activity could be an important factor in the initial elaboration of topographic maps and so a strobe frequency of 1Hz was used in subsequent experiments to remove this non-evoked activity from the tectum. Periodic and non-periodic bursting, of the type seen in response to each strobe flash, has been reported in the firing patterns of RGCs (Stiles *et al.*, 1985) but its function is uncertain. It has previously been shown (Chung *et al.*, 1973), using a different mode of analysis, that stroboscopic illumination alters the temporal characteristics of neural activity in the tectum but Chung *et al.* did not examine the effect this phenomenon would have on correlated firing patterns across the tectum. Visual stimulation of overlapping receptive fields did result in the correlation of firing patterns. More importantly, this was true for binocularly driven inputs to different tectal lobes. However, no indication of correlated firing was observed when the two inputs arose from non-overlapping receptive fields be they recorded from the same or opposite tectal lobes. This represents the first demonstration that visual stimulation in *Xenopus* results in correlated patterns of activity at those disparate tectal locations receiving matched binocular input.

1Hz stroboscopic illumination induced correlated firing between non-overlapping receptive fields indicating that constant stroboscopic illumination does entrain neural activity across the tectum. In constant stroboscopic illumination all points on the tectum, irrespective of whether or not they are binocularly driven, exhibit correlated patterns of neural activity. In the case of overlapping receptive fields, recorded from the same or opposite tectal lobes, it was noted that they immediately exhibited a large degree of correlation when exposed to stroboscopic illumination. A central peak in the correlelogram was observed when analyzing the initial firing patterns recorded from these tectal locations and the size of this peak would increase after prolonged exposure to stroboscopic illumination. Therefore, those points on the tectum receiving matched binocular input exhibited greater degrees of correlation in the strobe environment. In conclusion, the results from this feasibility study indicate that constant stroboscopic illumination, at a frequency of

1Hz, could provide an adequate visual environment for masking novel patterns of correlated neural activity across the tectum.

When *Xenopus* were strobe-reared from before the onset of visually driven activity no change in the topographic order of the retinotectal projection and no change in the average size of individual event-type MURFs was noted in the mature animal. The size of MURFs recorded through the retinotectal projection is believed to reflect the magnitude of the RGCs terminal arborization in the tectal neuropil. The more precise the retinotectal projection the smaller the calculated MURF size should be. However, the size of retinotectal MURFs recorded from normal animals was no different to that observed in strobe-reared animals. The distribution of sustained, event and dimmer units within the tectal neuropil was also the same in normal and strobe-reared animals indicating that no change had occurred in this aspect of the projections organization. Keating *et al.* (1986) reported that dark-rearing did not disrupt the topographic order, MURF size or laminar distribution of unit types in the retinotectal projection of *Xenopus*. This data challenges the importance of correlated patterns of spontaneous neural activity in the developing retinotectal projection in this species of frog. Neither visually driven or spontaneous neural activity seems to play a role in the normal development of the retinotectal projection in *Xenopus*.

The disruptions observed in the connections of the intertectal system, following prolonged exposure to stroboscopic illumination, were not as drastic as those seen when the animal was reared in total darkness. Dark-rearing totally obstructs the intertectal system in its attempts to make synaptic modifications following normal developmental changes in eye position. Prolonged dark-rearing during the critical period of development produces a lack of registration between binocular inputs (Grant and Keating, 1989b) and a characteristic compression of the isthmotectal visual projection. If stroboscopic illumination does interfere with the cues necessary for these changes then this environment should disrupt intertectal plasticity in an analogous manner to dark-rearing. The disorder we have described in the intertectal system of some strobe-reared *Xenopus* is reminiscent of that seen in visually deprived animals. However, this was not a consistent finding with the intertectal projections in 7 out of 12 animals appearing normal after strobe-rearing. However, statistical analysis of the absolute disparity values from all these animals did suggest that the alignment of the isthmotectal projection was significantly disturbed but the degree of this disruption was not as great as that observed following dark-rearing.

The capacity for intertectal plasticity to take place following a 90° or more

single eye rotation was disturbed by strobe-rearing with all 5 animals showing a severe lack of registration between isthmotectal and retinotectal inputs. However, if the eye rotation was less than 90° then quite substantial intertectal plasticity was observed following strobe-rearing with 69 out of 72 isthmotectal inputs in modified locations. This would not be the case with dark-rearing. This could reflect an inadequacy in the visual environment produced by stroboscopic illumination. The contrast information available during each strobe flash may be enough to facilitate minor changes but bot sufficient for the larger changes enforced by 90° eye rotations. However, the general trend of the data does support the hypothesis that detection of visually driven correlated patterns of neural activity contributes to the correct alignment of binocular inputs on each tectal lobe. Subsequent experiments examine the involvement of specific postsynaptic receptors of relevance to the coincidence detection hypothesis in this remarkable form of experience-dependent synaptic plasticity.

Correlated firing patterns in the tectal neuropil

Non-overlapping receptive fields:
maximum number of events at t=0 seconds

Control	Start	1 hour	% change
30	380	450	18.42
48	520	1020	96.15
5	350	280	-20.00
10	610	1300	113.11
12	3800	6100	60.53
4	40	225	462.50
		mean	121.79
		sem	64.84

Overlapping receptive fields:
maximum number of events at t=0 seconds

Control	Start	1 hour	% change
160	1100	2150	95.45
38	275	320	16.36
13	1500	1300	-13.33
60	1800	2500	38.89
430	480	600	25.00
4	185	470	154.05
		mean	52.74
		sem	22.82

Table 4.1. The acute effect of stroboscopic illumination on coincident neural activity calculated from the cross-correlation recorded simulataneously from two MURFs.

Strobe-rearing and normal binocular connections

Experiment	Retinotectal	Isthmotectal	congruent	incongruent	Absolute disparity
LNS4	19	16	16	0	7.2
LNS8	50	41	41	0	15.7
LNS9	36	29	7	22	24.0
LNS14	46	43	43	0	13.1
XSC21	68	65	65	0	8.3
XSC23	31	26	26	0	9.8
XSC24	16	10	10	0	5.5
XSC25	24	13	13	0	4.8
LRS6	48	44	18	26	18.7
LRS8	21	18	18	0	14.5
LRS17	39	33	24	9	13.7
LRS18	46	39	33	6	13.1
Total	444	377	314	63	
				Average	12.37
				Std	5.39

Strobe-rearing and single eye rotation experiments

Experiment	Retinotectal	Isthmotectal	congruent	incongruent	rotation(degrees)
LRS12	10	10	0	10	120
LRS13	88	75	10	65	120
LRS14	36	26	4	22	140
LRS15	41	35	2	33	180
LRS16	28	17	13	4	90
Total	203	163	29	134	
				Average	130.00

Table 4.2. The chronic effects of strobe-rearing on binocular visual connections in the optic tectum.

Chapter 5

Synaptic transmission *in vivo*

5.1. Introduction

The classification of postsynaptic excitatory amino acid receptors into non-NMDA (AMPA and kainate type glutamate receptors) and NMDA preferring is well established. Drugs that selectively block the NMDA recognition site, D,L-2-amino-5-phosphonovaleric acid (AP5), have been available for some time (Evans *et al.*, 1982). However, previous non-NMDA antagonists were relatively impotent and poorly selective (Collingridge *et al.* 1983a,b; Crunelli *et al.*, 1983; Koerner and Cotman, 1982). More recently, quinoxalinedione derivatives, such as 6-cyano-7-nitroquinoxaline-2,3-dione (CNQX), have been shown to be potent antagonists at non-NMDA receptor sites (Drejer and Honoré 1988; Honoré *et al.*, 1988) and have enabled a reasonable degree of selectively between NMDA and non-NMDA type glutamate receptors. Excitatory synaptic transmission in the CNS is lergely mediated by glutamate receptors with NMDA receptor being implicated in many forms of activity-dependent synaptic plasticity. However, it is evident from several studies in the mammalian CNS that NMDA receptors contribute to normal synaptic transmission (Crunelli *et al.*, 1987; Jones, 1987; Salt, 1986; Thomson *et al.*, 1985). It has recently been suggested that NMDA receptors are involved in retinotectal (Cline *et al.*, 1987) and intertectal plasticity (Scherer and Udin. 1989). In these experiments chronic exposure to an unknown concentration of AP5 was shown to block retinotectal and intertectal plasticity. However, we need to delineate the exact involvement of non-NMDA and NMDA type glutamate receptors in the transmission of visually elicited neural activity in the optic tectum. Do the chronic effects of AP5 merely reflect interference with normal synaptic transmission or do they reflect the blockade of a specific postsynaptic mechanism involved in neural development and plasticity?

First, we decided to investigate the effect of specific pharmacological antagonists on visually elicited neural activity in the optic tectum of the anaesthetized whole animal. Due to the arrangement of visual connections in lower vertebrates neural activity, originating from pre- and postsynaptic locations, can be recorded independently in response to visual stimulation. In the enucleated animal visually evoked activity recorded at the contralateral tectal lobe is largely presynaptic,

representing the firing patterns of terminal arbors in the retinotectal projection. The activity recorded at the ipsilateral tectal lobe is contingent upon synaptic transmission at the opposite tectal lobe and at another mid-brain nuclei: the nucleus isthmi (NI). Specifically, visually elicited activity at the ipsilateral tectal lobe represents firing patterns recorded from terminal arbors of the crossed isthmotectal projection (figure 1.1). Postsynaptic receptor antagonists were topically applied to the tectum to assess the role of specific receptor complexes in the processing of visual information in the tectum. What effect would these specific receptor antagonists have on the pre- and postsynaptic activity recorded in response to visual stimulation? The primary motivation was to establish whether, in *Xenopus laevis*, the transmission of visually elicited activity was mediated by glutamate receptors and if any aspect of this transmission required the activation of NMDA receptors. An important consideration in this study was to assess the role of the previously purported retinotectal neurotransmitter, acetylcholine, in the visual system of this frog.

5.2. Results

I. Physiology

The visual activity recorded at the contralateral tectal lobe, in this type of preparation, is believed to be predominately presynaptic in origin. Visually evoked activity recorded from the ipsilateral tectal lobe depends upon postsynaptic transmission through retinotectal synapses and thus affords an indirect assay of the receptors that mediate this transmission. In these experiments, visually evoked firing patterns were recorded simultaneously at the tectal lobes contralateral and ipsilateral to the remaining eye of acutely monocularly enucleated *Xenopus*. ON and OFF responses were recorded in response to an LED placed in the visual field of this eye. The exact time at which neural activity occurred at the two recording locations was recorded. Post-stimulus time histograms (PSTHs) were constructed from the information obtained from 10 consecutive stimulus presentations at a repetition rate of 1/30sec (figure 5.1). The ON and OFF responses were of very long duration. The ON response lasted 500msec post-stimulus but the OFF response consistently exhibited a late burst of activity 1 second or more after the stimulus. This periodic bursting property of visual responses in the tectum has been reported in the literature (Stiles *et al.*, 1985) and was noted in the previous chapter in response to stroboscopic illumination. Transient early, intermediate and late events could be clearly identified

in the PSTHs for both the ON and OFF response in the contralateral and ipsilateral tectal lobes.

The firing rate for the ON and OFF response was calculated by counting the number of events recorded during a 1 second period post stimulus. 10 consecutive responses were used to calculate the average firing rate. The spontaneous firing rate was calculated during a 25 second period between stimuli when no visually evoked activity was present in the recording. Due to the late bursting behaviour of visually evoked activity the response was not considered to have finished until at least 4 seconds after the LED had been turned off. The contralateral response as well as being greater in magnitude was considerably more robust than the ipsilateral response. The intertectal delay between the first response at the contralateral and the first response at the ipsilateral tectal lobe was 61msec $\pm$ 19msec (sem, n=10) for the ON and 45msec $\pm$ 8msec (sem, n=10) for the OFF response. The latency to first response was calculated when a minimum of 5 spikes had occurred in one 5msec time bin following 10 consecutive visual stimuli. Previous data (Scherer and Udin, 1991) reported much shorter intertectal delays of ~10msec in *Xenopus*. However, the different anaesthetic regimes coupled with dissimilar stimulus paradigms and independent recording apparatus could account for this discrepancy.
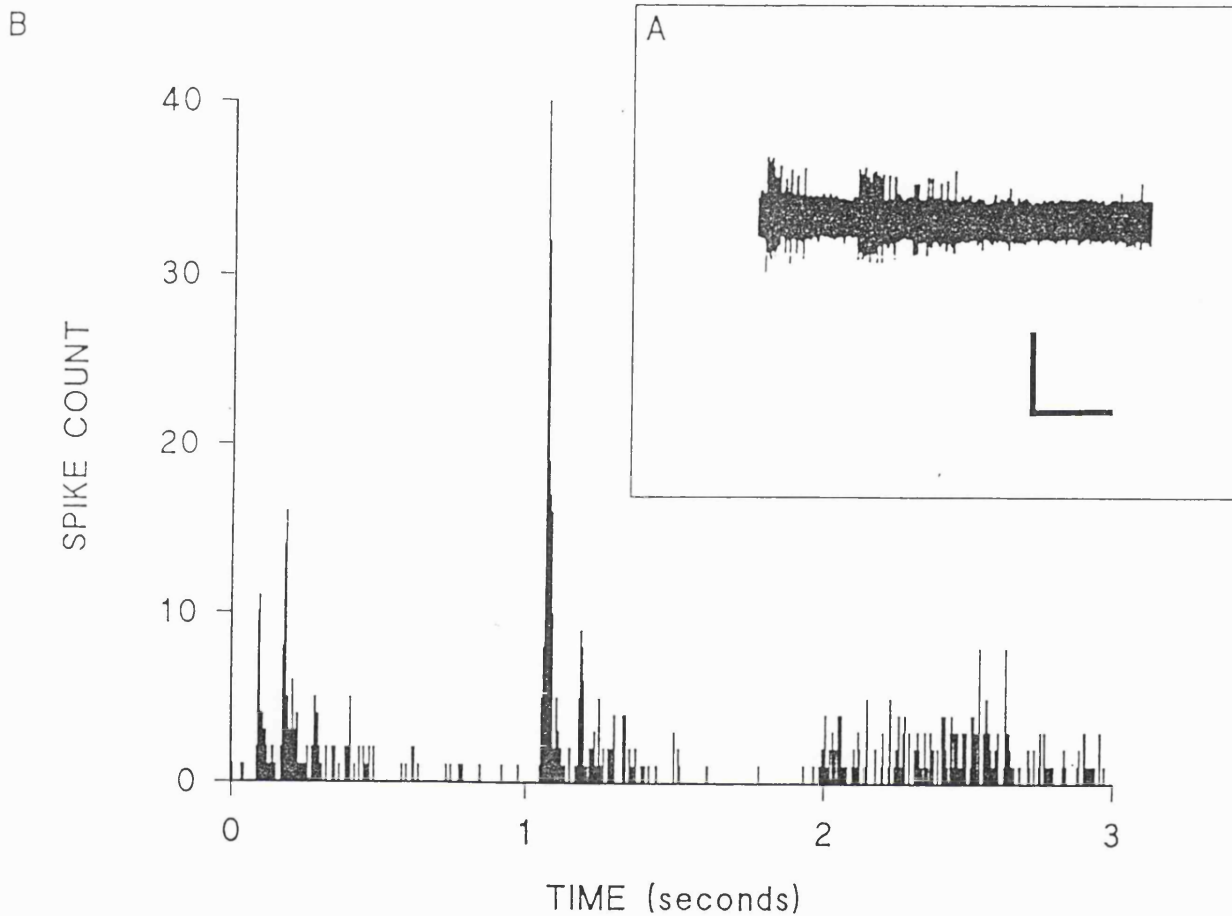
Figure 5.1. Example of an extracellular recording made from the optic tectum in response to visual stimulation and a post-stimulus histogram (PSTH) constructed from event data extracted from 10 consecutive tectal responses.

A is an oscilloscope trace of an extracellular recording from the optic tectum made in response to the ON and the OFF of an LED placed in the multi-unit receptive field (MURF) of the retinotectal projection. The scale bar represents a time base of 1 second and an amplitude of 1mV.

B is the post-stimulus histogram (PSTH) which was constructed from 10 consecutive responses. The event data was extracted from each extracellular recording using a window discriminator. The abscissa shows the time post stimulus at which the events occurred. The ordinate counts the number of events which occur in each 500μsecond epoch.

5.2.1. Control experiments.

7 animals were used in a control group to assess the stability of the preparation over time and following changes in normal perfusion medium. The average firing rate was calculated for the ON and OFF response recorded at each tectal lobe following 10 consecutive visual stimuli (see table 5.1). The average number of spikes per stimulus during the control period had to exceed 1 spike/stimulus before the data was included in the final analysis. Over a period of 1 hour the visually elicited responses remained at control levels for the contralateral ON response and the ipsilateral ON and OFF responses. However, a ~50% reduction was observed in the firing rate of the contralateral OFF response. This reduction was significant (p=0.02). The spontaneous firing rate was also calculated during the 25 seconds between each visual stimuli (Table 5.2). In the control series no significant change was observed in the contralateral or ipsilateral spontaneous firing rates. The average firing rates recorded in each experimental group were not significantly different when compared with control values (One-way analysis of variance, ANOVA).

II. Pharmacology

5.2.2. Effect of non-NMDA-type glutamate receptor antagonists.

The role of non-NMDA-type glutamate receptors in mediating visually elicited activity at the contralateral and ipsilateral tectal lobes was assessed by topical application of CNQX, a selective blocker of this receptor. The effect of 25μM CNQX was monitored in 7 animals (Table 5.1). This concentration was an order of magnitude above the effectve dose which will block 50% of a pure non-NMDA mediated response (ED$_{50}$) for this drug (~2μM; Lambert and Jones, 1990). A high concentration of CNQX was used in anticipation of the poor access conditions encountered in this whole animal preparation. However, in all 7 experiments a reduction in the ipsilateral firing patterns was observed in the presence of this drug with variable apparent effects on the contralateral firing patterns. In 5 of the 7 experiments abolition of visually evoked activity occurred at the ipsilateral tectal lobe. An example of this block is shown in figure 5.2. In this experiment, within a few minutes of drug application a large decrease in the visually evoked activity at the ipsilateral tectal lobe was observed with only slight reductions in the activity recorded at the contralateral tectal lobe. The average 34% and 20% reduction in the firing rate of the contralateral ON and OFF response was not statistically significant.

However, statistical significance was achieved for the 80% (p=0.03) and 75% (p=0.03) reductions observed in the firing rates for the ipsilateral ON and OFF responses. In 3 of the 7 cases, where an effect was seen at the ipsilateral tectum, the removal of the antagonist from the bathing medium did not result in recovery of the evoked response. Consistent with the effect of CNQX on the evoked activity, the ipsilateral spontaneous firing rate was also significantly (p=0.03) reduced (65%) with no significant reduction in the spontaneous rate of activity recorded at the contralateral tectal lobe (Table 5.2).
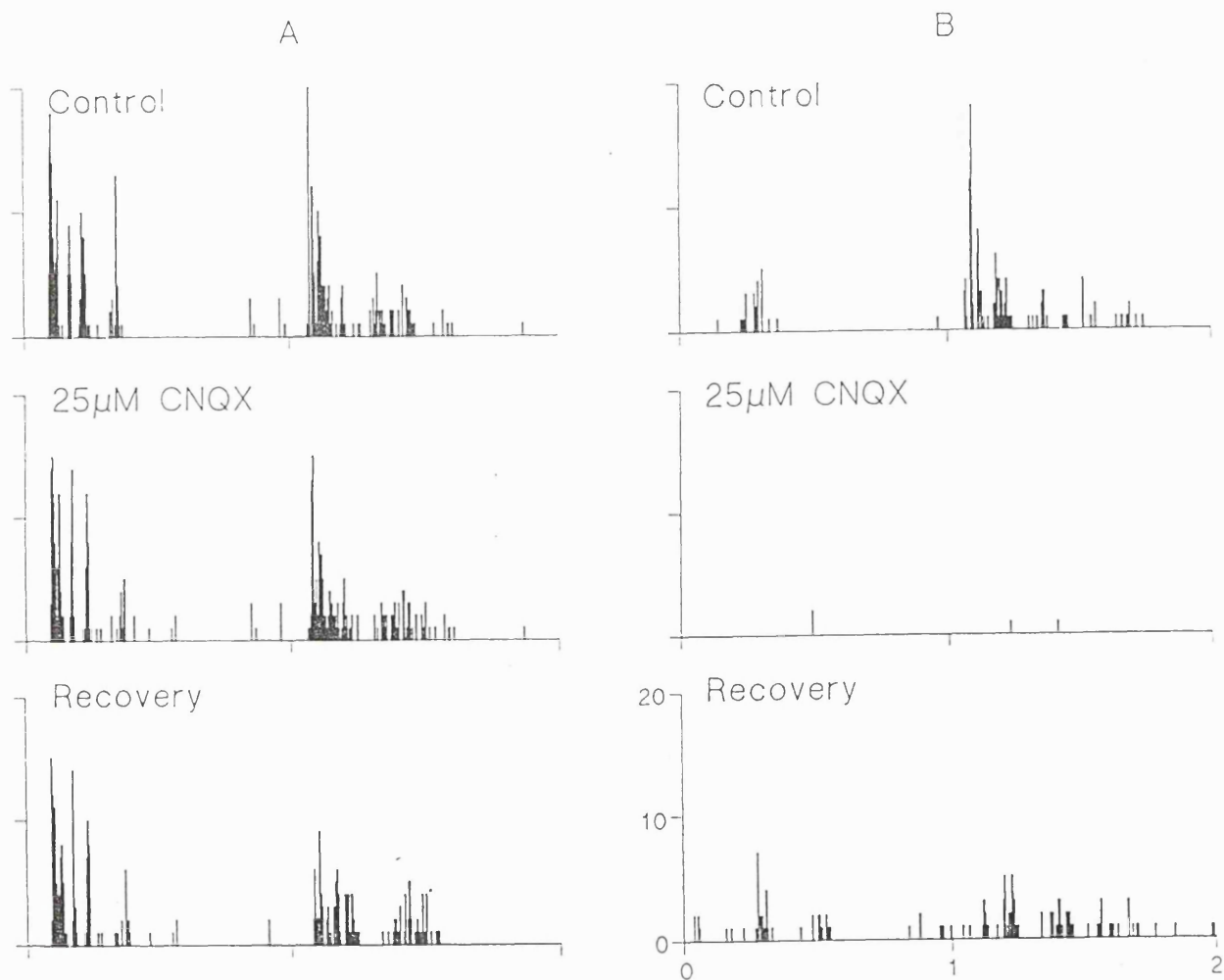
Figure 5.2. The effect of CNQX on PSTHs constructed from the visually evoked extracellular responses recorded at the contralateral and ipsilateral optic tectum.

Under general anaesthesia simultaneous recordings were made from the contralateral **A** and ipsilateral **B** tectal lobes of the enucleated animal. PSTHs were constructed from event data before, during and after the application of 25μM CNQX.

An LED was placed in the receptive field of the one remaining retinotectal projection. The LED was turned on for a 1 second period every 30 seconds and window discriminators were used to time events at both recording locations. The events from 10 consecutive responses were used to construct a PSTH. The abscissa shows the time at which events occur during visual stimulation. The LED was turned on at 0 seconds and off 1 second later. The ordinate depicts the number of events recorded during each 500μsecond period.

The control PSTH was calculated from 10 responses immediately before CNQX was applied to the exposed optic tectum. The effect of 25μM CNQX was assessed in the PSTH constructed from 10 responses following 20 minutes of exposure to the drug and finally, after 20 minutes of washing with normal control medium, the extent of recovery was established in the final PSTH.

5.2.3. Effect of NMDA-type-glutamate receptor antagonists.

5 preparations received a 250μM concentration of the NMDA receptor antagonist AP5. The dose of antagonist required to block 50% (ED_{50}) of the response to NMDA in mouse cultured hippocampal neurons was $\sim 1\mu$M D-AP5 (Benveniste *et al.*, 1990). In rat hippocampal slices D-AP5 had an ED_{50} of $\sim 7\mu$M when monitoring the depolarization elicited by ionophoretically applied NMDA (Harris *et al.*, 1984). The inactive L-isomer was reported to have little effect on the NMDA mediated response. Once again we started with a high concentration of antagonist to obviate any possible problem associated with poor access in this type of preparation. However, no change in the visually evoked or spontaneous activity recorded at either tectal lobe was noted in the presence of 250μM AP5 even though at this high concentration the NMDA antagonist could well be non-specific (see figure 5.3). Further analysis revealed an increase in the average firing rate for the contralateral ON and OFF response, of $\sim 100\%$ and $\sim 50\%$ respectively, but this effect was not statistically significant (Table 5.1). A large $\sim 90\%$ increase was also calculated in the spontaneous contralateral rate of activity but this was also not statistically significant. In the ipsilateral tectum a $\sim 40\%$ and $\sim 5\%$ increase was also observed in the ON and OFF response with a $\sim 20\%$ increase in the spontaneous activity. Once, again none of these changes were statistically significant.
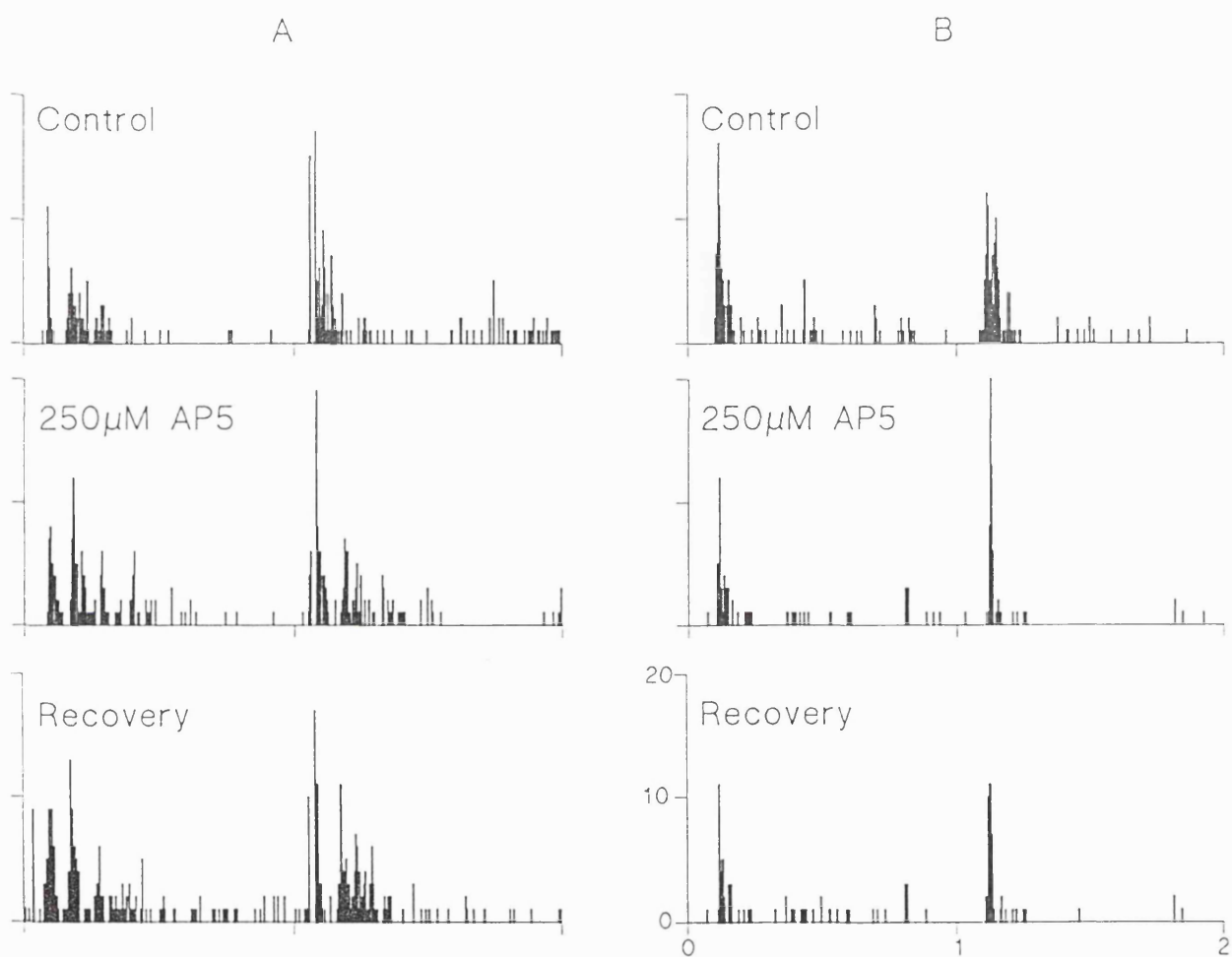
Figure 5.3. The effect of AP5 on PSTHs constructed from the visually evoked extracellular responses recorded at the contralateral and ipsilateral optic tectum.

Under general anaesthesia simultaneous recordings were made from the contralateral **A** and ipsilateral **B** tectal lobes of the enucleated animal. PSTHs were constructed from event data before, during and after the application of 250μM AP5.

An LED was placed in the receptive field of the one remaining retinotectal projection. The LED was turned on for a 1 second period every 30 seconds and window discriminators were used to time events at both recording locations. The events from 10 consecutive responses were used to construct a PSTH. The abscissa shows the time at which events occur during visual stimulation. The LED was turned on at 0 seconds and off 1 second later. The ordinate depicts the number of events recorded during each 500μsecond period.

The control PSTH was calculated from 10 responses immediately before AP5 was applied to the exposed optic tectum. The effect of 250μM AP5 was assessed in the PSTH constructed from 10 responses following 20 minutes of exposure to the drug and finally, after 20 minutes of washing with normal control medium, the extent of recovery was established in the final PSTH.

5.2.4. Effect of nicotinic and muscarinic receptor antagonists.

To investigate the role of cholinergic synaptic transmission in the optic tectum the nicotinic receptor antagonist D-Tubocurarine (D-TC) was topically applied to the tectal lobes of 13 animals. In the 4 preparations which received a 15μM concentration of D-TC it was difficult to identify any effect on any aspect of the evoked or spontaneous activity recorded at either tectal lobe. However, following further analysis (Table 5.1 and 5.2) it was shown that the average firing rate of the contralateral ON and OFF response was reduced by $\sim 50\%$ and $\sim 15\%$ respectively at this concentration of antagonist. At the ipsilateral tectal lobe the ON response was decreased by $\sim 20\%$ but the OFF response was increased by a similar amount. The spontaneous contralateral firing rate was also reduced, this time by $\sim 56\%$, but the level of spontaneous activity recorded at the ipsilateral tectal lobe was increased by $\sim 20\%$. Due to the large standard deviation associated with these changes no statistically significant effects were observed in the contralateral and ipsilateral firing rates. At a higher 250μM concentration 7 out of 9 animals exhibited increases in some aspect of neural activity recorded from the contralateral tectal lobe. This increase in the visually evoked contralateral activity can be observed in the representative example shown in figure 5.4. However, even with the $\sim 125\%$ increase calculated for the contralateral ON response the error associated with the average was too great to allow statistical significance to be reached. The $\sim 300\%$ increases in the contralateral spontaneous activity, with 250μM D-TC, were caused by the emergence of very pronounced phasic discharges in the portion of the recording which normally consisted of random spontaneous activity. The frequency of these phasic discharges varied between preparations (figure 5.5). Similar changes were observed in the level of spontaneous activity recorded from the ipsilateral tectal lobe. However, visually evoked activity at the ipsilateral ectal lobe was decreased by $\sim 35\%$ for both the ON and OFF response. In contrast to the rather erratic results obtained with D-TC the muscarinic receptor antagonist, atropine sulphate (Hulme *et al.*, 1978), even at 100μM dose had no effect on any aspect of the firing patterns recorded in this preparation (n=4).

A   B
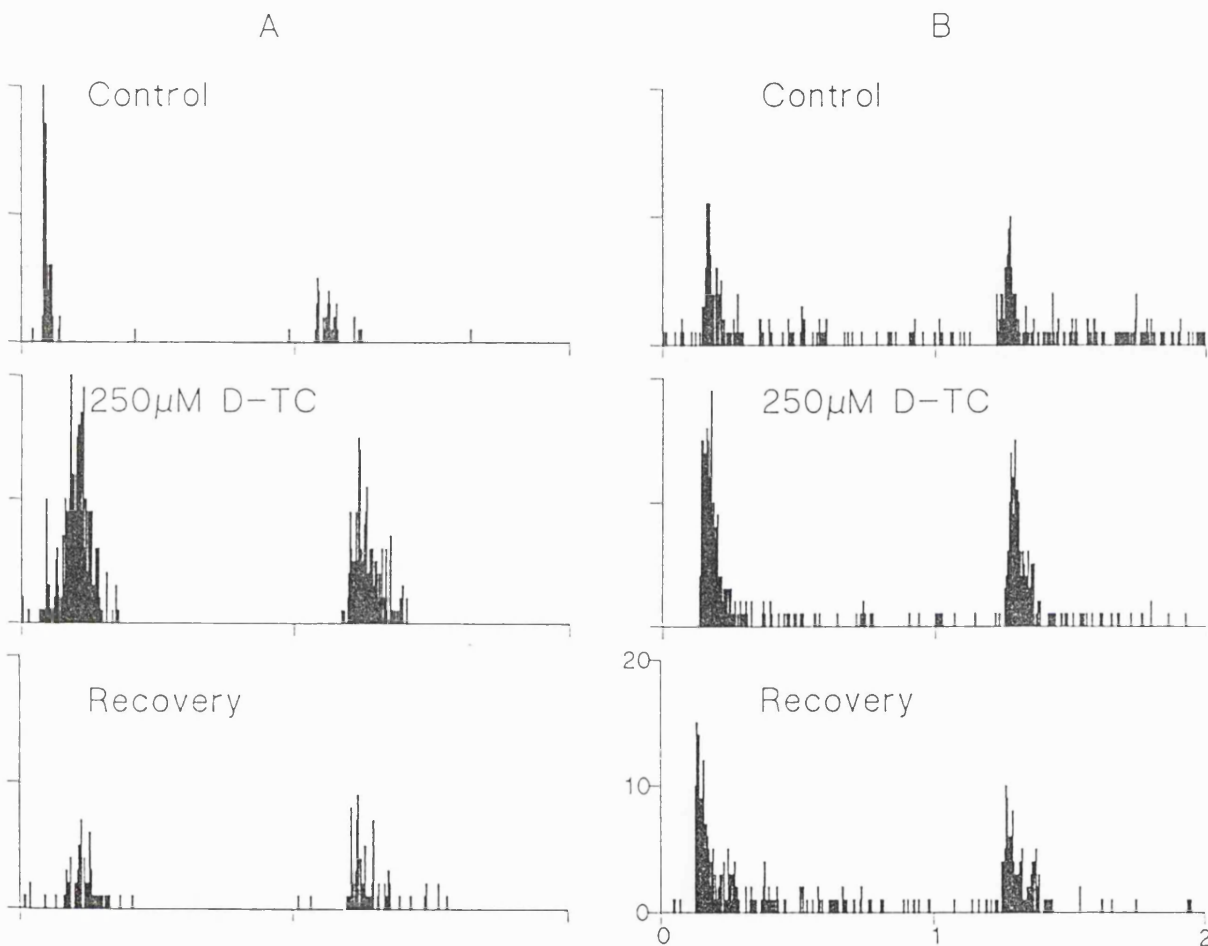
Figure 5.4. The effect of D-Tubocurarine on PSTHs constructed from the visually evoked extracellular responses recorded at the contralateral and ipsilateral optic tectum.

Under general anaesthesia simultaneous recordings were made from the contralateral A and ipsilateral B tectal lobes of the enucleated animal. PSTHs were constructed from event data before, during and after the application of 250μM D-TC.

An LED was placed in the receptive field of the one remaining retinotectal projection. The LED was turned on for a 1 second period every 30 seconds and window discriminators were used to time events at both recording locations. The events from 10 consecutive responses were used to construct a PSTH. The abscissa shows the time at which events occur during visual stimulation. The LED was turned on at 0 seconds and off 1 second later. The ordinate depicts the number of events recorded during each 500μsecond period.

The control PSTH was calculated from 10 responses immediately before D-TC was applied to the exposed optic tectum. The effect of 250μM D-TC was assessed in the PSTH constructed from 10 responses following 20 minutes of exposure to the drug and finally, after 20 minutes of washing with normal control medium, the extent of recovery was established in the final PSTH.

109
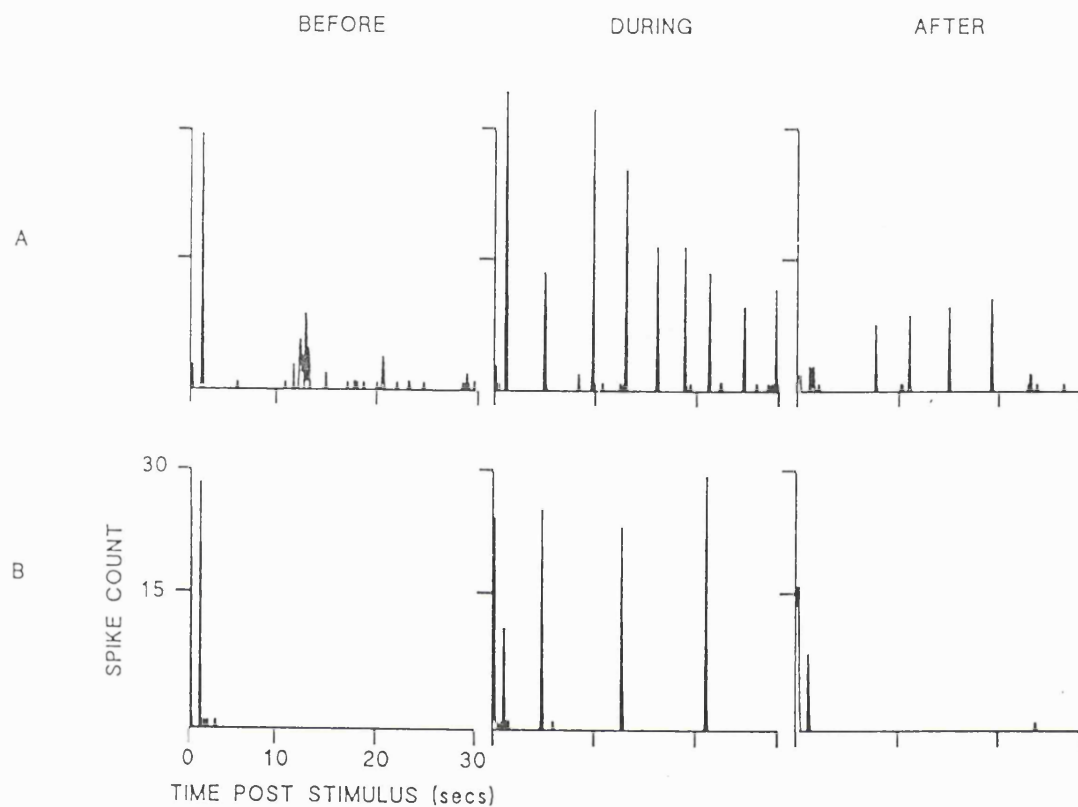
Figure 5.5. Examples of phasic discharges induced in the spontaneous firing patterns which were recorded in the optic tectum following the application of D-Tubocurarine.

Under general anaesthesia simultaneous recordings were made from the contralateral tectal lobe of the enucleated animal. PSTH's were constructed from event data before, during and after the application of 250μM D-TC.

An LED was placed in the receptive field of the one remaining retinotectal projection. The LED was turned on for a 1 second period every 25 seconds and window discriminators were used to time events at both recording locations. The events from 10 consecutive responses were used to construct a PSTH. The abscissa shows the time at which events occur during visual stimulation. The LED was turned on at 0 seconds and off 1 second later. The ordinate depicts the number of events recorded during each 0.001 second period.

110

5.3. Discussion

The antagonists which have recently been developed for the non-NMDA and NMDA type glutamate receptors are potent and highly selective enabling a reliable characterisation of glutamatergic synaptic transmission to be made. At a 25μM concentration, the non-NMDA type glutamate receptor antagonist CNQX, produced a significant reduction in visually elicited postsynaptic activity recorded from the ipsilateral tectal lobe. This was true for both the ON and OFF response and a significant reduction was also observed in the ipsilateral spontaneous activity. The NMDA type glutamate receptor antagonist, AP5, even at a 250μM concentration, did not reduce any component of the evoked or spontaneous response. The results of these experiments suggest that visual information is transmitted between the two tectal lobes via non-NMDA type glutamate receptors. This further supports the hypothesis that the effects of chronic AP5 treatment on retinotectal and intertectal synaptic plasticity reflect interference with a specific postsynaptic mechanism.

The site of CNQX action following topical application of the antagonist to the tectal surface is unclear. We know that presynaptic neural activity recorded via the retinotectal projection is not affected by topical application of CNQX and so the possibility that synaptic transmission is impeded at the retina is ruled out. The tectal neuropil lies immediately below the surface of the tectum but the effects of CNQX in our preparation may not reflect the blockade of retinotectal synaptic transmission. If synaptic transmission at the NI is governed by non-NMDA receptors then the reduction in activity at the ipsilateral tectum, in the presence of CNQX, may reflect the blockade of synaptic transmission at this site and not at synapses in the contralateral tectal lobe. However, the deep location of the NI makes this unlikely. Autoradiographic localisation of glutamatergic binding sites have confirmed the excitatory amino acid involvement in the circuitry of the optic tectum of *Xenopus* (Henley *et el.*, 1991). Therefore, it is possible that CNQX is blocking retinotectal synaptic transmission. Specific NMDA receptor activity has also been reported in layer 9 of the optic tectum in *Rana pipiens* (McDonald *et el.*, 1989). NMDA receptor function could be subserved for specific postsynaptic mechanisms concerned with experience and activity-dependent synaptic plasticity within the tectum.

We currently believe that the extracellular activity recorded from the contralateral tectal lobe following visual stimulation is presynaptic in origin. It is presumed that this electrical activity represents the arrival of action potentials at the densely arranged

terminal arbors of retinal ganglion cell axons. Therefore, the multi-unit activity recorded from the tectum merely reflects the firing properties of RGCs (Maturana *et al.*, 1960). Similarity between the response properties of RGCs and recordings made from the tectal neuropil has reinforced this general opinion. Also, anatomical data demonstrates that there are very few soma in the superficial layers of the tectum, this being the major site of afferent termination onto the apical dendrites of tectal neurons. This conclusion is also supported by the results we obtained with CNQX. This receptor blocker had no significant affect on the activity recorded from the contralateral tectal lobe but decreased the activity recorded from the ipsilateral tectum. However, the suggestion has recently been made that a portion of the electrical transients recorded from the superficial tectum represent action potentials generated postsynaptically in the apical dendrites of tectal neurons (Grant and Lettvin, 1991). This conclusion was based upon the interpretation of extracellular recordings and as such is not very satisfactory. However, in light of this suggestion it is interesting to note that during the experiments described in this Chapter postsynaptic receptor antagonists had, in some cases, apparent effects on the activity recorded from the contralateral tectal lobe. These observations could strengthen the hypothesis that these electrical transients reflect postsynaptic activation of tectal neurons. However, the large fluctuations that occur in tectal firing rates during experiments of this kind makes interpretation of this type of data very difficult. For example, in the control group (Table 5.1) a significant ~50% reduction in the contralateral OFF response was observed in the absence of any pharmacological agent. In the ipsilateral tectum, following application of 15μM D-TC the ON response increased at the same time as the OFF response decreased. There is no reason to believe that these two ipsilateral responses should be generated by very different postsynaptic events and so it is difficult to attribute any significance to these data.

Previous *in vivo* studies on the optic tectum of goldfish concluded that retinotectal transmission was nicotinic (Freeman *et al.*, 1980). In these previous studies the nicotinic antagonist α-bungarotoxin produced a complete block of retinotectal synaptic transmission. Some doubt has been cast on the validity of these results with the suggestion that impurities exist in the purified toxin. Studies using D-TC reported no such block (Stevens, 1973; Schmidt and Freeman, 1980; Langdon and Freeman, 1987) but all report a prolongation of the evoked response and phasic bursting in the spontaneous activity indicative of loss of inhibition. In our experiments, at a 15μM concentration of D-TC, no significant change was observed in either the evoked or

spontaneous activity recorded from either tectal lobe. Only at a 250μM concentration did we observe a large increase in the evoked contralateral response and the spontaneous contralateral and ipsilateral activity. The increase in the spontaneous activity was a reflection of the phasic discharge phenomenon which was first reported by Stevens (1973). Monoclonal antibody studies, generated against nicotinic acetylcholine receptors, suggest a presynaptic localisation of nicotinic receptors on RGC axons in the optic tectum (Sargent *et al.* 1989). The changes in firing patterns observed in the contralateral tectal lobe could reflect a loss of presynaptic inhibition due to the blockade of these receptors. The existence of nicotinic neurotransmitter systems in the optic tectum has also been studied using immunohistochemical methods to assay choline acetyltransferase activity. These experiments suggest a role for nicotinic mechanisms in the intrinsic circuitry of the tectum linked with a strong nicotinic input from the NI (Ricciuti and Gruberg 1985, Migani *et al.* 1980; Zotilli *et al.*, 1988). In view of this information it is interesting that in the presence of D-TC the visually evoked firing patterns of the isthmotectal input were consistently reduced in the ipsilateral tectal lobe. However, once again due to the large fluctuations normally present in this assay no statistical significance could be attached to these changes. Also, the concentration of antagonist required to produce this effect was high and so it is also possible that the loss of inhibition reflects non-specific antagonism of an inhibitory input such as that mediated by γ-Aminobutyric acid (GABA) receptors, which are present in the tectum (Arakawa and Okado 1989; Antal, 1991). Indeed, Curtis *et al.* (1974) have shown that GABA mediated inhibitory effects in spinal interneurons and Renshaw cells of the cat can be antagonised by D-TC. It was not surprising that the muscarinic antagonist, atropine sulphate, had no effect on visually elicited activity in the tectum as a previous study (Frances *et al.*, 1980) has shown that muscarinic receptor activity was not affected in the deafferented retinotectal pathway.

A more sensitive assay of synaptic transmission within the optic tectum is required to evaluate more precisely the role of NMDA and non-NMDA receptors in retinotectal synaptic transmission. The role of nicotinic receptors within the tectum is also speculative and so an *in vitro* preparation of the optic tectum is needed to investigate retinotectal synaptic transmission further. Therefore, we developed an *in vitro* preparation of the optic tectum in which postsynaptic responses could be recorded following controlled pharmacological manipulation.

Control

	n	% change	std	significance
contralateral on	6	-12.19	32.56	N/S
contralateral off	7	-51.45	20.95	0.02
ipsilateral on	7	-13.34	40.99	N/S
ipsilateral off	7	-12.36	27.18	N/S

25uM CNQX

	n	% change	std	significance
contralateral on	6	-34.00	37.27	N/S
contralateral off	6	-20.34	27.14	N/S
ipsilateral on	6	-80.28	21.95	0.03
ipsilateral off	6	-74.81	30.92	0.03

250uM AP5

	n	% change	std	significance
contralateral on	5	99.04	66.81	N/S
contralateral off	5	49.61	100.76	N/S
ipsilateral on	5	43.23	89.77	N/S
ipsilateral off	5	4.82	42.12	N/S

15uM D-TC

	n	% change	std	significance
contralateral on	4	-52.19	26.15	N/S
contralateral off	4	-15.75	80.15	N/S
ipsilateral on	4	-24.06	26.99	N/S
ipsilateral off	4	20.71	52.60	N/S

250uM D-TC

	n	% change	std	significance
contralateral on	7	125.94	142.60	N/S
contralateral off	5	20.99	72.71	N/S
ipsilateral on	3	-33.94	34.38	N/S
ipsilateral off	3	-35.00	78.81	N/S

Table 5.1. Change in visually evoked activity recorded from the optic tectum.

The average firing rate was first calculated from 10 consecutive responses to visual stimuli before and after a given perturbation. The % change in firing rate was determined from these values and also the statistical significance of the change was established using a paired non-parametric two-tailed t-test.

114

Control

	n	% change	std	significance
contralateral	7	-2.50	61.38	N/S
ipsilateral	7	4.29	56.93	N/S

25uM CNQX

	n	% change	std	significance
contralateral	6	51.72	116.07	N/S
ipsilateral	6	-65.26	26.87	0.03

250uM AP5

	n	% change	std	significance
contralateral	5	93.82	91.11	N/S
ipsilateral	5	21.00	36.19	N/S

15uM D-TC

	n	% change	std	significance
contralateral	4	-56.34	26.99	N/S
ipsilateral	4	20.71	52.60	N/S

250uM D-TC

	n	% change	std	significance
contralateral	7	299.47	420.53	N/S
ipsilateral	3	355.17	620.57	N/S

Table 5.2. Change in spontaneous activity recorded from the optic tectum.

The average spontaneous firing rate was first calculated during 10 consecutive periods of quiescence before and after a given perturbation. The % change in firing rate was determined from these values and also the statistical significance of the change was established using a paired non-parametric two-tailed t-test.

Chapter 6

Synaptic transmission *in vitro*

6.1. Introduction

The development of a physiologically viable *in vitro* preparation of the optic tectum would allow more controlled pharmacological classification of tectal synaptic transmission. An *in vitro* preparation containing an isolated portion of the frog brain, for use in electrophysiological experiments, was first described by Libet and Gerard (1939). Sometime later, Teylor *et al.*, (1981) described an *in vitro* preparation of the goldfish optic tectum in which neurophysiological and biochemical properties could be examined. Since then numerous studies have utilised *in vitro* preparations of the optic tectum to study retinotectal synaptic transmission. In these studies the effect of various antagonists was monitored on extracellular field potentials recorded from the tectal neuropil in response to electrical stimulation of the optic nerve or tract. Responses of this type are caused by the laminar synaptic activation of radially oriented neurons and reflect the transient potential difference which is set up by the extracellular current flow between the cell bodies and the synaptic inputs (Nicholson and Freeman, 1975). In the goldfish, *Carassius auratus*, Langdon and Freeman (1986 & 1987) showed a complete reversible block of this postsynaptic response using the non-NMDA excitatory amino acid antagonists Kyurenic acid but no disruption in synaptic transmission was observed with the potent NMDA receptor antagonist AP5; with or without Mg^{2+} ions present. However, Deusen and Meyer (1990) did report a partial suppression of the field potentials recorded from goldfish optic tectum in the presence of AP5. Nistri *et el.* (1990) found no indication of NMDA mediated retinotectal synaptic transmission in the frog *Rana temporaria*. Also, the recent work of Debski *et al.* (1991), using a cannulated tadpole preparation has not been able to demonstrate an NMDA receptor mediated event in field potentials recorded from the tectum of *Rana pipiens*. Their results indicate a bizarre increase in the amplitude of this postsynaptic response in the presence of AP5. The only demonstration that the NMDA receptor mediates synaptic transmission in *Rana pipiens* comes from the observation that increases in intracellular Ca^{2+}, in cultured tectal neurons, are mediated by the direct activation of NMDA receptor channels (Cline and Tsien, 1991).

An *in vitro* preparation of the optic tecum in *Xenopus laevis* was developed so that extracellular field potentials could be recorded from the tectal neuropil in response to electrical stimulation of the optic tract. The physiological integrity of this *in vitro* preparation was assessed by direct comparison with the physiological results obtained from a previous *in vivo* preparation (Chung *et al.*, 1974a,b). Response latencies, strength response curves, depth profiles, paired pulse experiments and response to tetanic stimulation were carried out on this *in vitro* preparation. The postsynaptic nature of these responses was further clarified by monitoring the effect of various ion substitutions on the electrically evoked tectal field potential. Pharmacological experiments were then undertaken to investigate the role of various postsynaptic receptor complexes in tectal synaptic transmission. The *in vitro* studies cited so far have not used the more selective non-NMDA antagonist CNQX (Honoré *et al.*, 1988) to distinguish between NMDA and non-NMDA mediated synaptic transmission. Moreover, none of these studies have investigated synaptic transmission in the optic tectum of *Xenopus laevis*. The primary motivation for this study was to investigate the role of NMDA and non-NMDA mediated synaptic transmission in the optic tectum of *Xenopus*.

6.2. Results

I. Physiology

Extracellular field potentials were recorded *in vitro* from the superficial layers of the *Xenopus* optic tectum in response to electrical stimulation of the optic tract. When recordings were made from the surface of the tectum two pronounced negative deflections were elicited similar to those reported *in vivo* (Chung *et al.*, 1974a). These were identified as the U1 and U2 responses, with latencies to peak amplitude of 9.6 ± 2.0 msec (std, n=61) and 29.1 ± 4.8 msec (std, n=55) respectively (figure 6.1). The earlier U1 response could be identified in all 181 preparations examined so far but the later U2 response was only evident in 144 preparations. That is, the U2 response was never observed in the absence of the U1 response. The exact placement of the stimulating and recording electrode was critical for the successful recording of the U2 response. However, in all experiments the recording electrode was placed in the rostral half of the tectum where the binocular visual field is represented. It was also possible to identify earlier so called M1 and M2 responses but these were not as prominent as the later events and were not sufficiently isolated from the rest of the trace to be reliably examined. In all illustrated traces stimulus artifact has been

117

removed from the recordings and negativity is downwards. In a few cases it was also possible to discern an even longer latency event which occurred subsequent to the U2 response. This very long latency response has not been commented on *in vivo* but was only ever present in the early stages of these experiments or following the removal of Mg^{2+} ions.

The strength-response curves for the U1 and U2 responses were in accordance with the results of Chung *et al.* (1974a). In all 37 preparations examined the threshold for the U2 response was at a higher stimulus intensity than that of the U1 response (figure 6.2). In the pharmacological experiments described in this study the stimulus intensity was set to supra-threshold intensity for the U2 response. In 35 preparations the U1 and U2 response was recorded at different tectal depths following supra-threshold stimulation of the optic tract. In all cases the U1 potential was most pronounced at the surface of the tectum (50-100μm) and the U2 response attained maximal negativity at a depth of $\sim$150μm (figure 6.3). Radial penetrations of the tectum with the microelectrode resulted in a reversal of the waveform from a negative to a positive going polarity at approximately 300μm below the pial surface. We interpret this reversal as being due to the variation in the recording position with respect to the active current sink, the synaptic input, and the passive current source, which corresponds to the cell body layer. The reversal of the field potential at the cell body layer is taken as evidence for the postsynaptic nature of these responses. These *in vitro* depth profiles were identical to those reported previously *in vivo*.

The only results which were not in full accordance with the previous *in vivo* study involved paired pulse stimulation of the optic tract. A conditioning stimulus, of threshold intensity for the U2 response, was delivered to the optic tract and the peak amplitude of the U1 and U2 response recorded at a depth of 150μm in the tectal neuropil. A test shock, of equivalent strength, was then delivered to the tract at a specified inter-stimulus interval. In 10 preparations inter-stimulus intervals between 100 and 1000msec were used in stimuli applied to the optic tract (figure 6.4). In all 10 preparations the U1 peak amplitude was potentiated at these inter-stimulus intervals in accordance with previous *in vivo* data. The peak amplitude of the U2 response was depressed at all inter-stimulus intervals between 100msec and 1000msec. This effect was not noted in the earlier *in vivo* experiments (Chung *et al.* 1974a) which reported a facilitation in both the U1 and U2 response at similar inter-stimulus intervals.

In a series of control experiments the % change in the U1 and U2 peak amplitude was calculated over a 1 hour period to assess the stability of the preparation

over time. An average 6.5% ± 2.2% (n=10, std) increase in the U1 peak amplitude and a 4.0% ± 4.7% increase in the U2 peak amplitude was observed in these control experiments. This change not statistically significant (paired non-parametric two-tailed t-test).
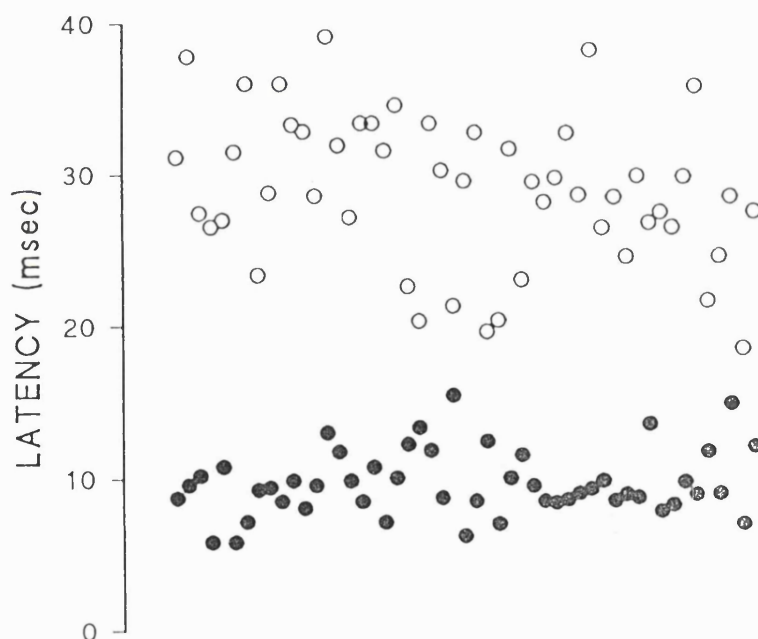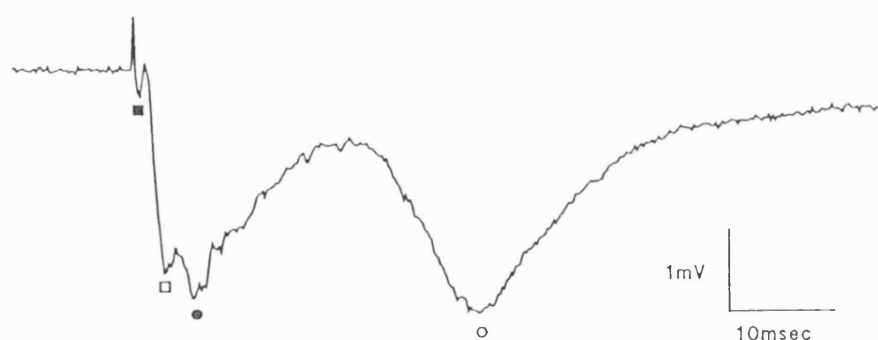
Figure 6.1 A typical field potential recorded at a depth of 150μm in the tectal neuropil in response to electrical stimulation of the optic tract *in vitro*.
        In this example a rectangular pulse 50μsec in duration, 100mA and 8V in amplitude was used to elicit this supra-maximal response. The stimulus artifact has been removed from the trace and negativity is downwards. Early M-type responses (open and solid rectangles) are elicited within the first 5msec post-stimulus. The U1 response (solid circle) occurred at ~10msec post-stimulus and the U2 response (open circle) had a latency to peak of ~30msec. The latency to peak amplitude for the U1 (filled circle) and U2 response (open circle) from 51 separate preparations have been plotted.

119
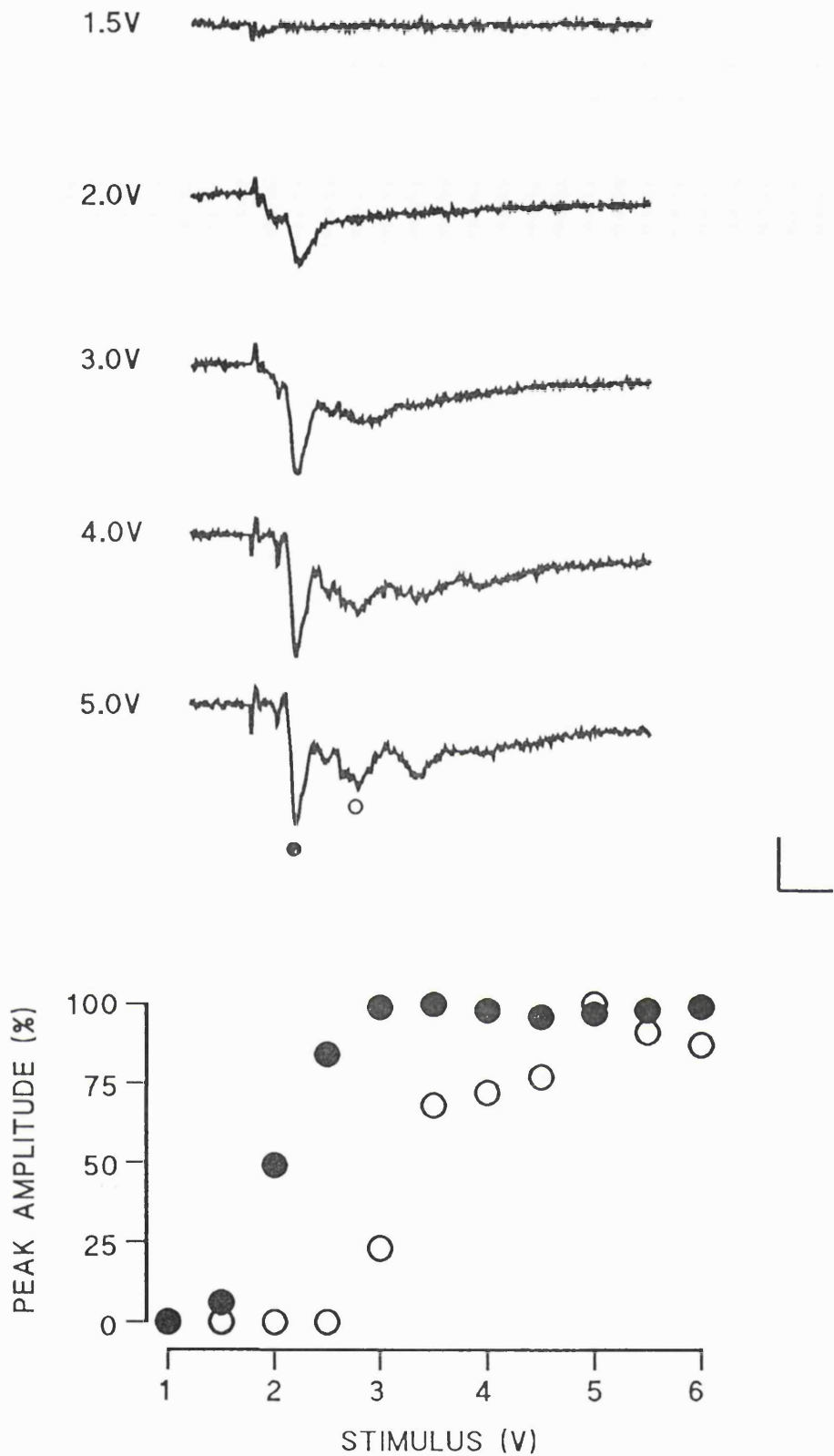
Figure 6.2 The effect of increased stimulus strength on the peak amplitude of the U1 and U2 response recorded 150μm below the pial surface.

In this example the voltage applied during a constant 50μsec, 100mA stimulus pulse to the optic tract was varied between 1 and 6V. In the top half of the figure representative traces are shown in which the stimulus artifact has been removed and negativity is downwards. At a stimulus intensity of 1.5V early negative deflections were observed. At 2.0V a distinct U1 response (filled circle) was present with no later U2 response. At 3.0V the U2 response (open circle) was evident but this did not reach maximal amplitude until 4.0V. In this example a later response occurring at ~40msec post-stimulus was also present at a 5.0V stimulus intensity.

120
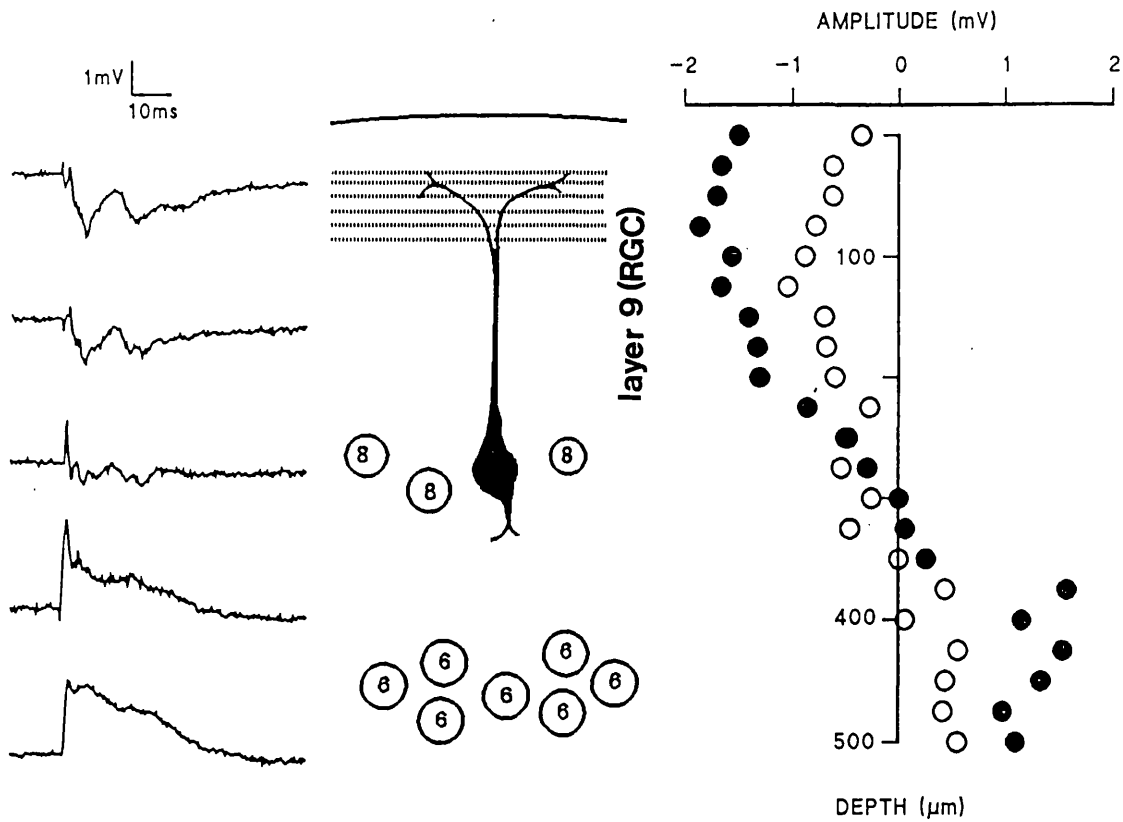
Figure 6.3 Effect of a radial penetration through the tectal neuropil.

This composite figure illustrates a phenomenon common to all field potentials recorded from highly laminated structures such as the optic tectum. The left side of the figure consists of a series of responses recorded during a radial penetration of the tectum. The top trace was recorded at $100\mu m$ below the pial surface and shows two marked negative deflections at $\sim 10msec$ and $\sim 30msec$. The trace recorded at $300\mu m$ shows the negative polarity potentials about to reverse polarity. At $400\mu m$ all the responses are now positive deflections.

The middle schematic demonstrates how this reversal phenomenon is related to the architecture of the tectal neuropil. The retinal ganglion input makes the majority of its synaptic contact with the apical dendrites of tectal neurons in the superficial fibre layer 9, which spans approximately the first $200\mu m$ of the tectal neuropil. The first cell body layer, layer 8, is situated $\sim 300\mu m$ below the pial surface approximately at the depth where the field potentials reverse polarity.

The right half of the figure shows in greater detail from a different experiment how the amplitude of the U1 response (filled circle) and U2 response (open circle) varies with the recording position of the microelectrode. Note how the reversal of both responses takes place at $\sim 300\mu m$ in accordance with the *in vivo* findings of Chung *et al.* in 1974.

121
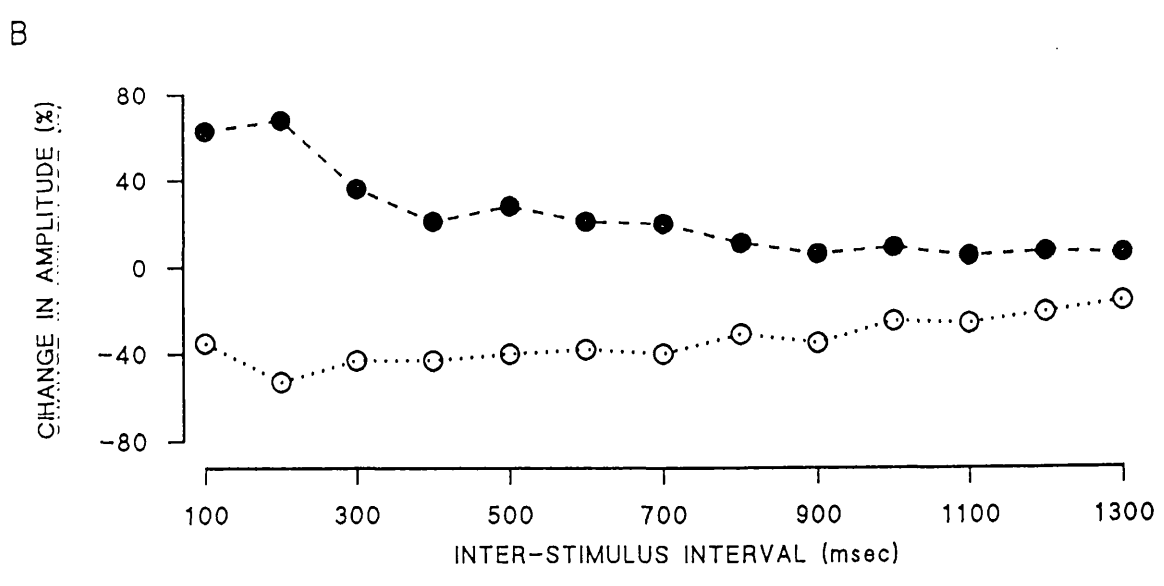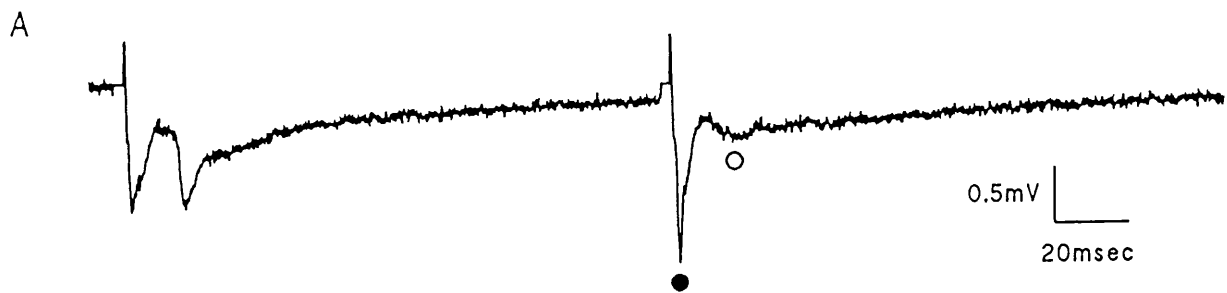
Figure 6.4 The effect of paired pulse stimulation on the amplitude of U1 and U2 responses.

The optic tract was electrically stimulated at different paired pulse intervals to determine the nature of the U1 and U2 response. Recordings were made from the tectal neuropil at a constant depth of 150μm.

A shows the result of a paired pulse experiment in which an inter-stimulus interval of ~ 150msec was used. The early U1 response (closed circle) was clearly facilitated and the later U2 response (open circle) depressed at this particular inter-stimulus interval.

B summarises the results from a series of experiments in which paired pulsing was performed with inter-stimulus intervals ranging from 100 to 1300msec. The percent change in the peak amplitude of the U1 response (filled circles) and U2 response (open circles) are shown at the different inter-stimulus intervals chosen. The U1 response was facilitated at all inter-stimulus intervals between 100 and 1300msec whereas the U2 response was depressed.

This result is consistent with the hypothesis that the U1 response reflects mono-synaptic activation and the U2 response reflects poly-synaptic activation of tectal circuitry.

122

6.:.2.1. Effect of anoxia.

To assess the nature of the extracellular responses, recorded in response to opptic tract stimulation, the O_2/CO_2 supply to the frog ringer was removed (figure 6.5 A).). Postsynaptic responses should be preferentially effected by this procedure but evventually presynaptic responses should also be removed. Recordings were made at a coonstant $150\mu m$ depth and the optic tract was stimulated 1/50sec. Robust U1 and U2 reesponses were recorded for a control period of 1 hour and then the O_2 supply to the tisssue was removed. After ~40 minutes all negative deflections were lost from the evvoked response. The U1 and U2 responses were the first to be reduced by oxygen reemoval (circles) with the earlier M type responses (star) the last deflections to be affffected. The full irreversible effects of anoxia took at least 30 minutes to become appparent.

6.:.2.2. Effect of removing Ca^{2+} or Mg^{2+} ions from the bathing medium.

Once a reliable U1 and U2 response was achieved the normal frog ringer was exxchanged for a notionally Ca^{2+} or Mg^{2+} free frog ringer.

In the 2 preparations examined in Ca^{2+}-free medium, at a tectal depth of $1550\mu m$, all negative deflections were abolished from the response after a 40 minute peeriod (figure 6.5 B). The effects of Ca^{2+} ion removal could be reversed when the prreparation was returned to normal frog ringer. The U1 and U2 responses were the firrst to be abolished by Ca^{2+} ion removal, with the earlier M waves the last to disappear.

In another group of experiments, in which the normal frog ringer was replaced byy a notionally Mg^{2+}-free solution, all 13 preparations exhibited elevated postsynaptic reesponses. In 8 preparations the peak amplitude of the U1 and U2 response could be maeasured before and after the removal of Mg^{2+} ions. The remaining 5 preparations beecame epileptiform with very erratic and convulsive field potentials resulting in a loøss of all evoked activity. In the 8 preparations which did not become epileptic the prrocedure resulted in a 5.6% ± 5.2% increase in the peak amplitude of the U1 reesponse and a 34.4% ± 4.5% increase in the U2 response. The changes observed in thee U1 response were varied, ranging from a 23% reduction to a 27% increase in peeak amplitude and the average change observed in the U1 response was not siegnificant. However, the U2 response was consistently and significantly ($p < 0.001$) inccreased in all 8 preparations. The results from one of these experiments (figure 6.6) illtustrates this selective increase in the peak amplitude of the U2 response. This

increase was reversed when the preparation was returned to a normal 1.5mM Mg^{2+} containing frog ringer.
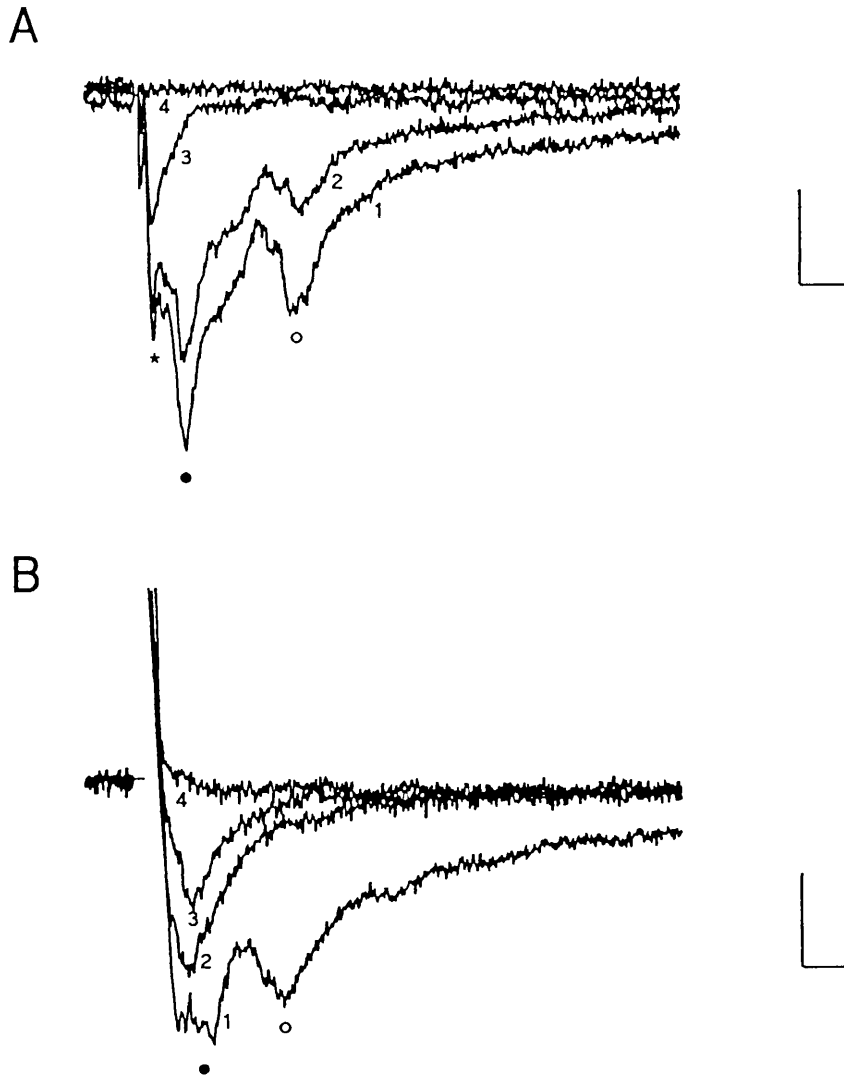
Figure 6.5. Effect of anoxia and Ca^{2+} ion removal on postsynaptic responses recorded from the tectal neuropil.

A. Supra-threshold stimulation of the optic tract initially elicited a robust field potential (trace 1) which included the U1 (filled circle) and U2 (open circle) response. Earlier events were also identified in the trace (star). The O_2/CO_2 supply was turned off and the effect of anoxia was first noted ~30 minutes later (trace 2). The later U1 and U2 responses were the first to be affected and were completely removed by 40 minutes (trace 3). The earlier M responses were the last to be abolished leaving a completely flat record post-stimulus (trace 4).

B. A similar effect was observed when the normal frog ringer, containing 2.5mM Ca^{2+}, was replaced by a notionally Ca^{2+} free solution. In this experiment supra-threshold stimulation of the optic tract elicited a robust field potential (trace 1). The U1 and U2 responses (filled & open circle) were the first to be abolished by Ca^{2+} ion removal after ~30 minutes (trace 2) and by 40 minutes all responses were lost (trace 4). Scale bar = 15msec, 1mV
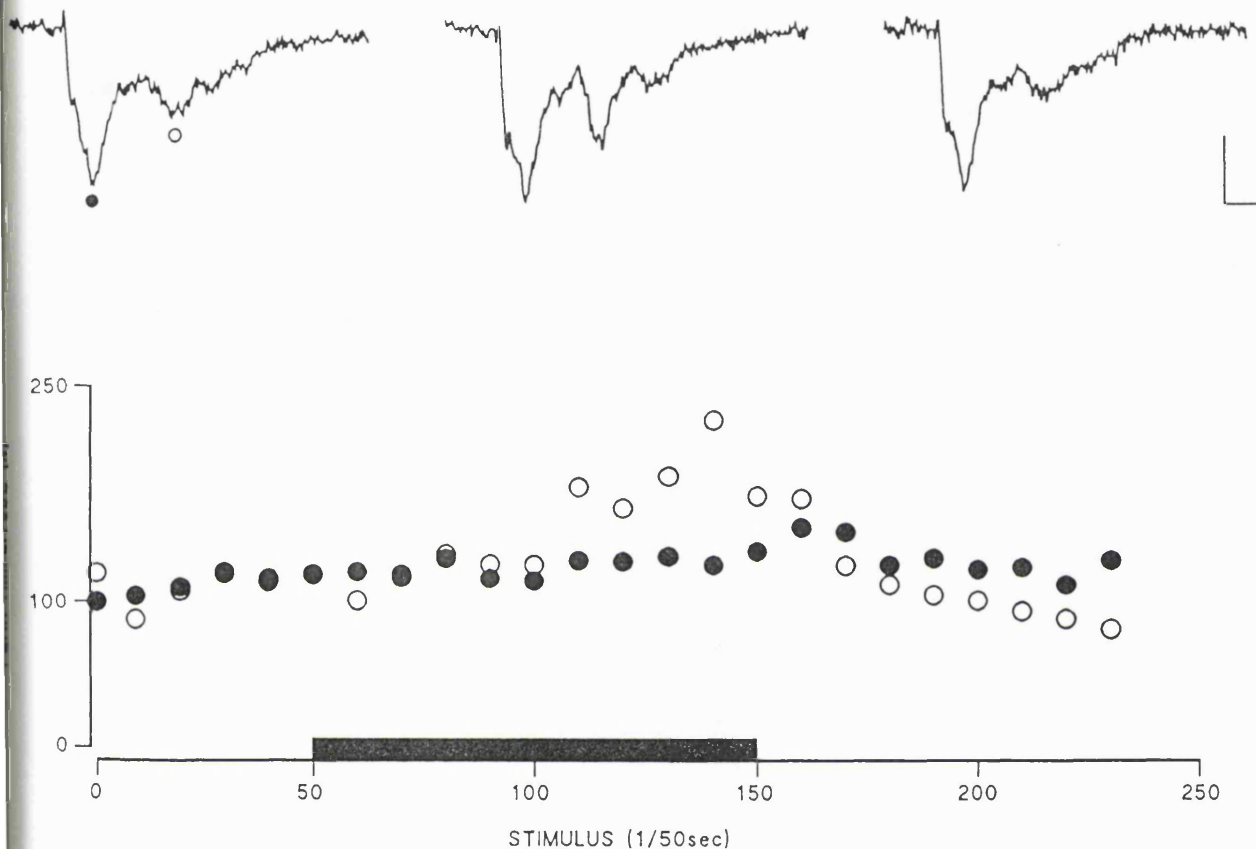
Figure 6.6 Effect of Mg^{2+} ion removal on the peak amplitude of the U1 and U2 response.

The top 3 traces result from identical supra-threshold stimulation of the optic tract. In the left hand trace a U1 (filled circle) and U2 (open circle) response was elicited in the presence of 1.5mM Mg^{2+} ions. The preparation was then exposed to Mg^{2+} free frog ringer. After 30 minutes the middle trace shows how, in this single experiment, the peak amplitude of the U2 response has been increased by the removal of Mg^{2+} ions with little effect on the earlier U1 response. When the preparation was returned to normal 1.5mM Mg^{2+} the U2 response was restored to control levels. Scale bar = 15msec, 1mV. The bottom graph illustrates how the peak amplitudes of the U1 (filled circle) and U2 responses (open circle) changed during this experiment. The abscissa plots the stimulus number and the ordinate plots the normalised peak amplitude data as a percentage of control. The filled bar covers the period of the experiment in which Mg^{2+} free solution was applied to the preparation.

125

6.2.3. Effect of high frequency stimulation.

In 5 experiments, in which a robust U1 and U2 response could be recorded, the optic tract was tetanically stimulated at a frequency of 100Hz for a total period of 2 seconds. This tetanus regime consisted of 4 groups of 50 stimuli delivered at a frequency of 100Hz with each burst separated by 500msec. These stimulus parameters would usually induce long-term potentiation (LTP) in the perforant path to dentate gyrus pathway of the hippocampus (Bliss and Colingridge, 1993). In this preparation the effect of this high frequency stimulation paradigm was monitored on the peak amplitude of the U1 and U2 response which was recorded at a constant 150μm below the tectal surface. First, stable responses were recorded from the tectum (at a stimulation rate of 1/50 sec) for at least 30 minutes before the tetanus was delivered. The stimulus intensity was at threshold for the U2 response and so did not elicit the maximal peak amplitude for this response (figure 6.7 A). The same stimulus strength was employed during the tetanus as that used during the control period. The peak amplitude of the U1 and U2 response was then calculated for up to one hour post tetanus during which the optic tract was once again stimulated at the control frequency of 1/50 sec.

In 1 preparation we did observe a change in the magnitude of the U2 response (figure 6.7 A & B). Immediately following the 100Hz train a 50% increase in the peak amplitude of the U2 response was observed with no corresponding increase in the peak amplitude of the U1 response. However, in the remaining 4 experiments both the U1 and U2 response was depressed immediately following the tetanus and both responses recovered to basal levels within 10 stimuli. When all 5 experiments were normalised and averaged we could not detect any significant difference in the U1 and U2 peak amplitude following high frequency stimulation (figure 6.7 C).
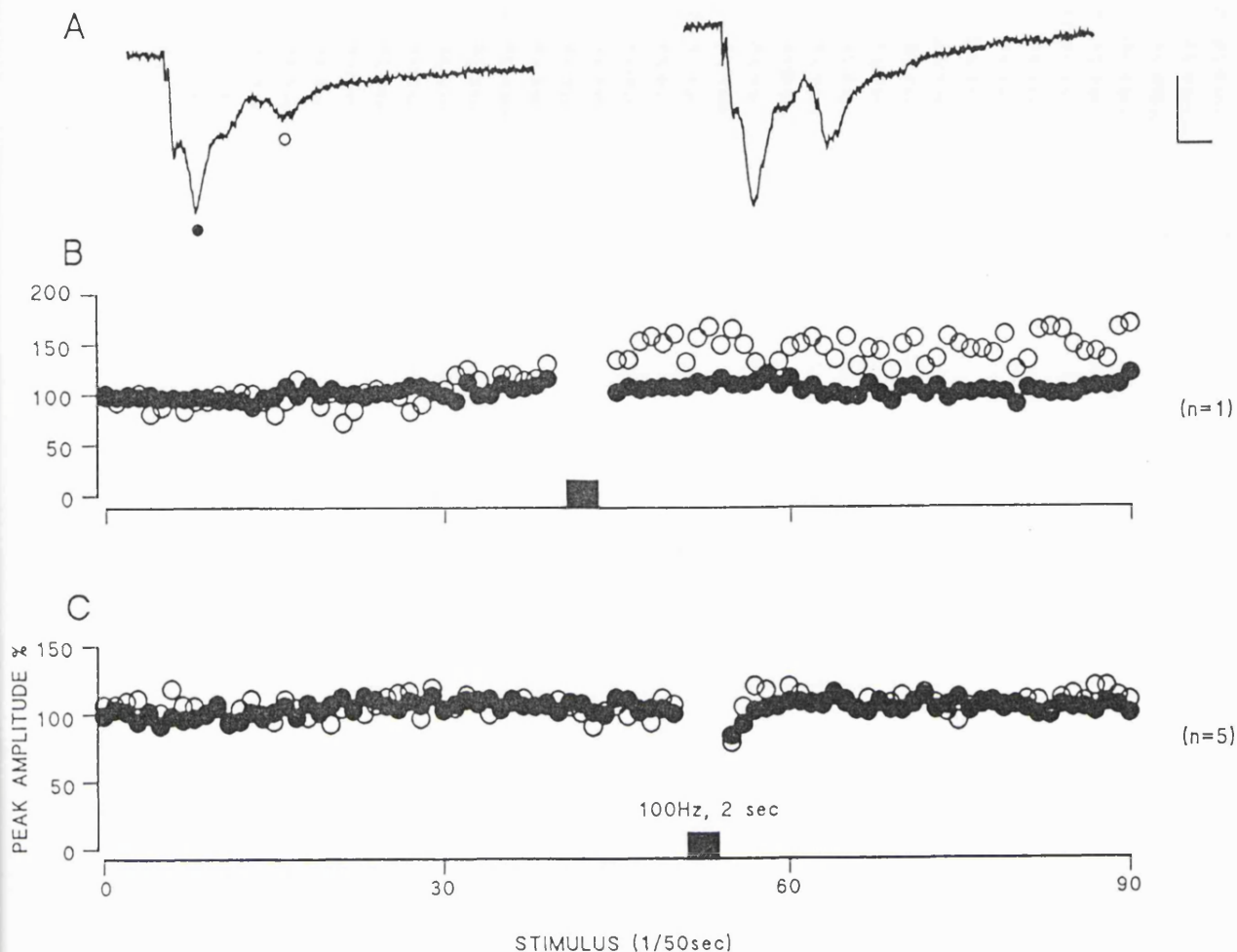
Figure 6.7 Effect of high frequency stimulation on the peak amplitude of the U1 and U2 response.

A. Two traces recorded 150μm below the tectal surface following optic tract stimulation. The left hand record was obtained during the control period immediately before a high frequency train was delivered to the optic tract. Stimuli were delivered at a rate of 1/50sec which were maximal for the U1 response (filed circle) but at threshold for the U2 response (open circle). The right hand trace was recorded from the tectum following the 100Hz tetanus. In this example the peak amplitude of the U1 response has not altered but the peak amplitude of the U2 response has noticeably increased. Scale bar = 10msec, 1mV

B. This graph depicts the peak amplitudes for the U1 responses (filled circles) and U2 responses (open circles) calculated for all stimuli delivered during experiment **A**. The stimulus time is on the abscissa with the normalised data on the ordinate. The peak amplitude values for the U1 and U2 response have been normalised to their 100% level relative to the first 10 response of the experiment. For over 30 minutes before the tetanus was delivered the peak amplitude of the U1 and U2 response remain at approximately this 100% level. The filled box illustrates the duration of the high frequency train. During the tetanus period the peak amplitudes of the U1 and U2 responses have not been calculated. Following this tetanus the peak amplitude of the U1 response remains at control levels but the peak amplitude of the U2 response has increased by 50%. The U2 peak amplitude remains at this elevated level for over 30 minutes post-tetanus.

C. The average of 5 separate experiments in which the U1 (filled circle) and U2 peak amplitudes (open circle) were calculated before and after high frequency stimulation (filled box). The peak amplitude for the U1 and U2 response does not change from its 100% control level following the tetanus.

127

II. Pharmacology

Extracellular field potentials were recorded at a constant depth of $150\mu m$ below the pial surface and the peak amplitude of the U1 and U2 response was calculated following supra-threshold stimulation of the optic tract at a repetition rate of 1/50sec. The peak amplitude of the U1 and U2 response was monitored for a control period of at leat 30 minutes before the antagonist was added to the bathing medium at a defined concentration. One-way analysis of variance (ANOVA) demonstrated that there was no statistical significance ($p > 0.05$) between the average peak amplitudes recorded in the different experimental groups. In each experimnetal group one concentration of antagonist was tested on a naive preparation. The effect of each drug was allowed to stabilise for at least 30 minutes and then the tissue was returned to normal frog ringer. The % change in the peak amplitude of the U1 and U2 response was calculated for a given perturbation and any statistical significance in this change was determined using a paired non-parametric two-tailed t-test.

6.2.4. Effect of non-NMDA-type glutamate receptor antagonists

The selective non-NMDA-type glutamate receptor competitive antagonist CNQX was added to the bathing medium in a total of 23 preparations at specific concentrations ranging from 50nM to $50\mu M$. Figure 6.8 shows the results of one experiment in which $50\mu M$ CNQX was added. In this experiment a stable U1 and U2 response had been recorded for 30 minutes and the addition of CNQX caused a very rapid decrease in the peak amplitude of the U1 response. The decrease in the U2 response was not observed until ~5 minutes subsequent to CNQX application by which time the U1 response had been reduced by ~30% its original value. It was noted that the U1 and U2 responses were transiently elevated during the initial inclusion of the antagonist into the bathing medium. However, after 30 minutes of drug application the U1 and U2 response had completely disappeared. At this concentration of antagonist it was not possible to reverse this block.

The effect of CNQX was dose dependent (Table 6.1) but was not reversible in all experiments. At a $10\mu M$ concentration a significant suppression was observed in both the U1 peak amplitude (47.3% $\pm$ 5.1%; $p < 0.001$) and the U2 peak amplitudes (61.4% $\pm$ 6.9%; $p < 0.001$). At a $50\mu M$ concentration a 71.4% $\pm$ 5.7% suppression in the U1 peak amplitude and a 70.4% $\pm$ 9.0% suppression in the U2 peak amplitude was observed. However, at a very low 50nM concentration of CNQX the U2

response was increased by an average of 30%, ranging from a 16% decrease in one preparation to an 81% increase in another. The U1 response did not exhibit such a marked fluctuations in the presence of 50nM CNQX.
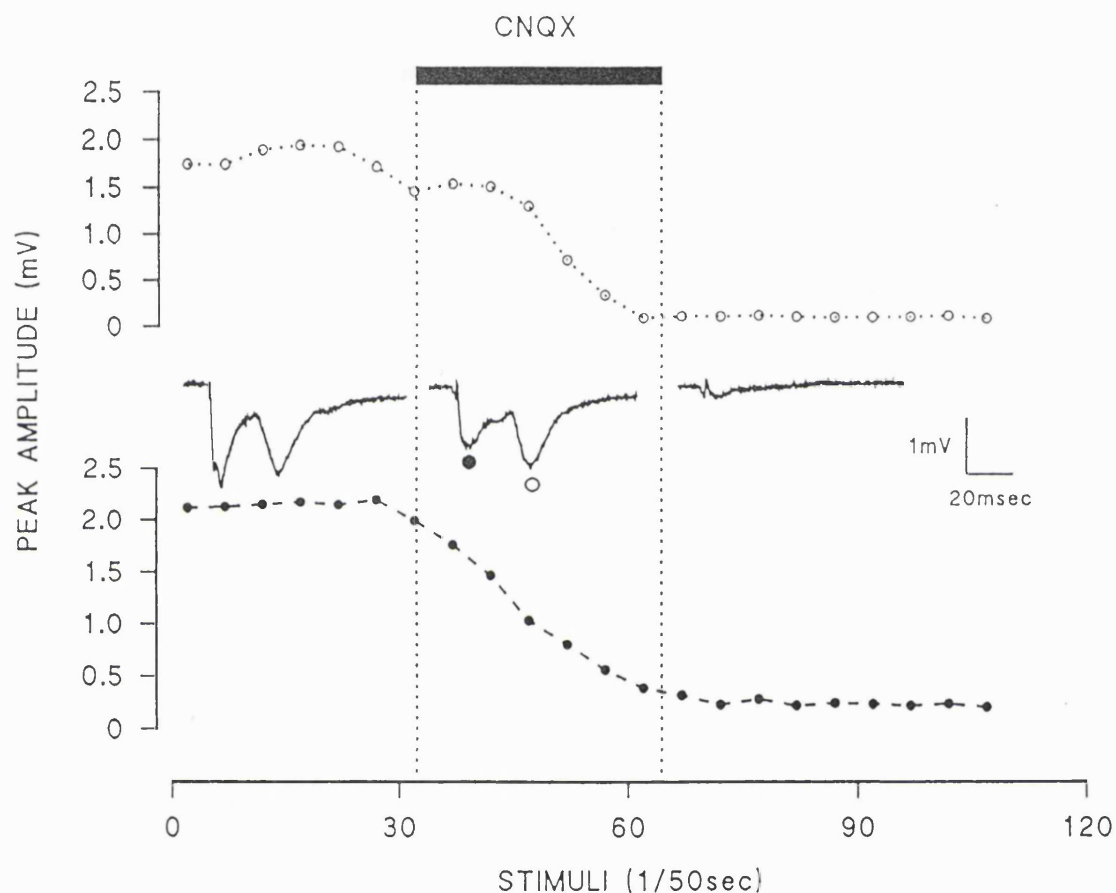
Figure 6.8 Effect of a non-NMDA-type glutamate receptor antagonist on postsynaptic field potentials recorded from the tectal neuropil.
    This figure describes the results of a typical experiment in which the effect of $20\mu M$ CNQX was assessed on tectal field potentials recorded *in vitro*. The optic tract was stimulated at a rate of 0.02 Hz. The peak amplitudes, plotted as positive values, for the U1 responses (filled circles) and U2 responses (open circles) were calculated for each stimulation. Representative traces are shown for responses before, during and after the inclusion of antagonist into the bathing medium. The solid bar indicates the period for which CNQX was present.   Both the U1 and U2 peak amplitudes were significantly reduced by CNQX. In this experiment the effect was irreversible but this was not the case for all experiments. Note how the U1 response was reduced by CNQX before the later U2 response was affected. In some cases a transient enhancement of both peak amplitudes was observed when CNQX containing medium was added but this result was not consistent.

129

6.2.5. Effect of NMDA-type glutamate receptor antagonists.

Only the peak amplitude of the long latency U2 postsynaptic potential was significantly reduced by bath application of the selective NMDA receptor antagonist AP5. Varying concentrations, 5,50,100,150 and 200μM, were applied to 24 preparations (Table 6.1). At all effective concentrations only the U2 response was reduced by AP5. An example of this highly selective effect is depicted in figure 6.9. In this experiment the highest 250μM concentration of AP5 was applied following 30 minutes of consistent U1 and U2 responses. The reduction in the peak amplitude of the U2 wave was observed after 2 minutes and the effect was fully reversible after wash out. Even at this high concentration of AP5 no reduction was noticed in the peak amplitude of the U1 response.

Even at the highest (250μM) AP5 concentration the U1 response was only reduced by an average of 10.9% $\pm$ 2.6% and this change was not statistically significant ($p > 0.1$). Lower concentrations did not affect the peak amplitude of the U1 response at all. This small reduction in the peak amplitude of the U1 wave only at the highest AP5 concentrations was in stark contrast to the results obtained for the U2 wave. A highly selective dose dependent reduction in the U2 peak amplitude was consistently observed. At the highest AP5 concentration of 200μM a ~60% decrease was seen, a ~50% decrease at 150μM, a ~30% decrease at 100μM and a ~30% decrease at 50μM. A statistically significant reduction in the U2 peak amplitude was first observed at a concentration of 50μM ($p < 0.001$). 5μM AP5 had no significant effect on the peak amplitude of the U2 response.

A more potent competitive antagonist to the NMDA receptor 3-(($\pm$)-2-carboxypiperazin-4-yl)propyl-1-phosphonic acid (CPP) was also applied to the optic tectum. This antagonist had similar effects to AP5 (data not shown). The U1 response was not affected by this NMDA receptor blocker but the long latency U2 response was significantly reduced at a 50μM CPP concentration (51.5% $\pm$ 2.6%, n=3).
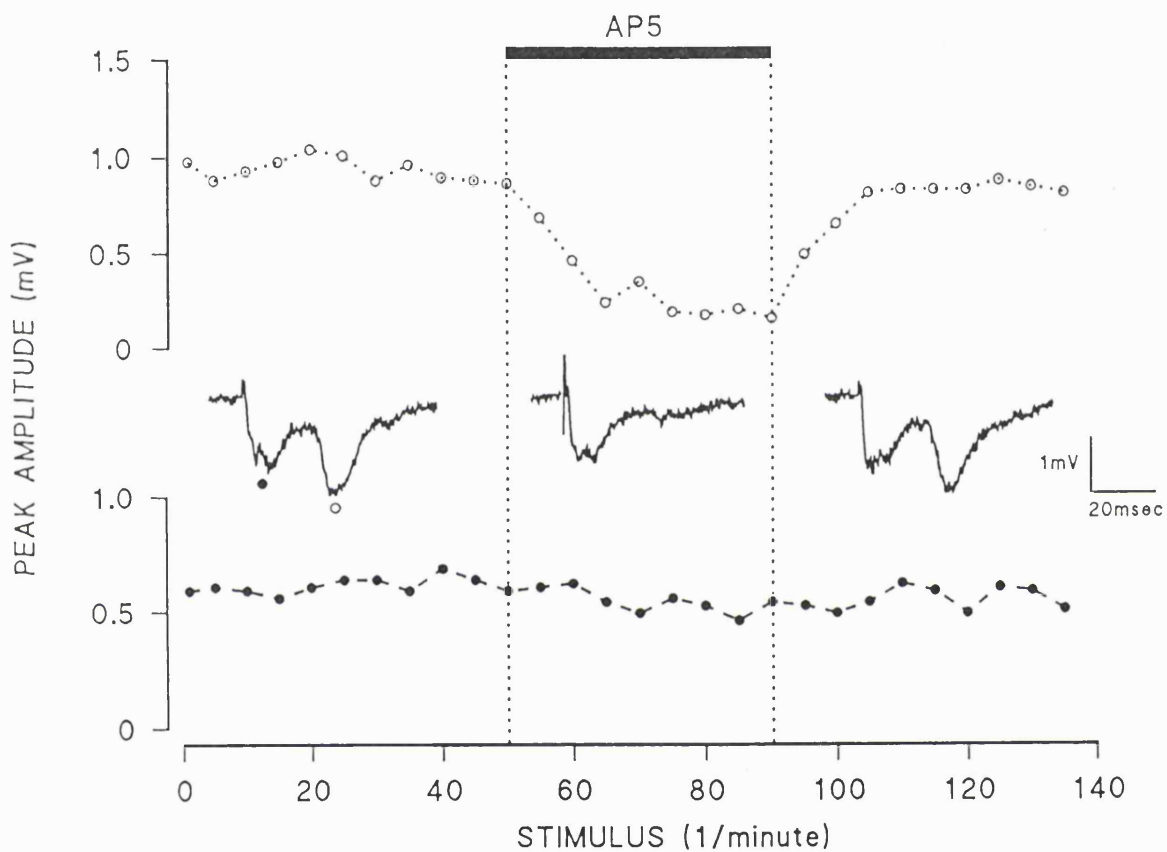
Figure 6.9 Effect of an NMDA-type glutamate receptor antagonist on postsynaptic field potentials recorded from the tectal neuropil.

In this experiment a 250μM concentration of AP5 was applied to the preparation. The conventions are essentially the same as those used in figure 6. Only the long latency U2 response was affected by the NMDA receptor antagonist and in this example, as in most cases, full recovery was achieved.

6.2.6. Effect of blocking cholinergic synaptic transmission.

250μM D-TC, a nicotinic receptor antagonist, was included in the bathing medium of 5 preparations. In all cases a large increase in the duration of the field potential was induced within 1 minute of drug application (figure 6.10). A large +ve deflection followed the early U1 response which peaked at $\sim$150msec post-stimulus. This very long duration response, typically lasting for over 1 second, was not normally present at any depth in the tectum. Following full washout of the antagonist the evoked response returned to its normal duration of $\sim$100msec but was reduced in amplitude relative to the control response. The muscarinic receptor antagonist, atropine sulphate, had no effect on any aspect of the evoked response (n=2) even at a very high 250μM concentration.

6.2.7. Effect of GABA$_A$ receptor antagonists.

A very similar effect to that described with D-TC was observed with the non-competitive GABA$_A$ receptor antagonist picrotoxin (n=4). In the presence of 50μM picrotoxin a large +ve deflection was induced after the U2 response which was very long lasting (figure 6.11). This effect was very rapid and fully reversible but resulted in a reduction in the amplitude of the U1 and U2 response.
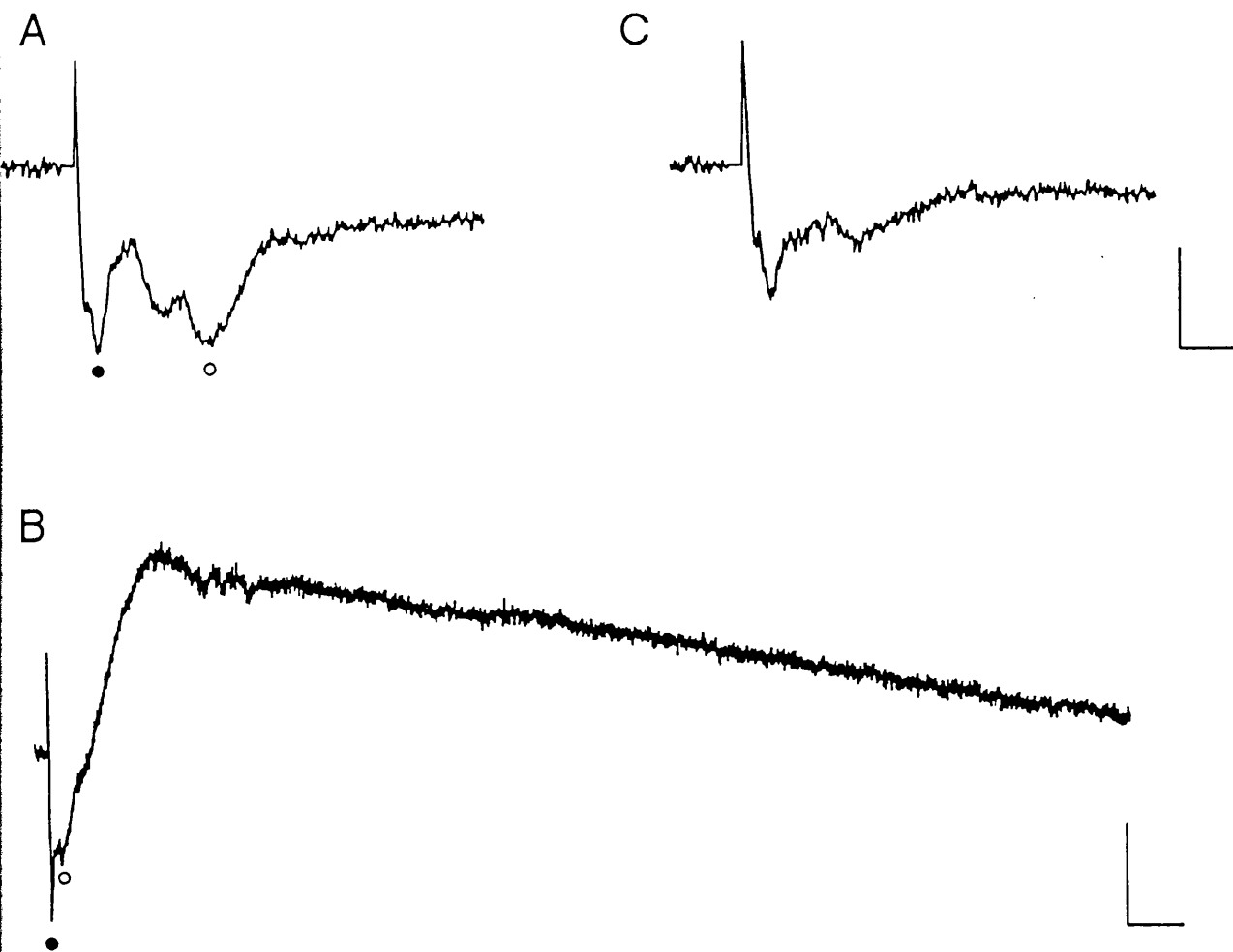
Figure 6.10 Effect of a nicotinic antagonist on postsynaptic field potentials recorded from the tectal neuropil.

All 3 traces were recorded at 150μm below the tectal surface and result from supra-threshold stimulation of the optic tract. A is a control response obtained in normal frog ringer. The U1 response (solid circle) occurs at 10msec and the U2 response (open circle) peaks at 30msec. The entire response returns to base line by 100msec post-stimulus. Trace C is taken after full washout of the nicotinic antagonist (20μM D-TC) from the bathing medium. The U1 and U2 response are diminished in amplitude following this perturbation. Scale bar = 15msec, 1mV in A & C. However, in the presence of 20μM D-TC record B illustrates the elongation of the response with the large positive deflection lasting well over 1 second. Time base = 50msec, 1.5mV.

133
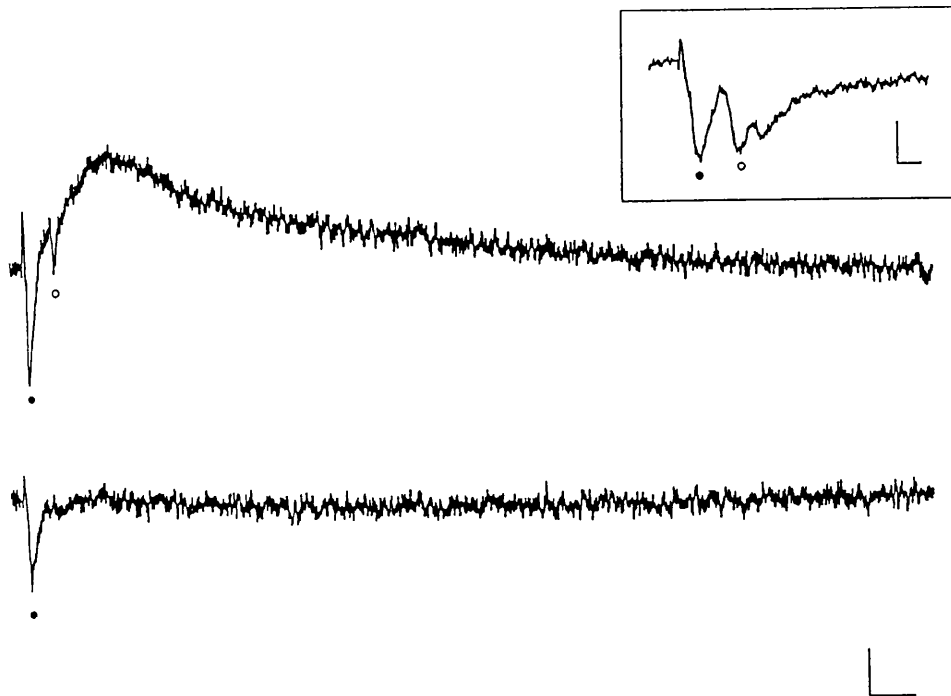
Figure 6.11 Effect of a GABA$_A$ antagonist on postsynaptic field potentials recorded from the tectal neuropil.

Once again all 3 traces were recorded at a constant 150μm depth below the pial surface in response to supra-threshold stimulation of the optic tract. The inset shows the control response with a discreet U1 (filled circle) and U2 response (open circle) over by 100msec post stimulus. Scale bar; 10msec and 1mV. The top trace, in the main figure illustrates, the elongation of the evoked response in the presence of 50μM picrotoxin. Once this GABA$_A$ antagonist was removed from the bathing medium the large +ve going deflection was lost from the response (bottom trace). The long latency U2 response was not present following this perturbation. Scale bar; 50msec, 1mV.

6.3. Discussion

This *in vitro* preparation displayed many of the characteristics reported in the previous *in vivo* study (Chung *et al.* 1974a). These similarities indicate that the *in vitro* preparation is physiologically viable. The extracellular field potentials recorded from the tectum *in vivo* were characterised by 4 distinct events at specific latencies post-stimulus. These were classified as the M1, M2, U1 and U2 waves by Chung *et al.* (1974a) and we have decided to maintain this nomenclature. In this *in vitro* preparation the M1 and M2 response occur at ~ 1 and ~ 3.5msec post-stimulus and the U1 and U2 responses occur at ~ 10 and ~ 30msec post-stimulus. It was difficult to reliably study the M1 and M2 responses because of their very short latency. They both occur within the first 5msec of the response and so are difficult to isolate consistently from the stimulus artifact. Therefore, no strong conclusions as to the exact nature of these responses has been made and attention was focused on the late U1 and U2 responses.

The U1 and U2 response reflects the potential difference transiently propagated by extracellular current flow between the cell bodies and the synaptic inputs of tectal neurons. The optic tectum is a highly laminated structure with a well defined afferent input separated spatially from the cell body layer (see Chapter 8). On the basis of current source density (CSD) analysis Chung *et al.* (1974a) suggested that the synaptic contacts giving rise to the U1 response were positioned within the first 100μm of the pial surface whereas the synaptic connections responsible for the U2 response were positioned deeper in the tectum at $\sim 150\mu$m below the pial surface. They also concluded that the dendrites of cell bodies situated in layer 8 of the tectum received the retinal inputs responsible for the U1 and U2 response. Therefore, it is postulated that the U1 and U2 response reflect postsynaptic current flow following the activation of two distinct populations of synaptic connections spatially separated on the apical dendrites of layer 8 tectal neurons. The postsynaptic nature of these recordings was confirmed by the similar effects of O_2 removal and Ca^{2+} ion removal. Both manipulations resulted in a complete loss of all responses with the later U2 response the first to be affected. These data suggest that the late U1 and U2 components we record *in vitro* are postsynaptic in origin and are also Ca^{2+}-dependent. In contrast to these global effects on postsynaptic activity the effect of Mg^{2+} ion removal was restricted to the long latency U2 response. It is possible that the increase in the U2 response observed following Mg^{2+} ion removal results from the removal of the Mg^{2+} ion block on the NMDA receptor. In further support of this conclusion the LTP-like

effect of high frequency stimulation was also selective for the long latency U2 response causing a marked 50% increase in the peak amplitude of this response. However, this was not consistent between experiments and was only observed in 1 out of 5 preparations.

Consistent with results obtained *in vivo*, the postsynaptic events we record *in vitro* were blocked in a dose dependent manner by the non-NMDA-type glutamate receptor antagonist CNQX. This result is also consistent with the present hypothesis that retinotectal synaptic transmission is glutamatergic and not, as earlier believed, cholinergic (Langdon and Freeman, 1987). It also supports the view that these extracellular recordings represent postsynaptic current flow. The increases which were sometimes observed at lower 50nM CNQX concentrations have been reported perviously (Lambert and Jones, 1990) but it is not certain why they occur. However, a 10μM concentration of CNQX produced a maximum 60% reduction in the U1 and a maximum 70% reduction in the U2 peak amplitude. In a previous study, on the perforant path to granule cell synaptic response in a hippocampal slice preparation, the excitatory postsynaptic potential (EPSP) was depressed by $\sim$80% in the presence of 10μM CNQX (Lambert and Jones, 1990). Therefore, the concentration of CNQX required to produce a comparable reduction in the postsynaptic response in this whole midbrain preparation is not that different from previous studies using slice preparations. Access of the drug into the tissue does not seem to be a great problem. The tectal lobes are small, with a total volume of $\sim$4mm^3, and passive diffusion of the antagonist into the synaptic layer $\sim$100μm below the tectal surface should not be difficult.

NMDA receptors are present in the optic tectum, as shown by autoradiographic techniques (McDonald *et al.*, 1989). In support of this observation the late U2 component of tectal synaptic transmission was blocked by the NMDA-type glutamate receptor antagonist AP5. However, the earlier U1 response was not affected by AP5 indicating that no aspect of this postsynaptic response is mediated by NMDA-type-glutamate receptors. Even at a very high 250μM concentration of AP5 no significant reduction in the U1 response was observed. This could explain why, in Chapter 5, the topical application of 250μM AP5 had no effect on the transmission of visually elicited neural activity between the tectal lobes. However, AP5 did have marked effects on the long latency U2 component of retinotectal synaptic transmission. 50μM D,L-AP5 reduced the peak amplitude of the U2 response by $\sim$30% and a higher 100μM concentration still only produced a $\sim$30% reduction. At even higher

concentrations of AP5 we observed larger decreases in the amplitude of the U2 response but this could represent non-specific binding. Indeed, in the study of Harris *et al.* (1984) a 100μM dose of D,L-AP5 blocked over 90% of the NMDA mediated response. Therefore, it seems likely that in the adult animal $\sim$30% of the late U2 response is mediated by NMDA receptors. The remainder of the U2 response is probably mediated by non-NMDA type glutamate receptors. In support of this suggestion 10μM CNQX was calculated on average to block $\sim$60% of this U2 response.

What else is special about the long latency U2 response? It was first suggested that the long latency of the U2 response reflected the slow conduction velocity of a class of unmyelinated RGC fibres (Chung *et al.*, 1974a). Chung *et al.* electrically stimulated the extra-cranial portion of the optic nerve. In the present *in vitro* study the optic tract was stimulated approximately 500μm rostral to its innervation of the tectal lobe. If the long latency of the U2 response did reflect the slow conduction velocity of unmyelinated fibres then the change in propagation distance should have affected the latency to peak. Moreover, the change in stimulation site should have altered the separation between the two responses but, evidently, it did not. Teyler *et al.* (1981) calculated, in an *in vitro* preparation of the goldfish optic tectum, that the amplitude of the long latency component had 95% response variability whereas the earlier postsynaptic component exhibited a 37.5% response variability. This was in stark contrast to the 5% response variability calculated for the presynaptic fibre volley. The present *in vitro* preparation does appear more stable than that of Teyler *et al.* but, the peak amplitude and latency to peak of the U2 response is certainly more variable than that of the U1 response. We also find that the U2 response is generally a more labile response absent completely from $\sim$20% of preparations. Also, the U1 and U2 response show opposite behaviour to paired pulse stimulation: a marked suppression of the U2 response was induced at inter-stimulus intervals between 100msec-1000msec in marked contrast to the facilitation observed in the U1 response. This suppression of the U2 response following paired pulse stimulation is characteristic of a poly-synaptic event (Richards and Sercombe, 1970). The facilitation of the U1 peak amplitude during paired pulse stimulation could reflect the removal of presynaptic inhibition on a mono-synaptically activated postsynaptic response. Given all these observations we now postulate that the U2 response is a poly-synaptic event mediated by as yet unidentified intra-tectal circuitry. Moreover, it is this poly-synaptic U2 response which is in part mediated by NMDA-type glutamate

137

receptors while the mono-synaptic U1 response is entirely mediated by non-NMDA-type glutamate receptors. The possible significance of this finding is examined in the following chapter.

So what circuitry generates the polysynaptic U2 respoonse? King and Schmidt (1991) have reported a facilitation of the long latency response in the goldfish optic tectum following stimulation of the ipsilateral NI. A crossed isthmotectal projection is not present in goldfish but in all lower vertebrates a reciprocal set of connections is present between each tectal lobe and its ipsilateral NI. The physiological function of the uncrossed projection in the processing of visual information in lower vertebrates is unclear. King and Schmidt (1990) suggest that the uncrossed ishmotectal part of this X link is responsible for the modulation of the U2 response. In *Rana pipiens* most of the cholinergic input to the optic tectum is believed to arise from this uncrossed isthmotectal projection (Ricutti and Gruberg, 1985). It could be that the long latency response in goldfish is generated by the reverberating projection between the tectal lobe and its ipsilateral NI. In this scenario the excitatory input to the tectum which generates the long latency polysynaptic response would be nicotinic in origin. In support of this hypothesis King and Schmidt (1991) reported that, following optic tract stimulation, the long latency response in goldfish is blocked by nicotinic antagonists. Our results imply that the nature of the long latency polysynaptic (U2) response in *Xenopus* is different from that described in goldfish. The U2 response was not mediated by nicotinic recptors and so it would seem unlikely that it reflects an input from the ipsilateral NI. However, more experiments are needed to identify the circuitry which gives rise to the polysynaptic U2 response in lower vertebrates and intracellular recordings of the type described in Chapter 8 should be used to do this.

The nicotinic antagonist D-TC caused a pronounced elongation of the evoked response within minutes of application but a very similar effect was observed in the presence of picrotoxin, a $GABA_A$ receptor antagonist. A large positive going deflection occurred immediately following the U1 and U2 response and this disinhibited response ultimately leads to synaptic fatigue with the amplitude of the recovery response very much reduced in comparison to the control level. It has been reported that D-TC can antagonise inhibitory inputs such as the GABA receptor (Curtis *et al.*, 1974) and so it is possible that the effect of D-TC in this preparation is a non-specific one. The distribution of GABA immunoreactivity in the optic tectum (Antal, 1991) and the effect of GABA in frog tectal slices (Arakawa and Okado 1989) suggest an inhibitory role for GABA mediated synaptic transmission in the intrinsic

circuitry of the tectum. However, a presynaptic localisation of nicotinic receptors on RGC axons in the optic tectum (Sargent *et al.* 1989) and the strong nicotinic input from the NI (Ricciuti and Gruberg 1985, Migani *et al.* 1980) could be the site of action for D-TC in the current study.

In conclusion, the early mono-synaptic U1 response is mediated predominantly by non-NMDA type glutamate receptors. The fact that the U1 response was not affected by AP5, Mg^{2+} ion removal or tetanus indicates that this aspect of tectal synaptic transmission has little or no NMDA mediated component in the adult system. The selective effect of AP5 suggests that a component of the long latency poly-synaptic U2 component is in part NMDA receptor mediated. This conclusion is further supported by the selective enhancement of the U2 response by Mg^{2+} ion removal and its potentiation by tetanic stimulation. Strong inhibition of tectal postsynaptic responses can be removed by blocking the nicotinic and GABAergic system. Further analysis, at the single cell level, is needed to delineate more directly the involvement of the various postsynaptic receptors in the circuitry of the optic tectum (see Chapter 8).

NQX SENSITIVITY (% change)

	50nM		5uM		10uM		20uM		50uM	
	U1	U2	U1	U2	U1	U2	U1	U2	U1	U2
	18	81	-20	22	-49	-70	-78	-55	-73	-46
	10	65	-13	-23	-62	-38	-42	-75	-62	-83
	-4	36	-22	35	-34	-68	-74	-42	-53	-47
	7	-16	-13	-24	-44	-69	-53		-79	-81
	-20	-10					-58	-63	-89	-95
mean	2.1	31.3	-16.9	2.3	-47.3	-61.4	-61.1	-58.7	-71.3	-70.4
std	13.2	38.8	4.0	26.4	10.1	13.8	13.3	12.1	12.7	20.1
n	5.0	5.0	4.0	4.0	4.0	4.0	5.0	4.0	5.0	5.0

P5 SENSITIVITY (% change)

	5uM		50uM		100uM		150uM		200uM	
	U1	U2	U1	U2	U1	U2	U1	U2	U1	U2
	-5	7	3	-42	-5	-47	-2	-66	-12	-54
	-16	-3	2	-34	-11	-27	-5	-63	-0	-58
	12	28	-1	-25	-11	-39	-8	-31	-11	-74
	-5	26	-8	-33	-15	-32	-6	-47	-15	-62
			3	-31	9	-25	-3	-33	-16	-65
mean	-3.6	14.4	-0.1	-33.0	-6.6	-34.1	-4.8	-48.1	-10.9	-62.4
std	10.1	13.1	3.9	5.7	8.5	8.2	2.3	14.5	5.7	6.8
n	4.0	4.0	5.0	5.0	5.0	5.0	5.0	5.0	5.0	5.0

Table 6.1. Dose-response characteristics of the U1 and U2 response in the presence of CNQX and AP5.

140

Chapter 7

Intertectal plasticity:

AP5 sensitivity of the long latency U2 response

7.1. Introduction

Keating (1968) first suggested that intertectal plasticity in *Xenopus* involves the detection of correlated patterns of neural activity between binocularly convergent inputs in the tectum. Synaptic plasticity in the retinotectal projection is also considered to depend upon the recognition of temporally correlated neural activity, but in this case derived from the spontaneous activity of neighbouring retinal ganglion cells (review by Cline, 1991). It has been postulated that the NMDA-type glutamate receptor has properties which explain its involvement in processes which require the detection of coincident neural activity. This receptor mechanism has already been implicated in mediating activity-dependent changes in the adult hippocampus (Collingridge and Bliss, 1987) and in the developing visual cortex (Kleinschmidt *et al*, 1987). A role for the NMDA-type glutamate receptor in retinotectal synaptic plasticity has recently been suggested. It has been shown that eye specific stripes are actively desegregated in the presence of the NMDA receptor antagonist AP5 (Cline *et al.*, 1987). The NMDA-type glutamate receptor has also been implicated in the synaptic modifications described in the intertectal system of *Xenopus* (Scherer and Udin, 1989). Continuously perfused AP5 did not alter the topography of the retinotectal projection but the intertectal system was unable to adapt its series of connections to a single eye rotation.

However, until recently there has been no direct demonstration that NMDA-type glutamate receptors actually mediate synaptic transmission in the optic tectum of *Xenopus*. In Chapter 6 we described how the long latency U2 response in adult *Xenopus* was reduced by $\sim 30\%$ in the presence of $50\mu M$ AP5 leading to the suggestion that this poly-synaptic event is in part mediated by NMDA-type glutamate receptors. What relevance does this NMDA receptor mediated event have in the coincidence detection processes which are thought to underlie intertectal plasticity? As discussed previously (Section 1.7), the NMDA receptor has properties which make it an ideal candidate as a molecular coincidence detector. However, when considering intertectal plasticity the coincidence detection hypothesis does not take into account the delay which is inherent to the crossed isthmotectal input. The crossed isthmotectal

input involves a very circuitous route with at least two synaptic delays (Gruberg and Udin, 1978). The poly-synaptic nature of this indirect input means that the arrival of visual information at the tectum is delayed by approximately 20msec relative to the arrival of binocularly convergent information via the retinotectal projection (Chapter 5; Scherer and Udin, 1991). It could be that the NMDA receptor mediated U2 response occurs at a latency consistent with the arrival of binocularly driven visual information through the intertectal relay. As such, the NMDA mediated U2 response could form the basis of the coincidence detection mechanism thought to underlie intertectal synaptic plasticity. These considerations lead to the prediction that the efficacy of NMDA receptor function in *Xenopus*, and hence the U2 responses sensitivity to AP5, will be maximal during the critical period for intertectal plasticity, rather than earlier in life. As a control for generalised changes in glutamate receptor efficacy, the sensitivity of the U1 and U2 responses to CNQX were also examined. To further test this hypothesis we examined the AP5 sensitivity of the U2 response following periods of visual deprivation, a situation known to influence intertectal plasticity. Finally, if the AP5 sensitivity of the U2 response is related to intertectal plasticity then we would expect it to be reduced or even absent in *Rana pipiens*, a species of frog which does not exhibit intertectal plasticity.

7.2. Results

Extracellular field potentials were recorded *in vitro* from the superficial layers of the *Xenopus* optic tectum in response to electrical stimulation of the optic tract. When recordings were made from the surface of the tectum two pronounced negative deflections were elicited analogous to those reported in Chapter 6. In the previous Chapter it was found that in the adult animal $50\mu M$ AP5 selectively depressed the U2 peak amplitude by $\sim 30\%$ and $20\mu M$ CNQX decreased both the U1 and U2 responses by $\sim 60\%$. When assessing the effects of these concentrations of AP5 and CNQX in this study recordings were made at a constant depth of $150\mu m$ below the pial surface. The peak amplitude of the U1 and U2 response was calculated following supra-threshold stimulation of the optic tract at a repetition rate of 1/50sec. The U1 and U2 response was monitored for a control period of at leat 30 minutes before the antagonist was added to the bathing medium. The effect of each drug was allowed to stabilise for at least 30 minutes before the % change in the peak amplitude of the U1 and U2 response was calculated.

7.2.1. Developmental change in the postsynaptic response.

The postsynaptic response was monitored in 7 groups of animals; those at stage 60 of late larval life (n=5), at metamorphic climax (n=4), and at 1 (n=5), 3 (n=5), 6 (n=3), 12 (n=5) and 18 (n=3) months after metamorphosis (Nieuwkoop and Faber, 1967). The earliest stage at which this *in vitro* preparation could be successfully prepared was stage 55 of late larval life. Both U1 and U2 postsynaptic responses were present in all age-groups (figure 7.1). Depth profiles, stimulus strength dependency and paired pulse profiles of the postsynaptic responses in the younger animals were similar to those previously described in the adult preparation.

Analysis of variance (ANOVA) indicated that the peak amplitude of the U1 responses (p=0.71) and the U2 responses (p=0.07) did not significantly differ at any developmental stage and also revealed no difference between the latency to peak amplitudes for the U1 (p=0.73) and U2 (p=0.21) responses (Table 7.1).
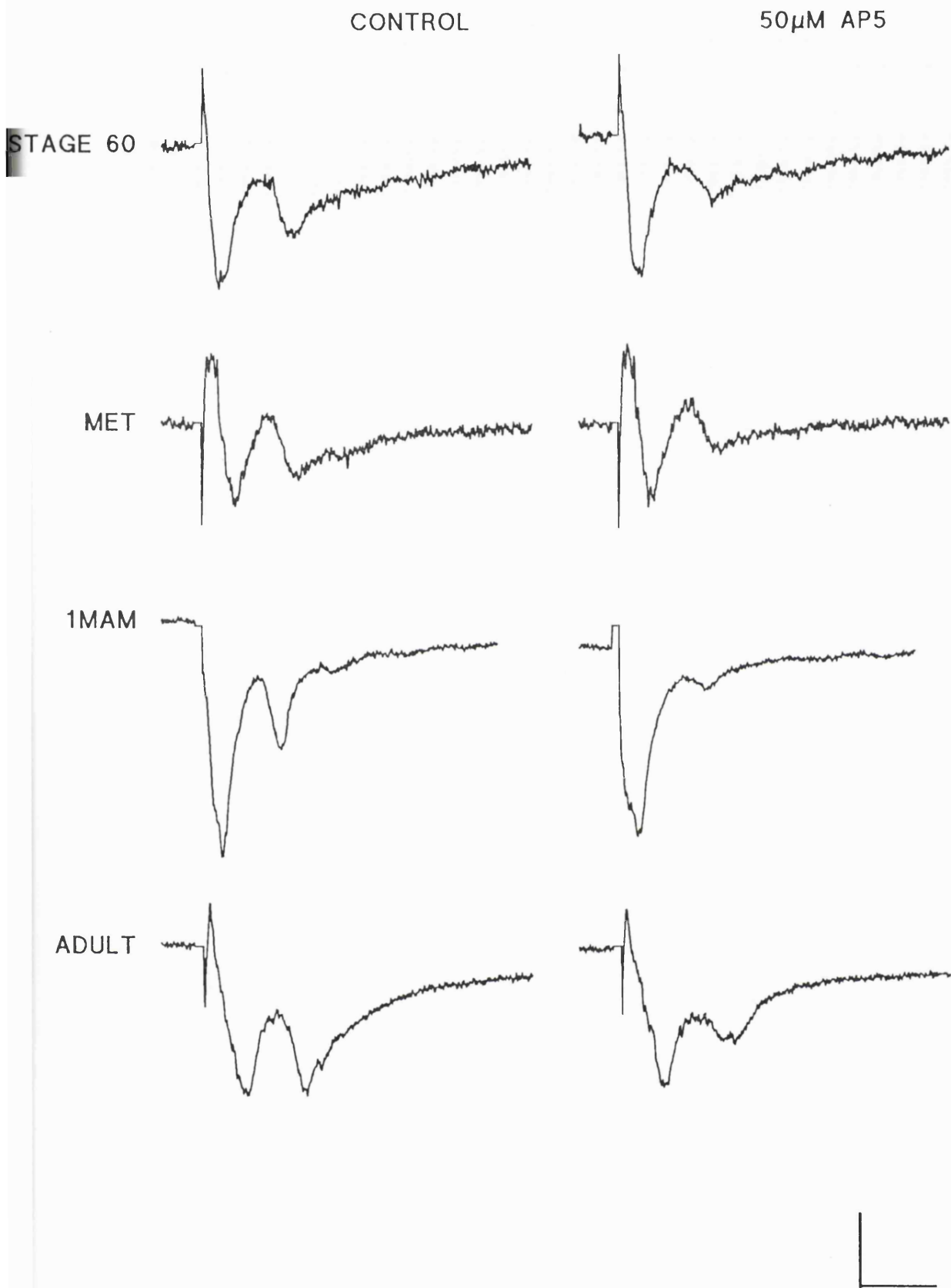
Figure 7.1. U1 and U2 response recorded from the tectum at different stages of development.
    4 sets of extracellular field potentials were recorded from the tectal neuropil in response to supra-threshold stimulation of the optic tract. A robust U1 and U2 response was recorded at stage 60 of development, from animals at metamorphic climax, animals 1 month after metamorphosis and adult animals 18 months after metamorphosis. Moreover, the U2 response was noticeably reduced by 50μM AP5 at each developmental stage and little effect was observed, at any stage, on the earlier U1 response. Scale bar; 20msec, 1mV.

7.2.2. Developmental change in CNQX sensitivity.

In 15 preparations the effect of $20\mu M$ CNQX was monitored at 4 developmental stages; stage 60 (n=4), metamorphic climax (n=4), and 1 (n=3) & 12 (n=4) months after metamorphosis (Table 7.2). In 3 of these preparations it was only possible to monitor the peak amplitude of the U1 response, because the poly-synaptic U2 response was either too small or absent, consistent with its reported fragility. At all developmental stages, bath application of the non-NMDA-type glutamate receptor antagonist CNQX produced a major depression in the peak amplitudes of the U1 and the U2 responses by ~60% (Table 7.2). ANOVA revealed that the depression in the peak amplitude of both responses was not significantly different across age groups.

7.2.3. Developmental change in AP5 sensitivity.

In a further 30 preparations the effect of $50\mu M$ AP5 was determined at all 7 developmental stages (Table 7.2). At each developmental stage a significant reduction was observed in the U2 peak amplitude with little or no effect on the U1 peak amplitude (figure 7.1). The reduction in the U2 response in the stage 60 animals was no different from that observed in animals 6, 12 and 18 months after metamorphosis. However, at metamorphic climax (stage 66) the mean reduction was nearly 40%, and by 1 month after metamorphosis was over 60%. Two months later the level of reduction had decreased to ~40% and by 6 months after metamorphosis was back to control levels. So, the AP5 sensitivity of the long latency U2 response reached a peak 1 month after metamorphosis and had returned to pre-metamorphic levels by 6 months after metamorphosis (figure 7.2). ANOVA demonstrated that the small reduction observed in the peak amplitude of the early mono-synaptic U1 response did not alter at any developmental stage $(p > 0.1)$. However, the reduction observed in the peak amplitude of the long latency poly-synaptic U2 response did significantly change during development $(p = 0.0003)$. These age-related changes in AP5 sensitivity, occurring between metamorphic climax and 3 months after metamorphosis, were significantly different to those existing at earlier and later ages.
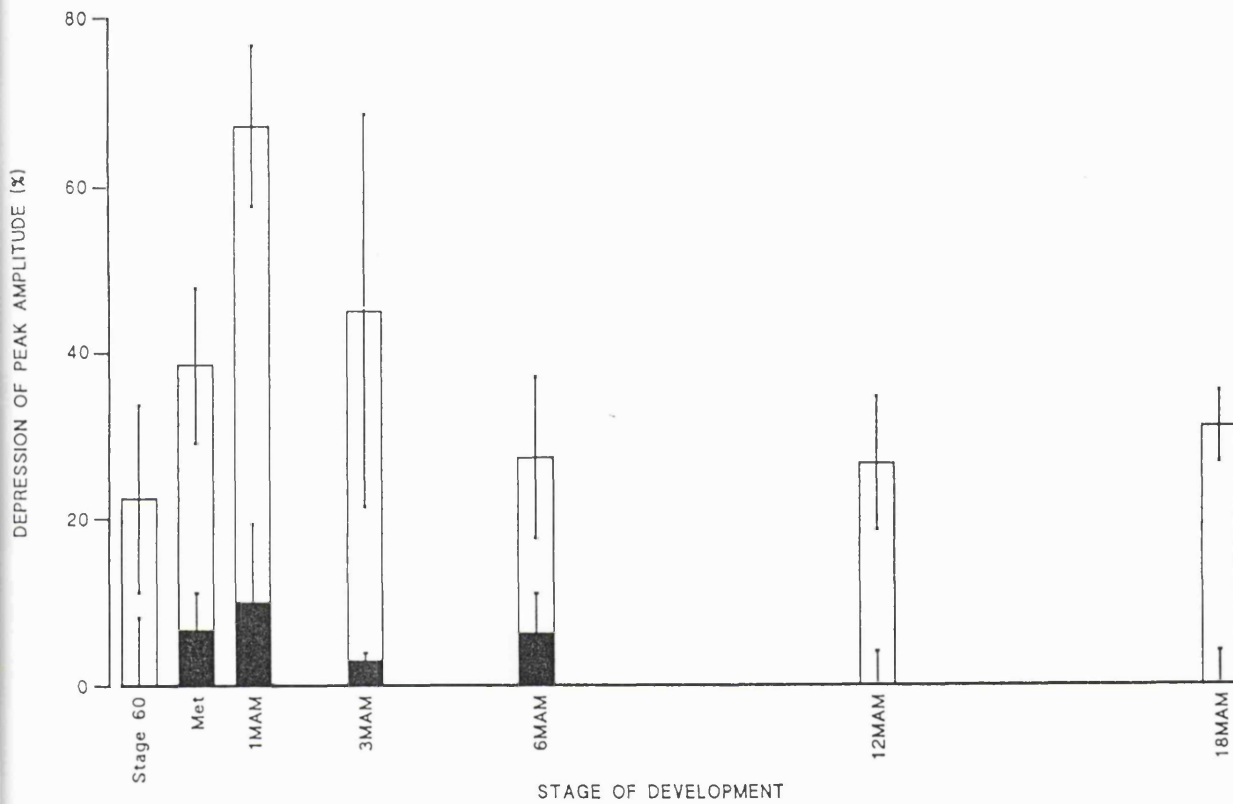
Figure 7.2. The developmental change in AP5 sensitivity.

The effect of 50µM AP5 was established on the peak amplitude of the U1 and U2 response recorded 150µm below the pial surface in response to electrical stimulation of the optic tract. The depression of the peak amplitude (%) for the U1 response (filled bar) and the U2 response (open bar) is plotted at different stages of development. Each value represents the average reduction observed in 5 animals with the standard deviation of the mean plotted on the error bars.

7.2.4. Effect of dark-rearing on the postsynaptic response.

Next, we examined the effect of dark-rearing on the AP5 sensitivity of the long latency U2 response. Animals were dark-reared for 1 year from stage 55 onwards and the effect of $50\mu M$ AP5 was established *in vitro* immediately following this period of dark-rearing and also subsequent to 1 month of visual experience. A total of 15 successful preparations contributed to this study with all animals descending from a single hatching. 10 animals were dark-reared for 1 year and the remaining 5 were given normal visual experience for the same period. 5 animals were sacrificed immediately following dark-rearing and the other 5 were first given 1 month of normal visual experience.

The postsynaptic responses of these visually deprived animals appeared no different to their age-matched controls. Following dark-rearing the U1 and U2 response was still present in the postsynaptic response (Figure 7.3) and the peak amplitude and latency to peak of the responses were no different from those obtained from control animals (Table 7.3). This was also true for the group of animals exposed to one month of visual experience immediately subsequent to 12 months of dark-rearing. In each case ANOVA revealed no difference $(p > 0.1)$ between the peak amplitudes and latencies to peak amplitude recorded in these three groups of animals.
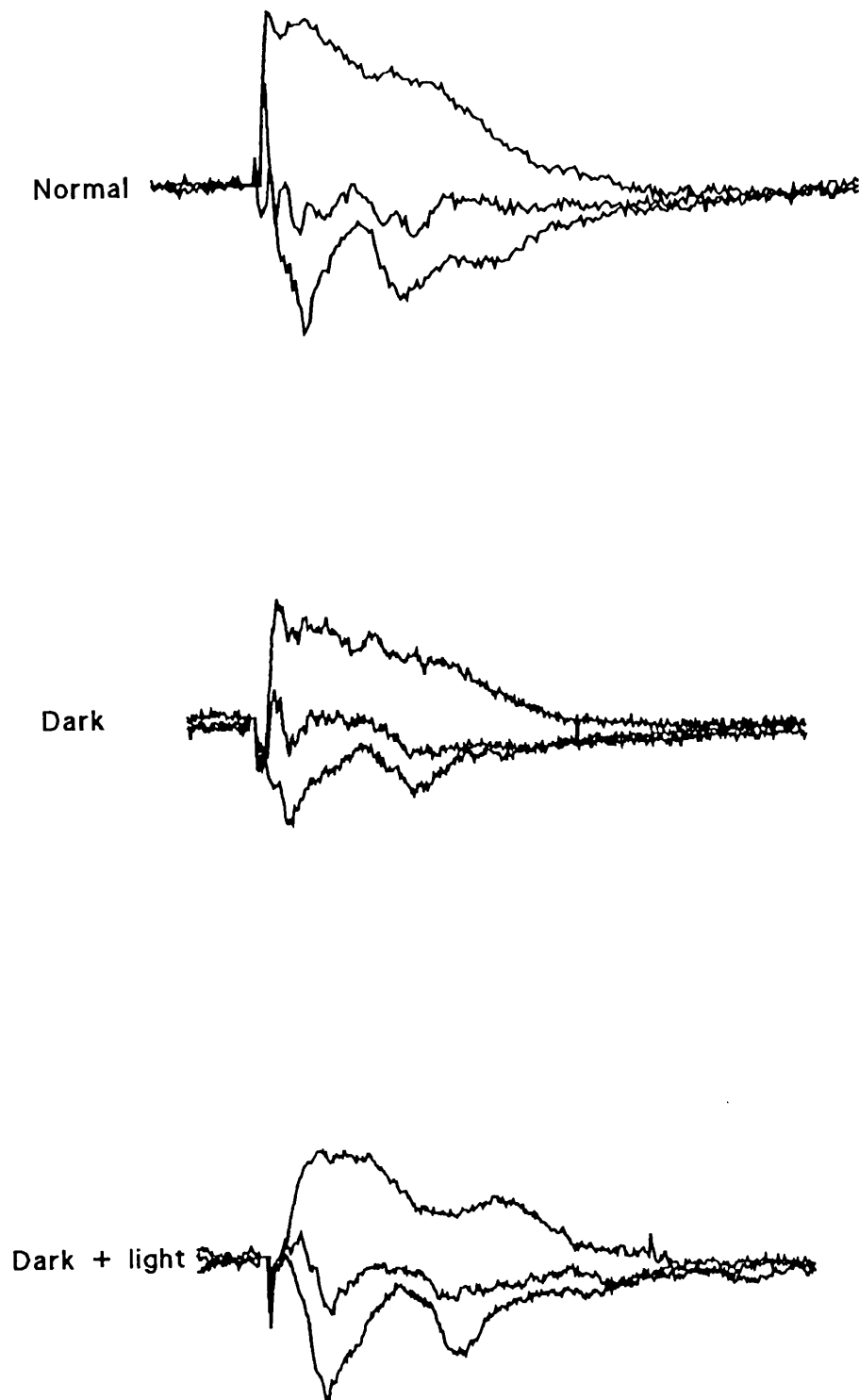
Figure 7.3. No effect of visual deprivation on extracellular responses recorded from different depths of the optic tectum *in vitro*.

The top trace shows 3 responses recorded from different depths in the tectal neuropil in response to supra-threshold stimulation of the optic tract. This in vitro preparation was obtained from an animal 12 months after metamorphosis which had been reared in normal diurnal lighting. The larger negative going deflections were recorded at 150μm below the pial surface. The next trace was recorded at $\sim 300\mu$m below the surface. The polarity of the signal is seen to be reversing at this depth. The large positive going deflections were recorded at a depth of 450μm.

The middle 3 traces were recorded at 150μm, 300μm and 450μm below the pial surface in response to supra-threshold stimulation of the optic tract. This *in vitro* preparation was obtained from an animal 12 months after metamorphosis which had been reared, since stage 55-58 of larval life, in complete darkness. Once again the polarity of the signal reverses at $\sim 300\mu$m below the pial surface.

The bottom 3 traces were also recorded at 150μm, 300μm and 450μm below the pial surface in response to supra-threshold stimulation of the optic tract. However, this preparation was obtained from an animal which had been dark-reared for 12 months, from stage 55-58 of development, and then exposed to 1 month of normal diurnal lighting. In all traces the scale bar = 20msec, 1.5mV

7.2.5. Effect of visual experience on AP5 sensitivity.

In the control group of animals which were reared in normal diurnal lighting for 1 year $50\mu M$ AP5 reduced the U2 response by $\sim 37\%$ (Table 7.3). In the group of animals which had been dark-reared for 1 year $50\mu M$ AP5 still only reduced the U2 response by $\sim 33\%$. Therefore, dark-rearing did not appear to alter the AP5 sensitivity of the U2 response. However, in the group of 5 animals which had been given normal visual experience immediately following 1 year of dark-rearing the depression of the U2 peak amplitude appeared to have changed. In this group of animals the U2 peak amplitude was now reduced by $\sim 58\%$. No change in the insensitivity of the U1 response to $50\mu M$ AP5 was noted in any of the three groups of animals.

As expected ANOVA between the AP5 sensitivity of the U1 response in these animals indicated that the variability between the three groups was not significant $(p > 0.8)$ but the AP5 sensitivity of the U2 response had significantly changed $(p = 0.04)$. Therefore, after exposure to 1 month of normal visual experience the AP5 sensitivity of the long latency poly-synaptic U2 response in dark-reared animals increased (Figure 7.4).
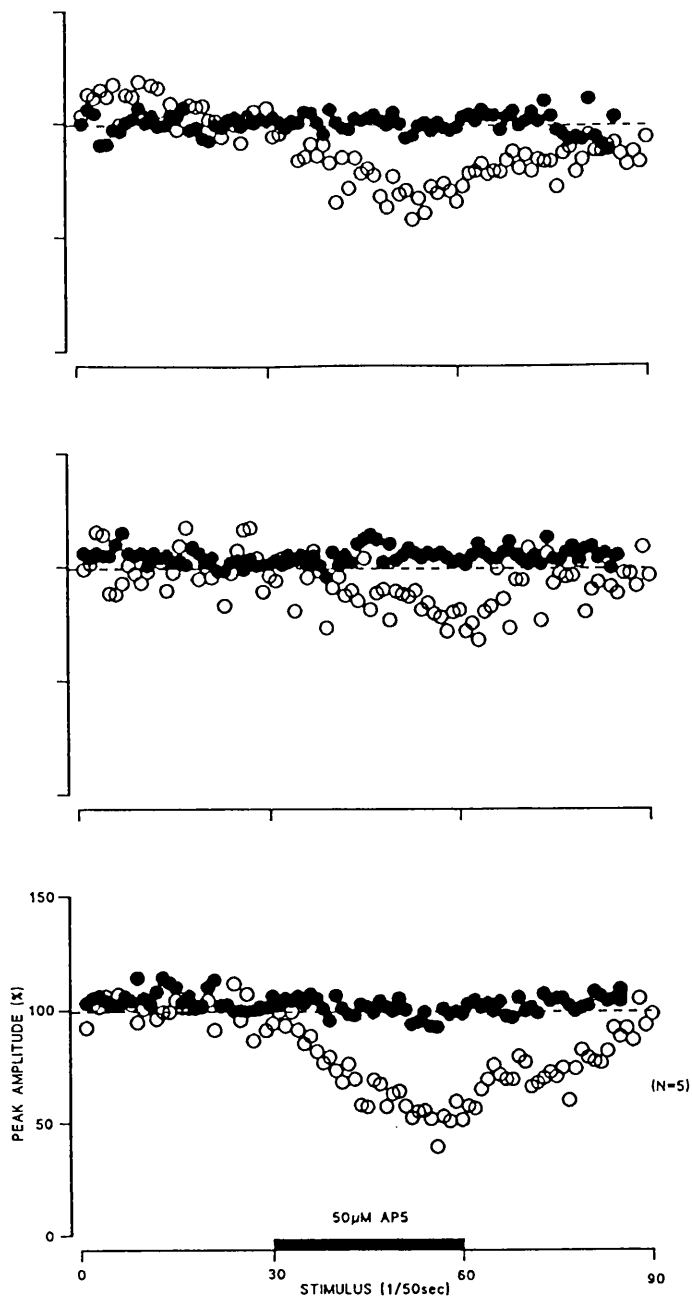
Figure 7.4. The effect of visual experience on the AP5 sensitivity of the U1 and U2 response *in vitro*.

The peak amplitude of the U1 and U2 response was calculated following supra-threshold stimulation of the optic tract. Control responses were recorded for 30 stimulations and then 50μM AP5 was included in the bathing medium. After a further 30 stimuli the AP5 was removed. The data from 5 separate experiments was normalised and averaged. The top diagram shows the average results from preparations obtained from normal animals .12 months after metamorphosis. The peak amplitude of the U1 response (filled circles) and the peak amplitude of the U2 response (open circles) are shown as percentages of control. So, for the 30 minute control period the responses are stable at the 100% level but addition of 50μM AP5 induces a ~30% decrease in the peak amplitude of the U2 response with little effect on the U1 response. This selective decrease is fully reversible on washout of the drug.

The middle plot illustrates the results of identical experiments in which the *in vitro* preparation was obtained from 5 animals which had been dark-reared for 12 months from stage 55 onwards. Again little depression was observed in the peak amplitude of the U1 response but the U2 peak amplitude was selectively and reversibly reduced. However, the reduction observed in this case was smaller than in the normal animals.

The bottom plot was obtained from animals which had also been dark-reared for 12 months but, in this case, they were subsequently reared in normal diurnal lighting for 1 month before being sacrificed for the *in vitro* preparation. Once again 50μM AP5 can be seen to have little effect on the peak amplitude of the U1 response but the U2 response was reduced on average by over 50% in the 5 experiments.

150

7.2.6. Comparison of the postsynaptic responses in *Xenopus* and *Rana*.

The physiological characteristics of the postsynaptic responses recorded *in vitro* from the two species were, in most respects, identical. In both species a radial penetration of the tectal neuropil resulted in reversal of the negative going deflections at $\sim 300 \mu m$ below the tectal surface (figure 7.5). The U1 response reached its maximal negativity more superficially than the U2 response. Also, at a depth of $150 \mu m$ below the tectal surface the U1 response was consistently elicited at a lower stimulus strength than the U2 response (figure 7.6). The latency to peak amplitude for the U1 and U2 responses were no different in the two species although in *Rana* the peak amplitudes of both responses were larger than those recorded in *Xenopus* (Table 7.4). Mann-Whitney unpaired nonparametric statistics was used to ascertain significance between the values obtained in the two species. No difference was found in the latency to peak amplitudes for the U1 or U2 responses in the two species $(p > 0.4)$. However, the peak amplitudes were significantly different for the U1 $(p = 0.005)$ and the U2 $(p = 0.01)$ responses. The reaction of the U2 response to paired pulse stimulation was also different in the two species (figure 7.7). When a test shock of threshold intensity for the U2 response was delivered to the optic tract 100-1000msec after a conditioning shock of equivalent strength the U1 peak amplitude was potentiated but the peak amplitude of the U2 response was depressed in *Xenopus* $(n = 10)$. In *Rana pipiens* $(n = 10)$ the U1 peak amplitude was not altered and the long latency U2 peak amplitude was potentiated under these circumstances.
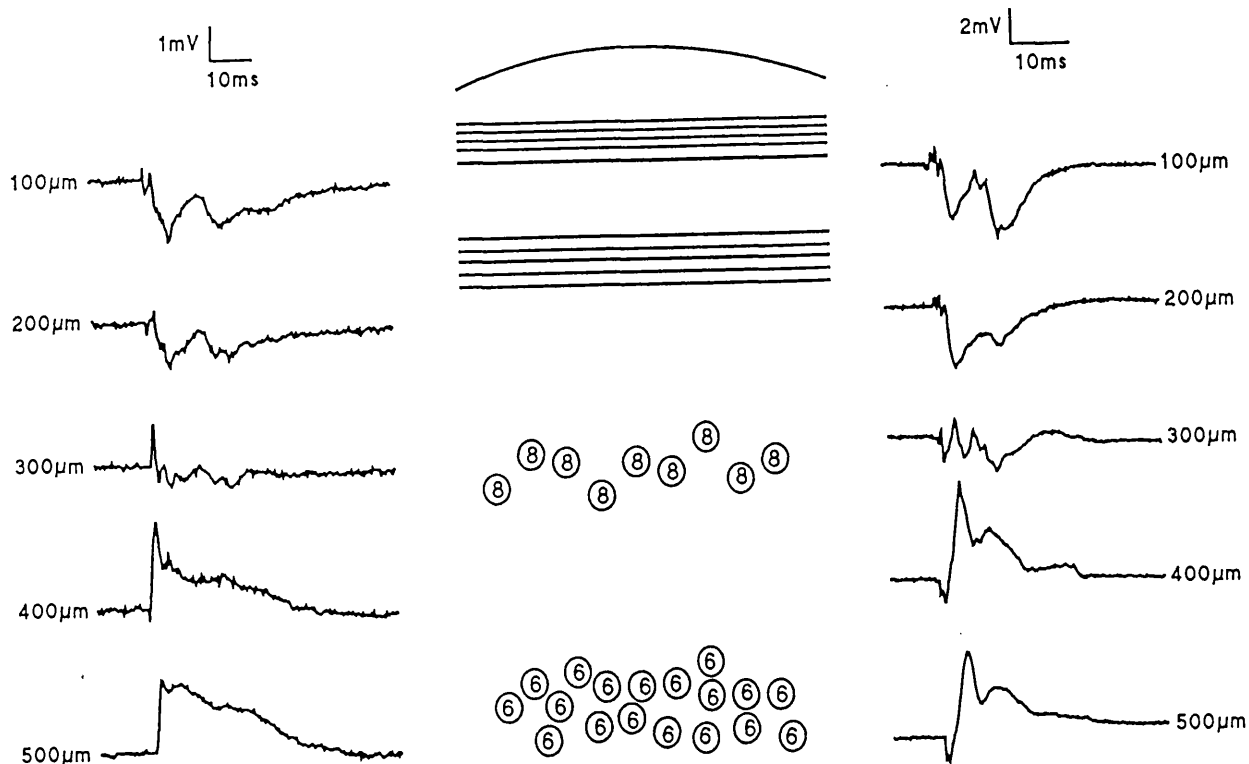
Figure 7.5. Effect of radial penetrations of the optic tectum in Xenopus and Rana.

The middle schematic illustrates the laminar organisation of the optic tectum at the corresponding depths of teach radial penetration. Afferent input arises in layer 9 of the tectum from the pial surface to a depth of $\sim 200 \mu m$ where layer 8 cell bodies begin to appear. Layer 6 cell bodies are situated approximately $500 \mu m$ below the surface.

The left hand side of this figure consists of responses recorded *in vitro* from the optic tectum of *Xenopus laevis* in response to supra-threshold stimulation of the optic tract. Illustrated traces are from recordings made at $100 \mu m$, $200 \mu m$, $300 \mu m$, $400 \mu m$ and $500 \mu m$ below the pial surface. The traces on the right hand side of the figure are recorded from the optic tectum of *Rana pipiens* at similar depths. Scale bar in both cases = 10msec, 1mV
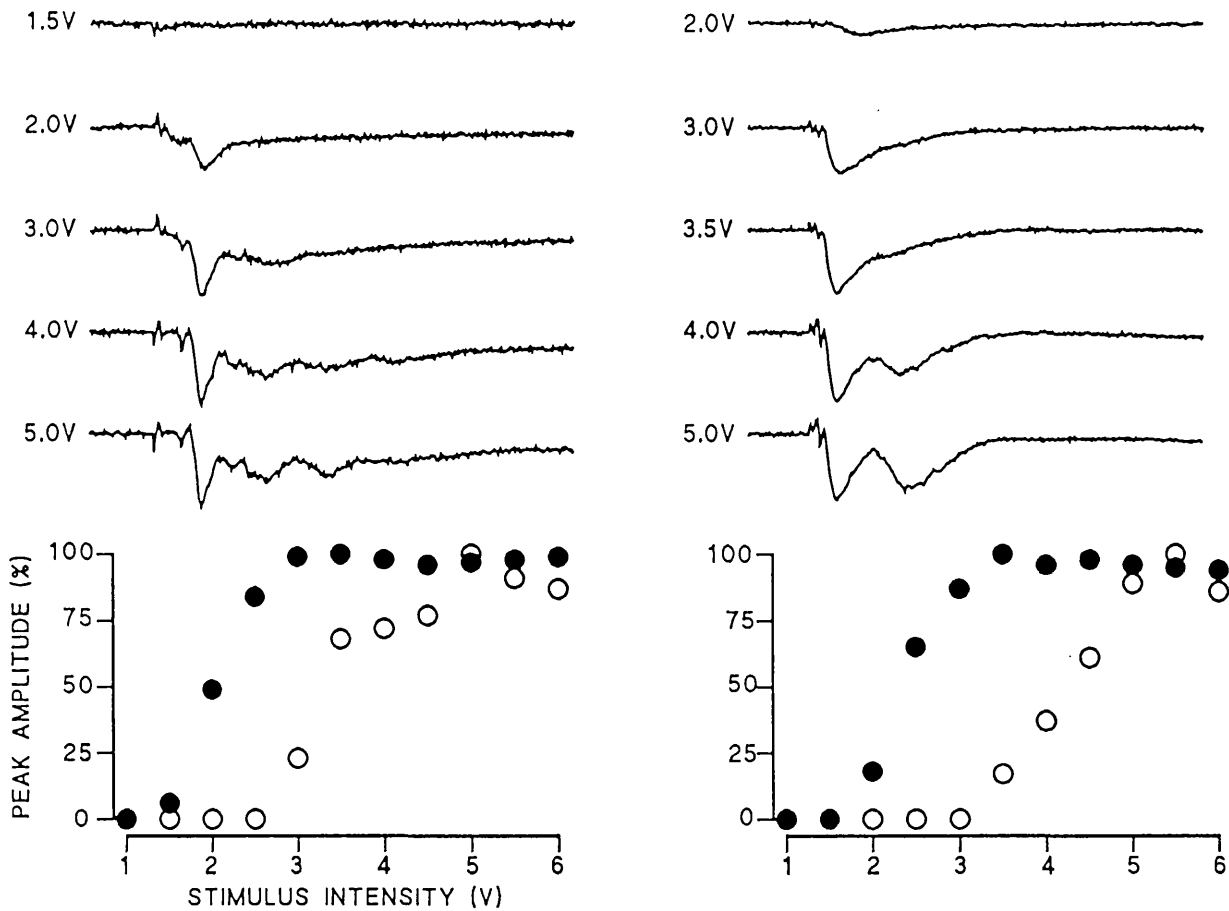
Figure 7.6. Stimulus strength dependency of the U1 and U2 response in *Rana* and *Xenopus*.

The optic tract of *Xenopus* (left hand side of figure) and *Rana* (right hand side of figure) was stimulated at varying intensities from 1 to 5 V and the response recorded at a constant 150μm depth below the pial surface. The peak amplitude of the U1 (filled circle) and U2 (open circle) was normalised to the maximum response and the stimulus-response relationship plotted for *Xenopus* and *Rana*.
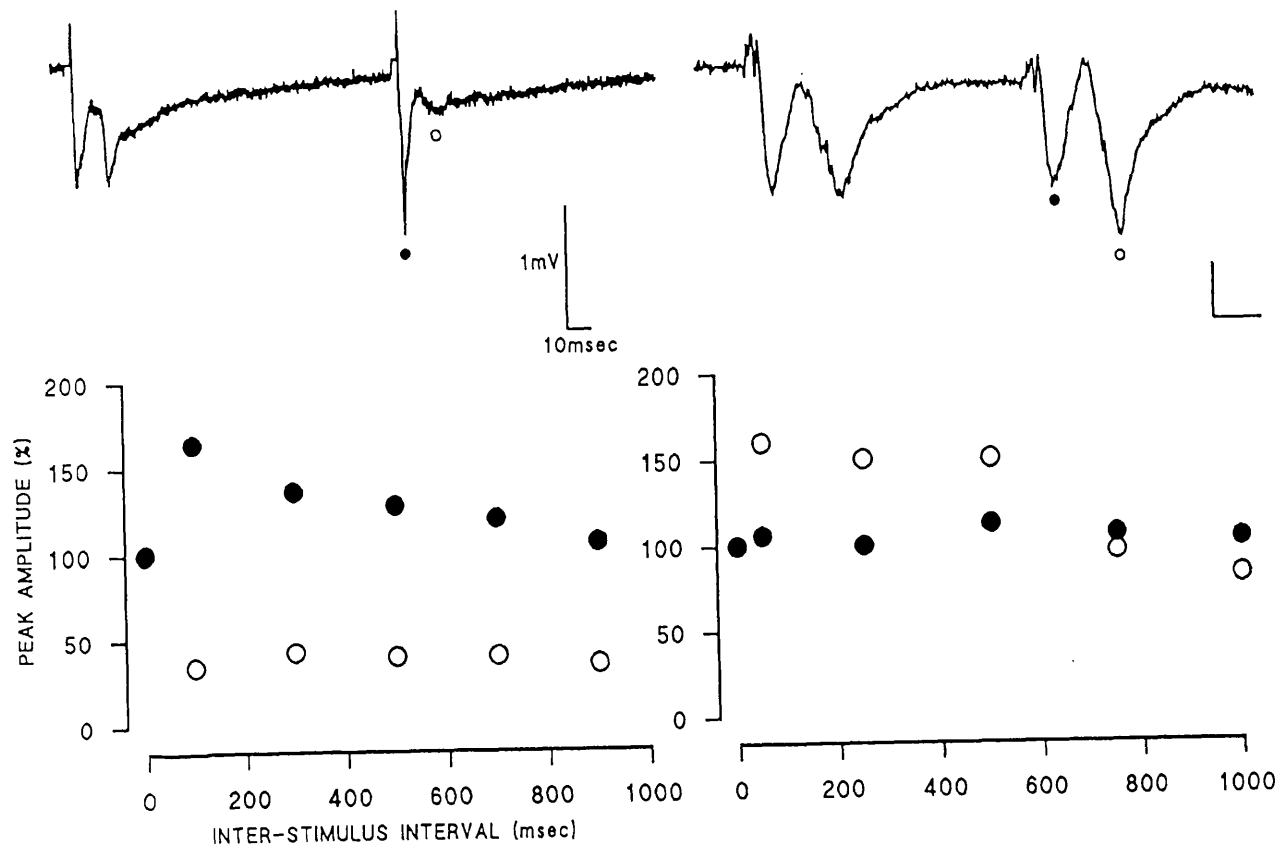
Figure 7.7. Paired pulse stimulation in *Xenopus* and *Rana*.

Results for *Xenopus* are on the left and *Rana* on the right of the figure. The top traces show the results of a single paired pulse experiment in which the optic tract is stimulated at supra-threshold intensity and a second identical stimulus is delivered to the tract a short interval later. The scale bar = 10msec and 1mV for *Xenopus* and *Rana*.

The peak amplitude of the U1 (filled circle) and U2 (open circle) response is then recorded at a depth of 150μm below the pial surface. The % increase in the amplitude of the second response is then calculated and plotted in the lower graph at inter-stimulus intervals between 0 and 1000msec. At an inter-stimulus interval of 0 seconds only one stimuli is delivered to the tract and so the U1 and U2 response remain at the 100% level.

154

7.2.7. CNQX sensitivity in *Xenopus* and *Rana*.

The effects of the non-NMDA-type glutamate receptor antagonist CNQX were equivalent in the two species (figure 7.8 & 7.9). Within minutes of the application of 20μM CNQX the U1 and U2 response was depressed. This depression was sometimes proceeded by a transient increase in the peak amplitude of the U1 response. However, in both species 20μM CNQX ultimately resulted in a ~60% reduction in the U1 and U2 responses (Table 7.4). The reduction in the U1 and U2 peak amplitudes was calculated in 4 *in vitro* preparations obtained from *Xenopus laevis* aged 12 months after metamorphosis and in 4 preparations obtained from adult *Rana pipiens*. An unpaired nonparametric t-test demonstrated that the difference in the calculated reductions in the two species were not significant (**p > 0.9**).

7.2.8. AP5 sensitivity in *Xenopus* and *Rana*.

50μM AP5 had little effect on the U2 response recorded in *Rana*. The effect of 50μM AP5 on the U1 and U2 peak amplitude was monitored in total of 5 preparations (Table 7.4). In all cases no consistent reduction was observed in peak amplitude of the U1 or U2 response (figure 7.10). However, on average the U2 peak amplitude was increased by ~16%. This ranged from an 85% increase in one preparation to an 18% reduction in another. Using a paired nonparametric two-tailed t-test it was shown that this average change in the U2 peak amplitude was not statistically significant. (**p > 0.1**). Therefore, in contrast to those results previously obtained using *Xenopus*, AP5 had no effect on the peak amplitude of the U2 response in another species of frog *Rana pipiens*.

In a series of inter-leaved control experiments it was shown once again that, in 5 *Xenopus* aged 12 months after metamorphosis, the U2 peak amplitude was reduced by ~30%, in accordance with previous findings (figure 7.11). Moreover, a paired nonparametric two-tailed t-test demonstrated that this change in the U2 peak amplitude was significant (**p < 0.1**).
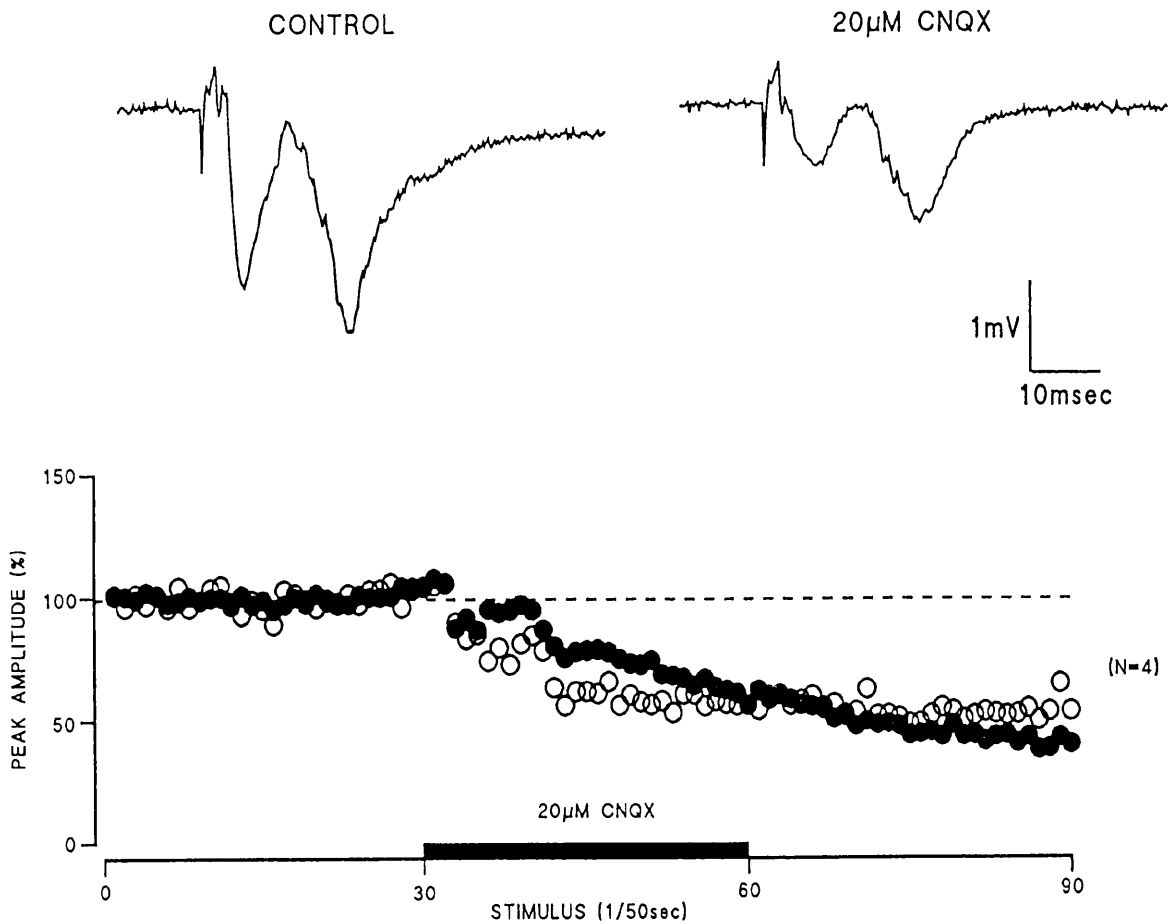
Figure 7.8. The effect of non-NMDA receptor antagonists on the U1 and U2 response in *Xenopus*.

The control trace shows the extracellular response recorded at a 150μm depth in the tectal neuropil following supra-threshold stimulation of the optic tract. On addition of 20μM CNQX in the bathing medium the amplitude of both the U1 and U2 response was noticeably reduced. Scale bar = 10msec and 1mV

The peak amplitude of both the U1 and U2 response was calculated for the entire experiment and in the bottom graph. The peak amplitude values represent the average of 5 separate experiments in which the peak amplitude values were normalised to the maximum value. Control responses were monitored in normal bathing medium for 30 stimuli before the effect of 20μM CNQX was established. 30 responses were recorded in the presence of CNQX and then the preparation was returned once again to normal bathing medium.

156
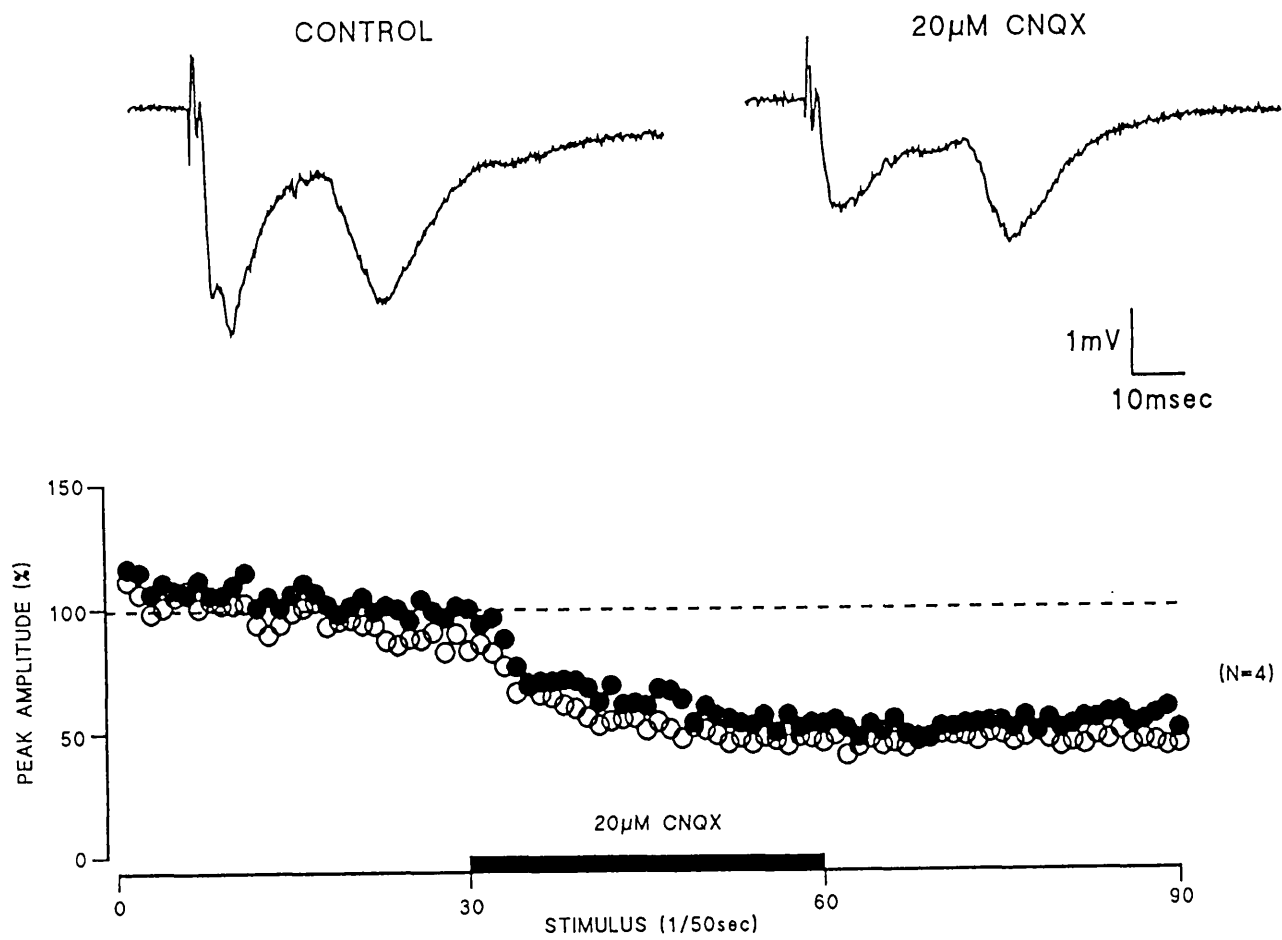
Figure 7.9. The effect of non-NMDA receptor antagonists on the U1 and U2 response in *Rana*.

This figure is identical in its format to figure 7.8 but the *in vitro* preparations were now obtained from *Rana pipiens*.
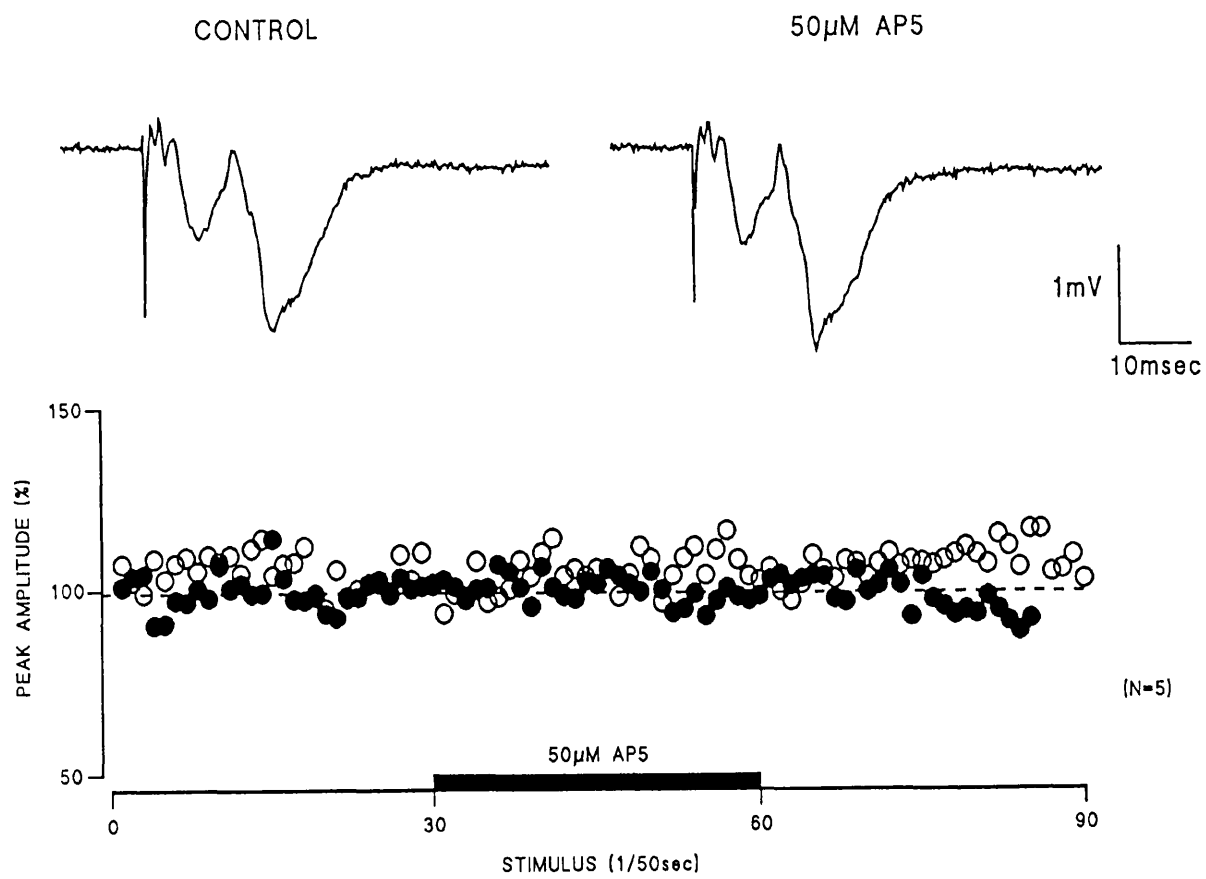
Figure 7.10. The effect of NMDA receptor antagonists on the U1 and U2 response in *Rana*.

In this example 50μM AP5 was added to the bathing medium of *in vitro* preparations obtained from *Rana pipiens*. Conventions are identical to those used in figure 7.8.
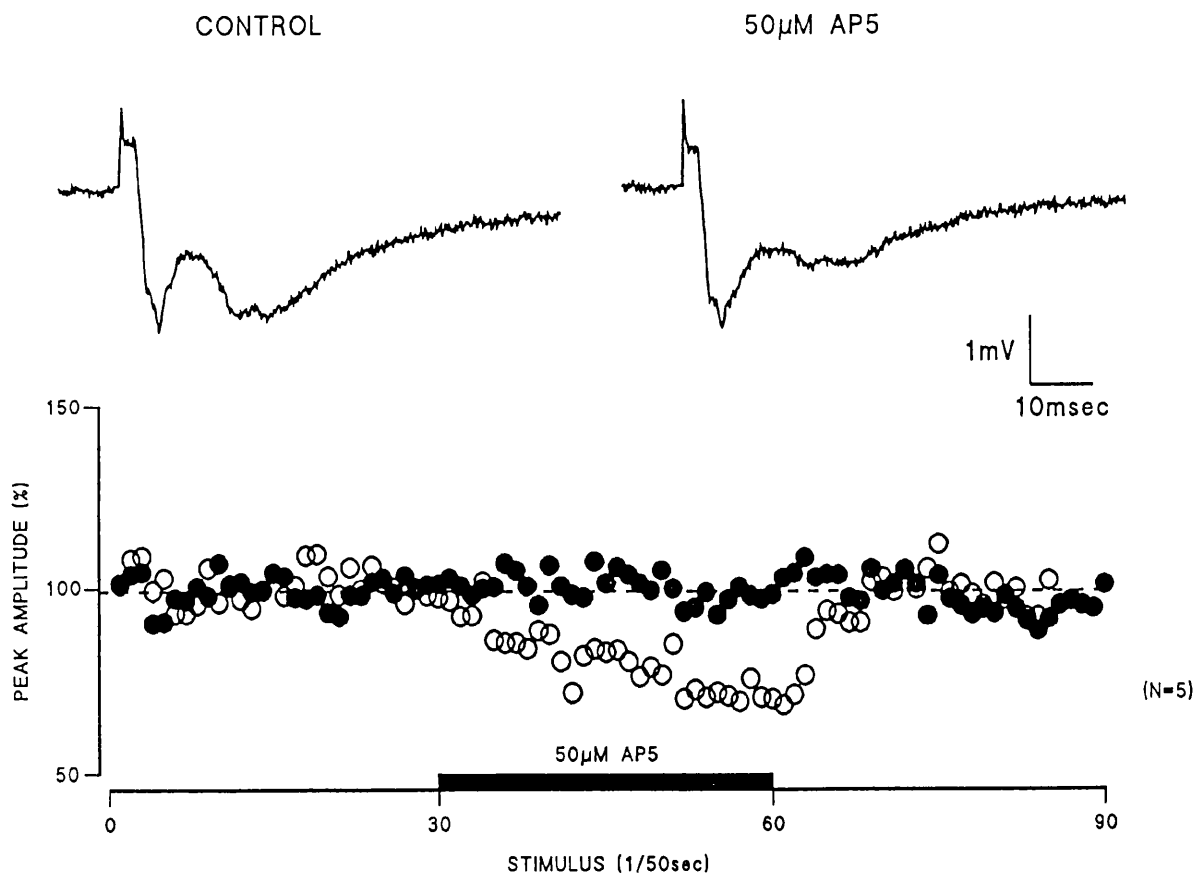
Figure 7.11. The effect of NMDA receptor antagonists on the U1 and U2 response in *Xenopus*.

In this example 50μM AP5 was added to the bathing medium of *in vitro* preparations obtained from *Xenopus laevis*. Conventions are identical to those used in figure 7.8.

7.3. Discussion

Studies documenting the chronic effect of applying the NMDA receptor antagonist AP5 to the developing frog optic tectum have implicated this receptor in both retinotectal (Cline et al., 1987) and intertectal (Scherer and Udin, 1989) synaptic plasticity. In Chapter 6 we have identified a late poly-synaptic response to RGC stimulation in adult Xenopus which is sensitive to AP5. The temporal profile of this NMDA receptor mediated response implicate it as a component of the coincidence-detection mechanism for intertectal plasticity. To test this hypothesis further the AP5 sensitivity of the response was examined in circumstances in which intertectal plasticity is known to be altered. The results of these experiments established further correlations between the NMDA receptor mediated component of the response and the age-, experience- and species-dependence of intertectal synaptic plasticity.

Preparation of the whole midbrain in vitro was not feasible before stage 60 of late larval life. The fragile constituency of the brain at earlier stages hindered the removal of the intact midbrain from the animal. However, robust U1 and U2 responses have been reported in vivo from larval animals as early as stage 40 (Chung et al., 1974b). Therefore, it was not surprising that in vitro preparations from stage 60 animals also contained a robust U1 and U2 response. The physiological characteristics of the U1 and U2 response, their amplitude, and their latency did not change throughout development. More importantly the highly selective effect of AP5 on the long latency poly-synaptic U2 response and the $\sim 60\%$ reduction in the peak amplitude of the U1 and U2 response in the presence of $20\mu M$ CNQX was consistently observed during development. Indeed, at all developmental stages examined so far little change was detected in the CNQX sensitivity of the U1 and U2 response and no change in the AP5 insensitivity of the mono-synaptic U1 response. However, significant changes were found in the AP5 sensitivity of the U2 response. The AP5 sensitivity of the response in the larval animals, before stage 60, was comparable ($\sim 30\%$) with that seen in the animals at 6, 12 and 18 months after metamorphosis. At these late larval stages of development rapid retinal and tectal growth is still occurring but binocular overlap is small but beginning to increase. Therefore, in late larval-life there is a functional requirement for both retinotectal and intertectal plasticity. However, the increase in AP5 sensitivity of the U2 response occurred at a time in development when intertectal plasticity is required but there is little necessity for retinotectal plasticity. The AP5 sensitivity remained elevated until 6 months after metamorphosis when retinotectal plasticity has ceased but eye

positional changes still necessitate minor modifications in the intertectal system.

It also appears that the peak in AP5 sensitivity can be recapitulated later in development but a period of visual experience subsequent to the 12 months of visual deprivation is required to elicit this change. It is difficult to explain this result in terms of retinotectal synaptic plasticity as this phenomenon does not rely upon visual experience. However, the increase in AP5 sensitivity could correlate with the extension of intertectal plasticity which has been shown to be induced by dark-rearing (Grant *et al.*, 1992). This delayed intertectal plasticity is also dependent upon visual experience following the period of visual deprivation. It could be that visual experience is a trigger for the change in AP5 sensitivity observed following long periods of dark-rearing. It would be interesting to establish whether the normal peak in AP5 sensitivity occurred at ~1 month after metamorphosis during dark-rearing. If vision is the cue for this developmental change in AP5 sensitivity then we would expect to see no change in AP5 sensitivity when the animal is denied visual experience through the critical period.

Finally, we have shown that the U2 response elicited in the optic tectum of *Rana pipiens* is not affected by the NMDA receptor antagonist AP5 at a $50\mu M$ concentration. This species of frog does not exhibit intertectal plasticity but does display retinotectal synaptic plasticity. However, it should be noted that the physiological properties of the U1 and U2 response in *Rana* are not identical to those observed in *Xenopus*. Though the latency to peak amplitude, stimulus strength dependency and depth profile of these two responses were very similar in both species the behaviour of these two responses to paired pulse stimulation was different. Facilitation of the U1 response at inter-stimulus intervals between 100 and 1000msec was very evident in *Xenopus* but absent completely from *Rana*. Also, the very marked depression of the U2 response in *Xenopus*, at similar inter-stimulus intervals, did not occur in *Rana*. In fact at inter-stimulus intervals between 100 and 500msec the U2 response was facilitated in *Rana*. This suggests that the mode of propagation of these two responses differs in the two species.

The results of all these studies further implicated the NMDA mediated U2 response of *Xenopus laevis* with intertectal plasticity. The molecular events contributing to this change in AP5 sensitivity are discussed in the General Discussion. However, it was realised that the information supplied by extracellular recordings of this kind would not be sufficient to determine the exact nature of these changes. To these ends, the next Chapter describes a thin slice preparation of the optic tectum in

which whole-cell recordings were made from identified tectal neurons with the intention of establishing, in greater detail, the contribution of NMDA and non-NMDA receptors to synaptic transmission within the circuitry of the optic tectum.

DEVELOPMENTAL CHANGE IN PEAK AMPLITUDE (mV)

	Stage 60		Metamorphosis		1MAM		3MAM		6MAM		12MAM		18MAM	
	U1	U2	U1	U2	U1	U2	U1	U2	U1	U2	U1	U2	U1	U2
	-0.37	-0.279	-1.143	-0.296	-0.742	-0.329	-1.189	-0.222	-1.043	-0.474	-0.982	-0.375	-0.472	-0.519
	-1.004	-0.259	-1.313	-0.437	-0.443	-0.187	-0.731	-0.699	-1.121	-0.641	-0.31	-0.198	-0.79	-0.792
	-0.595	-0.469	-0.439	-0.372	-0.93	-0.535	-0.805	-0.531	-0.754	-0.623	-1.487	-0.198	-1.134	-0.572
	-0.737	-0.448	-0.828	-0.638	-0.43	-0.355	-0.435	-0.182			-0.427	-0.39		
	-0.515	-0.301			-0.711	-0.198	-0.709	-0.259			-0.748	-0.522		
mean	-0.64	-0.35	-0.93	-0.44	-0.65	-0.32	-0.77	-0.38	-0.97	-0.58	-0.79	-0.34	-0.80	-0.63
std	0.22	0.09	0.33	0.13	0.19	0.13	0.24	0.20	0.16	0.07	0.42	0.12	0.27	0.12
n	5	5	4	4	5	5	5	5	3	3	5	5	3	3

DEVELOPMENTAL CHANGE IN LATENCY TO PEAK (msec)

	Stage 60		Metamorphosis		1MAM		3MAM		6MAM		12MAM		18MAM	
	U1	U2	U1	U2	U1	U2	U1	U2	U1	U2	U1	U2	U1	U2
	8.44	57.64	7.6	31.38	6.66	28.3	7.88	26.24	7.06	26.52	9.82	23.36	11.2	25
	6.02	27.6	7.16	29.26	9.26	26.32	8.04	25.3	4.32	23.62	1.112	25.94	8.8	22.2
	8.84	33.28	11.4	32.78	13.96	39.38	11.65	28.54	9.86	31.26	7.16	25.94	9.2	23.4
	9.68	28.72	9	31.24	6.28	26.48	8.38	31.2			5.58	29.54		
	8.81	27.36			10.06	34.52	8.76	23.26			4.84	28.06		
mean	8.36	34.92	8.79	31.17	9.24	31.00	8.94	26.91	7.08	27.13	5.70	26.57	9.73	23.53
std	1.24	11.56	1.65	1.25	2.77	5.14	1.39	2.74	2.26	3.15	2.86	2.10	1.05	1.15
n	5	5	4	4	5	5	5	5	3	3	5	5	3	3

Table 7.1. The characteristics of the U1 and U2 response during development.
The peak amplitude (mV) and latency to peak amplitude (msec) were measured at different stages of development.
MAM: months after metamporphosis.

DEVELOPMENTAL CHANGE IN AP5 SENSITIVITY

	Stage 60		Metamorphosis		1MAM		3MAM		6MAM		12MAM		18MAM	
	U1	U2	U1	U2	U1	U2	U1	U2	U1	U2	U1	U2	U1	U2
	5	-1	-10	-51	0	-57	-4	-75	-8	-14	2	-12	-1	-35
	1	-34	-12	-44	-25	-67	-3	-27	0	-31	2	-34	0	-25
	-15	-28	-3	-28	-12	-62	-2	-22	-11	-37	-1	-24	8	-33
	9	-23	-2	-31	0	-85	-2	-31			-8	-32		
	1	-26			-13	-65	-4	-74			3	-31		
mean	0.20	-22.40	-6.75	-38.50	-10.00	-67.20	-3.00	-45.80	-6.33	-27.33	-0.40	-26.60	2.33	-31.00
std	8.16	11.29	4.32	9.39	9.36	9.52	0.89	23.61	4.64	9.74	4.03	8.04	4.03	4.32
n	5	5	4	4	5	5	5	5	3	3	5	5	3	3

DEVELOPMENTAL CHANGE IN CNQX SENSITIVITY

	Stage 60		Metamorphosis		1MAM		12MAM	
	U1	U2	U1	U2	U1	U2	U1	U2
	-49	-65	-55	-44	-79	-81	-78	-55
	-29	-60	-63	-86	-41	-70	-42	-75
	-36	-63	-55		-60		-74	-42
	-37	-41	-96				-53	-62
mean	-37.75	-57.25	-67.25	-65.00	-60.00	-75.50	-61.75	-58.50
std	7.19	9.55	16.92	21.00	15.51	5.50	14.84	11.93
n	4	4	4	2	3	2	4	4

Table 7.2. Changes in the pharmacology of the U1 and U2 responses during development.

The % change in the U1 and U2 peak amplitudes in the presence of $20\mu M$ CNQX and $50\mu M$ AP5 were calculated at different stages of development.

Normal vision

U1(mV)	U2(mV)	U1(msec)	U2(msec)
-0.45	-0.40	9.28	26.62
-1.56	-0.57	11.68	31.34
-0.62	-0.37	11.20	33.90
-1.01	-0.36	5.84	27.40
-0.20	-0.15	8.38	31.70
mean -0.77	-0.37	9.28	30.19
std 0.48	0.14	2.10	2.75
n 5	5	5	5

Dark-reared

U1(mV)	U2(mV)	U1(msec)	U2(msec)
-0.91	-0.24	8.18	32.04
-0.30	-0.08	9.78	35.85
-0.65	-0.07	9.30	27.86
-0.85	-0.26	6.88	28.30
-0.77	-0.20	8.32	28.14
mean -0.70	-0.17	8.49	30.44
std 0.22	0.08	1.00	3.11
n 5	5	5	5

Dark-reared + light

U1(mV)	U2(mV)	U1(msec)	U2(msec)
-0.58	-0.13	10.28	26.44
-0.74	-0.20	7.20	25.18
-0.41	-0.37	6.64	28.48
-0.83	-0.18	10.62	26.72
-0.92	-0.35	5.90	26.96
mean -0.70	-0.24	8.13	26.76
std 0.18	0.10	1.94	1.06
n 5	5	5	5

AP5 sensitivity

Normal vision		Dark-reared		Dark-reared + light	
U1(%)	U2(%)	U1(%)	U2(%)	U1(%)	U2(%)
0	-11	-7	-36	0	-54
-1	-59	0	-42	0	-90
0	-56	0	-51	-7	-45
-9	-22	0	-19	0	-43
		0	-16	-7	-61
mean -2.50	-37.00	-1.40	-32.80	-2.80	-58.60
std 3.77	20.89	2.80	13.41	3.43	16.98
n 4	4	5	5	5	5

Table 7.3. The effect of visual experience on the U1 and U2 responses.

The peak amplitude (mV) and latency to peak amplitude (msec) was calculated for the U1 and U2 responses in the three groups of animals: (**Normal vision**) animals which had received normal visual experience for 12 months after metamorphosis; (**Dark-reared**) animals dark-reared since stage 55 of larval life until 12 months after metamorphosis; (**Dark-reared + light**) animals given 1 month of normal visual experience subsequent to the 12 months of dark-rearing.

The % change in the peak amplitude of the U1 and U2 responses in the presence of $50\mu M$ AP5 were then calculated in each group.

Difference in response properties

	Xenopus laevis U1(msec)	Xenopus laevis U2(msec)	Rana pipiens U1(msec)	Rana pipiens U2(msec)		Xenopus laevis U1(mV)	Xenopus laevis U2(mV)	Rana pipiens U1(mV)	Rana pipiens U2(mV)
	6	27	12	38		-0.45	-0.40	-2.87	-1.58
	11	34	5	19		-1.56	-0.57	-1.27	-0.36
	12	31	16	19		-0.62	-0.37	-1.87	-1.38
	9	27	7	35		-1.01	-0.36	-2.07	-1.90
	7	27	7	16		-0.75	-0.52	-1.40	-0.68
	4	24	16	29		-0.98	-0.37	-1.09	-0.40
	10	31	9	31		-0.31	-0.20	-2.08	-0.64
	9	24	8	16		-1.49	-0.20	-1.38	-0.45
	8	24	12	38		-0.43	-0.39	-1.96	-1.24
mean	8.44	27.67	10.22	26.78	mean	-0.84	-0.38	-1.78	-0.96
std	2.36	3.40	3.76	8.79	std	0.43	0.12	0.52	0.54
n	9	9	9	9	n	9	9	9	9

Difference in AP5 sensitivity

	Xenopus laevis U1(%)	Xenopus laevis U2(%)	Rana pipiens U1(%)	Rana pipiens U2(%)
	1	-31	0	8
	3	-31	-3	82
	-11	-37	-4	17
	-8	-15	-6	-18
	-8	-40	2	-7
mean	-4.78	-30.58	-2.01	16.29
std	5.43	8.59	2.65	34.97
n	5	5	5	5

Difference in CNQX sensitivity

	Xenopus laevis U1(%)	Xenopus laevis U2(%)	Rana pipiens U1(%)	Rana pipiens U2(%)
	-78	-55	-72	-56
	-42	-75	-65	-42
	-74	-42	-74	-85
	-58	-63	-57	-63
mean	-63.15	-58.73	-67.08	-61.60
std	14.16	12.14	6.71	15.50
n	4	4	4	4

Table 7.4. Comparison of the U1 and U2 response in *Rana* and *Xenopus*.

The peak amplitude (mV) and latency to peak amplitude (msec) was calculated for the U1 and U2 responses in *Xenopus* and *Rana*.

The % change in the peak amplitude of the U1 and U2 responses in the presence of $20\mu M$ CNQX and $50\mu M$ AP5 were then calculated in each group.

Chapter 8

Slice preparation of the optic tectum

8.1 Introduction

8.1.1. Anatomy of the optic tectum.

The structure of the optic tectum in *Xenopus laevis* is very similar to that of other anuran amphibians and has been extensively reviewed (see Lázár, 1984). In terms of its cytoarchitecture the tectum can be divided into alternating cellular (1,2,4,6, and 8) and fibrous layers (3,5,7,and 9). The most superficial fibre layer 9 is further subdivided into laminae A through to F. There are approximately 450,000 neurons in the tectum of *Rana pipiens* which is roughly equal to the number of retinal ganglion cells (RGCs) which innervate the structure. In *Xenopus laevis* there are half this number of RGCs and tectal neurons. Layer 8 cell bodies are $< 10\mu$m in diameter and represent the smallest neurons in the tectum whereas the largest cell bodies are found in the deeper periventricular layers of the tectum. Golgi staining studies have revealed that the majority of neurons possess axons which arborize within the tectum, a few are devoid of axons, and the rest have efferent axons projecting to associated areas of the frog brain. Therefore, the neuronal types in the optic tectum can be broadly divided into two groups, intrinsic neurons with axons arborizing in the tecta; and, projective neurons which send axons into layer 7 before leaving the tectum (figure 8.1).

The main afferent connections to the tectum originate from the contralateral retina. Horse radish peroxidase (HRP) and cobalt chloride studies, visualizing RGC fibres, showed that, in *Xenopus*, layer 9 is evenly labelled but laminae D is irregularly stained. There are a variety of non-retinal inputs to the tectum. Degeneration techniques have revealed an ipsilateral thalamo-tectal projections to laminae 9, mainly in layer A, and in the deep layers of the tectum. HRP injections also show an ipsilateral thalamo-tectal projection but no link with the Lateral Geniculate Nucleus (LGN) has been observed in either case. Afferents from the brainstem and the spinal cord exist with a low number of afferents terminating in the periventricular tectal layers and an ipsilateral link between the tegmentum mesencephali. There is a projection from the dorsal column of the spinal cord and the suprapenduncular nucleus on both sides. A more substantial bilateral topographic innervation exists from the Nucleus Isthmi (NI) (demonstrated using HRP tracing techniques) and ipsilateral isthmo-tectal fibres distribute to the whole of layers 9

and 8. Contralateral isthmo-tectal fibres only terminate in layer A and 8.

Possible anatomical correlates between the afferent inputs and tectal neurons have been examined. The main targets for the retinal afferent input are large pyriform and pyramidal cells and 5 or 6 different inputs may converge on the same cell. Retinal afferents extend from the pial surface with 6 alternating myelin-unmyelinated retinal fibre inputs through layer 9, with the 7th lamina below layer 8 receiving the thickest myelinated input. The majority of tectal periventricular neurons send dendrites to layer 9. The cells in layer 6 and 8 do the same. Pyriform neurons with wide dendritic trees (Maturana *et al.,* 1960) may be activated by myelinated fibres in B,D and F, with unmyelinated fibres on the thicker dendrites, dendritic appendages, and spines. Pyramidal cells receive connections on their widely arborizing dendritic trees. Layer 8 cells receive synaptic contact from retinal axons in layers A to F which may terminate on their dendrites. Fusiform, stellate and amacrine cells only receive input from one or two layers. Large ganglionic cells receive thick myelinated fibres in layer F and G (Matsumoto and Bando, 1980). Many of these large neurons send their axons to the spinal cord and could be involved in escape reflexes. Non-retinal afferents from the ipsilateral diencephalon and the NI send their projections to layer 9 and make connections with the same neurons that receive retinal input. The contralateral NI input connects in lamina A on narrow dendritic trees and the proximal dendritic trunk of layer 8 cells. Pretectal afferents connect to layer 3 and 5 mainly onto the basal dendrites of these cells. Efferent pathways of the optic tectum include the crossed projection to the spinal cord, a crossed projection to the thalamus, a projection to the LGN, and a crossed and uncrossed projection to the NI.
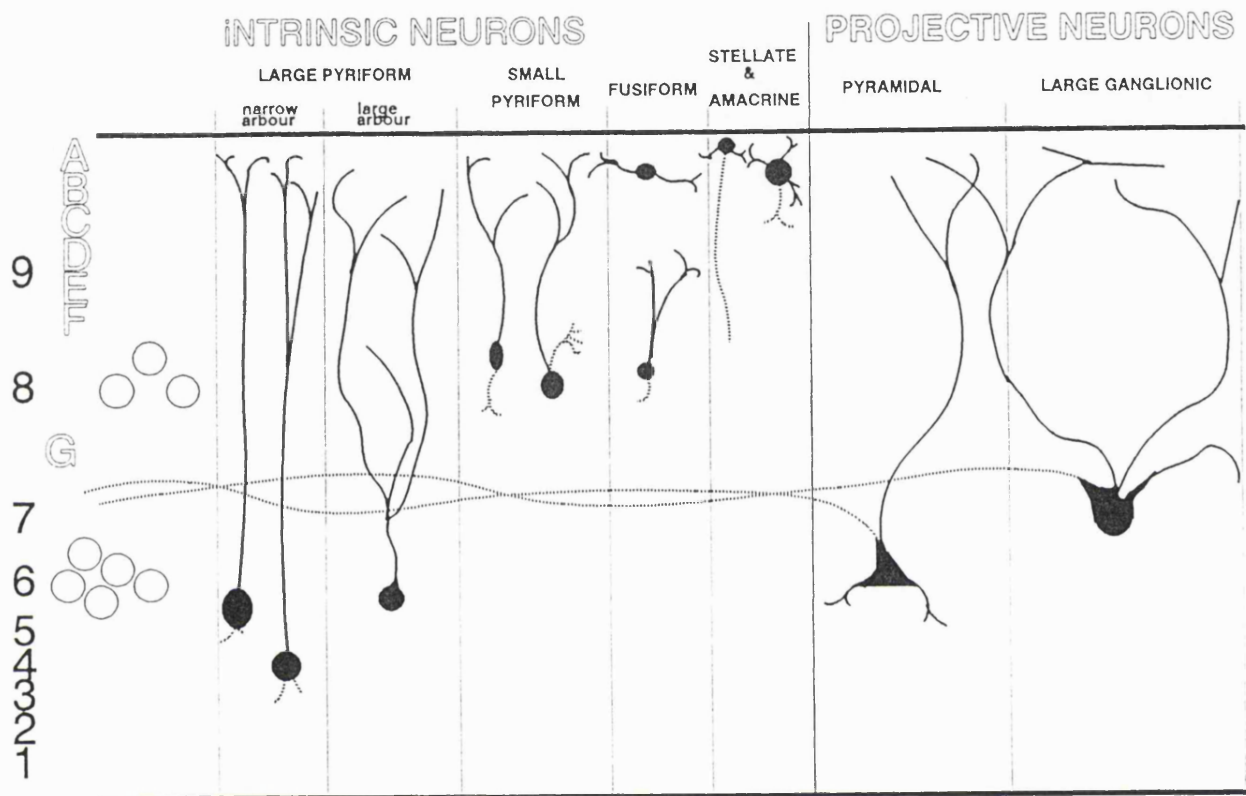
Figure 8.1. A schematic diagram of the neuronal cell types present in the optic tectum.
    The main neuronal types in the optic tectum and the organisation of the alternating fibre and cell body layers are depicted in cartoon form. Layer 9 is the most superficial layer where the retinal ganglion cell input terminates and layer 1 is the deepest layer next to the tectal ventricle. The main cell body layers are 6 and 8 which mainly comprise non-projecting pyriform type (pear shaped) neuronal cell bodies. The apical dendrites of these layer 6 and 8 cell bodies are the main recipients of the retinal input to layer 9. The main efferent layer is layer 7 and the majority of projective neurons are situated in the periventricular layers below this (see text for further details).

8.1.2. Intracellular recording from the tectum.

Electrophysiology of the optic tectum has been mainly based upon extracellular recording of single- or multi- unit responses following physiological stimuli (Chapter 5) or through the analysis of extracellular field potentials recorded from neuronal clusters in response to electrical stimulation of the optic nerve or tract (Chapter 6 & 7). Due to the small size of tectal neurons few attempts have been made to classify their intracellular properties. Stable intracellular recording is difficult as impalement with conventional sharp electrodes invariably damages the cell. However, intracellular recordings have been made *in vivo* from adult *Rana catesbeiana* (Matsumoto and Bando, 1980) and *Rana temporaria* (Matsumoto *et al.*, 1986). Standard DC recordings were made of excitatory and inhibitory postsynaptic potentials (EPSPs and IPSPs) following visual stimulation of identified receptive fields and in response to electrical stimulation of the optic nerve. Intracellular staining techniques were employed to enable any correlative morphology to be identified.

In *Rana catesbeiana*, two major neuronal types were identified in response to electrical stimulation of the optic nerve; Type I consisting of an EPSP followed by an IPSP; and Type II consisting of two successive EPSPs followed by an IPSP (Matsumoto and Bando, 1980). Staining with Procion Yellow revealed that large multipolar cells, presumably large ganglionic cells, gave rise to both types of response. Another set of neurons which resemble pyriform neurons exhibited a type I response. Later, visual stimulation experiments (Antal *et al.*, 1986) using cobalt filled electrodes revealed that pyriform type cells in layers 8,6,4, and 2 could be subidivided into two populations; those with beaded dendrites and short axons which responded with an IPSP and were classified as interneurons, and those with smooth dendrites and long axons projecting into layer 7 which responded with EPSP's and action potentials and were classified as projective neurons. Large ganglionic cells were also identified but these showed a variety of complex responses to visual stimuli. ELectrical stimulation of the uncrossed NI in *Rana catesbeiana* has been shown to result in a single IPSP indicating strong isthmic inhibition (Wang and Matsumoto, 1990).

In *Rana temporaria*, similar experiments (Matsumoto *et al.*, 1986) described response properties consisting of EPSP's and action potentials interrupted by small IPSP's. Co^{3+}-lysine fills demonstrated that this response profile was shared by pyriform, pyramidal and large ganglionic cells situated in layers 6,7 and 8 of the tectum. Using a variety of visual stimuli this study was able to divide this seemingly homogeneous population into 5 different classes based upon receptive field properties. Electrical

stimulation of the optic tract confirmed that the majority of neurons (54%) respond like a Type I neuron with an EPSP followed by an IPSP. A quarter of the cells encountered responded with a single EPSP which could elicit an action potential and 10% responded with two EPSP's followed by an IPSP, characteristic of a Type II neuron. However, the action potentials that are illustrated from the *in vivo* recordings were very small with little overshoot. It could be, as the authors suggest, that tectal neurons do not spike very often *in vivo* and that processing of neuronal information in the frog optic tectum occurs via dendro-dendritic connections. However, this observation may simply result from the poor condition of tectal cells following impalement with sharp electrodes.

Little is known about the basic intracellular properties of neurons in the optic tectum of *Xenopus*. Therefore, it is uncertain which population of tectal neurons receive non NMDA and NMDA mediated synaptic input of the type described in Chapter 6. The aim of this study was to characterise the intracellular properties of tectal neurons with the intention of evaluating the role of NMDA and non NMDA receptors in synaptic transmission within the tectum. The relatively small size of tectal neurons, the vast majority of which are under $15\mu m$ in diameter, has meant that impalement with conventional sharp microelectrodes has been difficult and the data obtained unsatisfactory. Recently, Edwards *et al* (1989) described a preparation which allows patch clamp recordings to be made on mammalian CNS neurons *in situ*. This methodology has been adopted in this study in order to make high resolution electrical recording of membrane current in visually identified tectal neurons. Physiologically viable thin slice preparations of the optic tectum, $200\mu m$ thick parasagittal sections, were developed with the use of vital dyes to fluorescently stain healthy cell bodies. The high level of visual resolution which can be attained using thin slice techniques enabled intracellular recordings to be made from identified tectal neurons in specific layers of the tectal neuropil. After establishing the viability of this slice preparation the electrophysiological and morphological properties of tectal neurons were ascertained. Localized cleaning of cell somata, with physiological saline, to expose the cell membrane allowed the formation of a high resistance seal between the membrane and the patch pipette. Tight-seal whole cell voltage and current clamped recordings were made and lucifer yellow (LY) was incorporated into the cell and photographs taken of the labelled fluorescent neurons. The electrical properties of morphologically identified tectal neurons were measured in voltage-clamp and current-clamp configurations.

8.2. Results

A maximum of six 200μm thick parsagittal slices could be prepared from one *Xenopus* brain. In this study animals were staged between 1 and 3 months postmetamorphosis and no attempt was made to prepare slices from younger or older animals. Within each section the highly laminated structure of the tectum was conserved from the pial surface down to the tectal ventricle (figure 8.2). Other nuclei rostral and caudal to the optic tectum were also intact and could be visualised if necessary. For example, in some sections the ipsilateral nucleus isthmi was present caudal to the tectal lobe. The relatively high optical density of myelinated fibres allowed the afferent and efferent layers of the tectal neuropil to be indentified. This in turn enabled the identification of cell body layers 8 & 6 and the periventricular cell body layers on the basis of their position within the slice. In some slices a portion of the optic tract and the location at which fibres from the tract invaded the superficial layers of the tectal neuropil could also be visualised. Individual tectal soma could be visualised in every cell body layer and what appeared to be healthy cell bodies were often apparent on the exposed surface of the slice (Figure 8.3). The microvilli and cilia associated with the ependyma, a ciliated columnar epithelium lining the tectal ventricle, could be seen moving in healthy slices.

8.2.1. Vital-dye staining.

Parasagittal 200μm thick slices of the optic tectum which were incubated with Fluorescein diacetate (FDA) exhibited strong fluorescence from a substantial number of cell bodies in every cell body layer of the optic tectum (see figure 8.2). Fluorescence was exhibited by cells on the cut surface and by those located deeper in the tectal slice. When the slicing procedure was successful little ethidium bromide (EB) staining was observed anywhere in the preparation.

Figure 8.2. Photographs of the tectal slice preparation.

The top photograph shows a representative parasagittal tectal slice under bright field illumination at low magnification (x10).

The bottom photograph is a portion of the tectal slice incubated with fluoresceine diacetate viewed at higher magnification (x40 water immersion, 0.75 NA) under epifluerescence illumination.

Page 174

Figure 8.3. Photographs of the tectal slice preparation at higher magnification and following a lucifer yellow injection.

A & B. Photographs of 200μm thick parasagittal tectal slices viewed under bright field Normaski optics (x40 water immersion, 0.75 NA). In **A**, the darker fibre layer 7 is in the top half of the photograph and individual pyriform type cell bodies of layer 6 can be visualised in the lower half. **B** shows the periventricular layers of the tectum with a portion of the ventricle visible in the left hand corner of the photograph. In this section the cell bodies of large ganglionic cells can be seen.

C. Epifluorescent illuminated photographs of Lucifer Yellow filled neurons *in situ* made during whole cell recordings illustrating dye coupling between a large ganglionic cell situated in the periventricular layers of the tectum. Fluorescence from LY in the patch pipette can be seen in the bottom half of the photograph. The brightly fluorescent soma of the large ganglionic cell is out of focus in this picture. The primary and secondary dendrite of the filled cell is in focus and below the right hand branch of the dendrite a second soma can be seen. This dye filled neuron also has a primary dendrite travelling out of focus towards the top of the photograph. Where the dye coupling is occurring the dendrite of the large ganglionic cell appears to be swollen.

Page 175

Figure 8.4. Reconstructions of lucifer yellow fills from the various layers of the tectal slice preparation.

A, 10 neurons traced from LY fills in the periventricular layer. The lower thin horizontal running line represents the position of the tectal ventricle. The top two thin lines depict the border of fibre layer 5.

B, 8 neurons traced from LY fills in layer 6 of the tectum. The horizontally running parallel lines depict the border of the layer 7 fibre tract.

C, 8 neurons traced from LY fills in layer 8 & 9 of the optic tectum. The top thin line shows the location of the tectal surface and the lower two lines show the upper and lower borders of layer 8.

A, B & C Scale bar = 10μm

Page 176

C

B

A
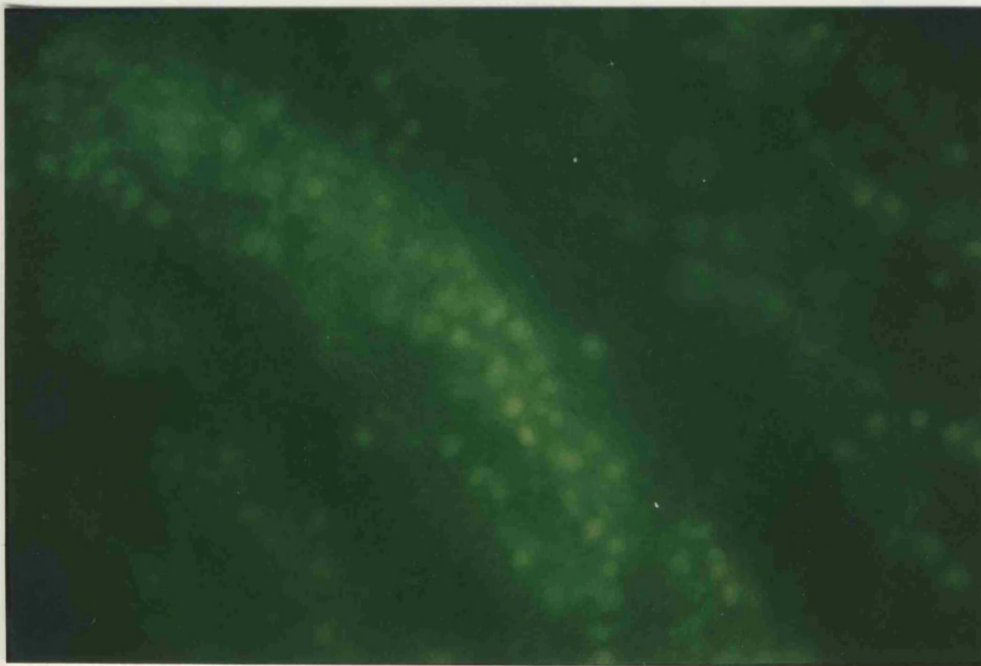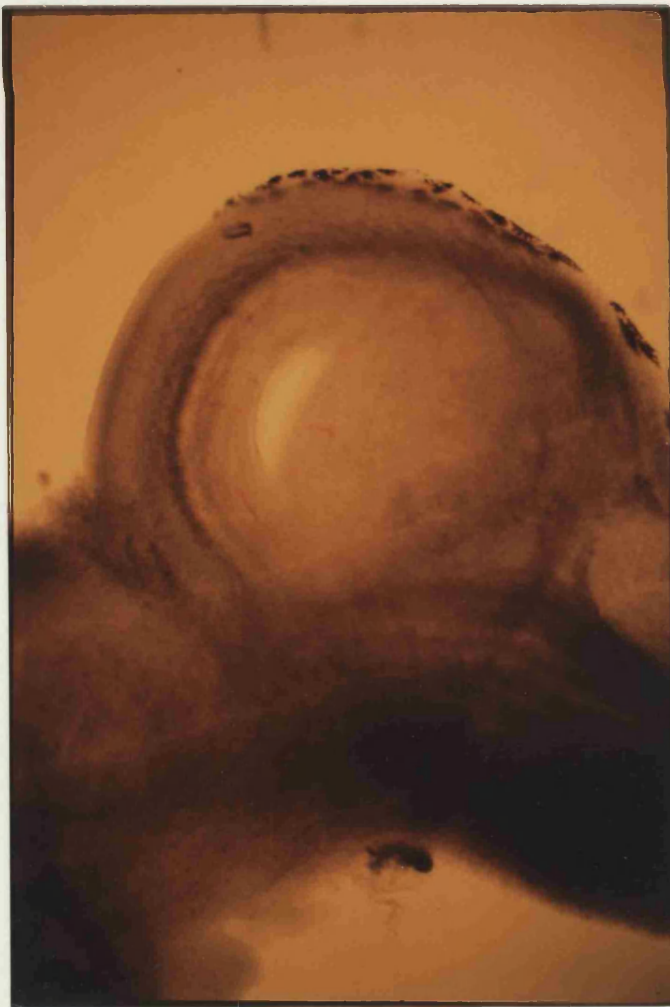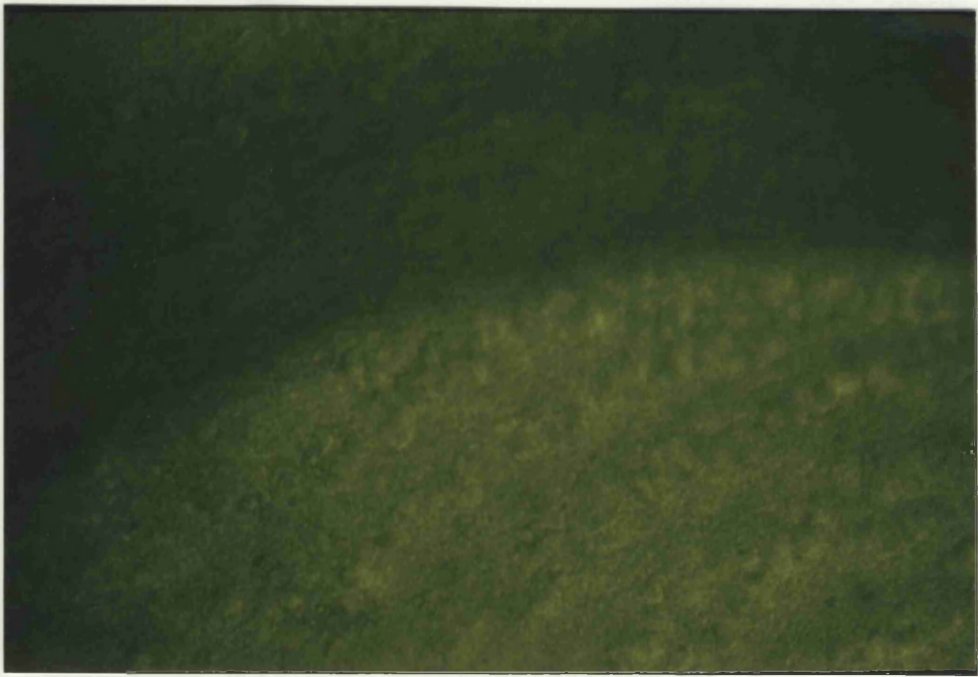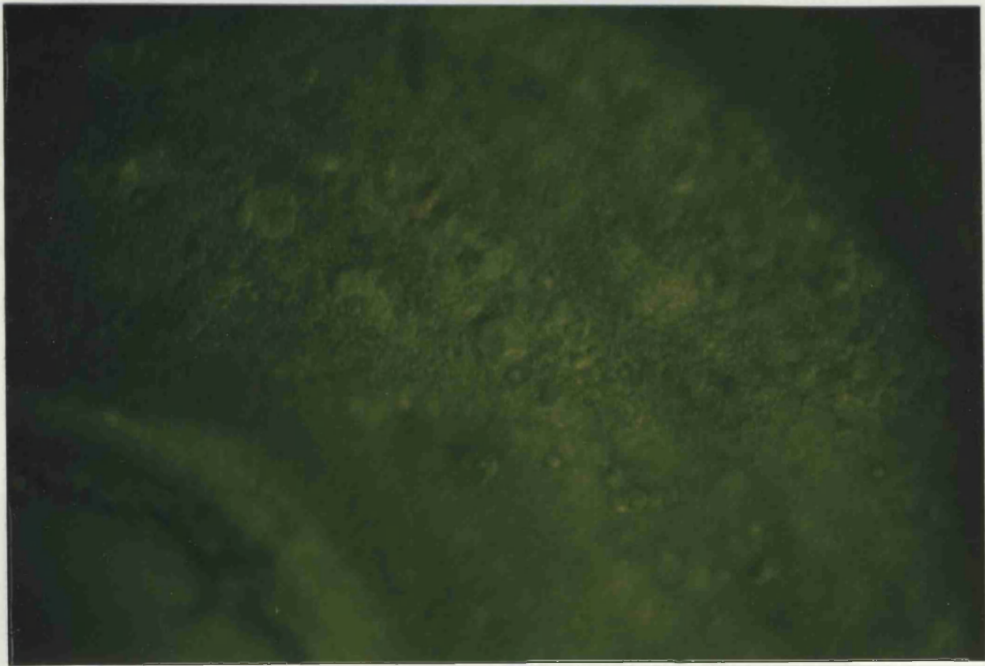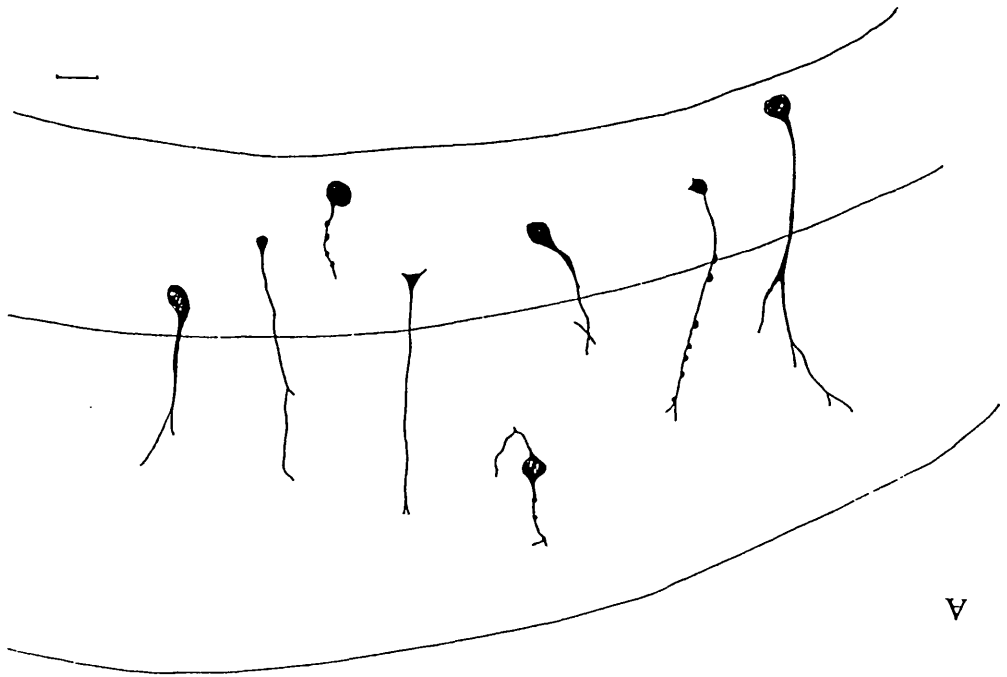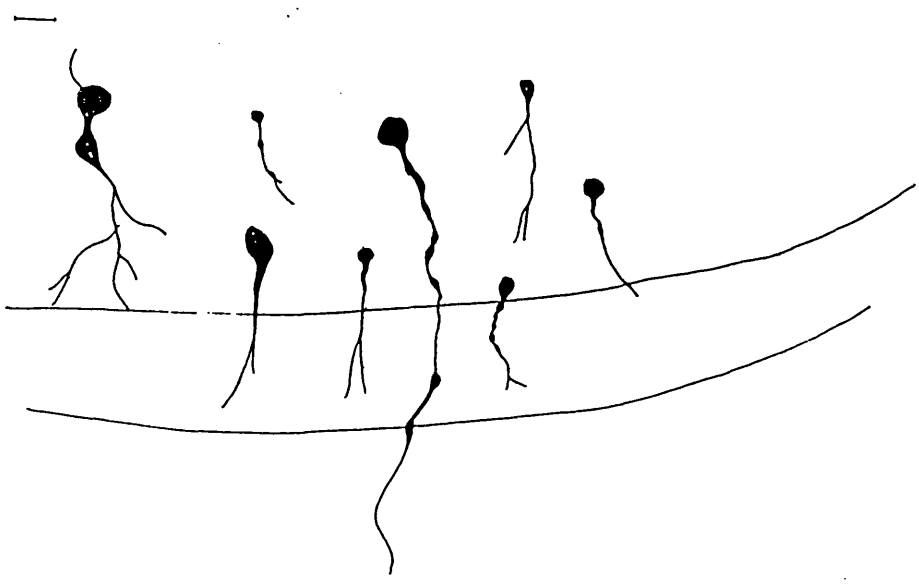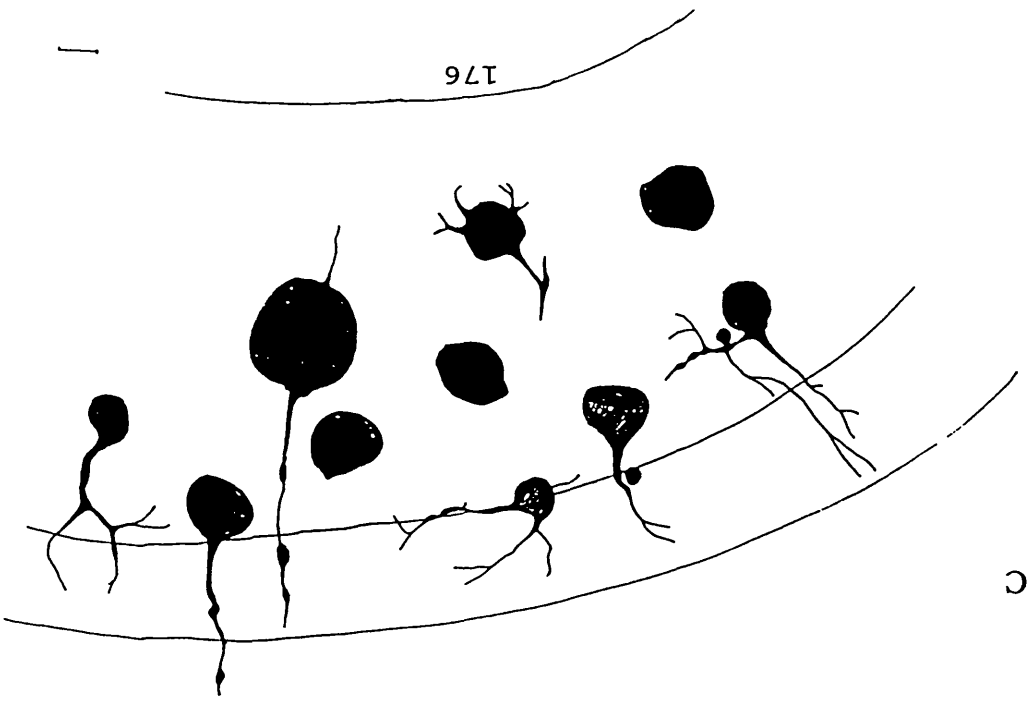
8.2.2. Lucifer Yellow injection.

After establishing a GΩ seal no LY was observed passing from the pipette to the tectal cell. Only on rupturing the cell membrane and entering whole cell configuration did LY rapidly diffuse into the soma. Diffusion of LY into the cell continued for several seconds until equilibrium between the contents of the cell and the pipette had been achieved. Unfortunately, the tight seal between the tip of the pipette and the membrane of the cell made removal of the pipette impossible. Therefore, histological preparation of dye-filled neurons was not feasible and we had to rely on the fluorescence of LY *in situ* for morphological classifications. Photographs of LY fluorescence were taken at various focal depths to reconstruct the extent of the fill (figure 8.3). Bright field photographs were also taken to record the position of the cell bodies within the tectal neuropil. Using this technique we could identify the dendrites of pyriform type neurons in layer 9, 8 & 6 and large ganglionic cells in the periventricular layers (see figure 8.3) of the slice.

The largest cells encountered were situated in the deep periventricular layers (figure 8.4). In the majority of these cells fluorescence was detectable in primary and secondary dendrites travelling superficially towards layer 5. The cell bodies were 30-50μm in diameter typical of large ganglionic cells. In two cases what appeared to be a second soma, in contact with the primary dendrite of the cell, would also fluoresce indicative of dye-coupling. In one of these instances dendrites could also be observed travelling superficially from the dye-coupled cell body (figure 8.3). When LY was incorporated into cells in layer 6 what appeared to be primary dendrites were always observed extending towards more superficial layers (figure 8.5). However, very little tertiary dendrite was detectable in any of the fills. Cell body diameter ranged from 10-20μm and all were pyriform shaped. Layer 8 cell bodies had diameters of 10-15μm with very little tertiary dendrite (figure 8.4). However, the primary dendrite of these pyriform-shaped cels sometimes had a beaded appearance. Cells situated in layer 9 could also be filled with LY and these had a bipolar appearance with very short often beaded dendrites (figure 8.4). Axons were not visible with LY in any of the neuronal populations studied in this preparation.

8.2.3. Voltage-clamp recording.

In whole cell configuration macroscopic current, which represents the sum of the current through many ionic channels, can be recorded. The capacitance (C) and the series resistance (R_s) for each cell population was calculated from the area and the time

constant of the current transients initially recorded during a 5mV step in holding potential (see Methods). Layer 9 cells = 5.33 pF ± 4.11 pF (std, n=3); layer 8 pyriform cells = 6.88 pF ± 6.01 pF (std, n=8); layer 6 pyriform cells = 4.2 pF ± 4.2 pF (std, n=5, range 1 to 8pF); and large ganglionic cells = 39.5 pF ± 22.1 pF (std, n=8). The R_s encountered in these cells, with electrodes of 1-5 MΩ resistance, ranged from 10 to 50 MΩ. During experiments in which the Axopatch 2A was used to make whole cell recordings the capacitance and series resistance values obtained directly from the amplifier were comparable to our calculated valuesmade from the capacitance transients (see Methods). The decay of the transient current associated with the capacitance of the membrane, in the large ganglionic cell population, was described by a single exponential decay (figure 8.5) which implies that the quality of voltage clamp was sufficient for this neuronal population.

Voltage step experiments performed on tectal neurons during whole cell recording revealed standard inward and outward voltage activated conductances (figure 8.6). What appeared to be fast inactivating inward Na^{2+} current and slower outward K^+ current were present in all neurons examined. However, it was obvious that the characteristics of the current records obtained from the pyriform (n=7) and large ganglionic (n=5) cells were different. Firstly, larger conductances were observed in the macroscopic current elicited in the large ganglionic cells and obvious tail currrents were observed in the records obtained from this neuronal population. The current-voltage relationship, measured from the steady state outward K^+ current demonstrates that the degree of outward rectification present in the large ganglionic cells was greater than that observed in the pyriform cells. The outward K^+ current were activated at more negative potentials ($\sim$-50mV holding potential) in the large ganglionic cell population. Activation of the outward K^+ current in the pyriform cells occurred when the holding potential was stepped to -20mV. From the results of the voltage step experiments it also appeared that the quality of the voltage clamp in the large ganglionic cells was poor with obvious spikes in the current record as the neuron escaped voltage clamp (figure 8.6). This was not observed in the smaller pyriform cells in which the quality of voltage clamp was much improved.

At holding potentials close to the resting membrane potential (average -67.36 mV ± 3.75 mV; std & n=11) spontaneous postsynaptic events were observed in the current record in 5 out of 11 whole cell recordings made from pyriform type neurons. These spontaneous postsynaptic current were negative going deflections of varying amplitude, between 5 and 40pA, with a duration of up to 100msec (figure 8.7). At more hyperpolarised potentials the amplitude of the postsynaptic inward current increased and

as the holding potential was depolarised the inward current got progressively smaller (figure 8.8). These inward currents reversed polarity at positive holding potentials, typically +25mV (figure 8.8).

5pA

1msec

10mV

Single exponential decay:

y = A·exp(-k·x)

k = 1215.744 ± 51.6018 t Ratio 23.56

A = 1.457E-6 ± 9.814ε-7 t Ratio 1.48

r = 0.997331

Goodness-of-fit Index = 0.999673
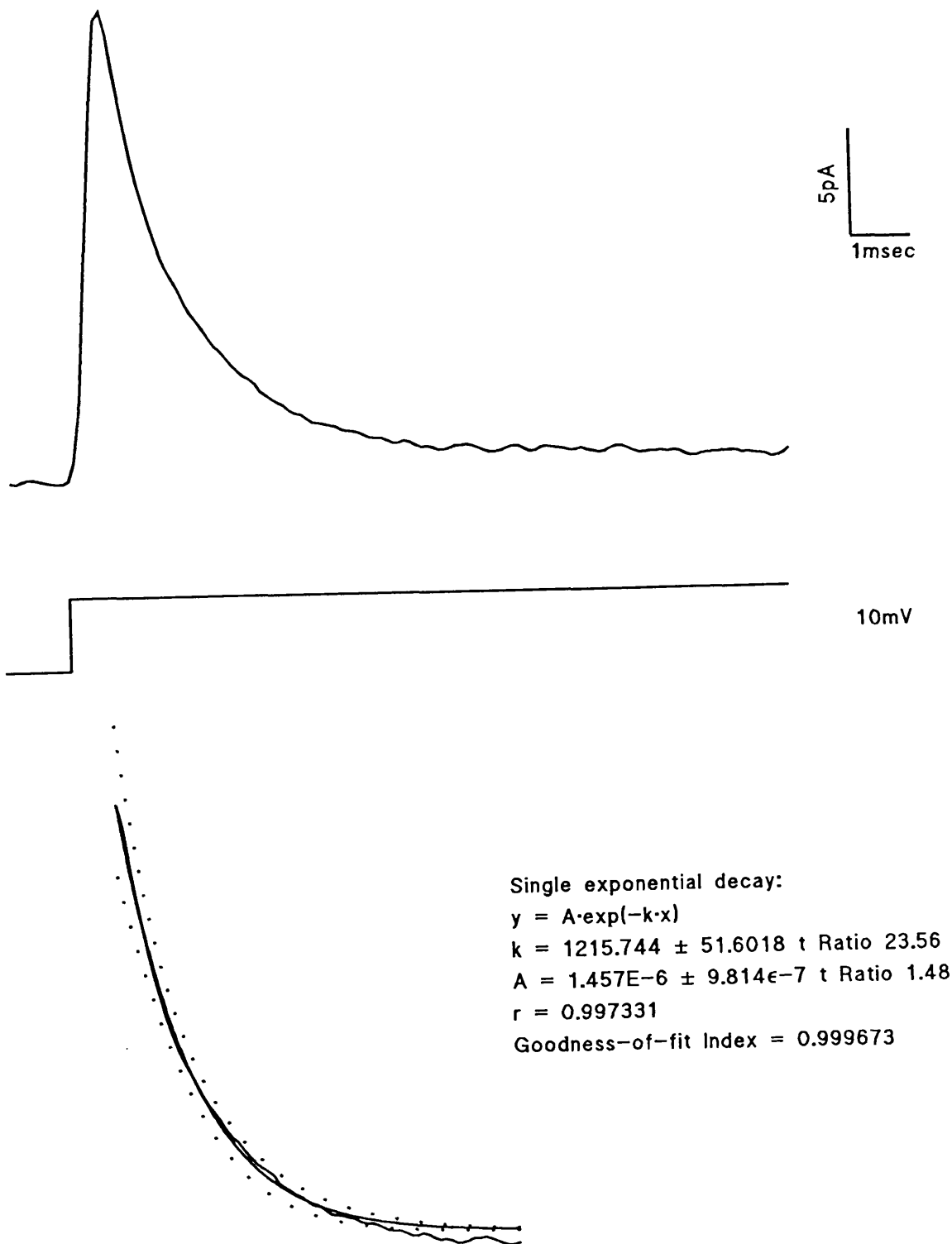
Figure 8.5. Slow capacitive transient recorded from a large ganglionic cell.

The top trace is an average of 5 records made following a 10mV step in holding potential during a tight seal whole cell voltage clamp recording from a large ganglionic neuron. In the bottom plots the results of a single exponential fit is shown superimposed over the decay of this capacitance transient. The upper and lower confidence limits for this fit are taken from the standard deviations for the averaged record (dotted line).

179
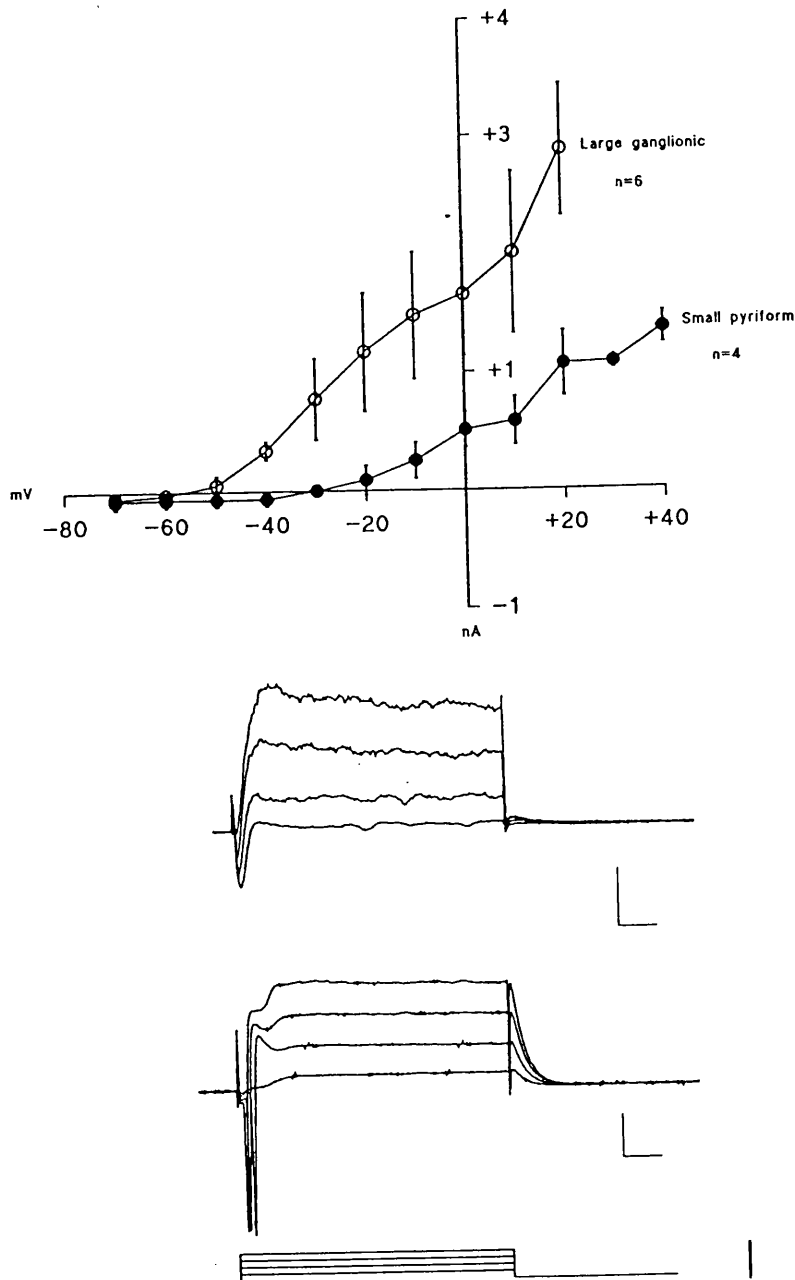
Figure 8.6. Voltage step experiments in pyriform neurons and large ganglionic neurons.

The bottom trace shows the current record from a tight seal whole cell voltage clamp experiment on a same large ganglionic neuron. In this experiment the holding-potential was stepped from -70mV to -50mV, -30mV, -10mV and finally +10mV for a duration of 50msec as depicted by the solid line drawing at the bottom of the figure. An attempt has been made to compensate for the slow capacitance transients present at the start and the end of the step in holding potential (C=38pF. R_s=35MΩ). Immediately following the step in holding potential a fast inward current occurs which rapidly inactivates within 10msec. Then an outward current occurs which does not inactivate but reaches a steady state. In this cell type when the holding potential is stepped back to -70mV a tail current is apparent in the current record. Scale bar = 1nA, 10msec.

The middle current traces are taken from a voltage clamp experiment performed on a pyriform type neuron. Once again the holding potential is stepped from -70mV to -50mV, -30mV, -10mV and +10mV for a duration of 50msec. The slow capacitance transient was compensated for (C=6pF. R_s=15MΩ) and once again a fast inactivating inward current occurred during the first 10msec of the response and a slower outward current reached a steady state level immediately afterwards. Scale bar = 1nA, 10msec.

The top plot demonstrates how the steady state outward current varies with the size of the voltage step. The holding potential (mV) is plotted against the current (pA) for large ganglionic (open circles) and pyriform (filled circles) type neurons. The error bars represent the standard deviation for these average values of current flow.
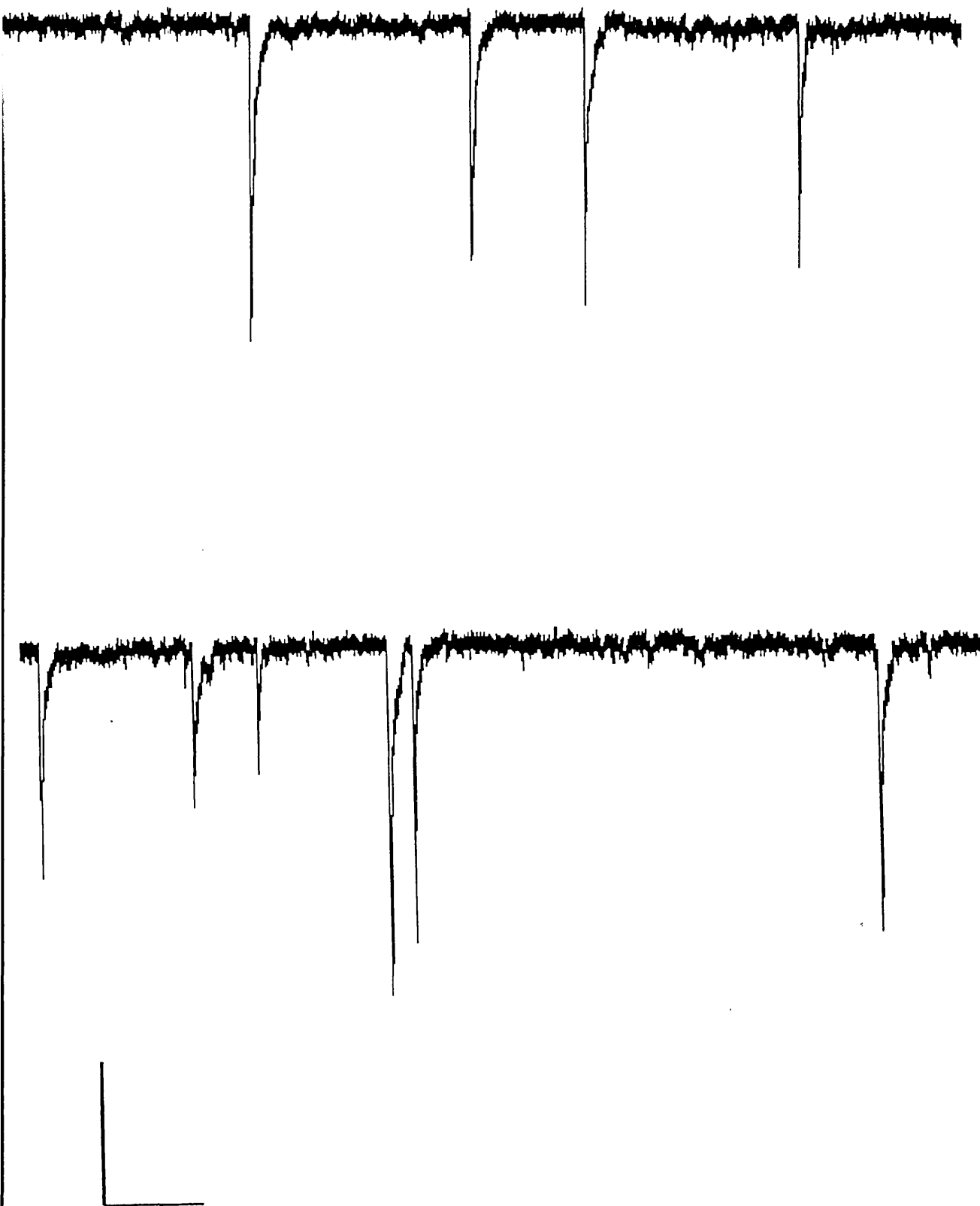
Figure 8.7. Spontaneous postsynaptic current recorded from a pyriform neuron in the tectal slice preparation.

A tight seal whole cell voltage clamp recording from a pyriform type neuron in layer 8 (C=10pF, R_s=18MΩ, rmp=-67mV) with 20mM Cl$^-$ ion in the patch pipette.

Scale bar = 100msec, 20pA.

181
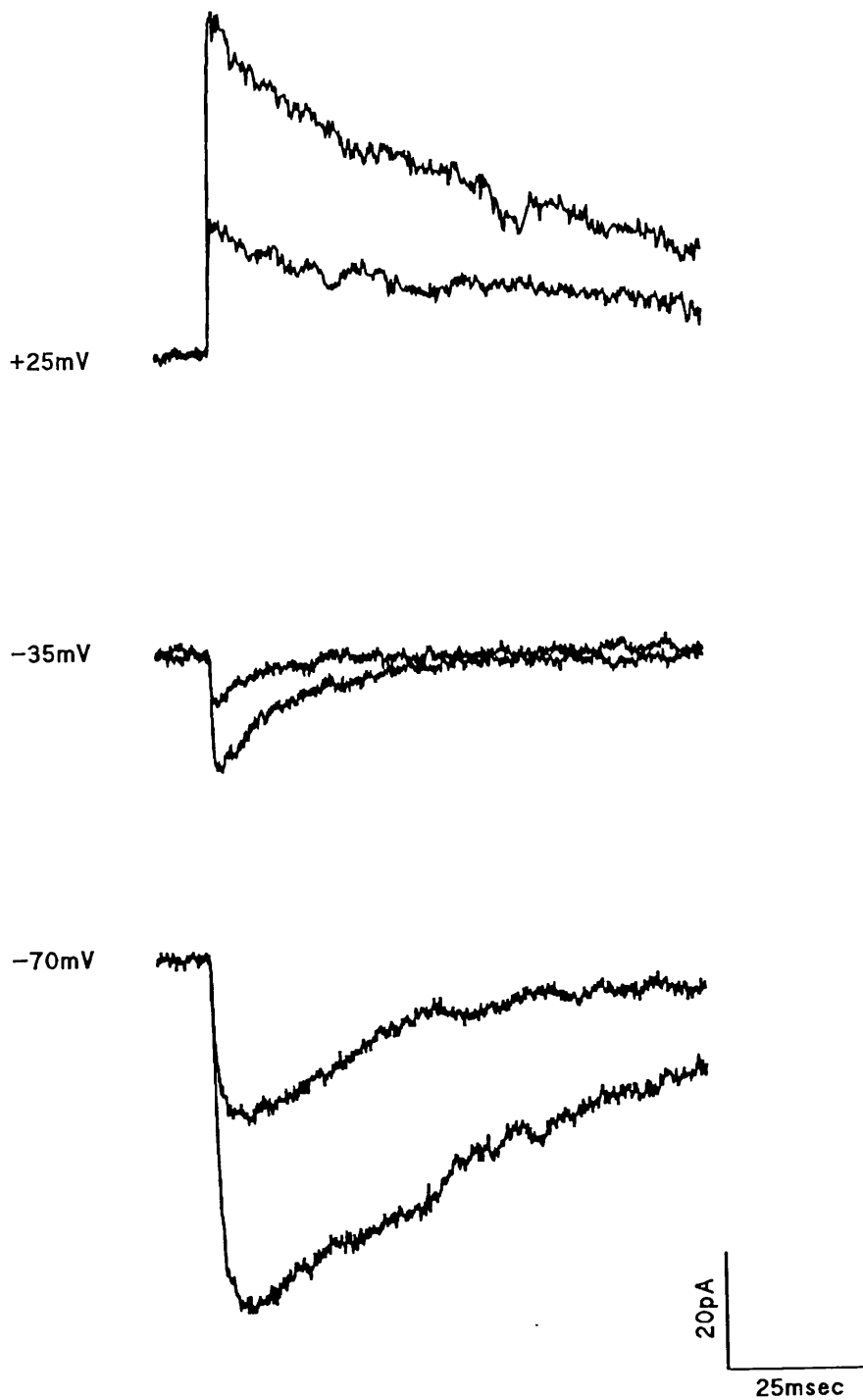
Figure 8.8. Effect of holding potential on spontaneous postsynaptic current recorded from the tectal slice preparation.

Tight seal whole cell voltage clamp recording from a pyriform neuron in layer 8 (C=22pF, $R_s = 16M\Omega$) with 20mM Cl⁻ ion in the patch pipette. In this experiment the holding potential was maintained at -70mV, -35mV and +25mV. The smallest and largest spontaneous current recorded at each holding potential are shown.

8.2.4. Current-clamp recording.

In current clamp mode the membrane voltage (Vm) of a cell was measured during tight-seal whole cell recording. Layer 9 pyriform neurons had resting membrane potentials (RMPs) of -61.33mV $\pm$ 10.21mV (std, n=3); layer 8 pyriform neurons had RMPs of -59.00mV $\pm$ 15.85mV (std, n=8); layer 6 pyriform neurons had RMPs of -49.8mV $\pm$ 13.89mV (std, n=5); and large ganglionic cells below layer 5 had RMPs of -52.63mV $\pm$ 14.91mV (std, n=8). The firing properties of these different neuronal populations were then analyzed by injecting depolarising current into the cell. When depolarised with current steps of 100-300msec duration two modes of firing were consistently observed from neurons in this preparation. Type 1 neurons responded with a continuous firing of action potentials whose frequency increased when current strength was raised (figure 8.9). Type 2 neurons responded to current injection with a short burst of action potentials, typically 10, at the beginning of the current step which accommodated rapidly to continued depolarisation (figure 8.10). However, in one instance after the initial burst of action potentials a second burst of action potentials would occur ~50msec later. During whole cell recording in these experiments LY was included in the recording pipette so that the morphology could be confirmed. The Type 1 neurons encountered (n=4) were pyriform cells of layer 8 and 6 whereas the Type 2 neurons (n=6) were all large ganglionic cells situated in the deeper periventricular layers of the tectum. Further examination of the individual action potentials generated in the two groups showed that the shape of the action potential differed in the two populations (figure 8.11). The action potentials recorded from the pyriform cell population were much broader than those recorded from the large ganglionic cells. The width of the action potentials, measured from the threshold of the action potential to the trough produced during the action potentials after hyperpolarization, was 3.02 $\pm$ 1.77 msec for the large ganglionic cells and 13.45 $\pm$ 0.05 msec for the pyriform cells. The rate of rise for the action potential was 86.33 $\pm$ 44.17 V/sec for the large ganglionic cells and 10.3 $\pm$ 2.7 V/sec for the pyriform cell population. The rate of the action potentials decay in the pyriforn cells (-15.6 $\pm$ 2.4 V/sec) was also much slower than that calculated for the large ganglionic cells (114.17 $\pm$ 67.4 V/sec).
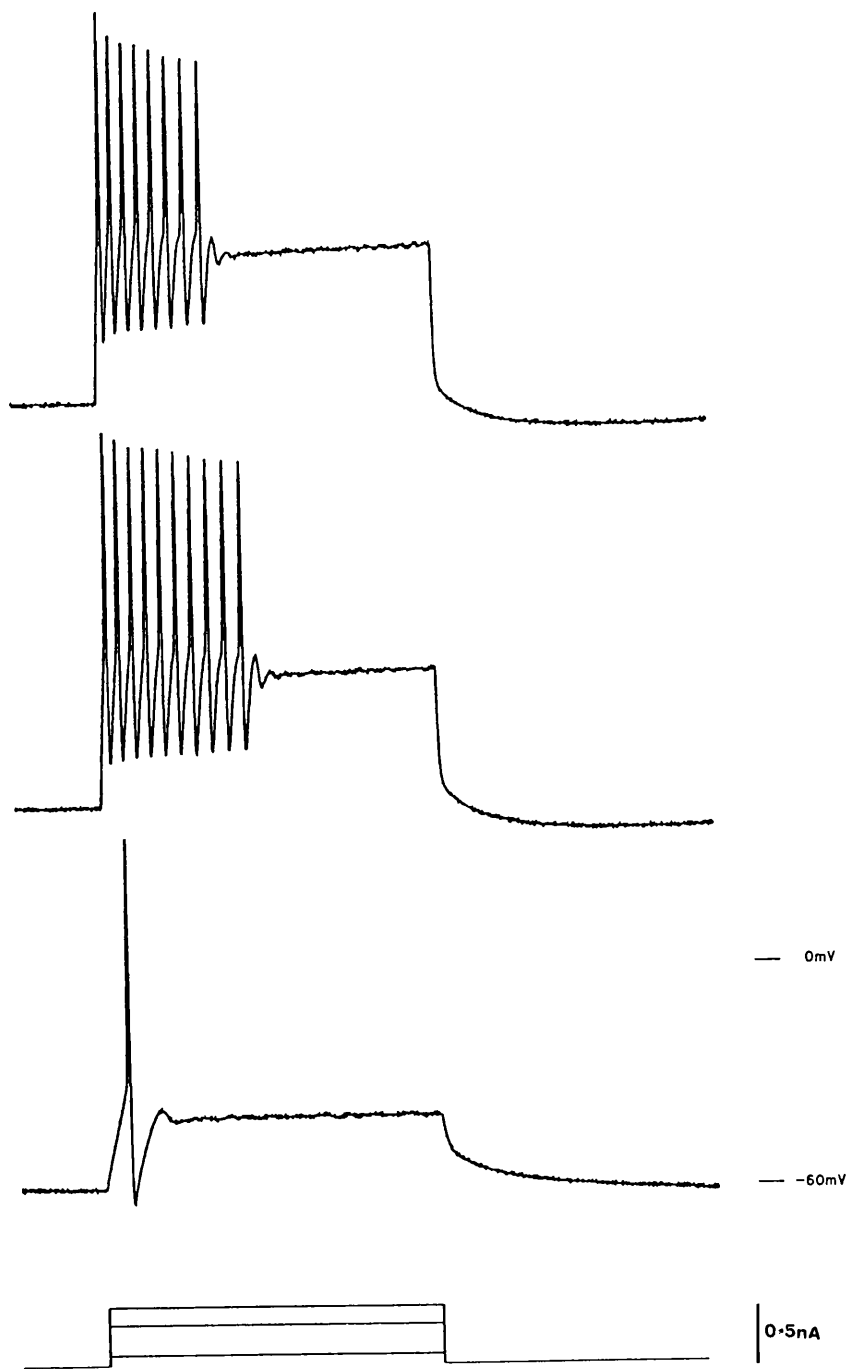
Figure 8.9. Firing properties of large ganglionic cell.

Tight seal whole cell current clamp recording from a large ganglion cell in layer 4 (C=28pF, rmp=-70mV). Increasing levels of depolarising current are injected into the cell for 100msec; as depicted by the line drawing at the bottom of the figure. The bottom voltage record shows the cells response to the lowest level of depolarisation with a single action potential being generated. As more current is injected a burst of 10 action potentials is generated in the first 50msec of the depolarisation but the cell accommodates to this stimuli. Higher levels of depolarisation do not elicit any greater number of action potentials.
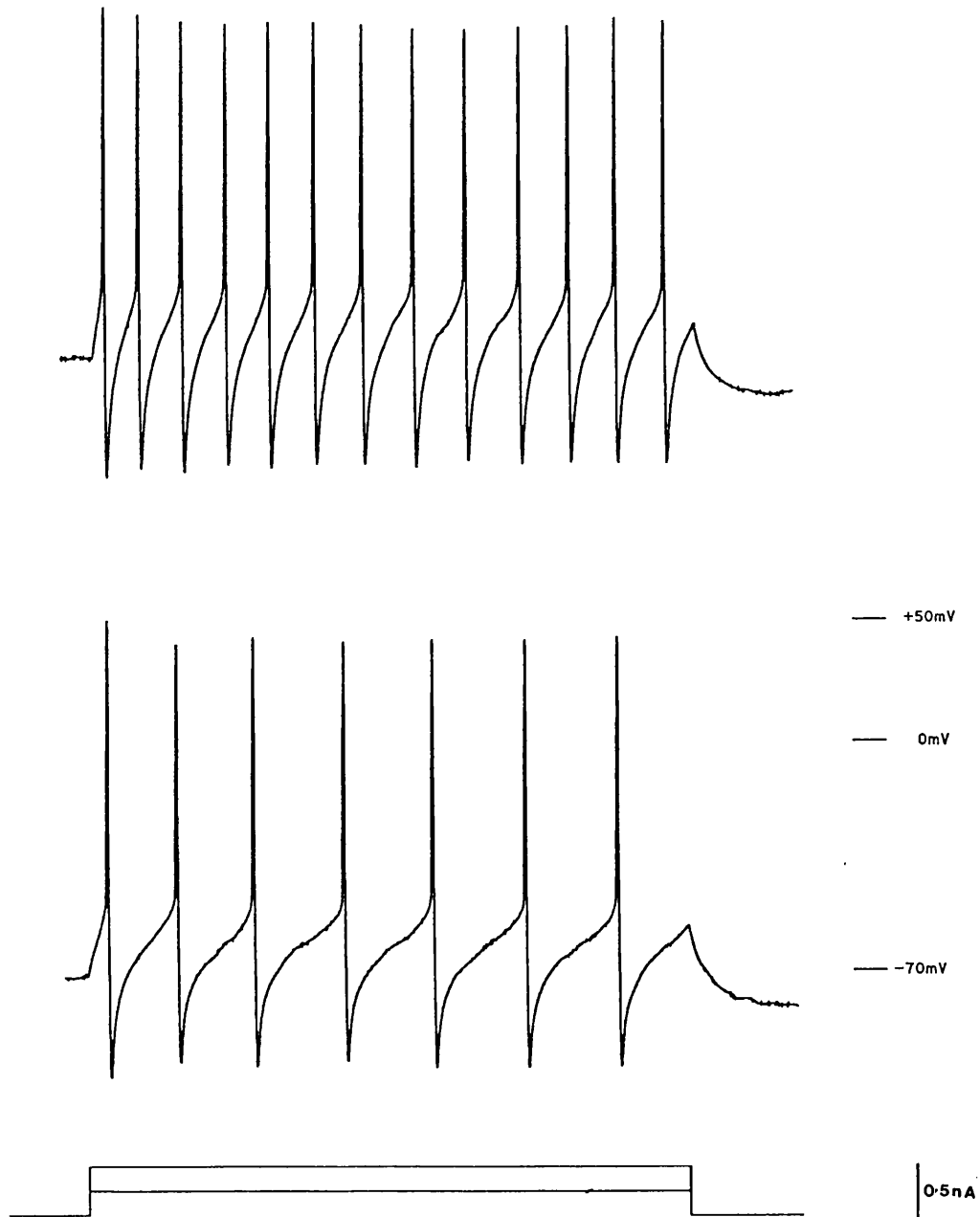
Figure 8.10. Firing properties of pyriform neuron.

Tight seal whole cell current clamp recording from a pyriform cell in layer 8 (C=5pF, rmp=-73mV). Once more increasing levels of depolarising current are injected into the cell but in this experiment for 350msec; as depicted by the line drawing at the bottom of the figure. The bottom voltage record shows the cells response to the lowest level of depolarisation and the top trace shows the increased rate of firing induced by a larger depolarising current. No accommodation is observed in the firing of the cell to this longer duration stimuli.
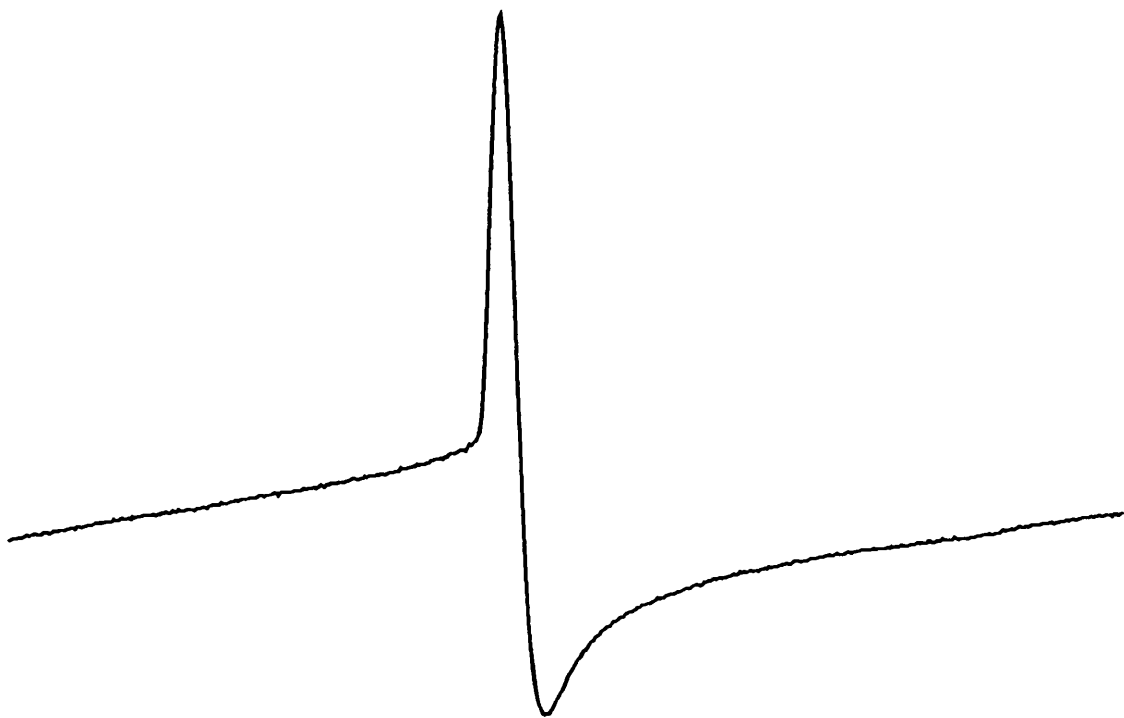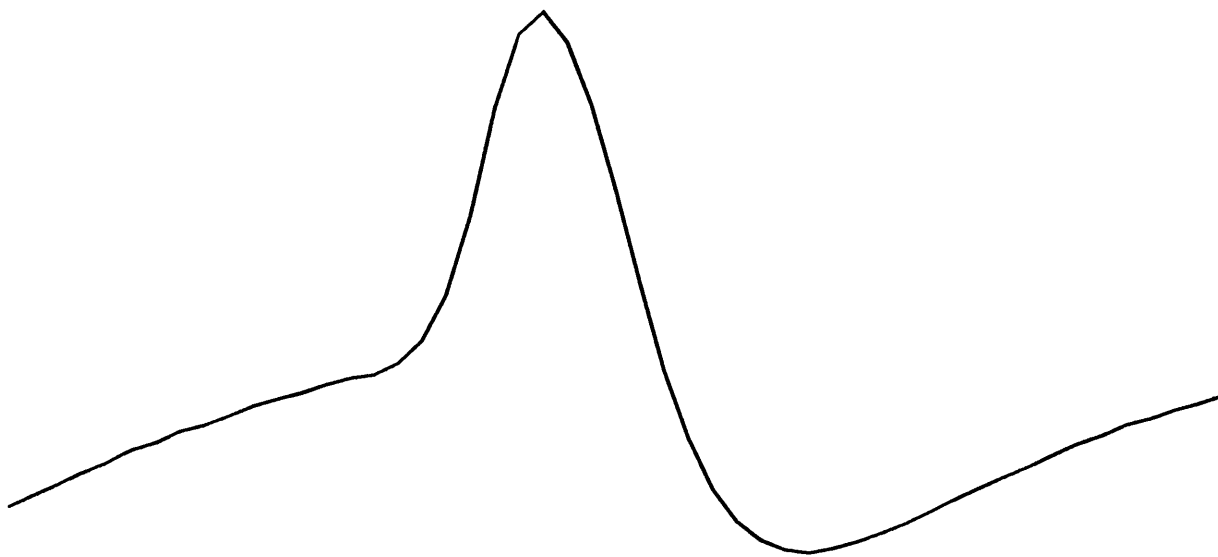
Figure 8.11. Difference between individual action potential recorded from a large ganglionic neuron and a pyriform neuron.

Single action potentials extracted form the voltage records in figure 8.10 and 8.11 showing the difference in duration of an action potential generated in a pyriform cell (top) and ganglionic cell (bottom).

Scale bar = 5msec

8.3. Discussion

Once the efficiency of the slicing procedure had been optimised using vital dye staining 35 successful whole cell recordings were made from a total of 30 preparations. 26 of these voltage and current clamp recordings have been included in this study because they combined LY filling enabling norphological correlates to be made. It appears from the morphological and electrophysiological data that in all cases examined the recordings were made from from tectal neurons. No obvious differences were observed in the electrophysiological properties of tectal neurons in the presence or absence of LY in the recording pipette. Stable intracellular recording from these healthy tectal neurons (exhibiting respectable rmp, C and R_i) was possible for up to 30 minutes. The thin slice preparation enabled very good visual resolution of individual cell bodies with the optics available (figure 8.3). It was possible to identify different neuronal types on the basis of their location in the tectum and their soma shape and size. Using this criteria we could make an initial identification of large ganglionic cells in the periventricular layers and the smaller pyriform type neurons which constitute the majority of cells in the superficial layers 6 and 8 of the tectum. We could also identify the soma of alleged interneurons in the superficial tectal layer 9 in which the main afferent input to the tectum terminates. LY fills enabled the primary and secondary dendritic structure of all these neuronal cell types to be visualised. The beaded appearance of the dendrites in a small proportion of layer 6 and 8 neurons (3 out of 15) could represent synaptic specialisations suggesting that the afferent connections to these neurons could still be intact. LY injection also revealed dye-coupling between neurons in the periventricular layers. This is the first preliminary demonstration of this phenomenon in the optic tectum of lower vertebrates and implies the presence of gap junctions in the circuitry of the tectum.

Unfortunately, in several large ganglionic cells, which maintained healthy resting membrane potentials and could propagate action potentials, no dendritic arbour was visible. This may result from low levels of LY incorporation into the dendritic appendages or, more likely, the fact that the neurons full dendritic tree was not present in this preparation. This could well be the case for the large ganglionic cells whose dendritic arbour is reported to span up to a millimetre of the tectum. It would be very surprising if, in a 200μm thick slice, the dendritic arbour of large ganglionic cells was not severed. Therefore, this slice preparation may not be ideal for studying synaptic transmission as the full dendritic morphology of all cell types may not be preserved. However, spontaneously occurring postsynaptic current were observed in pyriform type neurons recorded from this preparation suggesting that some synaptic inputs onto these

tectal dendrites were intact. Unfortunately, it was not possible to elicit an evoked postsynaptic response by electrical stimulation of the optic tract or layer 9 of the tectal neuropil. It could be that the chances of recording from a tectal neuron which receives retinal input may be very low in this thin slice preparation due to the orientation in which the slices were cut. Indeed, very recently Hickmott and Constantine-Paton (1993) published a report on synaptic transmission in a slice preparation of the optic tectum in *Rana*. In this preparation the slices were not parasagittal in orientation but were cut at an unspecified angle to the mid-line and afferent stimulation did result in postsynaptic current recorded intracellularly from layer 6 and 8 tectal neurons. This difference in methodology, in combination with the larger number of retinal ganglion cells present in the visual system of *Rana*, may account for the success of this slice preparation.

Data on the firing properties of identified tectal neurons demonstrated for the first time that *Xenopus* tectal neurons situated in layers 6 and 8 are capable of consistently generating action potentials, over 60mV in height, in response to membrane depolarisation. In the pyriform cell population increasing levels of depolarisation resulted in a greater frequency of action potential firing. In the large ganglionic cells the accommodation in the firing of action potentials was a consistent observation and as such does not merely reflect damage to the neuron under study. This rapid accommodation in response to continued depolarisation may reflect greater levels of inhibition in this class of neuron. Similar results were obtained in an *in vitro* slice preparation of the pigeon optic tectum (Hardy *et al.*, 1987). In this study three distinct classes of neurons were identified according to their firing properties in response to depolarising current. The majority of neurons responded to injected current with continuous firing similar to the behaviour of pyriform cells in this preparation. Another group also exhibited continuous firing throughout the current step but this time in discrete bursts of 2-6 action potentials per group. At this preliminary stage we are not certain whether this particular behaviour is present in the optic tectum of *Xenopus* as it was only observed on one occasion. The final set of neurons accommodated rapidly following depolarisation producing a rapid burst of action potentials at the start of the current step. So, similar patterns of firing behaviour have been noted in the optic tectum of another species but no attempt was made to classify these differences in terms of tectal neuron morphology. However, the most common behaviour encountered was the regular firing patterns observed in pyriform cells which constitute the majority of neurons in the optic tectum. The division of the two modes of firing into the pyriform and large ganglionic cell type population was very distinct in this preparation, as was the difference in the shape of

action potentials recorded from the two neuronal populations. The reason for the broader action potentials recorded from the pyriform cell population is unknown. However, the voltage clamp experiments also suggested that the ionic current giving rise to the action potentials in the two populations of neurons were different. The degree of outward rectification in the large ganglionic cells was greater than that observed in the pyriform cells. This may reflect a real difference in the properties of the K^+ channels underlying this outward current in the two neuronal populations. These very obvious differences in firing behaviour may reflect the physiological function of these two cell types. Pyriform type neurons in the superficial layers of the tectum are the primary recipients of retinal input and as such represent the first level of visual processing in the tectum. The larger ganglionic cells in the deeper periventricular tectal layers are considered the main output stage to motor structures of the brainstem and spinal cord, that initiate escape and reorienting behaviour.

Though we did record spontaneous EPSCs in this preparation it was not possible to elicit evoked activity. It is hoped that future work will help classify the postsynaptic receptors which contribute to the sponataneous EPSCs we record from tectal neurons. From the results of a very recent study by Hickmott and Constantine-Paton (1993) it seems that the difficulty we experienced in evoking a synaptic response may be overcome by reorienting the angle of the slice to maximize on the number of tectal neurons receiving the appropriate afferent input. In this study obliquely oriented slices were produced from the optic tectum of *Rana pipiens*. Electrical stimulation of the optic tract resulted in, what was interpreted as being, mono- and polysynaptic responses recorded in whole cell configuration from tectal neurons. Voltage-clamp experiments revealed that under normal conditions (*ie.* at resting membrane potential and in the presence of extracellular Mg^{2+} ions) only the polysynaptic component of retinotectal synaptic transmission was blocked by $100\mu M$ AP5.

Chapter 9

General Discussion

In the formation of precisely and topographically ordered sets of synaptic connections, between any group of neurons and their target structure(s), a number of problems have to be surmounted. Neurons in the presynaptic array have to send their growing axons over considerable distances, usually by-passing inappropriate targets on the way and sometimes navigating across other developing fibre tracts. Having arrived at their chosen destination the axons must then deploy their terminations with the correct orientation or polarity, over an appropriate extent of the three-dimensional target space. Having now staked a claim to this territory, the axon terminals must manufacture synaptic contacts with the target cells in a pattern that precisely reflects the ordered distribution of their parent cell bodies in the array from which they originate. The experiments reported in this thesis are primarily concerned with the mechanisms responsible for surmounting the problems associated with this last phase of map formation.

9.1. The retinotectal projection and chemoaffinty

The mechanisms responsible for orderly synaptogenesis during the formation of visual maps in the lower vertebrate optic tectum have been extensively studied during the last 50 years, beginning with the seminal work of Sperry (1943) on the regenerating retinotectal projection. His elegant series of experiments seemed to refute the then prevalent notion that synaptogenesis is governed solely by functional usefulness, and lead him to propose that the ordering of connections between retina and tectum relies upon a specific matching of complementary gradients of membrane bound molecules present in the two neuronal arrays. During recent years, candidate molecules with some of the characteristics envisaged by Sperry (1963) have been identified in the retina and tectum. The first of these was discovered by Trisler and colleagues (Trisler et al., 1981; Trisler & Collins, 1987), and rather presumptively was named TOP, deriving from "topynomic" meaning place name. TOP is a cell surface molecule present in a graded fashion across the dorso-ventral axis of the chick retina and distributed in an opposite direction across the dorso-ventral axis of the tectum. However, the effect of monoclonal antibodies generated against TOP has not been established and so a role for this molecule in the developing retinotectal projection is at present only speculative (Stirling, 1991). Bonhoeffer and colleague

have presented evidence that a de-naturable membrane-bound molecule, located in the posterior tectum, causes repulsion of temporal retinal axons but not of nasal ones which normally innervate this region. Using an ingenious *in vitro* assay membrane fragments of anterior and posterior tectum are arranged as a carpet of very narrow alternating stripes. Axons growing on such striped carpets are simultaneously confronted with the two substrates. Nasal and temporal axons were found to grow well on both membrane environments but temporal axons show a marked preference for growth on anterior tectum especially during the period of normal retinotectal map development (Walter *et al.*, 1987a&b). However, the structural identity of this molecule, whether it is distributed across the tectum as a gradient, and whether it is bound to the membranes of tectal neurons, are all unknown. This latter point is not trivial, because similar types of results have been obtained in *Xenopus* with the observation, using time-lapse photography, that the growth cones of temporal retinal axons collapse on contact with glial cells prepared from posterior tectum (Johnston & Gooday, 1991). Also, no repulsive or attractive chemical gradients have been demonstrated which can explain the mediolateral polarity of the retinotectal projection. Therefore, although there has been considerable successes in identifying the nature and effect of certain molecules (eg, laminin, N-CAM, NGF etc.) on the promotion, selective fasciculation, adhesion and navigation of growing axons in the earliest phase of map formation, those responsible for signalling target polarity and the global deployment of terminals remain something of a mystery.
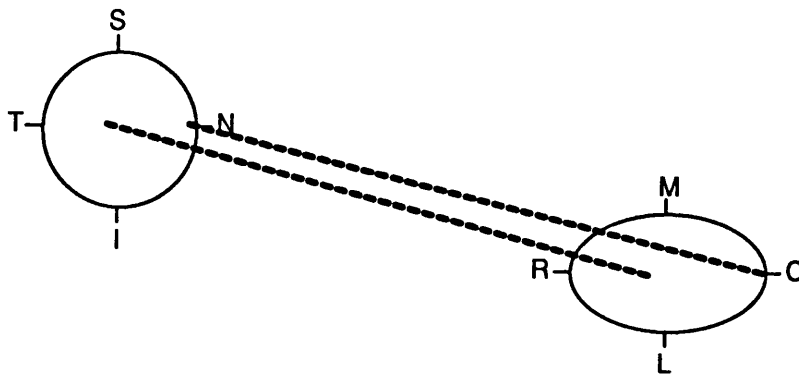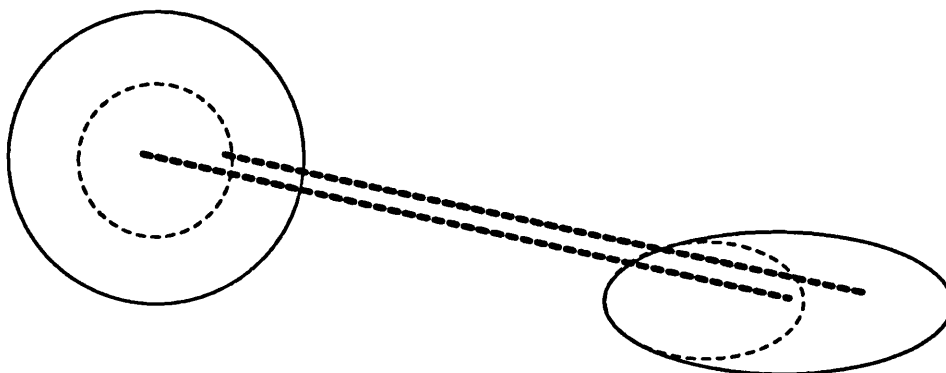
Figure 9.1. Shifting synaptic connections in the developing retinotectal projection.

A cartoon illustrating changes in the retinotectal projection during development**A**, illustrates the topographic organisation of the early projection with the circle representing the retina and the ovoid representing the contralateral tectal lobe. Central retina projects to the central region of the opposite tectal lobe and nasal retina is projecting to rostral tectum (dotted lines). **B**, illustrates the mature projection following the disparate growth of the retina and the tectum. Central retina is still projecting to central region of the tectum but due to the caudal growth of the tectum this has required the retinotectal connections (dotted line) to move caudally across the tectal surface. Due to the addition of cells to peripheral retina the point on the mature retina which used to be the extreme nasal position in the early retina is now more centrally located. Therefore, these retinotectal connections have also moved caudally across the tectal neuropil.

Conventions are Superior (S), Inferior (I), Nasal (N) and Temporal (T) for retina and Rostral (R), Caudal (C), Medial (M) and Lateral (L) for tectum. No particular scale intended.

9.2. The role of activity in the developing retinotectal projection

The experiments of Gaze and others were the first to directly challenge the chemospecificity model of retinotectal development. The results from "size-disparity" experiments contradicted the notion that rigid specificity exists between retinal axon terminals and the dendrites of tectal neurons but none of this data was sufficient to completely eliminate this model from current axioms of neural development. However, it has been demonstrated that the disparate growth patterns of the retina and tectum necessitate changes to be made in the synaptic connections of the developing retinotectal projection (Figure 9.1). Activity-dependent mechanisms have been implicated in this fine tuning of the projection once intrinsic mechanisms have guided the axons to the appropriate tectal location. The first evidence in support of this idea came from the observation that intraocular injection of TTX prevents the emergence of detailed order in the regenerating projection without affecting the initial processes of axonal growth (Meyer, 1983; Schmidt and Edwards, 1983). However, a role for neural activity in the normal development of the retinotectal map has proven less readily demonstrable following TTX-induced retinal impulse blockade (Harris, 1980; Stuermer *et al.*, 1990). In a previous study of retinotectal map development in *Xenopus* that had been reared in total darkness from embryonic life, the electrophysiologically derived retinotopic order, multi-unit receptive field (MURF) size, and depth distribution of different unit types in the projection were all shown to be normal (Keating *et al.*, 1986). These authors concluded that visually-driven activity is not required for the precise ordering of retinotectal synaptic connections, or for their normal shifting relations during development, but could not exclude the possibility that intrinsic (spontaneous) patterns of neural activity might be involved, if these were sufficiently correlated between neighbouring RGCs. However, Schmidt and Eisele (1985) oppose this view and have demonstrated that visually-driven neural activity does sharpen the regenerated retinotectal projection in goldfish.

In principle, correlated spontaneous neural activity can be removed from the firing patterns of RGCs by rearing animals in constant stroboscopic illumination. We have shown, for the first time, that during acute exposure to constant stroboscopic illumination, the evoked and spontaneous neural activity of all classes of retinal unit (as recorded in their terminations) are entrained to the strobe (figure 4.2), so that the entrained strobe-evoked activity recorded from quite disparate tectal locations become increasingly correlated with time (Figures 4.7). These experiments imply that the spatial information that may normally be imparted by correlated patterns of

spontaneous activity between neighbouring RGCs, and which is supposed to participate in the ordering of their synaptic connections in the tectum, may be masked by this non-local entrainment of evoked activity in the strobe-environment. Therefore, the effects of entraining neural activity on the developing projection was investigated by rearing *Xenopus*, from before the onset of visual function, in this visual environment. The electrophysiologically derived retinotopic order, MURF size and laminar distribution of unit types in the retinotectal projection were all unaffected by strobe-rearing, when compared with age-matched controls. Therefore, it would seem that the normal development of the retinotectal projection in *Xenopus* does not involve the detection of local patterns of correlated neural activity, whether generated intrinsically or extrinsically.

In a recent study Schmidt and Buzzard (1993) claim that the normal development of the goldfish retinotectal projection is impaired by strobe-rearing. Electrophysiological mapping experiments, following 1-2 years of strobe-rearing, revealed disturbed retinotopic order and increased MURF size. HRP labelling of RGC axons showed abnormal patterns of arbour branching consistent with the disorder documented in the electrophysiological maps and in their overlapping receptive fields. Both our study and that of Schmidt & Buzzard used a strobe frequency of 1Hz with animals placed in separate containers in a featureless environment. However, in the study of Schmidt & Buzzard the strobe-reared goldfish were kept in stroboscopic illumination for only 14 hours of each day. For the remaining 10 hours they were maintained in total darkness, an environment permissive for spontaneous patterns of correlated neural activity. How could it be that the fragmentary nature of the strobe environment implemented by Schmidt & Buzzard was successful in disturbing the normal sharpening of the projection when our constant strobe-rearing environment was not? If anything the strobe regime adopted in this Thesis should have been more effective than that adopted by Schmidt. However, the nature of the strobe environment is obviously very important to this type of investigation and how this influences spontaneous patterns of correlated neural activity in the tectum during chronic exposure to this regime is still not certain. In the strobe-rearing environment adopted in the present study (Chapter 4) sufficient contrast information may be visible during each strobe flash to generate local correlated firing patterns between neighbouring RGCs. This neural activity may be sufficient for the activity-dependent synaptic plasticity of the developing retinotectal projection in *Xenopus*. However, Cook and Rankin (1986) were only able to show that strobe-rearing affected the

regenerating retinotectal projection of the goldfish when the lens was concurrently removed so as to blur the retinal image. Given the difficulty Cook experienced in achieving any disturbance in the order of the regenerating rertinotectal projection it seems strange that normal development was so easily disturbed by the strobe rearing regime adopted by Schmidt.

Differences in the strobe environment may account for the different effects of this regime, but another possibility is that activity-dependent processes are used to a different extent in the orderly patterning of retinotectal synaptic connections in the frog and the fish. Activity-dependent plasticity may play only a minor role in the developing retinotectal projection of *Xenopus*. Is there any quantitative difference which could explain this species difference? The size of retinal axon terminal arbors in the retinotectal projection in *Xenopus* remain constant throughout development (Sakaguchi and Murphy, 1985; O'Rourke and Fraser, 1990). Quantitative analysis of arbor size suggests that any apparent decrease in size of terminal arbors, with respect to the tectum, is due to rapid growth of the tectal neuropil and not due to retraction of an initially diffuse arbor. This expansion in the size of the tectum could also account for increased precision in the developing retinotectal projection of goldfish (Stuermer and Raymond, 1989). Interestingly, this is not true for the regenerated retinotectal projection (Gaze and Keating, 1970). Anatomical and physiological studies have shown that, after nerve crush or section, the retinal projection initially forms a diffuse projection which is then pruned down to a more precise map (Gaze and Jacobson, 1963; Humphrey and Beazley, 1982; Murray and Edwards, 1982; Stuermer and Easter, 1984). This process does require a reduction in the size of terminal arbors and so the refinement in targeting of axonal arbors during development is a phenomenon distinct from that seen during regeneration. This process of arbor refinement in the regenerating retinotectal projection occurs in the frog and the fish. However, the size of mature MURFs in *Xenopus* is over twice that of mature MURFs in goldfish. Therefore, the topographic precision in the retinotectal projection of *Xenopus* is less than that encountered in other lower vertebrates. Also, both retina and tectum continues to grow for many years in the fish (Easter and Stuermer, 1984) but tectal histogenesis stops after metamorphosis in frogs (Straznicky and Gaze, 1971 & 1972). Therefore, the requirement for activity-dependent synaptic plasticity in the developing retinotectal projection could well be less in *Xenopus* than goldfish. However, there is circumstantial evidence to support the idea that neural activity may play some role in the developing retinotectal projection in *Xenopus*. Straznicky *et al.*

(1980) have shown that when two eyes are forced to co-innervate a single tectal lobe in *Xenopus*, they segregate into eye-specific stripes. In other frogs, and in goldfish, it is clear that TTX blocks this eye-specific segregation (Boss and Schmidt, 1982; Meyer, 1982; Reh and Constantine-Paton, 1985) and so it is widely believed that stripe formation is activity-dependent. However, no data is available on the effect of strobe-rearing on stripe formation in any species of frog or fish, but in the frog, *Rana pipiens*, dark-rearing apparently does not disrupt stripe formation (cited in Reh and Constantine-Paton, 1985).

In conclusion, the detection of correlated patterns of neural activity, whether spontaneously or visually evoked, may play little part in the developing retinotectal projection of *Xenopus*. Indeed, Fraser *et al.* (1984) have shown that antibodies to the neural cell adhesion molecule (N-CAM), when applied to the optic tectum of juvenile *Xenopus*, very rapidly distorts the retinotectal mapping precision and can increase MURF sizes, suggesting that such molecules are of greater importance for maintaining retinotectal topography than are patterns of neural activity. Therefore, in *Xenopus* the elaboration of the retinotectal projections topographic precision could be explained purely on the basis of genetically determined chemical guidance factors. Gradients of attractive or repulsive molecules could account for the dynamic nature of the developing retinotectal projection. However, this may not be the case for the developing retinotectal projection in other lower vertebrates such as the goldfish. Here, as in the mammalian retinocollicular and retinogeniculate pathways, the detection of correlated patterns of spontaneous neural activity could play a key role in refining the topographic precision of the pathway.

9.3. Plasticity in the crossed isthmotectal projection.

In *Xenopus laevis*, as the position of the two eyes changes during metamorphosis anatomical re-arrangements take place in the crossed isthmotectal projection in order to maintain alignment of this projection with the retinotectal map. However, intrinsic guidance mechanisms, probably similar to those described in the developing retinotectal projection, guide the early isthmotectal axon terminals to their appropriate location in the tectal neuropil. During metamorphosis the area of the optic tectum which receives binocular input via the isthmotectal projection gets larger. This correlates with the developmental change in eye position which occurs in *Xenopus* during metamorphosis. Electrophysiological mapping studies have demonstrated that the crossed isthmotectal projection initially forms a well ordered

topographic map in animals that have been deprived of vision or in animals that have previously received a single eye rotation (Grant and Keating, 1989b, 1992). Expansion of the isthmotectal projection across the tectum also seems to be intrinsically generated because, in a similar fashion to the retinotectal projection, shifting synaptic connections in the developing isthmotectal projection sill occurs in X visually deprived animals (Grant and Keating, 1989a&b). It also appears that spontaneous patterns of neural activity play no role in this shifting of synaptic connections, because they occur in dark-reared animals in which spontaneous activity should be normal and in strobe-reared animals in which this activity should be disrupted (figure 4.9).

In fact, it is only some time after the completion of metamorphosis that major indications of experience-dependent mechanisms operating in the crossed isthmotectal projection become apparent: in dark-reared animals the projection begins to develop signs of disorder and in eye-rotated animals it begins to change orientation to match the disparate visual input (Grant and Keating, 1989b, 1992). It could be that experience-dependent changes in the pathway normally appear after metamorphosis because they are important in the adapting the animal to the ecological niche it will now maintain until adulthood. However, the results reported in Chapter 3 demonstrated that the pathway is capable of completely reorganising the pattern of its synaptic connections even when both eyes have been apportioned a large rotation ? (figure 3.1). In these circumstances the inverted visuotectal environment induced by a double eye rotation means the animal should orient incorrectly to a visual stimuli (Sperry, 1943). Modifications in the crossed isthmotectal pathway, following eye rotation, do not confer any behavioral advantage to the animal as visuomotor behaviour will remain mal-adapted. Therefore, the functional usefulness of the intertectal synaptic plasticity in double eye rotated animals is, at best, negligible, but rather reflects a synaptic mechanism that can operate almost autonomously, without interference from other modulatory influences (see Udin *et al.*, 1983).
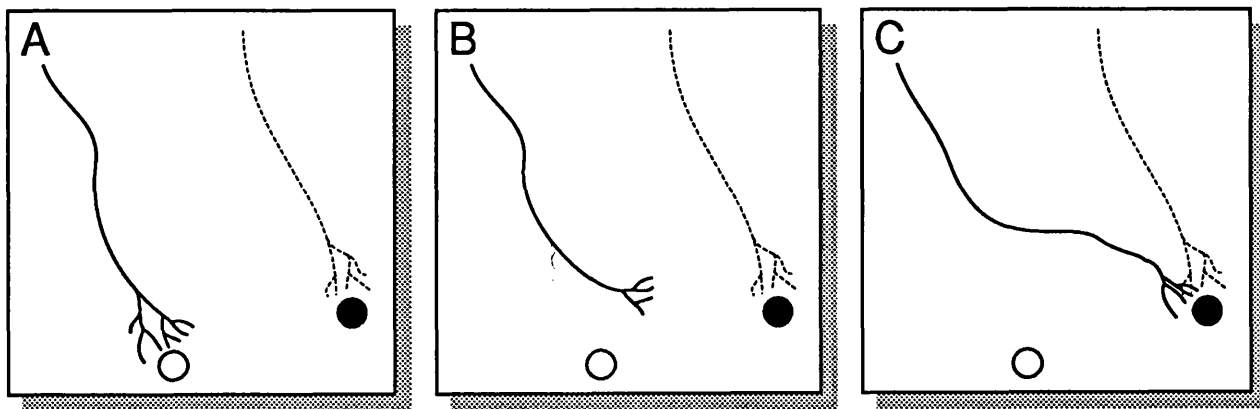
Figure 9.2. A 3-stage model for intertectal plasticity.

This cartoon illustrates the response of the crossed isthmotectal input to a single eye rotation. **A**, a crossed isthmotectal arbor (solid line) and a retinotectal arbor (dotted line), which are receiving visual information from areas of retinal correspondence, are now projecting to disparate tectal locations (open and filled circles) due to the eye rotation. **B**, the crossed isthmotectal arbor disconnects from its inappropriate tectal location (open circle) in search of the appropriate tectal location (filled circle) which is receiving matched binocular input. **C**, Retinotectal and isthmotectal arbors now terminate at the same tectal location.

See text for further explanation.

9.4. A model for intertectal plasticity

Intertectal plasticity, both during normal development and following an eye rotation in *Xenopus*, involves terminal arbors of axons in the crossed isthmotectal portion of the pathway leaving their original sites of tectal termination and selecting novel ones appropriate to the change in visual input (Udin and Keating, 1981; Udin, 1983, Grant and Keating, 1989a&b). The process could reflect the ability of these arbors to detect tectal termination sites that are coincidently activated by retinotectal arbors which receive their visual input from the same region of the binocular field. However, intertectal plasticity is a three stage process (figure 9.2). The first step is the removal of isthmotectal synaptic connections from inappropriate tectal locations; *ie* that position in the tectum which is not receiving matched binocular input. The second is the search, by isthmotectal fibres, for the newly appropriate position in the tectum which is receiving matched binocular input. The third is the establishment of synaptic connections at the newly appropriate tectal location where coincident neural activity occurs.

Data in Chapter 3 suggests that retinotectal arbors may actively discourage the formation of intertectal synaptic connections at inappropriate tectal locations. During visual stimulation, retinotectal synapses appeared to mask neural activity arising from inappropriately placed terminal arbors in the crossed isthmotectal projection. This masking of neural activity was lost once the retinotectal projection was removed by enucleation and dual inputs were subsequently recorded at a single tectal location (figure 3.2). Dual inputs have been seen before in enucleated *Xenopus* but were interpreted as intermediate stages of intertectal plasticity (Grant and Keating, 1990). Another possible interpretation is that the selective inhibition of neural activity arriving at inappropriately located crossed isthmotectal arbors could be the initial impetus for crossed isthmotectal fibres to disconnect. The construction of appropriate synaptic connections, with tectal neurons which receive matched binocular input, would not necessarily involve the loss of the original terminal arbor. This arbor would remain, but neural activity arriving at that location would be masked by the inhibition of the retinotectal projection. Udin *et al.*, (1990) reported no anatomical evidence to suggest that crossed isthmotectal synapses are present on retinotectal arbors. The majority of crossed isthmotectal arbors make connections directly with tectal cell dendrites. The presence of retinotectal synapses on crossed isthmotectal arbors has not been investigated. It is possible that this relationship would give rise to presynaptic inhibition which could mask neural activity arriving at the terminal arbors

of inappropriately located crossed isthmotectal arbors. The unmasking of ineffective synapses due to removal of an excitatory input has been described in lamina IV of the spinal cord (Merrill and Wall, 1972; Wall, 1977) and was also explained by the removal of presynaptic inhibition.

The cues which enable isthmotectal fibres to locate the newly appropriate tectal locations are not known. However, once the crossed isthmotectal fibres reach the appropriate tectal location a Hebbian-type mechanism could act to stabilize synaptic connections at newly appropriate tectal locations. Retinotectal and isthmotectal arbors, stimulated by the same position in visual space, are believed to exhibit correlated firing patterns. It has been hypothesized that these correlated firing patterns, resulting from binocular visual experience, are utilized by the intertectal system to stabilize appropriate crossed isthmotectal connections (Grant and Keating, 1989a, 1989b, 1992). Data in Chapter 4 demonstrated that correlated patterns of neural activity were produced during binocular vision (figure 4.4 & 4.5). Moreover, neural activity recorded from areas of the tectum not receiving matched binocular input became correlated after acute exposure to stroboscopic illumination (figure 4.7). However, the coincidence detection hypothesis of intertectal synaptic plasticity received only qualified support from the strobe-rearing experiments described in Chapter 4. Despite the strobe environments interference with correlated firing patterns the disruptions observed in the intertectal system following strobe-rearing were not as drastic, or as consistent, as those observed following visual deprivation. Quantitatively the crossed isthmotectal projections alignment with the retinotectal projection was disturbed in only a minority of cases but, in the main, the binocular tectal maps were normally aligned. The capacity for intertectal synaptic plasticity to occur during stroboscopic illumination was more substantially disturbed in eye rotated animals (figure 4.10). But, once again, the disturbances were not as great as those previously documented in visually-deprived animals; following any eye rotation of less than 90° quite substantial re-re-orientation of the crossed isthmotectal projection did occur. In contrast, long-term dark-rearing reliably perturbs the ipsilateral visuotectal map and disrupts its spatial alignment with the contralateral visuotectal projection. Therefore, strobe-rearing was not capable of removing all cues of relevance to intertectal plasticity.

Obviously, it is not possible to monitor firing patterns directly in the strobe-rearing environment. However, in experiments described in Chapter 4 it appeared that following stroboscopic entrainment correlated patterns of neural activity were

produced at tectal locations not receiving matched binocular input (figure 4.7). This implies that all positions across the tectum, irrespective of whether or not it they are receiving matched binocular input, exhibit correlated firing. However, when monitoring the neural activity recorded at those tectal locations which are receiving matched binocular input, the degree of correlation improved during stroboscopic entrainment (figure 4.6). In these experiments it was apparent that, even though correlated firing was now induced at inappropriate tectal locations, the correlated firing recorded between appropriate tectal locations was improved.

9.5. NMDA and non-NMDA receptor mediated synaptic transmission in the optic tectum.

A necessary component of the coincidence detection hypothesis is that synaptic mechanisms exist in the circuitry of the tectum to detect and respond to coincident patterns of visually evoked activity. Recent studies have implicated a postsynaptic glutamate receptor, the NMDA receptor, in this process (Scherer and Udin, 1989). Long-term exposure to the NMDA receptor antagonist AP5 was shown to block intertectal plasticity in eye-rotated animals in an analogous manner to dark-rearing. Scherer and Udin (1989) interpreted these results as indicating that visually-evoked excitatory retinotectal synaptic transmission was primarily mediated by non-NMDA-type glutamate receptors. However, when this direct input onto tectal neurons was paired with coincident input from crossed isthmotectal fibres then sufficient depolarisation would be achieved to remove the Mg^{2+} block and open NMDA-type glutamate receptors that are co-localised at the same synapses. Activation of the NMDA receptor would allow Ca^{2+} ions to flow into the tectal neuron, following the agonist induced opening of the NMDA receptors ion channel, and trigger a cascade of secondary events which serve to stabilize the co-active synaptic inputs in the intertectal pathway. These secondary events could also be involved in de-stabilizing those intertectal inputs that are coincidently inactive. Many unverified assumptions are involved in this interpretation including the important fact that retinotectal synaptic transmission is glutamatergic in *Xenopus*. If retinotectal synaptic transmission is glutamatergic then it would be important to establish which postsynaptic glutamate receptors are involved. If NMDA receptors actually mediate retinotectal synaptic transmission then the effects of AP5 on intertectal plasticity would merely reflect interference with levels of visually elicited activity and not the blockade of a specific postsynaptic mechanism concerned with synaptic stabilisation. Indeed, NMDA

receptors have been shown to contribute to synaptic transmission in other glutamatergic visual pathways such as the mammalian SC (Hestrin, 1992), and visual cortex (Stern *et al.* 1992). Therefore, it is possible that a similar phenomenon exists in the *Xenopus* retinotectal projection.

The *in vivo* studies (Chapter 5) established that glutamate (or some closely related analogue) was the neurotransmitter responsible for mediating retinotectal visual responses in *Xenopus*. The non-NMDA receptor antagonist CNQX, completely blocked postsynaptic visual output from tectal neurons without altering the presynaptic visual responses. By contrast, the NMDA receptor antagonist AP5, even at very high concentrations, had little effect on any aspect of visually evoked activity *in vivo*. During the course of this study a similar methodology was adopted to assess the physiological effects of topically applied NMDA and AP5 on activity in the optic tectum of *Xenopus laevis* (Scherer and Udin, 1991b) and *Rana pipiens* (Udin *et al.*, 1992). As in the present study, the visually evoked responses recorded at the ipsilateral tectal lobe were used to monitor the tectal output via the crossed isthmotectal projection and little or no change in the firing rates recorded through this projection were detected, even following chronic exposure to AP5. Thus, although the effects of the selective non-NMDA receptor antagonist CNQX were not investigated in either of these studies the common conclusion is that NMDA receptors do not participate in the normal transmission of visually-elicited activity from retina to tectum or between the tectal lobes. Therefore, the cumulative weight of evidence suggests that the chronic effects of NMDA receptor blockade on intertectal plasticity in Xenopus arises from the interference with a specific postsynaptic mechanism concerned with responding to the correlated firing patterns of binocular inputs to the tectum. This still raises the question as to where in the circuitry of the tectum NMDA receptors are located and how they participate in the activation of tectal neurons?

The *in vitro* preparations of the tectum were developed to further investigate these questions. Distinct early (U1) and late (U2) postsynaptic events could be identified in the evoked potentials recorded from the tectal neuropil in response to electrical stimulation of the optic tract in the whole mid-brain preparation. These responses were identical to those recorded *in vivo* by Chung *et al.* (1974a), but we have reached different conclusions as to their exact nature. Though my results confirm the postsynaptic character of both these responses, I now believe that the long latency (U2) response is polysynaptic in origin (Chapter 6). A similar

interpretation was placed upon the early and late components of the evoked response to retinal fibre stimulation in the goldfish optic tectum (Teylor *et al.*, 1981).

In accordance with the *in vivo* data of Chapter 5, and consistent with results from other species (Langdon and Freeman, 1986; Deusen and Meyer, 1990; Nistri *et el.*, 1990; Debski *et al.*, 1991; Cline and Tsien, 1991), the early monosynaptic component of the evoked response is clearly mediated by non-NMDA type glutamate receptors. Therefore, a large body of evidence now supports the suggestion that retinotectal synaptic transmission is mediated by non-NMDA type glutamate receptors. However, in *Xenopus* the long latency (U2) component of retinotectal synaptic transmission is mediated by both NMDA and non-NMDA type glutamate receptors. This is emerging as a common characteristic of many glutamatergic synapses in the vertebrate CNS. For example, Stern *et al.* (1992) describe whole cell recordings from a slice preparation of the visual cortex in which NMDA and non-NMDA mediated synaptic currents occur simultaneously. A similar co-existence of NMDA and non-NMDA receptors has been reported in synaptic connections of the mammalian hippocampus (Bekkers and Stevens, 1989) and cerebellum (Silver *et al.*, 1992). On the other hand, analysis of spontaneous EPSPs in the embryonic spinal cord of *Xenopus* (Sillar and Roberts, 1991) has revealed that NMDA and non-NMDA receptors are situated on separate synaptic connections. It is not possible to determine from our extracellular field potential recordings whether the NMDA mediated component of retinotectal synaptic transmission involves receptors situated on the same or different synapses to those which give rise to the non-NMDA mediated component of the response. This consideration is important because the NMDA receptors should be localised on the same tectal neuron which is receiving direct depolarising input via non-NMDA-type glutamate receptors. It is not necessary for the non-NMDA and NMDA receptors to be co-localised at the same synapse, only that the synaptic connections giving rise to NMDA and non-NMDA mediated inputs be present on the same tectal neuron. In this way it may be argued that coincident retinal and isthmotectal inputs could cause sufficient levels of depolarisation in the tectal neuron to allow the activation of NMDA receptors selectively on the tectal neuron receiving matched binocular input.

Unfortunately, we were not able to use the thin slice preparation (Chapter 8) to address this question, because we failed to evoke EPSCs during electrical stimulation of the retinal afferents. From the results of a very recent thin slice study Hickmott and Constantine-Paton (1993) demonstrated that under normal conditions (*ie.* at resting

membrane potential and in the presence of extracellular Mg^{2+} ions) only a late polysynaptic component of retinotectal synaptic transmission was blocked by AP5 in *Rana pipiens*. The monosynaptic component of retinotectal synaptic transmission was blocked by CNQX with no AP5 sensitivity at normal Mg^{2+} ion concentrations. These intracellular results appear to confirm our data from extracellular recordings made in the optic tectum of *Xenopus*. Moreover, they indicate that NMDA and non-NMDA receptor mediated postsynaptic events are activated in a single tectal neuron. However, Hickmott and Constantine-Paton went on to demonstrate that, in Mg^{2+} free solution, the monosynaptic component of retinotectal synaptic transmission was also sensitive to AP5. The significance of this NMDA mediated monosynaptic event was interpreted in terms of activity-dependent synaptic plasticity in the developing retinotectal projection. In this system neighbouring RGCs, which exhibit correlated spontaneous firing patterns, are stabilised onto common tectal neurons because of the coincident spontaneous activity they exhibit. This activity-dependent stabilisation of RGCs is also suggested to involve activation of the NMDA receptor and therefore, Hickmott and Constantine-Paton (1993) suggest that a monosynaptically activated NMDA receptor mediated event is required. It is also argued that the temporal delay introduced by the polysynaptically activated NMDA receptor mediated events would be insufficient to orchestrate this form of coincidence detection.
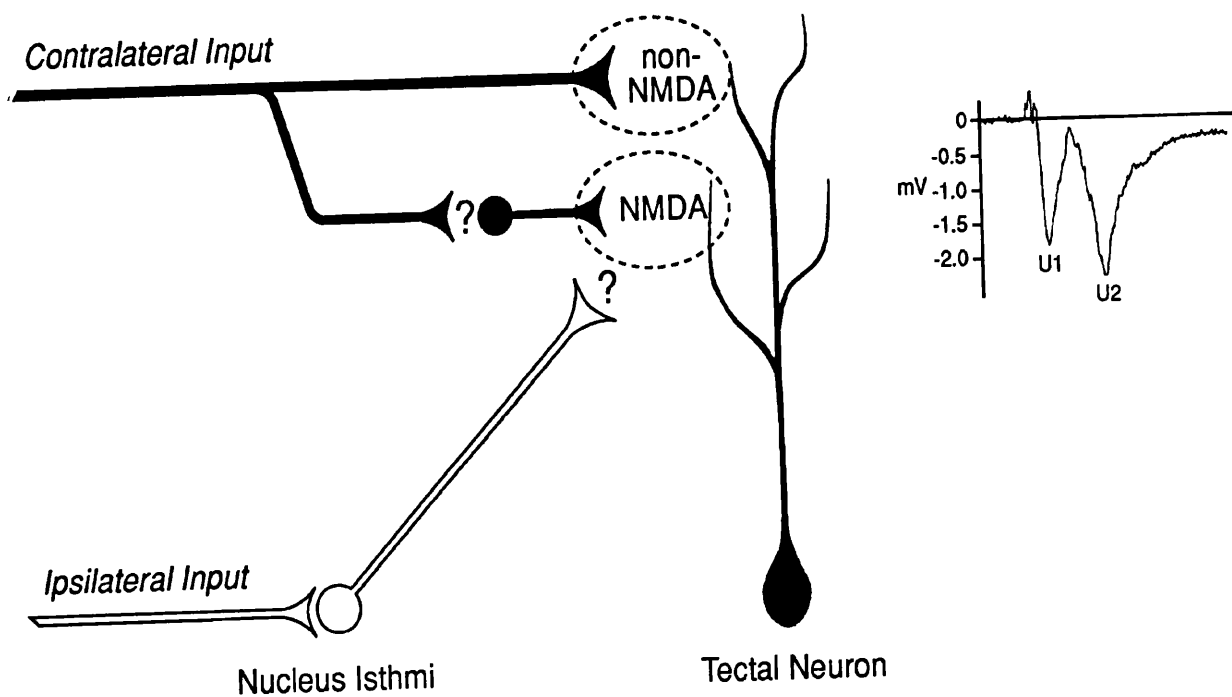
Figure 9.3. Possible significance of the NMDA mediated component of the U2 response.

A schematic illustrating our present understanding of how the U1 and U2 responses are generated and the possible relevance of these synaptic responses to intertectal plasticity.

A layer 8 tectal neuron is shown receiving direct monosynaptic activation via non-NMDA type glutamate receptors through the contralateral retinal input. This gives rise to the early U1 response. An unknown polysynaptic relay, probably involving an excitatory interneuron, then generates the longer latency NMDA mediated U2 response. The U2 response is only in part NMDA receptor mediated with the remainder of the U2 response being generated through non-NMDA receptors (not shown in diagram).

Due to the polysynaptic nature of the intertectal relay visual information through the ipsilateral eyes input at approximately the same time as the U2 response is generated by the retinotectal input. The NMDA receptors, which are located on the postsynaptic tectal neuron, could be acting as the molecular coincidence detector for these temporally correlated inputs. See text for further details.

205

9.6. Possible significance of the NMDA mediated component of the U2 response.

The onset of visually-evoked activity in the tectum following stimulation of the ipsilateral eye is delayed, on average, by at least 10msecs compared to that evoked directly from the contralateral eye (Scherer and Udin 1991a; Chapter 5); this delay being a reflection of the polysynaptic nature of the intertectal pathway. The appearance, following retinal stimulation, of the long latency, AP5 sensitive component of the polysynaptic U2 response could thus coincide, *in vivo*, with the arrival of inputs via this commissural pathway and it could provide a substrate for the vision- and NMDA-dependent coincidence detection processes thought to underlie the plasticity of this pathway in *Xenopus* (figure 9.3). That is, because the retinal activation of NMDA receptors is delayed via the intrinsic synaptic circuitry of the tectum by at least 10msec, compared to the direct monosynaptic activation, Ca^{2+} entry into tectal neurons would occur coincidently with the arrival of activity via the crossed isthmotectal projection. Hence, those co-active synaptic inputs become stabilized via the NMDA receptor activation of common tectal neurons. An alternative possibility, that the NMDA receptor mediated component of the response is related to developmental changes in the retinotectal projection, seems less likely based of the data in Chapter 7. First, as discussed above, in order for such NMDA receptor activation to participate in the stabilisation of co-active retinotectal synapses, it is mandatory that they monosynaptically excite the receptor. However, the monosynaptic (U1) response is mediated exclusively by non-NMDA type glutamate receptors at all stages of development examined in *Xenopus*. Second, it was found that the NMDA receptor contribution to the polysynaptic (U2) response only changes during situations of relevance to intertectal plasticity.

The retinotectal projection of *Rana pipiens* is also subject to the disparate growth patterns of the retina and the tectum but in an extracellular study in the cannulated tadpole (Debski *et al.*, 1991) AP5 failed to block any aspect of retinotectal synaptic transmission and an unexpected increase in the amplitude of the late U2 response was reported in the presence of this NMDA receptor antagonist. This result is in contrast to the recent intracellular study of Hickmott and Constantine-Paton (1993) using slices of *Rana* tectum prepared from animals during or shortly after metamorphic climax. At these later stages of development a small component of retinotectal synaptic transmission was blocked by high doses of AP5. Therefore, it seems that at metamorphic stages of development, NMDA receptors are involved in synaptic transmission within the optic tectum of *Rana* (Hickmott and Constantine-

Paton, 1993), but not in the tadpole (Debski et al., 1991) or the adult frog (Chapter 7, figure 7.10). Although eye position in this species of frog do not undergo such drastic changes at metamorphic climax (Grobstein and Comer, 1977) and its intertectal system will not reorganise its series of connections in response to a single eye rotation at any developmental stage (Kennard and Keating, 1985), dark-rearing does enlarge the size of multi-unit receptive fields recorded through the crossed isthmotectal projection (Jacobson, 1971). Therefore, it could be that even in *Rana* experience-dependent modifications in the isthmotectal projection do occur to accommodate for minor changes in eye position. The NMDA receptor mediated responses which are present at metamorphic climax in *Rana* may be involved in this intertectal plasticity.

As discussed previously the functional necessity for retinotectal synaptic plasticity arises from the disparate growth patterns of the retina and the tectum. This growth disparity is minimal after metamorphic climax and so is the degree of retinotectal plasticity (Grant and Keating, 1986). We were not able to monitor synaptic transmission during the period of development when retinotectal plasticity is most required. However, Chung *et al.* (1974b) have shown that the late U2 response can be evoked by optic nerve stimulation *in vivo* in *Xenopus* tadpoles at early larval stages. It would be interesting to adapt the methodology described in Chapters 6 & 7 to determine whether there is an NMDA mediated component to the U1 or U2 response at these early stages of development. It could be that there is an earlier peak in the AP5 sensitivity which coincides with the necessity for retinotectal plasticity. In contrast, intertectal plasticity is greatest during and shortly after metamorphic climax and continues well into adult life. Does the peak in the AP5 sensitivity of the NMDA mediated U2 response coincides with the critical period for intertectal plasticity? The critical period for intertectal plasticity was defined by the ability of the system to adapt its pattern of connections to a single eye rotation apportioned at different stages of development (Keating and Grant, 1992). Following surgical eye rotation in larval animals the intertectal system can completely alter its pattern of connectivity to restore binocular visual registration at the tectum (Keating, 1975). The capacity for intertectal plasticity to occur is restricted to a critical period of development which peaks at metamorphosis and is over approximately 3 months later (Keating and Grant, 1992 see figure 1.3). The large changes in eye position, which introduce the necessity for intertectal plasticity in *Xenopus*, also occur between stages 60 and 66 of matamorphosis (figure 1.2), corresponding to the peak of the critical period. However, the peak in AP5 sensitivity of the U2 response occurs approximately 1

month after metamorphosis (figure 7.2) and so does not correlate well with the critical period as expressed in terms of the ability of the intertectal system to adapt its pattern of connections to a single eye rotation. But, even if an eye rotation is apportioned at stage 55 of larval life actual modifications in the intertectal system are only evident 3-4 weeks post-metamorphosis (Grant and Keating, 1992). It is at this stage of development that the AP5 sensitivity of the late U2 response is greatest (figure 7.2). Also, in dark-reared animals disorder and lack of registration in the isthmotectal pathway is only apparent approximately 1 month after metamorphosis (Grant and Keating, 1989b). Therefore, the final stage of intertectal plasticity, the experience-dependent consolidation of appropriate synaptic connections, occurs at approximately 1 month after metamorphosis, a period in development when AP5 sensitivity of the U2 response was greatest. It is at this stage of development that coincident neural activity at co-active synapses would be required to result in the stabilisation of those connections via the activation of the NMDA receptor.

The normal developmental decline in the capacity for intertectal plasticity can be prevented by dark-rearing animals through the normal critical period (Grant *et al.*, 1992). When *Xenopus* were dark-reared throughout the critical period and up to 12 months after metamorphosis intertectal plasticity would still take place, in response to a single eye rotation, if the animals were exposed to normal visual experience. Consequently, it has been postulated that binocular visual experience could be the trigger for the expression of the synaptic mechanisms responsible for intertectal plasticity. We have now shown that a peak in AP5 sensitivity of the NMDA receptor mediated component of the U2 response can be induced at a much later stage in development and that the trigger for this phenomenon is also vision. When *Xenopus* were dark-reared until 12 months after metamorphosis and then given a short period of normal visual experience, the AP5 sensitivity was at a level reminiscent of that seen shortly after metamorphosis (figure 7.4). We do not know whether the peak in AP5 sensitivity which normally occurs ~ 1 month after metamorphosis still occurs in the dark-reared environment. The peak in AP5 sensitivity may be delayed by dark-rearing and triggered by subsequent visual experience or it may still occur in the absence of vision and could be recapitulated later in development. However, if vision triggers this change in NMDA receptor function then it should not be present in the dark-reared environment. Not only can intertectal plasticity be extended by dark-rearing but it can also be restored by infusion of NMDA after the critical period (Udin and Scherer, 1990). Continuous application of the glutamate receptor agonist,

NMDA, 8 months after the normal end of the critical period restores the ability of animals to adapt the crossed isthmotectal projection in response to a single eye rotation. Normal visual experience has not been denied in these animals but the mechanisms giving rise to intertectal plasticity were restored by exposure to the NMDA receptors agonist. A valid theoretical explanation of why this remarkable restoration of intertectal plasticity occurs has not been offered but the result does suggest that vision is not the only trigger responsible for the manifestation of this plasticity.

9.7. Possible changes in the NMDA receptor during development.

It has been argued above that NMDA receptor mediated events in the tectum are developmentally and visually regulated in a manner that correlates with the expression of synaptic plasticity in the crossed isthmotectal projection. The question now arises as to what aspect of the NMDA receptors function changes in the optic tectum during these situations of relevance to intertectal plasticity in *Xenopus*. Do the changes in AP5 sensitivity reported for the U2 response result from changes in NMDA receptor number or do they represent a change in the NMDA receptors affinity for the antagonist? At present, there is no available evidence to suggest that the affinity of AP5 for its binding site changes during development but there are examples of NMDA receptor number and contribution to synaptic transmission in the CNS altering during development. In the cat visual cortex experiments have been performed to assess changes in NMDA receptor number and binding affinity during situations of relevance to the age- and experience-dependent plasticity that occurs in this structure (see section 9.6.1). For example, in relation to modifications in the synaptic circuitry of the visual cortex which are induced by monocular enucleation during a critical period of postnatal development (Hubel and Wiesel, 1970) a quantitative autoradiographic technique was used to measure changes in radioactively labelled (+)-5-methyl-10,11-dihydro-5H-dibenzo[a,b]-cyclohepten-5,10-imine maleate ([^{3}H] MK-801) binding in the cat visual cortex during normal development and following periods of visual deprivation (Reynolds and Bear, 1991; Gordon *et al.*, 1991). MK-801 is a high affinity antagonist of the NMDA receptor which binds to the open channel in a use-dependent manner (Huettner and Bean, 1988). If the affinity of the antagonist for its binding site does not change then, it is reasonable to postulate, that any changes in the density of binding arise from changes in receptor number. In both studies it was shown that the affinity of the antagonist remained

constant during postnatal development, but that the amount of binding increased to a maximum level by about 6 weeks of age. The apparent increase in NMDA receptor number, however, did not strictly correlate with the critical period. Moreover, prolonged dark-rearing did not consistently alter MK-801 binding and so it seems that NMDA receptor number in the visual cortex of the cat is not modulated by visual experience. As yet similar experiments have not been performed in the optic tectum of *Xenopus*, but obviously they should be in the future.

During the critical period of postnatal development in the kitten, during which time the binocular responsiveness of cortical neurons are highly susceptible to monocular deprivation, ionophoretic application of AP5 has been shown to block the visually elicited response of cortical neurons much more effectively than in the adult cat (Tsumoto *et al.*, 1987). Fox *et al.* (1991) demonstrated, in similar types of experiments, that the NMDA component of the visual response decreases between 3 and 6 weeks of age for cortical cells located in layers IV, V and VI, and that this decrease was delayed by dark-rearing. It was later demonstrated, with the use of CNQX, that this decrease was due to changes in the relative contributions of NMDA and non-NMDA receptors to the visually evoked response (Fox *et al.*, 1992). A developmental change in the proportion of NMDA receptor mediated synaptic current has recently been reported in neurons of the rat visual cortex (Carmignoto and Vicini, 1992) and superior colliculus (Hestrin, 1992). In both these studies whole cell voltage clamp recordings from slice preparations revealed that NMDA mediated spontaneous and evoked EPSCs contributed a larger current in younger than in older animals. In layer IV cells of the visual cortex the relative contribution of the NMDA receptor mediated slow component of the EPSC decreased from ~90% at postnatal day 12 (eye-opening) to less than 20% two months later. In the visual cortex it was shown that this decrease in the kinetics of the NMDA mediated synaptic response could be stopped by dark-rearing the animal or by intraocular injection of TTX. Therefore, it was suggested that the developmental regulation of NMDA receptor mediated synaptic current is dependent on visual activity.

This type of phenomenon could explain the developmental changes we observed in the AP5 sensitivity of the U2 response in *Xenopus*. If the contribution of the NMDA mediated portion of the synaptic current is larger at earlier stages of development, compared to the adult, then the reduction observed in the extracellular population synaptic response in the presence of AP5 would also be larger. At a functional level, the increased Ca^{2+} entry which this change makes available at earlier

stages of development would also be favourable to the theoretical model of intertectal synaptic plasticity described above. Ca^{2+} entry is postulated to trigger intracellular events which could orchestrate the morphological changes which underlie the stabilisation of appropriate isthmotectal synapses. However, it still remains to be seen if these types of changes occur in the NMDA receptor mediated synaptic events we record in *Xenopus*. Moreover, it has not yet been established whether synaptic activation of NMDA receptors in the circuitry of the optic tectum leads to increased levels of intracellular Ca^{2+}.

9.8. Developmental plasticity in the mammalian CNS.

Synaptic plasticity demonstrated in the retinotectal and intertectal systems seems to occur to counter problems associated with normal growth. Information imparted by spontaneous neural activity intrinsic to the retina may be sufficient for the developmental refinement and maintenance of the spatial order of this monocular map, whereas the precise integration of inputs from two eyes mediated by the intertectal maps require the additional information provided by binocular visual experience. Similar principles seem to apply to the development of monocular and binocular maps in the mammalian visual system. Do similar synaptic mechanisms also exist in these neural systems?

The superior colliculus (SC) is the mammalian anatomical homologue of the optic tectum receiving a topographically organized projection from the contralateral and ipsilateral retina. In the adult rat the retinal projection to the contralateral SC is highly organized (Siminoff *et al.*, 1966) in contrast to the ipsilateral retinocollicular projection which is extremely sparse (Lund, 1965). Activity-dependent changes have been described in both of these direct retinocollicular pathways. The mature retinotopically ordered projection to the contralateral SC emerges during the first postnatal week from a diffuse early contralateral projection just before the eyes open at about postnatal day 13 (Simon and O'Leary, 1992). The remodelling which occurs during this period involves the elimination of aberrantly positioned retinal axon branches (O'Leary *et al.*, 1986). The correlated patterns of spontaneous neural activity that are exhibited by neighbouring RGCs even before they become synaptically connected to bipolar cells in the retina (Maffei and Galli-Resta, 1990) could underlie these changes, as blockade of NMDA receptors in the developing SC interferes with map remodelling, with the aberrant RGC axons remaining at topographically incorrect sites (Simon *et al.*, 1992; Bunch and Fawcett, 1993).

Developmental rearrangements in the ipsilateral retinocollicular projection mainly involve the preferential elimination during early postnatal life of uncrossed projection RGCs in the nasal retina (Martin, et al., 1983). The removal of these aberrant connections is disrupted by intraocular injection of TTX in the Syrian Hamster (Thompson and Holt, 1989).

The formation of eye-specific laminar projections to the lateral geniculate nucleus (LGN) of the mammalian thalamus is also believed to involve the detection of spontaneous neural activity present in the RGC population (Shatz, 1990). In adult mammals the terminal arbors of RGCs terminate topographically in a series of alternating eye-specific layers within the LGN. These eye-specific projections emerge from an initially intermingled population during a prenatal period, a pattern of segregation which can be blocked by the intracranial administration of TTX prior to their formation (Shatz and Stryker, 1988). The possibility that NMDA receptors are involved in this phenomenon has not yet been investigated. Wiesel and Hubel (1963a&b; 1965) were the first to demonstrate, at a functional level, experience-dependent plasticity in the developing mammalian binocular visual system. Their fundamental discovery was that occlusion of one eye in kittens for several months after birth leads to an almost total loss of responses from this eye in neurons of the striate cortex. This finding has since been confirmed in other mammals, and similar effects have been reported in extrastriate visual areas, such as area 18 and the lateral suprasylvian area of the cat (reviewed in Rauschecker, 1991). The NMDA receptor has recently been implicated in this form of experience-dependent synaptic plasticity: following monocular deprivation shifts in cortical ocular dominance towards the open eye were selectively reduced in regions of the striate cortex exposed to AP5 delivery from an osmotic minipump (Kleinschmidt et al., 1987). However, it is known that a large component of visually evoked activity in the cortex is blocked by NMDA receptor antagonists (Fox et al., 1989; Miller et al., 1989) indicating that the NMDA receptor, under normal physiological conditions, partially mediates the transmission of visual information in the cortex. Following NMDA receptor inactivation, the reduction in ocular dominance plasticity could reflect a general loss of visually elicited excitability in the cortex. For this reason, the interpretation that disrupting NMDA receptor function interferes with a specific postsynaptic mechanism concerned with cortical synaptic plasticity has been called into question (Fox and Daw, 1993 and others).

9.9. Spatial maps in the hippocampus

Investigations into the basis of long-term changes in synaptic efficacy in the hippocampus have led to a greater understanding of how events at the postsynaptic membrane involving the NMDA receptor can be transduced into chemical signals of relevance to pre- and postsynaptic change. The discovery of "place cells" (O'Keefe and Dostrovsky, 1971) prompted the cognitive map theory of hippocampal function (O'Keefe and Nadel, 1978). This theory entrusts the hippocampus with the special ability to store memories concerning the spatial layout of an environment and to use such memories for adaptive behaviour in the world. For this theory to be true the hippocampus should store many environmental representations only one of which is active at any given time. It is postulated that these "space maps" are represented in the hippocampus as distinct spatio-temporal patterns of neural activity. In order for these different neural maps to be stored in the circuitry of the hippocampus dynamic changes in the efficiency of the synaptic connections which convey this information is required. Indeed, activity-dependent changes in synaptic efficiency in the mammalian brain were first described in the excitatory connections made by perforant path fibres onto granule cells in the dentate gyrus of the hippocampus. Bliss and Lomo (1973) observed that brief trains of high-frequency electrical stimulation to this pathway caused an abrupt increase in the strength of synaptic transmission which lasted several hours. This phenomenon was termed long term potentiation (LTP) and now represents the primary experimental model for investigating mechanisms underlying synaptic plasticity in the CNS (for review see Bliss and Collingridge, 1993). An important consideration, in the context of the "coincidence detection" hypothesis of intertectal plasticity in *Xenopus*, is the phenomenon of "associative" LTP. This is the observation that weak or low frequency stimulation of one afferent input to hippocampal neurons which, by itself, is insufficient to change the strength of the activated synapses, can induce LTP in that input when coincidentally-paired with high frequency tetanic stimulation of another synaptic input to the same neurons. If the cognitive map theory is a valid definition of hippocampal function then the synaptic plasticity which has been described in the connections of the hippocampus may be essential to adapt the circuitry of the hippocampal spatial map to ongoing changes in the animals environment.

Several mechanisms are currently thought to be responsible for the expression of LTP in the hippocampus. Hippocampal glutamatergic synaptic transmission is predominantly through non-NMDA type glutamate receptors. The induction of LTP

by tetanic stimulation is, however, blocked by NMDA receptor antagonists, such as AP5 (Collingridge *et al.*, 1983a&b). Therefore, the manifestation of this form of synaptic plasticity is considered to depend upon the recognition of correlated patterns of presynaptic neural activity via postsynaptic activation of the NMDA receptor. The initial induction signal for this synaptic plasticity is proposed to be the Ca^{2+} transient which permeates into the postsynaptic neuron through the activated NMDA receptor channel (figure 9.4). The signal is amplified by the release of Ca^{2+} from internal stores leading to the activation of phosphorylation cascades such as the Ca^{2+}/phospholipid-dependent protein kinases (PKC) or Ca^{2+}/calmodulin -dependent protein kinases (CaMKII). This activation of protein kinases leads to the phosphorylation of substrate proteins which could include the NMDA and non-NMDA receptors themselves. This phosphorylation process could also lead to the cleavage of proteins such as neural cell adhesion molecules (N-CAMS) which may contribute to morphological changes.

A parallel pathway which may also be important in LTP is provided by the metabotropic glutamate receptor family (mGluRs). These receptors can couple, through G-proteins, to the phosphoinositide-specific phospholipase C (PLC), phospholipase A_2 (PLA$_2$) and adenylate cyclase (AC), to produce diacylglycerol (DAG) and arachidonic acid (AA). Other enzymes such as nitric oxide synthase (NOS) may be directly triggered by the Ca^{2+} transient. Biochemical changes in the presynaptic terminal may be initiated by the action of retrograde messengers such as arachidonic acid (AA) and nitric oxide (NO), because the long-term enhancement of transmitter release from activated presynaptic terminals, which is believed to participate in the maintenance of LTP (Errington *et al.*, 1987), appears to involve these putative retrograde messengers (Williams *et al.*, 1989 ; O'Dell *et al.*, 1991).

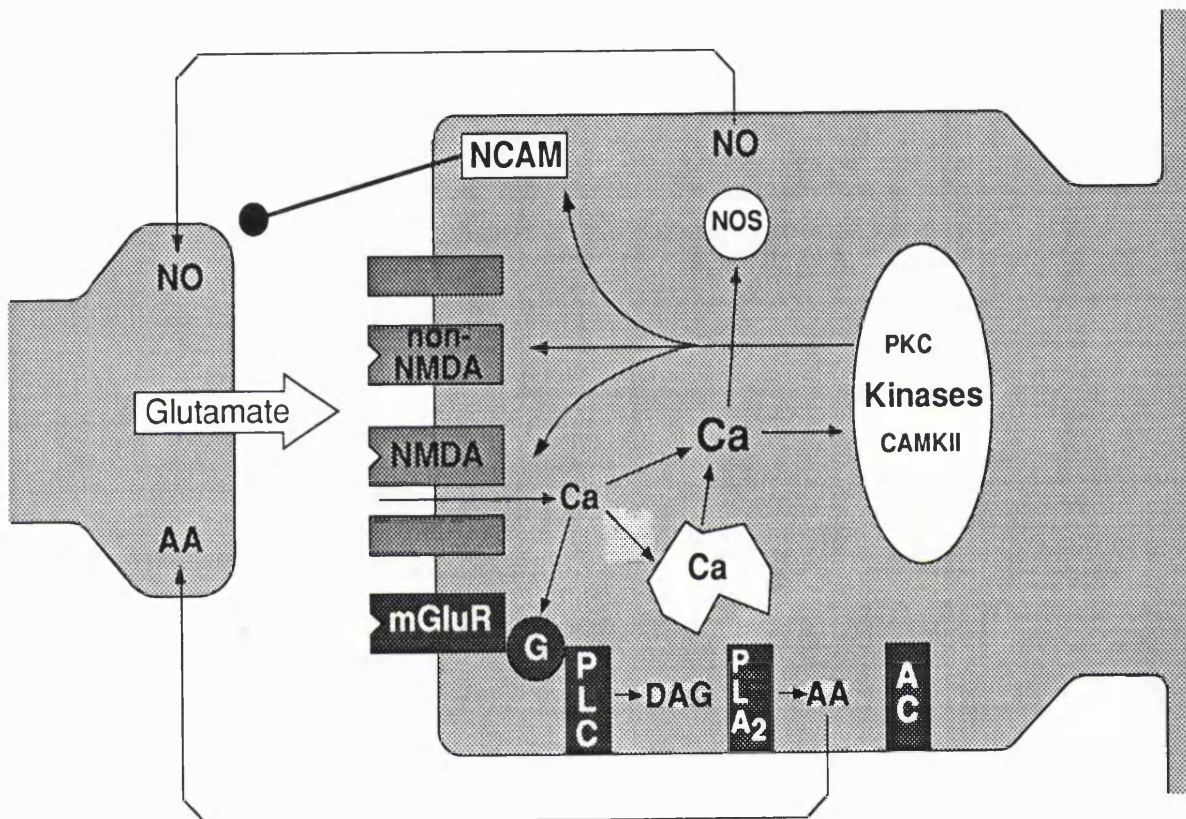**Figure 9.4. Possible signal transduction processes involved in synaptic plasticity.**

A cartoon illustrating possible biochemical cascades which could account for for this type of synaptic plasticity: the putative retrograde messengers AA & NO may either enhance or derpress transmitter release from the presynaptic bouton, depending on the level of coïcident depolarisation.
See text for details.

215

9.10. NMDA receptor-independent synaptic plasticity

While dynamic changes in synaptic strength are intuitively obvious ways of adapting developing and existing neural circuits to changes in the organisms circumstances, it must be emphasized that such synaptic plasticity can occur without involvement of NMDA receptors. Indeed, not all forms of LTP in the hippocampus require the activation of NMDA receptors. Mossy fibres terminate in the stratum lucidum of area CA3, a subfield devoid of NMDA receptors. Consistent with this observation, the LTP which is demonstrable in these synaptic connections is not blocked by AP5 (Harris and Cotman, 1986). Moreover, activity-dependent synaptic plasticity can take place in synaptic connections which are not even glutamatergic. The associative change in synaptic strength that underlies conditioning in adult *Aplysia* is mediated by the action of serotonin (Castellucci and Kandel, 1976). Temporally coincident neural activity in two converging pathways triggers presynaptic facilitation which increases the efficacy of synaptic transmission in the neural circuit of the gill-withdrawal reflex. The refinement of neuromuscular connections, in which synaptic transmission is mediated by acetylcholine, also requires neural activity. In mammalian muscles 2 or more motor axons innervate each muscle prior to birth, but during early postnatal life, branches of motor axons are retracted and remodelled such that muscle fibres become innervated by only one motor axon. Prolonged blockade of impulse activity during development of the neuromuscular junction stops this process (Thompson *et al.*, 1979). Sanes and Takacs (1993) have demonstrated that plasticity of inhibitory synapses can occur during the development of maps in the central auditory pathways. The medial nucleus of the trapezoid body (MNTB) sends an inhibitory glycinergic projection into the lateral superior olivary nucleus. Unilateral cochlea ablation in neonatal gerbils removed activity from this central projection and caused the inhibitory MNTB terminal boutons to spread along the frequency axis of the postsynaptic target. Thus, we should not assume that the NMDA receptor subserves all forms of activity-dependent synaptic plasticity in the developing and mature CNS. Indeed, it is clear that coincidence detection can be accounted for by a variety of diverse molecular mechanisms (for recent review see Bourne and Nicoll, 1993).

9.11. Conclusions.

Successful organisms are able to adapt as a result of previous experience. This ability ranges from the relatively simple capacity to re-wire nerve connections during brain development and to alter neuronal response properties in response to on-going changes in the external environment, to the little understood process of learning and recognition in maturity. These later manifestations of adaptive behaviour indicate that the mechanisms by which experience can modify the structure and function of the brain persist throughout life, rather than being confined to so-called "critical periods" of early ontogeny. Thus, neural systems that are affected by experience during these critical periods of development may afford a potential to broaden understanding of how the environment influences the brain in general.

It is evident that the earliest phases of topographic map formation are carefully orchestrated by genetically determined mechanisms, in which the products of gene expression serve to guide growing axons to their targets and cause them to distribute their synaptic terminations in a degree of topological order. Activity-dependent mechanisms then operate to a lesser or greater extent to fine-tune the synaptic connectivity, depending on the success of the initial order established by these genetic products. The results presented in this Thesis suggest a minimal involvement for neural activity in the development of the precisely ordered synaptic connections in the *Xenopus* retinotectal projection. However, it appears that intrinsically-derived, spontaneous patterns of neural activity are more important in fine-tuning the initially rather disordered monocular retinal maps in other lower vertebrates and in mammals. In some of these latter species (eg cats and monkeys) these activity-dependent events occur *in utero*, while in altricial ones (eg rats and hamsters) they occur postnatally, but behind closed eyelids. Certainly, there is no evidence, even in free-living lower vertebrates, that visually-evoked activity deriving from interactions with the environment are necessary for these processes.

However, visual experience is clearly involved in the integration and ordering of synaptic connections in the developing binocular maps found in the *Xenopus* tectum and the mammalian visual cortex. Experience-dependent dynamic changes in synaptic weighting and/or position are generally conceived as useful and convenient ways of adapting the organism to changes in the environment. Results presented in this Thesis indicate that experience-dependent changes in synaptic connectivity can occur without obvious behavioural or adaptive advantage. A role for the NMDA receptor in the detection of correlated or coincident patterns of activity generated by experience has

been suggested. Data obtained from *Xenopus* reared in stroboscopic illumination, which perturbs the spatial distribution of correlated firing in the tectum, offered qualified support for these ideas, but also high-lighted deficiencies in our understanding of the temporal parameters which define "coincidence" and which set its limits.

The major finding of this Thesis was that retinal synapses in *Xenopus* indirectly activate an NMDA receptor mediated response in the tectum, which seems to participate little in the processing of visual information in this nucleus, which is developmentally and visually regulated in ways that correspond to the synaptic plasticity of this commissural pathway, and which seems to be absent or diminished in a related species of frog in which the pathway exhibits only minimal experience-dependent synaptic plasticity. All of these observations are consistent with the NMDA receptors involvement in the mechanisms responsible for binocular visual integration in the tectum. However, many details concerning this receptors involvement in these processes are still to be clarified. Moreover, the relationship between the process of destabilization/stabilization and the physical reorienting/shifting of the crossed isthmotectal arbors, that is such a striking aspect of this plasticity in *Xenopus*, has not even begun to be seriously addressed.

Appendix 1. A computer program written for the calculation of peak amplitudes and latencies to peak in a series of tectal field potentials.

This program was written using a compiler supplied with CED software. It was designed so that large numbers of sampled waveforms could be analysed off-line by the simple placement of cursors between the response area of interest. The peak amplitude and latency to peak of the response is calculated between these fixed cursor positions for the entire series of traces. The results are transferred to a named ASCII file for future reference. Individual sampled waveforms can also be printed out and stored separately.

```
' Variable usage/declared global variables :
NUMVAR 11
NUMSTR 2
VAR ch
VAR av
VAR sst send
VAR sw
VAR st2 end2
VAR p2 t2
VAR outfile$
VAR tot
VAR dontp
Setup
Defaults
Keys
END

PROC Defaults
st2:=0; end2:=0
RETURN

PROC Setup
CLEAR
VIEW 1;CLEAR 1;NORMAL
OFF 2
WINDOW 0 5 100 95
v:=0
OFF 17; OFF XAXIS
COUNT 17 0 MAXTIME a
TOT:=a/2
YRANGE 1 -2.0 0.5
DRAW 0 0.1
PRINTTO "junk.txt"
ch:=1
RETURN

PROC Keys
FKEY 0
FKEY 1 2 Logfile "LOGFILE"
FKEY 1 3 Ranges1  "RANGES"
FKEY 1 4 Doall1   " DOALL1"
FKEY 1 6 Screen  "SCREEN"
FKEY 1 7 Pr1     " PRINT"
FKEY 1 8 Sa1     " SAVE"
FKEY 1 9 Files   " FILE"
FKEY 1 10 Stop   " QUIT"
REPEAT
```

```
 FKEY 5
UNTIL v
RETURN

PROC Logfile
 INPUTSTR outfile$ "Enter name of file"
 PRINTTO outfile$
RETURN

PROC Files
 FILE
 Setup
 Keys
RETURN

PROC Ranges1
IF p2=0
 send:=-1
 sst:=-1
 Go1
 CURSORS 2
 Seek1
ENDIF
 CURSORS 2
 SETC 1 sst+st2
 SETC 2 sst+end2
 PRINT 0 "Use cursors for -ve peak search"
 INTERACT
 st2:=C1-sst end2:=C2-sst
 MINMAX ch C1 C2 a b
RETURN

PROC Go1
 dontp:=0
 NEXTTIME 17 send sst
 NEXTTIME 17 sst send
 sw:=sw+1
 p2:=0
 t2:=0
RETURN

PROC Seek1
 MINMAX ch sst send x y
IF (y-x>.05)&(sst>0)
      YRANGE ch -2 0.5
      MINMAX ch sst+st2 sst+end2 p2 x t2 y-sst
      NEXTTIME 1 (sst+st2) c d
      NEXTTIME 1 (sst+end2) e f
      av:=f+d/2
      CURSORS 2
      SETC 1 (sst+st2) (sst+end2)
      DRAW sst send-sst
ELSE
 dontp:=1
ENDIF
RETURN

PROC Doall1
 sst:=-1
 send:=-1
```

```
sw:=0
PRINT 0 "Analysing and logging results Press any key to stop"
REPEAT
 Go1
IF sst<0
  MESSAGE "End of file"
  RETURN
ELSE
 seek1
ENDIF
 MOVETO 1 4
PRINT 1 "n= %2.0d peak= %6.5dmV latency= %6.5dsec" sw (p2-x) t2-(sst+0.01)
IF dontp<1
PRINT 3 "%6.0d     %6.5d     %6.5d" sw (p2-x) t2-(sst+0.01)
 t2:=0
ENDIF
UNTIL INKEY>0
RETURN

PROC Stop
 v:=1
RETURN

PROC Screen
 OFF TRAM
 OFF TITLE
 OFF LABELS
 CLEAR
 DRAW
 CURSORS 2
 MESSAGE " Select the view of the data "
 INTERACT
 CURSORS 0
 DRAW
 MOVETO 10 4
 INPUTSTR outfile$ "title 1"
 PRINT 1 outfile$
 MOVETO 40 4
 INPUTSTR outfile$ "title 2"
 PRINT 1 outfile$
 MOVETO 70 4
 INPUTSTR outfile$ "title 3"
 PRINT 1 outfile$
RETURN

PROC Pr1
 SCRNDUMP 2
 PRINT -2 "%C" 12
 setup
 defaults
RETURN

PROC Sa1
 CURSORS 1
 SETC 1 sst+st2
 PRINT 0 "Find that cursor and use it"
 INTERACT
 st2:=C1
 NEXTTIME 1 C1 a b
RETURN
```

ANTAL, M., MATSUMOTO, N. and SZEKELY, G., (1986), Tectal neurons of the frog: Intracellular recording and labeling with cobalt electrodes, J. Comp. Neurol., **246**, 238-253.

ANTAL, M., (1991), Distribution of GABA immunoreactivity in the optic tectum of the frog: A light and electron microscopic study, Neurosci., **42**, (3), 879-891.

ARAKAWA, T. and OKADA, Y., (1989), The effect of GABA on neurotransmission in frog tectal slices, Neurosci. Res., **6**, 363-368.

ARNETT, D. W., (1978), Statistical dependence between neighboring retinal ganglion cells in goldfish, Brain Res, **32**, 49-53.

ASCHER, P. and NOWAK, L., (1988), Quisqualate and kainate activated channels in mouse central neurones in culture, J. Physiol., **399**, 227-245.

ATTARDI, D. G. and SPERRY, R. W., (1963), Preferential selection of central pathways by regenerating optic fibers., Exp. Neurol., **7**, 46-64.

BEAR, M. F. and SINGER, W., (1986), Modulation of visual cortical plasticity by acetylcholine and noradrenaline, Nature Lond., **320**, 172-176.

BEAZLEY, L., KEATING, M. J. and GAZE, R. M., (1972), The appearance, during development, of responses in the optic tectum following visual stimulation of the ipsilateral eye in *Xenopus laevis.*, Vision Res., **12**, 407-410.

BEAZLEY, L. D., (1979), Intertectal connections are not modified by visual experience in developing *Hyla moorei.*, Exp. Neurol., **63**, 411-419.

BEKKERS, J. M. and STEVENS, C. F., (1989), NMDA and non-NMDA receptors are co-localized at individual excitatory synapses in cultured rat hippocampus, Nature, **341**, 230-233.

BENEDETTI, F., (1991), The postnatal emergence of a functional somatosensory representation in the superior colliculus of the mouse., Dev. Brain Res., **60**, 51-57.

BENVENISTE, M., MIENVILLE, J.-M., SERNAGOR, E. and MAYER, M. L., (1990), Concentration-jump experiments with NMDA antagonists in mouse cultured hippocampal neurons, J. Neurophys., **63**, (6), 1373-1384.

BLISS, T. V. P. and LOMO, T., (1973), Long-lasting potentiation of synaptic transmission in the dentate area of the anesthetised rabbit following stimulation of the perforant path, J. Physiol. (Lond), **232**, 331-356.

BLISS, T. V. P. and COLLINGRIDGE, G. L., (1993), A synaptic model of memory: long-term potentiation in the hippocampus, Nature, **361**, 31-39.

BONHOEFFER, F. and GIERER, A., (1984), How do retinal axons find their targets on the tectum?, Trends Neurosci, **7**, 378-381.

BOSS, V. and SCHMIDT, J. T., (1982), Tests for a role of activity in the formation of ocular dominance patches, Soc Neurosci Abstr , **8**, 668.

BOURNE, H. R. and NICOLL, R., (1993), Molecular machines integrate coincident synaptic signals, Cell, **72**, 65-75.

BRICKLEY, S. G., GRANT, S. and WILLIAMS, J. H., (1992), The frog optic tectum in vitro: differential effects of the NMDA receptor antagonist AP5 on postsynaptic potentials, Proc R Soc Lond, **452**, 63P

BUNCH, S. T. and FAWCETT, J. W., (1993), NMDA receptor blockade alters the topoography of naturally occuring ganglion cell death in the rat retina, Dev. Biol., **160**, 434-442.

CAREW, T. J., HAWKINS, R. D., ABRAMS, T. W. and KANDEL, E. R., (1984), A test of Hebb's postulate at identified synapses which mediate classical conditioning in Aplysia, J. Neurosci., **4**, (5), 1217-1224.

CARMIGNOTO, G. and VICINI, S., (1992), Activity-dependent decrease in NMDA receptor responses during development of the visual cortex, Science, **258**, 1007-1011.

CASTELLUCCI, V. F. and KANDEL, E. R., (1981), Presynaptic facilitation as a mechanism for behavioural sensitization in *Aplysia*, Science, **194**, 1176-1178.

CHUNG, S. H., GAZE, R. M. and STIRLING, R. V., (1973), Abnormal visual function in *Xenopus* following stroboscopic illumination, Nature, **246**, 186-189.

CHUNG, S. H., BLISS, T. V. P. and KEATING, M. J., (1974a), The synaptic organization of optic afferents in the amphibian tectum, Proc. R. Soc. Lond., **187**, (B), 421-447.

CHUNG, S. H., KEATING, M. J. and BLISS, T. V. P., (1974b), Functional synaptic relations during the development of retino-tectal projections in amphibians, Proc R. Soc. Lond., **187**, (B), 449-459.

CLINE, H. T., DEBSKI, E. A. and CONSTANTINE-PATON, M., (1987), NMDA receptor antagonist desegregates eye specific stripes, Proc.Natl.Acad.Sci.USA, **84**, 4312-4345.

CLINE, H. T. and CONSTANTINE-PATON, M., (1989), NMDA receptor antagonists disrupt the retinotectal topographic map, Neuron, **3**, (October), 413-426.

CLINE, H. T. and TSIEN, R. W., (1991), Glutamate-induced increases in intracellular Ca in cultured frog tectal cells mediated by direct activation of NMDA receptor channels, Neuron, **6**, (February), 259-267.

CLINE, H. T., (1991), Activity-dependant plasticity in the visual systems of frogs and fish, TINS, **14**, (3), 104-111.

COLLETT, T., (1977), Stereopsis in toads, Nature, **267**, 349-351.

COLLINGRIDGE, G. L., KEHL, S. J. and McLENNAN, H., (1983a), Excitatory amino acids in synaptic transmission in the Schaffer collateral-commissural pathway of the rat hippocampus, J. Physiol., **334**, 33-46.

COLLINGRIDGE, G. L., KEHL, S. J. and MCLENNAN, H., (1983b), The antagonisms of amino acid-induced excitations of rat hippocampal CA1 neurones in vitro, J. Physiol., **334**, 19-31.

COLQUHOUN, D., JONAS, P. and SAKMANN, B., (1992), Action of brief pulses of glutamate on AMPA/Kainate receptors in patches from different neurons of rat hippocampal slices, J. Physiol., **458**, 261-287.

CONSTANTINE-PATON, M. and LAW, M. I., (1978), Eye-specific termination bands in tecta of three-eyed frogs, Science, **202**, 639-641.

COOK, J. E. and RANKIN, E. C. C., (1986), Impaired refinement of the regenerated goldfish retinotectal projection in stroboscopic light: a quantatative WGA-HRP study, Exp Brain Res, **63**, 421-430.

COOK, J. E., (1987), A sharp retinal image increases the topographic precision of the goldfish retinotectal projection during optic nerve regeneration in stroboscopic light, Exp Brain Res, **68**, (319-328),

COOK, J. E., (1988), Topographic refinement of the goldfish retinotectal projection: sensitivity to stroboscopic light at different periods during optic nerve regeneration, Exp Brain Res, **70**, 109-116.

COOK, J. E. and BECKER, D. L., (1990), Spontaneous activity as a determinate of axonal connections, Eur J Neurosci, **2**, 162-169.

CRUNELLI, V., FORDA, S. and KELLY, J. S., (1983), Blockade of amino acid-induced depolarizations and inhibition of excitatory post-synaptic potentials in rat dentat gyrus, J. Physiol., **341**, 627-640.

CRUNELLI, V., KELLY, J. S., LERESCHE, N. and PIRCHIO, M., (1987), On the excitatory post-synaptic potential evoked by stimulation of the optic tract in the rat lateral geniculate nucleus, J. Physiol., **384**, 603-618.

CURTIS, D. R., GAME, C. J. A. and McCULLOCH, R. M., (1974), Antagonism of inhibitory amino acid action by tubocurarine, Br. J. Pharmacol., **52**, 101-103.

CYANDER, M., (1983), Prolonged sensitivity to monocular deprivation in dark-reared cats: effects of age and visual exposure., Dev. Brain Res., **8**, 155-164.

CYNADER, M. and MITCHELL, D. E., (1980), Prolonged sensitivity to monocular deprivation in dark reared cats, J. Neurophys., **43**, 1026-1040.

DAW, N. W., RADER, R. K., ROBERTSON, T. W. and ARIEL, M., (1983), Effects of 6-hydroxydopamine on visual deprivation in the kitten striate cortex, J. Neurosci., **3**, 907-914.

DAWES, E. A., GRANT, S., KEATING, M. J. and NANCHAHAL, K., (1984), The

elaboration of the contralateral visuotectal projection in the frog, *Xenopus laevis*, is unaffected by visual deprivation, J. Physiol., **350**, 62P.

DAWES, E. A., GRANT, S. and KEATING, M. J., (1984), Visual deprivation extends the 'critical period' for intertectal plasticity in the frog, *Xenopus laevis*, J. Physiol., **350**, 18.

DEBSKI, E. A., CLINE, H. T., MCDONALD, J. W. and CONSTANTINE-PATON, M., (1991), Chronic application of NMDA decreases the NMDA sensitivity of the evoked tectal potential in the frog, J. Neurosci., **11**, (9), 2947-2957.

DEUSON, E. B. v. and MEYER, R. L., (1990), Pharmacological evidence for NMDA, APB and Kainate/quisqualate retinotectal transmission in the isolated whole tectum of goldfish , Brain Res., **536**, 86-96.

DREJER, J. and HONORE, T., (1988), New quinoxalinediones show potent antagonism of quisqualate responses in cultured mouse cortical neurons, Neurosci. Letts., **87**, 104-108.

EASTER, S. S. and STUERMER, C. A. O., (1984), An evaluation of the hypothesis of shifting terminals in goldfish optic tectum., J. Neurosci., **4**, 1052-1063.

EDWARDS, F. A., KONNARTH, A., SAKMANN, B. and TAKAHASHI, T., (1989), A thin slice preparation for patch clamp recordings from neurones of the mammalian central nervous system, Eur. J. Physiol., **414**, 600-612.

ERRINGTON, M. L., LYNCH, M. A. and BLISS, T. V. P., (1987), Long-term potentiation in the dentate gyrus induction and increased glutamate release are blocked by D(-)aminophosphonovalerte, Neurosci., **20**, (1), 279-284.

EVANS, R. H., FRANCIS, A. A., JONES, A. W., SMITH, D. A. S. and WATKINS, J. C., (1982), The effects of a series of -phosponic -carboxylic amino acids on electrically evoked and excitant amino acid-induced responses in isolated spinal cord preparations, Br. J. Pharmac., **75**, 65-75.

EWERT, J. P., *The visual system of the toad: Behavioral and physiological studies on a pattern recognition system* (Academic Press, New York San Francisco London, 1976).

FELDMAN, J. D., (1975), Visual deprivation and intertectal neuronal connections in *Xenopus laevis.*, Proc. R. Soc. Lond., **191**,

FELDMAN, J. D., GAZE, R. M. and KEATING, M. J., (1983), Development of the orientation of the visuo-tectal map in *Xenopus*, Dev. Brain Res., **6**, 269-277.

FOX, K., DAW, N., SATO, H. and CZEPITA, D., (1991), Dark-rearing delays the loss of NMDA-receptor function in kitten visual cortex., Nature, **350**, (28 March), 342-344.

FOX, K., DAW, N., SATO, H. and CZEPITA, D., (1992), The effect of visual experience on development of NMDA receptor synaptic transmission in kitten visual cortex, J. Neurosci., **12**, (7), 2672-2684.

FOX, K. and DAW, N. W., (1993), Do NMDA receptors have a critical function in visual cortical plasticity, TINS, **16**, (3), 116-122.

FRANCES, A., JAGANNATH, A. and SCHECTER, N., (1980), Stability of Muscarinic-cholinergic receptor activity in the deafferented retinotectal pathway, Brain Res., **185**, 161-168.

FRASER, S. E., MURRAY, B. A., CHOUNG, C. M. and EDELMAN, G. M., (1984), Alterations of the retinotectal map in *Xenopus* by antibodies to neural cell adhesion molecules, Proc. Natl. Acad. Sci. USA, **81**, 4222-4226.

FREEMAN, J. A., SCHMIDT, J. T. and OSWALD, R. E., (1980), Effect of alpha-bungarotoxin on retinotectal synaptic transmission in the goldfish and the toad, Neuroscience, **5**, 929-942.

GAZE, R. M., (1958a), The representation of the retina on the optic lobe of the frog, J. Exp. Physiol., **43**, 209-214.

GAZE, R. M., (1958b), Binocular vision in frogs, J Physiol (Lond), **143**, 20P.

GAZE, R. M. and JACOBSON, M., (1963), A study of the retinotectal projection during regeneration of the optic nerve in the frog, Proc. R. Soc. Lond., **185**, 301-330.

GAZE, R. M., KEATING, M. J., SZEKELY, G. and BEAZLEY, L. D., (1970), Binocular interaction in the formation of specific intertectal neuronal connections., Proc. R. Soc. Lond., **175**, 107-147.

GAZE, R. M. and SHARMA, S. C., (1970), Axial differences in the reinnervation of the goldfish optic tectum by regenerating optic nerve fibers., Exp. Brain Res., **10**, 171-181.

GAZE, R. M. and KEATING, M. J., (1970), Further studies on the restoration of the contralateral retinotectal projection following regeneration of the optic nerve in the frog, Brain Res., **21**, 183-207.

GAZE, R. M., KEATING, M. J. and CHUNG, S. H., (1974), The evolution of the retinotectal map during development in *Xenopus*, Proc. R. Soc. Lond. B., **185**, 301-330.

GAZE, R. M., KEATING, M. J., OSTBERG, A. and CHUNG, S. H., (1979a), The relationship between retinal and tectal growth in larval *Xenopus*: implications for the development of the retino-tectal projection, J. Embryol. Morph., **53**, 103-143.

GAZE, R. M., FELDMAN, J. D., COOKE, J. and CHUNG, S. H., (1979b), The orientation of the visuotectal map in *Xenopus*: developmental aspects, J. Embryol. exp. Morph., **53**, 39-66.

GAZE, R. M. and GRANT, P., (1992), Spatio-temporal patterns of retinal ganglion cell death during *Xenopus* development., J. Comp. Neurol., **315**, 264-274.

GORDON, B., DAW, N. and PARKINSON, D., (1991), The effect of age on binding of MK-801 in the cat visual cortex, Dev. Brain Res., **62**, 61-67.

GRANT, S., DAWES, E. A. and NANCHAHAL, K., (1986), Visual deprivation and the maturation of the retinotectal projection in *Xenopus laevis*, J. Embryol. exp. Morph., **91**, 101-115.

GRANT, S. and KEATING, M. J., (1986a), Ocular migration and the metamorphic and postmetamorphic maturation of the retinotectal system in *Xenopus laevis*: an autoradiographic and morphometric study, J. Embryol. exp. Morph., **92**, 43-69.

GRANT, S. and KEATING, M. J., (1986b), Normal maturation involves systematic changes in binocular visual connections in *Xenopus laevis*., Nature, **332**, 258-261.

GRANT, S. and KEATING, M. J., (1989a), Changing patterns of binicular visual connections in the intertectal system during development of the frog, *Xenopus laevis*. I. Normal maturational changes in response to changing binocular geometry., Exp. Brain Res., **75**, 99-116.

GRANT, S. and KEATING, M. J., (1989b), Changing patterns of binocular visual connections in the intertectal system during development of the frog, *Xenopus laevis*. II. Abnormalities following early visual deprivation, Exp.Brain Res., **75**, 117-132.

GRANT, A. C. and LETTVIN, J. Y., (1991), Sources of electrical transients in tectal neuropil of the frog, *Rana pipiens*, Brain Res., **560**, 106-121.

GRANT, S. and KEATING, M. J., (1992), Changing patterns of binocular visual connections in the intertectal system during development of the frog, *Xenopus laevis*. III. Modifications following early eye rotation, Exp.Brain Res., **89**, 383-396

GRANT, S., DAWES, E. A. and KEATING, M. J., (1992), The critical period for experience-dependent plasticity in a system of binocular visual connections in Xenopus laevis: Its extension by dark rearing, Eur.J.Neurosci., **4**, 37-45.

GRANT, S., BRICKLEY, S. G. and KEATING, M. J., *Plasticity of Binocular Visual Connections in the Frog: From R.M. Gaze to NMDA* (Birkhauser, Boston Basel Berlin, 1993).

GROBSTEIN, P. and COMER, C., (1977), Post-metamorphic eye migration in *Rana* and *Xenopus*, Nature, **269**, 54-56.

GROBSTEIN, P., COMER, C., HOLLYDAY, M. and ARCHER, S. M., (1978), A crossed isthmotectal projection in Rana pipiens and its involvement in the ipsilateral visuotectal projection., Brain Res., **156**, 117-123.

GRUBERG, E. R. and UDIN, S. B., (1978), Topographic projections between the nucleus isthmi and the tectum of the frog Rana pipiens, J. Comp. Neur., **179**, 487-500.

HARDY, O., AUDINAT, E. and JASSIK-GERSCHENFELD, D., (1987), Electrophysiological properties of neurons recorded intracellularly in slices of the pigeon optic tectum, Neurosci., **23**, (1), 305-318.

HARRIS, W. A., (1980), The effects of eliminating impulse activity on the development of the retinotectal projection in salamanders., J. Comp. Neurol., **194**, 303-317.

HARRIS, W. A., (1984), Axonal pathfinding in the absence of normal pathways and impulse activity., J. Neurosci., 4, 1153-1162.

HARRIS, E. W., GANONG, A. H. and COTMAN, C. W., (1984), Long-term potentiation in the hippocampus involves activation of NMDA receptors, Brain Res., 323, 132-137.

HARRIS, E. W. and COTMAN, C. W., (1986), Long-term potentiation of guinea pig mossy fiber responses is not blocked by N-methyl-D-aspartate antagonists, Neurosci. Letts., 70, 132-137.

HEBB, D. O., The organization of behaviour New York, 1949).

HENLEY, J. M., BOND, A. and BARNARD, E. A., (1991), Autoradiographic localisations of glutaminergic binding sites in Xenopus brain, Neurosci. Lett., 129, 35-38.

HESTRIN, S., (1992), Developmental regulation of NMDA receptor-mediated synaptic currents at a central synapse, Nature, 357, 686-689.

HICKMOTT, P. W. and CONSTANTINE-PATON, M., (1993), The contribution of NMDA, non-NMDA and GABA receptors to postsynaptic responses in neurons of the optic tectum, J. Neurosci., 12, (10), 4339-4353.

HODOS, W., DAWES, E. A. and KEATING, M. J., (1982), Properties of the receptive fields of frog retinal ganglion cells as revealed by their response to moving stimuli, Neurosci., 7, (6), 1533-1544.

HONORE, T., DAVIES, S. N., DREJER, J., FLETCHER, E. F., JACOBSON, P., LODGE, D., NIELSEN, F. E., (1988), Quinoxalinediones: potent competetive non-NMDA glutamate receptor antagonists, Science, 241, 701-703.

HORDER, T. J., (1971), Retension, by fish optic nerve fibres regenerating to new terminal sites in the tectum, of chemospecific affinity for their original sites., J. Physiol., 216, 53P-55P.

HUBEL, D. H. and WIESEL, T. N., (1970), The period of susceptibility to the physiological effects of unilateral eye closure in kittens, J. Physiol., 206, 419-436.

HUETTNER, J. E. and BEAN, B. P., (1988), Block of NMDA activated current by the anticonvulsant MK-801: Selective binding to open channel, Proc. Natl. Acad. Sci. USA, 85, 1307-1311.

HULME, E. C., BIRDSALL, N. J. M., BURGEN, A. S. V. and MEHTA, P., (1978), The binding of antagonists to brain muscarinic receptors, Mol. Pharmac., 14, 737-750.

HUMPHREY, M. F. and BEAZLEY, L. D., (1982), An alactrophysiological study of early retinotectal projection patterns during optic nerve regeneration in Hyla moorei, Brain Res., 239, 595-602.

IINO, M., OZAWA, S. and TSUZUKI, K., (1990), Permeation of calcium through excitatory amino acid receptor channels in cultured rat hippocampal neurones, J.

Physiol., **424**, 151-165.

JACOBSON, M. and GAZE, R. M., (1965), Selection of appropriate tectal connections by regenerating optic nerve fibers in adult goldfish., Exp. Neurol., **13**, 418-430.

JACOBSON, M., (1971), Absence of adaptive modification in developing retinotectal connections in frogs after visual deprivation or disparate stimulation of the eyes., Proc. Nat. Acad. Sci., **68**, (3), 528-532.

JACOBSON, M. and HIRSCH, H. V. B., (1973), Development and maintenance of connectivity in the visual system of the frog. I. The effects of eye rotation and visual deprivation., Brain Res., **49**, 47-65.

JOHNSTON, A. R. and GOODAY, D. J., (1991), Xenopus temporal retinal neuritescolllapse on contact with glial cells from caudal tectum in vitro, Development, **113**, 409-417.

JONAS, P. and SAKMANN, B., (1992), Glutamate receptor channels in isolated patches from CA1 and CA3 pyramidal cells of rat hippocampal slices, J. Physiol., **455**, 143-174.

JONES, R. S. G., (1987), Complex synaptic responses of enthorinal cortical cells in the rat to subicular stimulation *in vitro* demonstration of an NMDA receptor-mediated component, Neurosci. Letts., **81**, 209-214.

KEATING, M. J., (1968), Functional interaction in the development of specific nerve connexions., J. Physiol., (Lond.), **198**, 75-77P.

KEATING, M. J., (1974), The role of visual function in the patterning of binocular visual connexions., Brit. Med. Bull., **30**, 145-151.

KEATING, M. J. and FELDMAN, J. D., (1975), Visual deprivation and intertectal neuronal connections in Xenopus laevis, Proc Roy Soc Lond (Biol), **191**, 467-474.

KEATING, M. J., (1975), The time course of experience dependent synaptic switching of visual connections in Xenopus laevis., Proc. R. Soc. Lond., **189**, 603-610.

KEATING, M. J., (1981), The effect of visual deprivation on the maturation of intertectal neuronal connections in Xenopus laevis., J. Physiol., (Lond.), **320**, 19-20P.

KEATING, M. J., GRANT, S., DAWES, E. A. and NANCHAHAL, K., (1986), Visual deprivation and the maturation of the retinotectal projection in Xenopus laevis, J Embryol Exp Morph, **91**, 101-115.

KEATING, M. J. and KENNARD, C., (1987), Visual experience and the maturation of the ipsilateral visuotectal projection in Xenopus laevis, Neurosci., **21**, 519-527.

KEATING, M. J. and GRANT, S., (1992), The critical period for experience-dependent plasticity in a system of binocular connections in Xenopus laevis: its temporal profile and relation to normal developmental requirements, Eur. J. Neurosci., **4**, 27-36.

KENNARD, C. and KEATING, M. J., (1985), A species difference between Rana and

Xenopus in the occurance of intertectal neuronal plasticity, Neurosci. Lett., **58**, 365-370.

KING, W. M. and SCHMIDT, J. T., (1991), The long latency component of retinotectal transmission: enhancement by stimulation of nucleus isthmi or tectobulbar tract and block by nicotinic cholinergic antagonists, Neurosci., **40**, (3), 701-712.

KLEINSCHMIDT, A., BEAR, M. F. and SINGER, W., (1987), Blockage of "NMDA" receptors disrupts experience-dependent plasticity of kitten striate cortex, Science, **238**, 355-358.

KOERNER, J. F. and COTMAN', C. W., (1982), Response of schaffer collateral-CA1 pyramidal cell synapses of the hippocampus to analogues of acidic amino acids, Brain Res., **251**, 205-115.

LAMBERT, J. D. C. and JONES, R. S. G., (1990), A reevaluation of excitatory amino acid-mediated synaptic transmission in rat dentate gyrus, J. Neurosci., **64**, (1), 119-132.

LANGDON, R. B. and FREEMAN, J. A., (1986), Antagonists of glutaminergic neurotransmission block retinotectal transmission in goldfish, Brain Res., **398**, 169-174.

LANGDON, R. B. and FREEMAN, J., (1987), Pharmocology of retinotectal transmission in the goldfish: effects of nicotinic ligands, strychnine, and kynurenic acid, J.Neurosci., **7**, 760-773.

LESTER, R. A. J., CLEMENTS, J. D., WESTBROOK, G. L. and JAHR, C. E., (1990), Channel kinetics determine the time course of NMDA receptor-mediated synaptic currents, Nature, **346**, 565-567.

LIBET, R. and GERARD, R. W., (1939), Control of the potential rhythm of the isolated frog brain, J. Neurophys., **2**, 153-169.

LUND, R. D., (1965), Uncrossed visual pathways of hooded and albino rats., Science, **149**, 1506-1507.

MAFFEI, L. and GALLI-RESTA, L., (1990), Correlation in the discharges of neighbouting retinal ganglion cells during prenatal life, Proc. Natl. Acad. Sci., **87**, 2861-2864.

MARTIN, P. R., SEFTON, A. J. and DREHER, B., (1983), The retinal location and fate of ganglion cells which project to the ipsilateral superior colliculus in neonatal albino and hooded rats., Neurosci. Lett., **41**, 219-226.

MATSUMOTO, N. and BANDO, T., (1980), Excitatory synaptic potentials and morphological classification of tectal neurons of the frog, Brain Res., **192**, 39-48.

MATSUMOTO, N., SCHWIPPERT, W. W. and EWERT, J. P., (1986), Intracellular activity of morphologically identified neurons of the grass frog's optic tectum in response to moving congigurational stimuli, J. Comp. Physiol., **159**, 721-739.

MATURANA, H. R., LETTVIN, J. Y., McCULLOCH, W. S. and PITTS, W. H., (1960), Anatomy and physiology of vision in the frog (*Rana pipiens*), J.Gen. Physiol.,

43, 129-175.

MAYER, M. L., WESTBROOK, G. L. and GUTHRIE, P. B., (1984), Voltage-dependent block by Mg^{2+} of NMDA responses in spinal cord neurones, Nature, **309**, 261-263.

McDONALD, J. W., CLINE, H. T., CONSTANTINE-PATON, M., MARAGES, W. F., JOHNSTON, M. V., YOUNG, A. B., (1989), Quantitative autoradiographic localization of NMDA, quisqualate and PCP receptors in the frog tectum , Brain Res., **482**, 155-158.

MEREDITH, M. A. and STEIN, B. E., (1986), Visual, Auditory, and somatosensory convergence on cells in superior colliculus results in multisensory integration., J. Neurophysiol., **56**, (3), 640-662.

MERRILL, E. G. and WALL, P. D., (1972), Factors forming the edge of a receptive field: the presence of ineffective afferent terminals, J. Physiol., **226**, 825-846.

MEYER, R. L., (1982), Tetrodotoxin blocks the formation of ocular dominance columns in goldfish, Science, **218**, 589-591.

MEYER, R. L., (1983), Tetrodotoxin inhibits the formation of refined retinotopography in goldfish, Dev. Brain Res., **6**, 293-298.

MIGANI, P., CONTESTABILE, A., CRISTINI, G. and LABANTI, L., (1980), Evidence of intrinsic cholinergic circuits in the optic tectum of teleosts, Brain Res., **194**, 125-135.

MILLER, K. D., CHAPMAN, B. and STRYKER, M. P., (1989), Visual responses in adult cat visual cortex depends on N-methyl-D-aspartate receptors, Proc. Natl. Acad. Sci. USA, **86**, 5183-5187.

MURRAY, M. and EDWARDS, M. A., (1982), A quantitative study of the reinnervation of the goldfish optic tectum following optic nerve cruush, J. Comp. Neurol., **209**, 363-373.

NICHOLSON, C., FREEMAN, J. A. and , (1975), Theory of current source-density analysis and determination of conductivity tensor for anuran cerebellum, J. Neurophys., **38**, 356-368.

NIEUWKOOP, P. D. and FABER, J., *Normal table of Xenopus laevis* (Daudin, North Holland, Amsterdam, 1967).

NISTRI, A., SIVILOTTI, L. and WELSH, D. M., (1990), An electrophysiological study of the action of NMDA on excitatory transmission in the frog optic tectum *in vitro*, Neuropharm., **29**, (7), 681-687.

NOWAK, L., BREGESTOVSKI, P., ASCHER, P., HERBERT, A. and PROCHIANTZ, A., (1984), Magnesium gates glutamate-activated channels in mouse central neurones, Nature, **307**, 462-465.

O'DELL, T. J., HAWKINS, R. D., KANDEL, E. R. and ARANCIO, O., (1991), Tests of the roles of two diffusable substances in long-term potentiation: Evidence for nitric oxide as a possible early retrograde messenger, Proc. Natl. Acad. Sci. USA, **88**, 11285-11289.

O'KEEFE, J. and DOSTROVSKY, J., (1971), The hippocampus as spatial map: Preliminary evidence from unit activity in the freely moving rat., Brain Res., **34**, 171-175.

O'KEEFE, J. and NADEL, L., *The hippocampus as a cognitive map* (Clarendon Press, London, 1978).

O'LEARY, D. D. M., FAWCETT, J. W. and COWAN, W. M., (1986), Topographic targeting errors in the retinocollicular projection and their elimination by selective ganglion cell death, Dev. Brain Res., **27**, 87-99.

O'ROURKE, N. A. and FRASER, S. E., (1990), Dynamic changes in optic fibre terminal arbors lead to retinotopic map formation: An *in vivo* confocal microscopic study, Neuron, **5**, 159-171.

OLSON, M. D. and MEYER, R. L., (1991), The effect of TTX-activity blockade and total darkness on the formation of retinotopy in the goldfish retinotectal projection., J. Comp. Neurol., **303**, 412-423.

PETTIGREW, J. D., (1974), The effect of visual expereience on the development of stimulus specificity by kitten cortical neurons., J. Physiol., **237**, 49-74.

RAUSCHECKER, J. F., (1991), Mechanisms of visual plasticity: Hebb synapses, NMDA receptors, and beyond, Physiological reviews, **71**, (2), 587-615.

REH, T. A. and CONSTANTINE-PATON, M., (1984), Retinal ganglion cell terminals change their projection sites during larval development of *Rana pipiens*, J Neurosci, **4**, 442-457.

REH, T. A. and CONSTANTINE-PATON, M., (1985), Eye-specific segregation requires neural activity in three-eyed *Rana pipiens*, J Neurosci, **5**, 1132-1143.

REITER, H. O., WAITZMAN, D. M. and STRYKER, M. P., (1986), Cortical activity blockade prevents ocular dominance plasticity in the kitten visual cortex., Exp. Brain Res., **65**, 182-188.

REYNOLDS, I. J. and BEAR, M. F., (1991), Effects of age and visual experience on [3H] MK801 binding to NMDA receptors in the kitten visual cortex, Exp. Brain Res., **85**, 611-615.

RICHARDS, C. D. and SERCOMBE, R., (1970), Calcium, magnesium and electrical activity of guinea-pig olfactory cortex *in vitro*, J Physiol Lond, **211**, 571-584.

RICUTTI, A. J. and GRUBERG, E. R., (1985), Nucleus Isthmi provides most tectal choline acetyltransferase in the frog *Rana pipiens*, Brain Res., **341**, 399-402.

SAKAGUCHI, D. S. and MURPHY, R. K., (1985), Map formation in the developing *Xenopus* retinotectal system: examination of ganglion cell terminal arborizations, J. Neurosci., **5**, (12), 3228-3245.

SALT, T. E., (1986), Mediation of thalamic sensory input by both NMDA receptors and non-NMDA receptors, Nature, **322**, 263-265.

SANES, D. H. and TAKACS, C., (1993), Activity-dependent refinement of inhibitory connections, Eur. J. Neurosci., **5**, 570-574.

SARGENT, P. B., PIKE, S. H., NADEL, D. B. and LINDSTROM, J. M., (1989), Nicotinic Acetylcholine receptor like molecules in the retina, retinotectal pathway, and optic tectum of the frog, J. Neurosci., **9**, (2), 565-573.

SCHERER, W. J. and UDIN, S. B., (1989), NMDA antagonists prevent interaction of binocular maps in *Xenopus* tectum, J.Neurosci., **9**, 3837-3843.

SCHERER, W. J. and UDIN, S. B., (1991a), Latency and temporal overlap of visually elicited contralateral and ipsilateral firing in *Xenopus* tectum during and after the critical period, Dev Brain Res, **58**, 129-132.

SCHERER, W. J. and UDIN, S. B., (1991b), Chronic effects of NMDA and APV on tectal output in *Xenopus laevis*, Vis. Neurosci., **6**, 185-192.

SCHMIDT, J. T., CICERONE, C. M. and EASTER, S. E., (1974), Reorganization of the retino-tectal projection in goldfish., Abstract Soc. Neurosci., 610.

SCHMIDT, J. T., CICERONE, C. M. and EASTER, S. E., (1977), Expansion of the half retinal projection to the tectum in goldfish: an electrophysiological and anatomical study., J. Comp. Neurol., **177**, 257-278.

SCHMIDT, J. T. and FREEMAN, J. A., (1980), Electrophysiological evidence that retinotectal synaptic transmission in the goldfish is cholinergic, Brain Res., **187**, 129-142.

SCHMIDT, J. T. and EDWARDS, D. L., (1983), Activity sharpens the map during the regeneration of the retinotectal projection in goldfish, Brain Res, **269**, 29-39.

SCHMIDT, J. T. and TIEMAN, S. B., (1985), Eye-specific segregation of optic afferents in mammals, fish and frogs, Cell.Mol.Neurobiol., **5**, 5-34.

SCHMIDT, J. T. and EISELE, L. E., (1985), Stroboscopic illumination and dark rearing block the sharpening of the regenerated retinotectal map in goldfish., Neurosci., **14**, (2), 535-546.

SCHMIDT, J. T. and BUZZARD, M., (1993), Activity-driven sharpening of the retinotectal projection in goldfish: development under stroboscopic illumination prevents sharpening., J. Neurobiol., **24**, (3), 384-399.

SEEBURG, P. H., (1993), The molecular biology of mammalian glutamate receptor channels, TINS, **16**, (9), 359-365.

SHATZ, C. J. and STRYKER, M. P., (1988), Prenatal tetrodotoxin infusion blocks segregation of retinogeniculate afferents., Science, **242**, 87-89.

SHATZ, C. J., (1990), Competetive interactions between retinal ganglion cells during prenatal development., J. Neurobiol., **21**, (1), 197-211.

SILLAR, K. T. and ROBERTS, A., (1991), Segregation of NMDA and non-NMDA receptors at seperate synaptic contacts: evidence from spontaneous EPSPs in *Xenopus* embryo spinal neurons, Brain Res., **545**, 24-32.

SILVER, R. A., TRAYNELIS, S. F. and CULL-CANDY, S. G., (1992), Rapid-time-course miniature and evoked excitatory currents at cerebellar synapses *in situ*, Nature, **355**, 163-166.

SIMINOFF, R., SCHWASSMANN, H. O. and KRUGER, L., (1966), An electrophysiological study of the visual projection to the superior colliculus of the rat, J. Comp. Neurol., **127**, 435-444.

SIMON, D. K. and O'LEARY, D. M., (1992), Development of topographic order in the mammalian retinocollicular projection, J. Neurosci., **12**, (4), 1212-1232.

SIMON, D. K., PRUSKY, G. T., O'LEARY, D. D. M. and CONSTANTINE-PATON, M., (1992), NMDA receptor antagonists disrupt the formnation of a mammalian neural map, Proc. Natl. Acad. Sci. USA, **89**, 10593-10597.

SINGER, W., TRETTER, F. and YINON, U., (1982), Central gating of developmental plasticity in kitten visual cortex, J. Phsiol., **324**, 221-237.

SPERRY, R., (1943), Effect of 180 degree rotation of the retinal field on visuomotor coordination, **92**, 263-279.

SPERRY, R. W., (1963), Chemoaffinity in the orderly growth of nerve fiber patterns and connections , Proc. Natl. Acad. Sci. USA, **50**, 703-710.

STERN, P., EDWARDS, F. A. and SAKMANN, B., (1992), Fast and slow components of unitary EPSCs on stellate cells elicited by focal stimulationin slices of rat visual cortex, J. Physiol., **449**, 247-278.

STEVENS, R. J., (1973), A cholinergic inhibitory system in the frog optic tectum: its role in visual electrical responses and feeding behaviour, Brain Res., **49**, 309-321.

STILES, M., MILHALAK, E., UNNIKRISHNAN, K. P., GOYAL, P., HARTH, E., (1985), Periodic and Nonperiodic Responses of Frog (*Rana pipiens*) Retinal Ganglion Cells, Exp. Neurol., **88**, 176-197.

STIRLING, R. V., (1991), Molecules, maps and gradients in the retinotectal projection, TINS, **14**, (12), 509-512.

STRAZNICKY, K. and GAZE, R. M., (1971), The growth of the retina in *Xenopus laevis*: an autoradiographic study., J. Embryol. exp. Morph., **26**, 67-79.

STRAZNICKY, K. and GAZE, R. M., (1972), The development of the tectum in *Xenopus laevis*: an autoradiographic study, J. Embryol. exp. Morph., **28**, (1), 87-115.

STRAZNICKY, C., TAY, D. and HISCOCK, J., (1980), Segregation of optic fibre projections into eye-specific stripes in dually innervated tecta in *Xenopus*, Neurosci Letts., **19**, 131-136.

STRYKER, M. P. and HARRIS, W. A., (1986), Binocular impulse blockade prevents the formation of ocular dominance columns in cat visual cortex., J. Neurosci., **6**, 2117-2133.

STUERMER, C. A. O. and EASTER, S. S., (1984), A comparison of the normal anmd regenerated retinotectal pathways of goldfish , J. Comp. Neurol., **223**, 57-76.

STUERMER, C. A. and RAYMOND, P. A., (1989), Developing retinotectal projection in larval goldfish, J. Comp. Neurol., **281**, 630-640.

STUERMER, C. A., ROHRER, B. and MUNZ, H., (1990), Development of the retinotectal projection of the zebrafish embryos under TTX-induced neural-impuls blockade., J. Neurosci., **10**, (11), 3615-3626.

SZEKELY, G., SETALO, G. and LAZAR, G., (1973), Fine structure of the frog's optic tectum: optic fibre termination layers, J. Hirnforsh., **14**, 189-225.

TEYLER, T. J., LEWIS, D. and SHASHOUA, V. E., (1981), Neurophysiological and biochemical properties of the goldfish optic tectum maintained in vitro., Brain Res. Bull., **7**, 45-56.

THOMPSON, W., KUFFLER, D. P. and JANSEN, J. K. S., (1979), The effect of prolonged, reversible block of nerve impulses on the elimination of polyneural innervation of new-born rat skeletal muscle fibres, Neurosci., **4**, 271-281.

THOMPSON, I. and HOLT, C., (1989), Effects of intraocular tetrodotoxin on the development of the retinocollicular pathway in the syrian hamster., J. Comp. Neurol., **282**, 371-388.

THOMSON, A. M., WEST, D. C. and LODGE, D., (1985), An N-methylaspartate receptor-mediated synapse in rat cerebral cortex: a site of action of ketamine?, Nature, **313**, 479-481.

TRISLER, G. D., SCHNEIDER, M. D. and NIRENBERG, M., (1981), A topographic gradient of molecules in retina can be used to identify neuron position, Proc. Nat. Acad. Sci. USA, **78**, (4), 2145-2149.

TRISLER, D. and COLLINS, F., (1987), Corresponding gradients of TOP molecules in the developing retina and optic tectum, Science, **237**, 1208-1209.

TRUSSELL, L. O. and FISCHBACH, G. D., (1989), Glutamate receptor desensitization and its role in synaptic transmission, Neuron, **3**, 209-218.

TSUMOTO, T., HAGIHARA, K., SATO, H. and HATA, Y., (1987), NMDA receptors

in the visual cortex of young kittens are more effective than those of adult cats, Nature, **327**, 513-514.

UDIN, S. B. and KEATING, M. J., (1981), Plasticity in a central nervous pathway in *Xenopus*: anatomical changes in the isthmotectal projection after larval eye rotation, J. Comp. Neurol., **203**, 575-594.

UDIN, S. B., (1983), Abnormal visual input leads to development of abnormal axon trajectories in frogs, Nature, (Lond.), **301**, 336-338.

UDIN, S. B., KEATING, M. J., DAWES, E. A., GRANT, S. and DEAKIN, J. F. W., (1985), Intertectal neuronal plasticity in *Xenopus laevis*: persistence despite cetacholamine depletion, Dev. Brain Res., **19**, 81-88.

UDIN, S. B. and FISHER, M. D., (1985), The development of the nucleus isthmi in *Xenopus laevis*: I. Cell genesis and formation of connections with the tecta., J. Comp. Neurol., **232**, 25-35.

UDIN, S. B., (1989), Development of the nucleus isthmi in *Xenopus*, II: Branching patterns of contralaterally projecting isthmotectal axons during maturation of binocular maps., Vis, Neurosci., **2**, 153-163.

UDIN, S. B., FISHER, M. D. and NORDEN, J. J., (1990), Ultrastructure of the crossed isthmotectal projection in *Xenopus* frogs., J. Comp. Neurol., **292**, 246-254.

UDIN, S. B. and SCHERER, W. J., (1990), Restoration of the plasticity of binocualr maps by NMDA after the critical period in *Xenopus*, Science, **249**, 669-672.

UDIN, S. B., FISHER, M. D. and NORDEN, J. J., (1992), Isthmotectal axons make ectopic synapses in monocular regions of the tectum in developing *Xenopus laevis* frogs., J. Comp. Neurol., **322**, 461-470.

UDIN, S. B., SCHERER, W. J. and CONSTANTINE-PATON, M., (1992), Physiological effects of chronic and acute application of N-methyl-D-aspartate and 5-amino-phosphonovaleric acid to the optic tectum of *Rana pipiens* frogs, Neurosci., **49**, (3), 739-747.

WALL, P. D., (1977), The presence of ineffective synapses and the circumstances which unmask them, Phil. Trans. R. Soc. Lond. B, **278**, 361-372.

WALTER, J., KERN-VEITS, B., HUF, J., STOLZE, B. and BONHOEFFER, F., (1987a), Recognition of position-specific properties of tectal cell membranes by retinal axons *in vitro*, Development, **101**, 685-696.

WALTER, J., HENKE-FAHLE, S. and BONHOEFFER, F., (1987b), Avoidance of tectal membranes by temporal retinal axons, Development, **101**, 909-913.

WANG, S. R. and MATSUMOTO, N., (1990), Postsynaptic potentials and morphology of tectal cells responding to electrical stimulation of the bullfrog nucleus isthmi, Vis. Neurosci., **5**, 479-488.

WIESEL, T. N. and HUBEL, D. H., (1963a), Effects of visual deprivation on morphology and physiology of cells in the cat's lateral geniculate body., J. Neurophysiol., **26**, 978-993.

WIESEL, T. N. and HUBEL, D. H., (1963b), Single-cell responses in striate cortex of kittens deprivede of vision in one eye., J. Neurophysiol., **26**, 1003-1017.

WIESEL, T. N. and HUBEL, D. H., (1965), Comparison of the effects of unilateral and bilateral eye closure on cortical unit responses in kittens., J. Neurophysiol., **28**, 1029-1040.

WILLIAMS, R. W., BASTIANI, M. J., LIA, B. and CHALPUA, L. M., (1986), Growth cones, dying axons and developmental fluctuations in the fiber population of the cat's optic nerve, J. Comp. Neurol., **246**, 32-69.

WILLIAMS, J. H., ERRINGTON, M. L., LYNCH, M. A. and BLISS, T. V. P., (1989), Arachidonic acid induces a long-term activity-dependent enhancement of synaptic transmission in the hippocampus, Nature, **341**, 739-742.

WITKOVSKY, P., GALLIN, E., HOLLYFIELD, J. G., RIPPS, H. and BRIDGES, C. D. B., (1976), Photoreceptor thresholds and visual pigment levels in normal and vitamin A deprived *Xenopus* tadpoles , J. Neurophysiol., **39**, 1272-1287.

YOON, M. G., (1972a), Reversibility of the reorganization of retinotectal projection in goldfish., Exp. Neurol., **35**, 565-577.

YOON, M. G., (1972b), Transposition of the visual projection from the nasal hemiretina onto the foreign rostral zone of the optic tectum in goldfish., Exp. Neurol., **37**, 451-462.

ZOTOLLI, S. J., RHODES, K. J., CORRODI, J. G. and MUFSON, E. J., (1988), Putative cholinergic projections from the Nucleus Isthmi and the Nucleus Reticularis Mesencephali to the Optic Tectum in the goldfish (*Carassius auratus*), J. Comp. Neurol., **273**, 385-398.